

MECHANISMS OF TREATMENT INDUCED CELL PLASTICITY IN PROSTATE CANCER

by

Daksh Thaper

BSc, Simon Fraser University, 2012

A THESIS SUBMITTED IN PARTIAL FULFILLMENT OF
THE REQUIREMENTS FOR THE DEGREE OF

Doctor of Philosophy

in

THE FACULTY OF GRADUATE AND POSTDOCTORAL STUDIES
(Experimental Medicine)

THE UNIVERSITY OF BRITISH COLUMBIA
(Vancouver)

August 2018

© Daksh Thaper, 2018

Examining Committee

The following individuals certify that they have read, and recommend to the Faculty of Graduate and Postdoctoral Studies for acceptance, the dissertation entitled:

Mechanism of treatment induced cell plasticity in prostate cancer

submitted by Daksh Thaper in partial fulfillment of the requirements
for

the degree of Doctor of Philosophy

in Experimental Medicine

Examining Committee:

Dr. Amina Zoubeydi, Associate Professor, Department of Urologic Sciences
Supervisor

Dr. Michael Cox, Associate Professor, Department of Urologic Sciences
Supervisory Committee Member

Dr. Christopher Maxwell, Associate Professor, Department of Pediatrics
Supervisory Committee Member

Dr. Shoukat Dedhar, Professor, Department of Biochemistry
Supervisory Committee Member

Dr. Calvin Roskelley, Professor, Department of Cellular and Physiological Sciences
University Examiner

Dr. Wan Lam, Professor, Department of Pathology and Laboratory Medicine
University Examiner

Abstract

While effective, resistance to 1st generation and 2nd generation androgen receptor (AR) pathway inhibitors is inevitable, creating a need to study the mechanisms by which prostate cancer (PCa) cells become resistant to these treatments. At its core, resistance can be categorized into AR driven and non-AR driven. The research presented in this thesis explores the hypothesis that non-AR driven resistance mechanisms exploit cellular plasticity to gain a survival advantage. Previous research has demonstrated that in response to 1st generation anti-androgens, epithelial PCa cells can undergo an epithelial-mesenchymal transition (EMT); a process implicated in metastatic dissemination of cancer cells throughout the body. Augmenting prior research demonstrating *LYN* tyrosine kinase's role in resistance to 1st generation anti-androgens, our research demonstrates *LYN* promoting both EMT and metastasis. Specifically, we discovered that signaling cascade downstream of *LYN* alters the sub-cellular localization and therefore stability of key EMT promoting transcription factors Slug and Snail. While *LYN* does contribute to both treatment resistance and metastasis in PCa, its role in EMT was a pan-cancer mechanism observed in both breast and bladder cancer.

Our research also explored the increased incidence of neuroendocrine PCa (NEPC) as a resistance mechanism to more potent 2nd generation anti-androgens (enzalutamide and abiraterone). Interrogating a model of *in vivo* derived enzalutamide resistance, our research uncovered the crucial role of neuronal transcription factor brain derived 2 (BRN2) in the transformation of epithelial prostate cells to neuroendocrine (NE) phenotype. Importantly, we discovered that AR inhibition relieves its' suppression of BRN2; thereby increasing BRN2 expression and initiating NE differentiation of epithelial PCa cells. Moreover, targeting BRN2 not only reduced the enzalutamide-induced NE differentiation but also reduced proliferation of enzalutamide resistant PCa cells and terminal NEPC cells. Building on this data, our research outlines the discovery of small molecule BRN2 inhibitors (BRN2i) that recapitulate the functional results demonstrated by conventional knockdown techniques. These BRN2i display specificity to BRN2 and selectivity in compromising growth of NEPC cells. Altogether, this thesis demonstrates

two possible mechanisms how PCa cells alter their identity as epithelial cells to more mesenchymal (*LYM*) and/or neuroendocrine (BRN2) and gain resistance to AR pathway inhibitors.

Lay Summary

Targeting the androgen receptor (AR) has been the cornerstone of treatment for men suffering from prostate cancer, essentially starving tumors of the fuel they need to grow and survive. While effective, resistance eventually emerges and tumors come back stronger and more aggressive than before. Research presented in this thesis studies the roles of two proteins, *LYN* and BRN2 in the aggressive nature of the recurrent prostate cancer.

We discovered that *LYN* activates a protein network that allow cells to gain enhanced invasive and migratory properties. These abilities enable the cancer cells to navigate around the human body to both close and distant metastatic sites.

We also studied the function of BRN2 in promoting a deadly form of prostate cancer called Neuroendocrine Prostate Cancer (NEPC). BRN2 is essential for the growth and survival of NEPC and we have developed drugs that can inhibit BRN2 and display therapeutic potential for treating NEPC.

Preface

Data presented in this thesis was conducted as part of my PhD program from January 2013 to January 2018. I was responsible for concept, design, experimentation or analysis for data presented in “Results” sections of Chapters 3, 4 and 5. Data presented in “Introduction” sections of Chapters 3, 4 and 5 were conducted by current/previous lab members and are an important preamble for the “Results” sections. Dr. Amina Zoubeidi is the principal investigator for all data presented in this thesis. Specifically for Chapter 4, I worked closely with Dr. Jennifer L. Bishop and Dr. Sepideh Vahid on study design and experiments. *In silico* modeling in the “Introduction” section of Chapter 5 was performed by Dr. Ravi Munuganti.

- In March 2017, Chapter 3 of this thesis was published as.

Targeting *LYN* regulates Snail family shuttling and inhibits metastasis.

Daksh Thaper, Sepideh Vahid, Ka Mun Nip, Igor Moskalev, Xhanghong Shan, Sebastian Frees, Morgan E Roberts, Kirsi Ketola, Kenneth W Harder, Cheryl Gregory-Evans, Jennifer L Bishop and Amina Zoubeidi. *Oncogene* (IF: 7) DOI:10.1038/onc.2017

- In January 2017, Chapter 4 of this thesis was published as:

The Master Neural Transcription Factor BRN2 Is an Androgen Receptor–Suppressed Driver of Neuroendocrine Differentiation in Prostate Cancer.

Jennifer L. Bishop, Daksh Thaper, Sepideh Vahid, Alastair Davies, Kirsi Ketola, Hidetoshi Kuruma, Randy Jama, Ka Mun Nip, Arkhjamil Angeles, Fraser Johnson, Alexander W. Wyatt, Ladan Fazli, Martin E. Gleave, Dong Lin, Mark A. Rubin, Colin C. Collins, Yuzhuo Wang, Himisha Beltran and Amina Zoubeidi. *Cancer Discovery* (IF: 25) DOI: 10.1158/2159-8290.CD-15-1263

- The data in Chapter 5 is unpublished and will be prepared as a manuscript for submission in late 2018 or early 2019.

Table of Contents

Abstract.....	iii
Lay Summary.....	v
Preface.....	vi
Table of Contents.....	vii
List of Tables.....	xi
List of Figures	xii
List of Abbreviations.....	xv
Acknowledgements.....	xviii
1. CHAPTER 1: Introduction	1
1.1. Prostate Cancer.....	1
1.1.1. History and Epidemiology	1
1.1.2. Staging	2
1.1.3. Androgen Receptor (AR) and Steroidogenesis	4
1.1.4. Disease progression	5
1.2. Treatments for PCa.....	5
1.2.1. Localized therapy (Radiation and Surgery).....	5
1.2.2. 1 st generation anti-androgens.....	6
1.2.3. 2 nd generation anti-androgens.....	7
1.3. AR driven mechanisms of resistance to hormone therapy	8
1.3.1. Resistance to 1 st line hormone therapy.....	8
1.3.2. Resistance to 2 nd generation anti-androgens.....	13
1.4. Cell plasticity driven responses to hormone therapy	15
1.4.1. Epithelial to Mesenchymal transition	15
1.4.2. Emerging clinical subtypes in PCa	17
1.4.3. Neuroendocrine Prostate Cancer	18
1.5. Treatment options: Beyond the AR	21
1.5.1. Chemotherapies (Taxanes)	21
1.5.2. Personalized Therapies (Immunotherapies and PARP inhibitors)	22

1.6.	Thesis Hypothesis and Objectives	23
2.	Chapter 2: Materials and Methods	25
2.1.	Generation of ENZ-resistant xenografts and cell lines:.....	25
2.2.	Human PCa specimens for RNA-Seq and immunohistochemistry (IHC):.....	25
2.3.	Cell culture.....	26
2.4.	Cell line transfections and treatments.....	26
2.5.	Proliferation, invasion and migration assays.....	28
2.6.	Gene expression profiling	29
2.7.	Western blotting (WB).....	30
2.8.	Subcellular fractionation	30
2.9.	Immunoprecipitation.....	30
2.10.	Reagents and antibodies	30
2.11.	Immunofluorescence	31
2.12.	Quantitative real time PCR (qRT-PCR)	31
2.13.	Luciferase assay.....	31
2.14.	Chromatin immunoprecipitation (ChIP).....	32
2.15.	Animal studies.....	32
2.16.	Zymography	33
2.17.	In vitro kinase assay	34
2.18.	RAC1 Activity assay.....	34
2.19.	Drug Affinity Responsive Target Stability (DARTS)	34
2.20.	BioLayer Interferometry.....	34
2.21.	Microsomal Stability	35
2.22.	Analysis of publically available databases	35
2.23.	Statistical analyses.....	35
3.	Chapter 3: <i>Targeting LYN regulates Snail family shuttling and inhibits metastasis</i>	36
3.1.	Background	36
3.1.1.	Src Family Kinase – <i>LYN</i>	36
3.1.2.	Roles of <i>LYN</i> in cancer.....	37
3.2.	Introduction.....	38
3.3.	Results	39

3.3.1.	<i>LYN</i> mRNA expression correlates with cancer metastasis and E-cadherin expression.	39
3.3.2.	<i>LYN</i> expression and activity modulates Epithelial and Mesenchymal cell states ..	43
3.3.3.	<i>LYN</i> regulates E-Cadherin through SNAI family proteins	48
3.3.4.	<i>LYN</i> kinase expression regulates Slug and Snail stability	51
3.3.5.	<i>LYN</i> kinase activates the VAV1-RAC1-PAK1 pathway translocating Slug and Snail to the nucleus.....	53
3.3.6.	<i>LYN</i> kinase facilitates metastasis in vivo.....	59
3.4.	Discussion	65
4.	Chapter 4: <i>The master neural transcription factor BRN2 is an Androgen Receptor-suppressed driver of neuroendocrine differentiation in Prostate Cancer</i>	68
4.1.	Background	68
4.1.1.	POU family transcription factor: BRN2.....	68
4.1.2.	Induced Neuronal differentiation	69
4.1.3.	Roles of BRN2 in other cancers.....	71
4.2.	Introduction.....	72
4.2.1.	Emergence of AR-driven and non- driven tumors in ENZ ^R CRPC	74
4.3.	Results	80
4.3.1.	The neural transcription factor BRN2 is highly expressed in NE-like ENZ ^R and in human NEPC	80
4.3.2.	BRN2 is inversely correlated with AR expression and activity	88
4.3.3.	Androgen Receptor directly represses BRN2 expression.....	95
4.3.4.	BRN2 and AR regulate SOX2 expression in NEPC	99
4.3.5.	BRN2 is required for NE marker expression and aggressive growth of ENZR cells in vitro and in vivo.	105
4.4.	Discussion.....	108
5.	Chapter 5: <i>Development and Characterization of small molecule inhibitors for BRN2 as a treatment strategy for NEPC</i>	112
5.1.	Introduction and <i>in silico</i> background.....	112
5.1.1.	<i>In silico</i> modeling of BRN2.....	112
5.2.	Results	115
5.2.1.	Exclusion Criteria for hits from <i>in silico</i> screening.....	115

5.2.2.	Compounds 7 and 18 directly bind to BRN2 DNA binding domain	118
5.2.3.	BRN2 inhibitors disrupt DNA binding	119
5.2.4.	Pathways downstream of BRN2 inhibition	121
5.2.5.	Targeting BRN2 greatly sensitizes cells to AR pathway inhibition	129
5.3.	Future Directions	131
6.	Discussion – Treatment resistance and cell plasticity	133
	Bibliography	143

List of Tables

Table 1-1: Gleason Grade system.....	2
Table 1-2: List of Androgen Receptor post-translational modifications:	10
Table 6-1: Models of NEPC	137

List of Figures

Chapter 1

Figure 1.1 – Prostate Cancer epidemiology (age adjusted):	1
Figure 1.2 – Androgen Endocrine Pathway:	4
Figure 1.3 – Prostate Cancer disease progression:	5
Figure 1.4 - Steroidogenesis pathways in Castration resistant prostate cancer:	12

Chapter 3

Figure 3.1 - <i>LYN</i> expression induced by androgen deprivation:	38
Figure 3.2 - <i>LYN</i> expression vs. Metastasis:	39
Figure 3.3 – <i>LYN</i> mRNA is up-regulated in metastatic cancers:	40
Figure 3.4 - <i>LYN</i> expression vs E-Cadherin:	41
Figure 3.5 – <i>LYN</i> modulates E-Cadherin <i>in vitro</i> :	42
Figure 3.6 – <i>LYN</i> kinase regulates EMT phenotype:	43
Figure 3.7 – <i>LYN</i> expression regulates EMT markers and cell migration and invasion:	44
Figure 3.8 – <i>LYN</i> mRNA correlates with EMT markers in patients:	45
Figure 3.9 – <i>LYN</i> 's kinase activity is required for EMT:	46
Figure 3.10 - Kinase activity of <i>LYN</i> is responsible for EMT:	47
Figure 3.11 - Targeting <i>LYN</i> kinase reduces expression of EMT factors Slug and Snail	48
Figure 3.12 - <i>LYN</i> kinase activity modulates protein levels of Slug and Snail:	49
Figure 3.13 - Targeting <i>LYN</i> does not alter Slug and Snail mRNA:	49
Figure 3.14 – Slug expression is higher in patients with high expression of <i>LYN</i>	50
Figure 3.15 - <i>LYN</i> expression modulates Slug and Snail protein stability:	51
Figure 3.16 - <i>LYN</i> expression and activity regulates Slug and Snail ubiquitination and degradation via proteasome	52
Figure 3-17 - <i>LYN</i> expression and activity promotes Slug and Snail nuclear localization	53
Figure 3.18 - Slug and Snail nuclear intensity in response to <i>LYN</i> mutant transfection:	54
Figure 3.19 - Inhibition of <i>LYN</i> causes cytoplasmic retention of Slug and Snail:	54
Figure 3.20 - PAK1 regulates protein levels of Slug and Snail:	55
Figure 3.21 - <i>LYN</i> activity alters interaction between PAK1 and Slug:	55
Figure 3.22 - PAK1 phosphorylates Slug at similar consensus domain as Snail:	56
Figure 3.23 - <i>LYN</i> activity regulates VAV-RAC1-PAK1 signaling pathway:	57
Figure 3.24 - Proposed model of <i>LYN</i> 's regulation of Slug, Snail and EMT	58
Figure 3.25 - PAK1 is required for <i>LYN</i> to stabilize expression of Slug and Snail:	58
Figure 3.26 - Inhibition of <i>LYN</i> reduces <i>in vivo</i> cell migration and invasion:	59
Figure 3.27 - Inhibition of <i>LYN</i> reduces <i>in vivo</i> cell migration and invasion:	60
Figure 3.28 - Inhibition of <i>LYN</i> reduced metastasis induced embryo mortality:	61
Figure 3.29 - Stable K/O of <i>LYN</i> reduces EMT in UC13 BICa cells:	61
Figure 3-30 - Targeting <i>LYN</i> reduces <i>in vivo</i> metastasis in orthotopic BICa model:	62
Figure 3.31 - Targeting <i>LYN</i> reduces <i>in vivo</i> metastasis in orthotopic BICa model:	63
Figure 3.32 - <i>LYN</i> expression is recovered at metastasis:	64

Chapter 4

Figure 4.1 - Binding orientation of POU domains:	68
Figure 4.2 - Binding orientation of PORE, MORE and NORE sites with POU domains:	69
Figure 4.3 - BRN2 expression in other cancers:	72
Figure 4.4 - Generation of ENZR Xenografts and Cell Lines:	75
Figure 4.5 - Emergence of AR-driven and non-driven phenotypes in an in vivo model of ENZR CRPC:	76
Figure 4.6 - AR status in ENZR ^R cell lines:	77
Figure 4.7 - 42D ^{ENZR} cells are AR non-driven:	79
Figure 4.8 - AR non-driven ENZR ^R cells display a NE differentiation signature:	81
Figure 4.9 - AR non-driven ENZR cells have increased levels of the neural transcription factor BRN2:	84
Figure 4.10 - BRN2 is highly expressed in human NEPC:	85
Figure 4.11 - BRN2 is increased in NEPC transdifferentiation model:	85
Figure 4.12 - BRN2 protein expression in human NEPC:	86
Figure 4.13 - BRN2 expression is higher in metastatic prostate cancer and correlates with NEPC markers:	87
Figure 4.14 - BRN2 expression is negatively correlated to AR activity:	88
Figure 4.15 - ENZR ^R cells with high AR activity do not display higher BRN2 or NEPC marker expression:	89
Figure 4.16 - Knockout of BRN2 prevents ENZ induced NE differentiation:	91
Figure 4.17 - BRN2 overexpression induces NE differentiation:	93
Figure 4.18 - BRN2 overexpression enhances NE differentiation, suppresses AR pathway and confers resistance to enzalutamide:	94
Figure 4.19 - Reactivation of AR suppresses BRN2 activity:	95
Figure 4.20 - Exogenous expression of BRN2 rescue NEPC gene expression:	96
Figure 4.21 - Active Androgen Receptor binds to BRN2 upstream enhancer:	97
Figure 4.22 - Inhibiting AR recruitment to BRN2 enhancer induces BRN2 and NE differentiation:	98
Figure 4.23 - SOX2 is upregulated in human NEPC:	99
Figure 4.24 - SOX2 co-operates with BRN2 to drive sub-set of NE differentiation genes:	100
Figure 4.25 - AR negatively regulates SOX2 expression in PCa:	101
Figure 4.26 - BRN2 positively regulates SOX2 expression:	102
Figure 4.27 - SOX2 does not regulate BRN2 and NEPC differentiation:	104
Figure 4.28 - Silencing BRN2 reduces NEPC marker expression:	105
Figure 4.29 - Inhibition of BRN2 reduces cell proliferation, migration and invasion:	106
Figure 4.30 - Stable knockout of BRN2 reduces tumor volume and NEPC markers:	107

Chapter 5

Figure 5.1 - Structural information of the BRN2 protein:.....	114
Figure 5.2 - Inhibition of BRN2 transcriptional activity:	115
Figure 5.3 - DARTS assay:.....	116
Figure 5.4 - Cell proliferation:	117
Figure 5.5 - Compounds inhibit BRN2 targets and NEPC markers:	118
Figure 5.6 - PIPE cloning of BRN2-DBD in pET vector:.....	118
Figure 5.7 - BioLayer Interferometry:	119
Figure 5.8 – Sub-cellular Fractionation:.....	120
Figure 5.9 - BRN2 Chromatin Immunoprecipitation:.....	120
Figure 5.10 - Expression changes in NEPC drivers/targets and markers:.....	121
Figure 5.11 - BRN2 autoregulation:.....	122
Figure 5.12 - BRN2i reduce NEPC cell proliferation and expression of NEPC drivers and markers:	123
Figure 5.13 - Rb1 status in ENZR cells relative to BRN2	124
Figure 5.14 – Cell cycle changes in response to BRN2 inhibition:.....	125
Figure 5.15 - G0/G1 separation:	126
Figure 5.16 - BRN2 inhibition recovers expression of p21 and p27:.....	127
Figure 5.17 - Targeting BRN2 via different mechanisms:	128
Figure 5.18 - Combination of AR and BRN2 inhibition on Proliferation:	129
Figure 5.19 - BRN2 inhibition hinders NE-differentiation induced by AR pathway inhibition : ...	130
Figure 5.20 - Lead optimization:	131
Figure 5.21 - BRN2 expression in NEPC patient derived xenograft models:	132

List of Abbreviations

ABL	abelson murine leukemia 1
ACK	activated cdc-42 Kinase
ADT	androgen deprivation therapy
AKT	ak strain transforming
AML	acute myeloid leukemia
AMP	adenosine mono-phosphate
AR	androgen receptor
ARD	ADP-ribosylation factor domain
ARE	androgen response element
ARV7	androgen receptor variant 7
ASCL1	achaete-scute complex-like 1
AURKA	aurora kinase a
BCR	breakpoint cluster region protein
BL21	b-strain lon protease deficient e-coli
BICa	bladder cancer
BLI	bioLayer interferometry
B-NHL	b-cell non-Hodgkin's lymphoma
BPE	bovine pituitary extract
BrCa	breast cancer
BRCA 1/2	breast cancer 1/2 (gene)
BRD4	bromodomain 4
BRN2	brain derived protein 2
CA	constitutively active
CNA	copy number alterations
CAS9	CRISPR associated protein 9
CBX	chromobox protein
CD133	cluster of differentiation 133
CD117	cluster of differentiation 117
CD29	cluster of differentiation 29
CD40	cluster of differentiation 40
CD56	cluster of differentiation 56
CDH	cadherin
CDK	cyclin dependent kinase
CDKN	cyclin dependent kinase inhibitor
cfDNA	cell free-DNA
CHGA	chromogranin A
CHGB	chromogranin B
CHIP	carboxyl terminus of HSC70-interacting protein

ChIP	chromatin immunoprecipitation
CHX	cycloheximide
CLL	chronic lymphoblastic leukemia
CML	chronic myeloid leukemia
Cpd	compound
CRISPR	clustered regularly interspaced short palindromic repeats
CRPC	castration resistant prostate cancer
CSC	cancer stem cell
CSK	c-terminal src kinase
CSS	charcoal stripped serum
CTLA4	cytotoxic T-lymphocyte-associated protein 4
CYP17A1	cytochrome p450 17A1
DARTS	drug affinity responsive target
DBD	DNA binding domain
DDR	DNA damage response
DHEA	dehydroepiandrosterone
DHT	dihydrotestosterone
DKO	double knock out
DMEM	dulbecco modified eagle's minimal essential medium
DMSO	dimethyl sulfoxide
DNA	deoxyribose nucleic acid
DNMT	DNA methyl transferase
DNPC	double negative prostate cancer
DRE	digital rectal exam
E2F1	E2 transcription factor 1
EBRT	external beam radiation therapy
EGF	epidermal growth factor
EGFR	epidermal growth factor receptor
EMT	epithelial mesenchymal transition
EMT/P	epithelial mesenchymal transition/plasticity
ENO2	enolase 2
ENZR	enzalutamide resistance
ESC	embryonic stem cells
EZH2	enhancer of zeste homolog 2
FAK	focal adhesion kinase
FDA	Food and Drug Administration

FKBP	FK506 Binding Protein
FOXA	Fox-head protein A
FSH	follicle stimulation hormone
GATA2	“GATA” family transcription factor 2
GBM	glioblastoma
GEM	genetically engineered mouse
GLIDE	grid-based ligand docking with energetics
GMCSF	granulocyte-macrophage colony-stimulating factor
gRNA	guide RNA
GSK3 β	glycogen synthase kinase 3 β
GTP	guanosine triphosphate
HSD	hydroxysteroid dehydrogenase
HSP	heat shock protein
HTH	helix turn helix
iN	induced neuron
IAC	intermediate atypical carcinoma
IGF	insulin growth factor
IHC	immunohistochemistry
IMDM	Iscove's modified dulbecco's medium
IPA	Ingenuity pathway analysis
IPTG	isopropyl β -D-1-thiogalactopyranoside
IVIS	in vivo imaging system
JAK	janus kinase
JARID1B	jumonji, AT rich interactive domain 1B
JNK	just another kinase
K/O	knock out
KD	kinase dead
kDA	kilo Dalton
KLF4	Kruppel like factor 4
KRT5	keratin 5
KRT8	keratin 8
LBD	ligand binding domain
LC/MS	liquid chromatography/mass spec
LHRH	luteinizing hormone releasing hormone
LSD1	lysine demethylase 1
MAPK	mitogen activated protein kinase
MCM7	mini-chromosome 7

MDM2	double minute 2 protein
MDR1	multi-drug resistant
MET	mesenchymal epithelial transition
MMP	matrix metalloproteases
MORE	more Pore sites
mRNA	messenger RNA
MYT1L	myelin transcription factor 1 Like
NCAM1	neural cell adhesion molecule 1
NCI	national cancer institute
NE	Neuroendocrine
NEPC	neuroendocrine prostate cancer
NES	nestin
NF κ B	nuclear factor kappa-light-chain-enhancer of activated B cells
NHT	neo-adjuvant hormone therapy
NI-NTA	nickle-nitrilotriacetic acid
nMYC	neuroblastoma MYC
NORE	N-Oct-3 responsive element
NPC	neural progenitor cell
NSE	neuron specific enolase
OCT	octamer
OD	optical density
OLIG2	oligodendrocyte transcription factor 2
OPTI-MEM	opti-minimum essential media
P300	histone acetyltransferase p300
PAK	p21-activated Kinase
PAP	prostatic acid phosphatase
PARP	poly [ADP-ribose] polymerase 1
PCa	prostate cancer
PKC	protein kinase c
PCoA	principle coordinate analysis
PD1	programmed death 1
PDL1	programmed death ligand 1
PDX	patient derived xenografts
PEG10	placental gene 10
PI3K	phosphatidyl inositol 3 kinase
PIM	proviral integration site 1
PIPE	polymerase incomplete primer extension
PORE	pallindromic oct response element
POU	pituitary octamer unc-86

PP1	protein phosphatase 1
PP2A	protein phosphatase 2A
PSA	prostate specific antigen
PTBP	polypyrimidine tract binding protein
QPCR	quantitative polymerase chain reaction
RAC1	ras-related c3 botulinum toxin substrate
RAS-GAP	rat sarcoma-GTPase activating protein
RB1	retinoblastoma 1
REST	RE1 silencing transcription factor
RFX4	regulatory factor x4
RIPA	radio-immunoprecipitation assay buffer
RMSD	root mean square deviation
RPKM	reads per kilo million
RPMI	Roswell park memorial institute
RPPA	reverse phase protein array
SALL2	spalt like transcription factor 2
SCLC	small cell lung cancer
SET9	SET domain containing lysine methyltransferase 7
SH2	src homology domain 2
SH3	src homology domain 3
shRNA	small hairpin RNA
siRNA	small interfering RNA
SIRT1	sirtuin 1
SKO	single knockout
SNAI	snail family transcriptional repressor
SOX	sex determining region-box
SPOP	speckle type BTB/POZ protein

SRC	steroid receptor co-activator
SRC	proto-oncogene SRC,
SRRM4	serine/arginine repetitive matrix 4
STAT	signal transducer and activator of transcription
SUV39H1	suppressor of variegation 3-9 homolog 1
SWOG	southwest oncology group
SYP	synaptophysin
TAX	taxane
TCGA	The Cancer Genome Atlas
TF	transcription factor
TMA	tissue microarray
TMPRSS2	transmembrane protease, serine 2
TNBC	triple negative breast cancer
TNC	tris-sodium-calcium
TNM	tumor node metastasis
TP53	tumor protein 53
T-PER	tissue protein extraction reagent
TRAMP	transgenic adenocarcinoma mouse prostate
TACSTD2	tumor associated calcium signal transducer 2
TSS	transcription start site
TURP	transurethral resection of the prostate
UTR	untranslated region
VAV	VAV guanine nucleotide exchange factor
VP-64	viral protein 16x4
WST1	water soluble tetrazolium
ZEB	zinc finger E-box-binding homeobox

Acknowledgements

I would like to begin by expressing my sincerest gratitude to my supervisor Dr. Amina Zoubeidi for all her guidance through the challenging yet rewarding world of research. I want to thank you for giving me a chance as a naïve undergraduate student and allowing me to be part of an amazing group of talented researchers in an environment that fostered my growth as a scientist. Thank you for trusting me, encouraging my scientific curiosity and providing with the tools to excel along this long journey. I truly enjoyed time as a student in your care and if I had a chance to do it all over again, I would not change a thing!

Next, I want to thank my supervisory committee, Dr. Michael Cox, Dr. Shoukat Dedhar and Dr. Chris Maxwell for all their insights and suggestions during my committee meetings over the last 4-5 years that helped me become a better researcher. Specifically Dr. Cox, I have really appreciated your friendship and advice over the last few years. I want to thank my chair Dr. Nelly Auersperg her charming management of my defense and my university examiners, Drs. Roskelley and Lam for their comments on my thesis and a genuinely enjoyable dialogue during my defense. Lastly, I would like to thank my external examiner Dr. David Rickman for his critical feedback as a leader in the field and for making the trip from New York!

Finally, I want to add a few extra words for some people very special to me.

Sepideh: We have both come a long way since we started as students back in 2013 and I am proud to have you as my best friend. You are one of the smartest people I know and I have seen you accomplish all the challenges set in front of you with poise and courage. Working together with you has inspired me to do the same and I hope to keep learning from you for years to come. Thank you for taking care of me (feeding me!), helping me and importantly, keeping me humble. You are amazing and you should know that when I call you “sir” all the time, I truly mean “senior in all respects”.

Jenna: It was an absolute privilege to learn from you and work with you and we all miss your calming and supportive presence in the lab. Personally, I was very lucky to have you in the lab because your wealth of experience in the fields of older sister and amazing scientist fused together into an amazing mentor and friend! Thank you for sharing your ideas and projects with me and I will always remember the brain storming sessions with coffee that solved so many of our problems. Together with Sepideh, the 3 of us made an amazing team/family and I hope we get to solve more problems together in the future!!

Eliana: It is not an understatement to say that I would not be at the Vancouver Prostate Centre without you. Thank you very much for hiring me as a co-op student, for helping to kindle my interest in research and for tolerating me while I was still immature! You are an absolute essential part of the prostate centre and are at the root of so many successful stories including my own.

My friends: I want to thank Ravi for joining the lab and helping mould an amazing story! I'm also grateful to Kevin, Kush and Peter as my "seniors" for all their advice! Also I want to thank Soojin, Chris, Gunjan, Davide, Shaghayegh, Morgan, Paul, Sahil, Max, Thomas, Alastair, Nader, Nada, Josselin, Lucia, Sebastian, Alex and also Hooman (honorary VPC member!) for all the laughing, crying and laughing while crying! There will always be a special place in my heart for my friends in the Zoubeidi lab and the Vancouver Prostate Centre. You all have made my time as an undergraduate and graduate student significantly more enjoyable! I have grown up within this centre, both personally and professionally and I will cherish my time with you all.

My parents, Rajan and Seema: Finally, I would like to thank my parents for their never-ending love and support. Thank you for all your hard work and sacrifice to get me access to all these opportunities in Canada, and then keeping me on track to realize my goals. I love you both from the bottom of my heart and I hope to continue to make you proud as progress further down the path of a scientist.

To my family

...

Both in and out of the lab.

1. CHAPTER 1: Introduction

1.1. Prostate Cancer

1.1.1. History and Epidemiology

Prostate Cancer (PCa) is a significant cause of cancer related mortality in men. In North America, approximately 1 in 7 Canadian men (Canadian Cancer Society) and 1 in 9 American men (American Cancer Society) are diagnosed with PCa in their lifetime. The observed prevalence of PCa has been subject to drastic changes over the last 40 years. Before the 1990s, the diagnosed prevalence of PCa was much lower and only possible with the presentation of clinical symptoms like urinary obstruction, bone pain and general fatigue and weakness. At point of diagnosis, localized treatments such as surgery were no longer beneficial and treatments were designed to extend life or in some cases were simply palliative. Thus, with the introduction of prostate specific antigen (PSA) screening and early detection, the option of curative intent became viable.

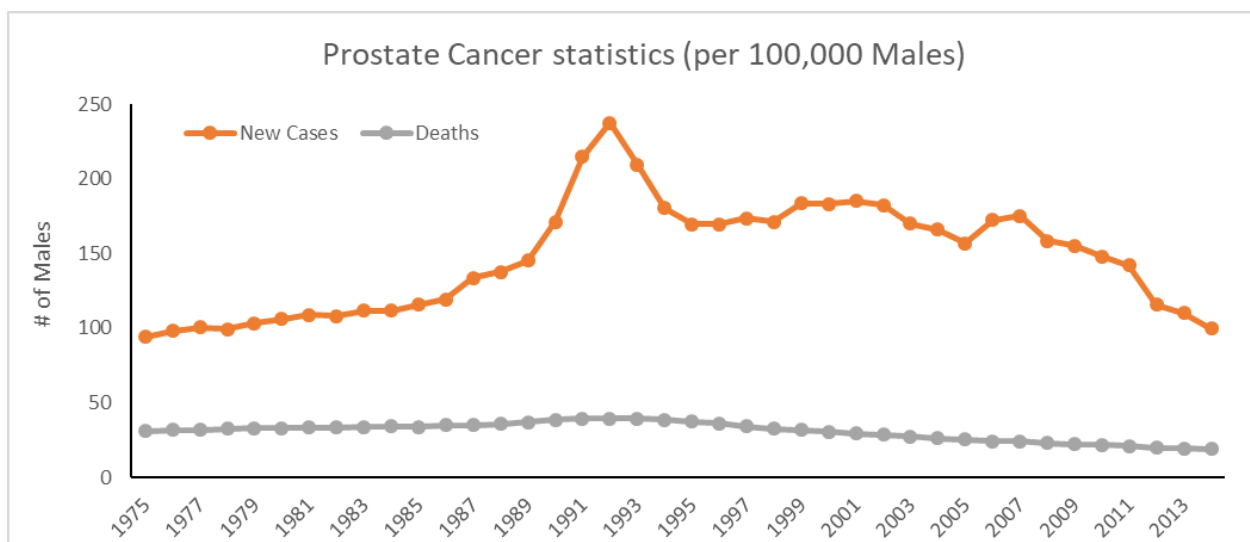


Figure 1.1 – Prostate Cancer epidemiology (age adjusted):

Statistics from National Cancer Institute (NCI) <https://seer.cancer.gov/statfacts/html/prost.html>

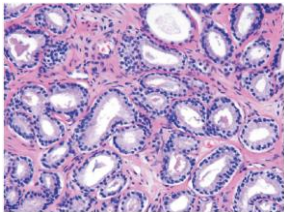
Due to these changes, there was a significant decrease in the number PCa related deaths (**Figure 1-1**). Furthermore, with the increase of awareness campaigns against PCa, men have been more vigilant about their doctor visits and the digital rectal exam (DRE) have combined to greatly increase the incidence/prevalence of PCa (3). However, the benefits of blanket PSA screening and its socioeconomic costs have been scrutinized by several studies. Initially, several large studies failed to find a significant improvement 10 year survival for patients whose

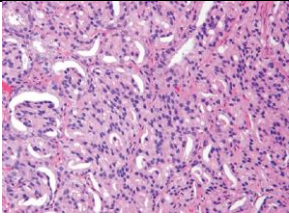
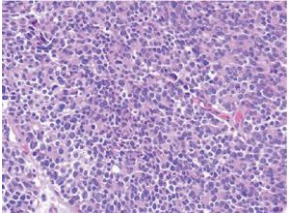
PCa was discovered using PSA screening vs. patients who were diagnosed by DRE or due to symptoms (4, 5). It is possible that the benefits of PSA screening were drowned out by the high survival rate of a majority of PCa patients with less aggressive disease. Interestingly, a recent bio-statistical reanalysis of the same studies found that PSA testing is beneficial to the patients (6). While more research will be required to settle this debate, Wilt et al. showed that even treatment options like surgery for patients with early stage PCa also did not provide any benefits to overall survival compared to active surveillance (7). Combined, this information strongly suggests the addition of other screening procedures are required to compliment PSA and the DRE to identify high-risk patients that would then require surgery and or anti-androgen treatments.

1.1.2. Staging

Gleason grading system is the primary means used to classify PCa pathologically. Scores of 1-5 are used to provide a primary and secondary pattern, although only patterns of 3, 4 and 5 are considered cancerous. Primary and secondary Gleason score sums greater than 6 (3+3) are considered malignant and Gleason scores sums of 1-5 are not. Newer guidelines recommend utilizing the Gleason grading system to report prognostic values as Gleason groups (8).

Table 1-1: Gleason Grade system

<u>Gleason Grade</u>	<u>Gleason Score (sum)</u>	<u>Histology details</u>
Grade 1	≤6	Well formed glands (8). 
Grade 2	3+4	Mostly well formed glands, with some poor/cirbriform glands
Grade 3	4+3	Predominantly poorly formed glands with sparse well formed structures (8).

		
Grade 4	4+4	Only poorly formed, fused, cribriform glands
Grade 5	4+5, 5+4, 5+5	No glandular formation at all (8). 

In addition to Gleason grading, PCa is further classified using the Tumor-Node-Metastasis (TNM) staging system. T_1 is defined by no palpable tumor; T_2 refers to a palpable tumor that is localized to the prostate; T_3 tumors have extended beyond the prostate and T_4 tumors have invaded into adjacent organs. The N category refers to tumor positivity in the lymph nodes, where N_0 means no tumor and N_1 indicates lymph node is positive for tumor. The final M category denotes the presence of distant metastasis (9).

Patients may undergo treatment, or they may select active surveillance based on their Gleason Score/Group and their TNM stage. These factors also combine together to give Stages I, II, III and IV. Patients with localized (T_1/T_2) disease presenting with a Gleason Group 1 (3+3) or Group 2 (3+4) are classified as Stage I or II. An important sub-staging for Stage II is Stage IIc where a patient with localized disease has Gleason Group 3 (4+3) histology as this distinction has considerable implications on overall survival (8). Stage III includes upgrades to Gleason Group 4 and or T_3/T_4 , but importantly N_0 and M_0 standing. Finally, any patient presenting with N_1 or M_1 is considered Stage IV regardless of Gleason Group. At diagnosis, approximately 70% of patients have Stage I or II (<https://seer.cancer.gov/statfacts/html/prost.html>) and are subject to active surveillance. If during surveillance, a patient is upgraded to Stage IIc, III or IV, treatment is recommended especially if life expectancy is greater than 10 years. Immediate treatment is also recommended for any patient diagnosed with stage III or IV PCa (10).

1.1.3. Androgen Receptor (AR) and Steroidogenesis

PCa is a hormone-responsive disease (testosterone) with the androgen receptor (AR) as the central driver. Since its characterization in the 1960s (11), AR has been the cornerstone of targeted therapy in prostate cancer. The AR is encoded on region q11-12 of the X-chromosome; structurally, it contains a regulatory N-terminal domain, the DNA binding domain, a hinge region and a ligand binding domain (LBD) (12). Once testosterone or dihydrotestosterone (DHT) bind to the LBD, the AR dimerizes and translocates to the nucleus. With the aid of a plethora of co-activators and co-repressors, the AR recognizes androgen receptor binding elements (ARE) and either transcribes or represses genes. For example, PSA is an AR dependent gene and a strong indicator of AR activity.

The production of androgens is a tightly controlled biological system beginning with the release of gonadotropin-releasing hormone (GnRH, also known as luteinizing hormone releasing hormone (LHRH)) and corticotropin-releasing hormone (CRH) from the hypothalamus.

This hormonal signal is received by the pituitary gland, which releases both luteinizing hormone

(LH) and follicle stimulating hormone (FSH) and in turn stimulate their release of testosterone from the testis (13). In parallel to the LH and FSH, the pituitary also releases adrenocorticotrophic hormone (ACTH) that stimulates the release of dehydroepiandrosterone (DHEA) from the adrenal gland. Importantly, DHEA can serve as a precursor to DHT and its presence in the blood is exploited by the tumor cells to produce intra-tumoral androgens, thus utilizing DHT for growth instead of testosterone (Fig. 1.2) (14). These ligands are used as important stimulants for AR activity and therefore PCa cell growth.

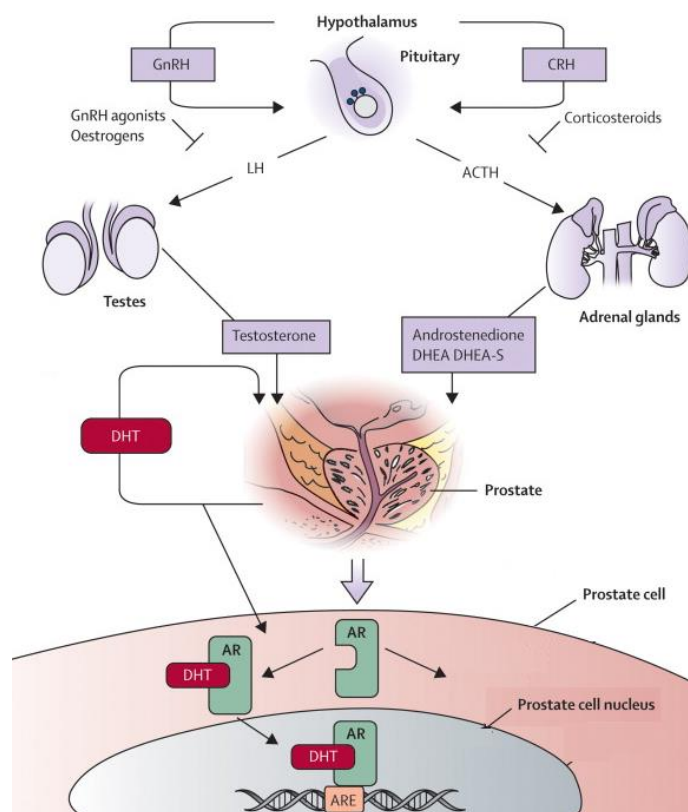


Figure 1.2 – Androgen Endocrine Pathway:

Endocrine pathways resulting in the production of Testosterone, DHT and DHEA. These hormones ultimately activate the AR and promote PCa cell growth. Extracted from Chen et al. 2009 (Lancet Oncology) with permission from publisher Elsevier.

1.1.4. Disease progression

Prostate Cancer tumor progression typically follows a pattern. As stated previously, unless patients are diagnosed with stage III or IV, they are advised to participate in an active surveillance program. This strategy avoids overtreatment of indolent cancers while patients on the program are subject to needle biopsies in 1-2 year cycles (15). If PSA velocity (rate of PSA increase) increases or if the Gleason score is upgraded during the surveillance period, patients are actively treated if their life expectancy is greater than 10 years. If the PCa is still localized at this stage, patients consider surgery or radiation as their treatment options. Despite efficient localized therapies, up to 35% of patients recur, and increasingly potent therapies manage the disease in order to extend the life until the patient (Fig. 1.3).

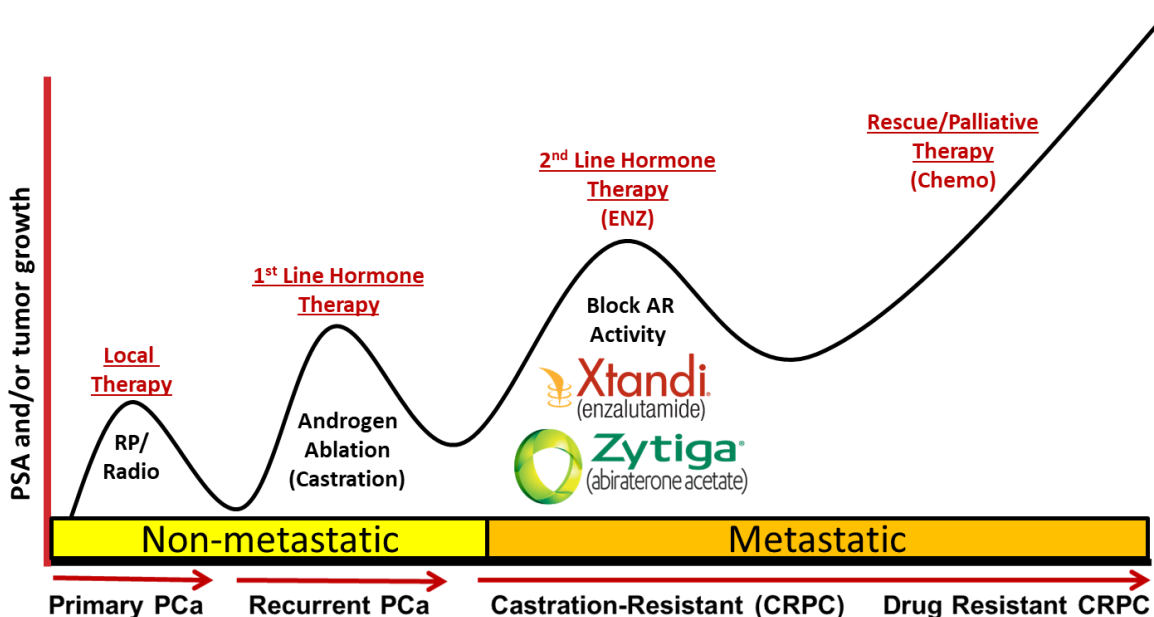


Figure 1.3 – Prostate Cancer disease progression:
Typical disease progression of PCa patients.

1.2. Treatments for PCa

1.2.1. Localized therapy (Radiation and Surgery)

The two most common treatments for localized PCa are radiation therapy and surgery (16).

Radiation therapy techniques-

- External Beam radiation (EBRT) – Beam of radiation delivered by a machine outside the body (16).

- Static high dose – Utilizes a 3D image of the prostate to deliver high dose of radiation to specific areas.
- Intensity modulated – Computer driven therapy that delivers a very precise dose of radiation.
- Proton – Delivers doses of protons instead of X-rays using similar computerized technology for precision to avoid damage to other organs.
- Brachytherapy – Utilizes small radioactive pellets that deliver constant radiation into the prostate. An injection through the perineal region delivers around 100 pellets that release low doses radiation over weeks or months (16).

Main surgery techniques-

- Reteropubic and Perineal – Reteropubic surgery accesses the prostate through the abdomen in the front of the body above the penis while perineal surgery occurs through the region between the anus and the scrotum. Both surgery techniques require large incisions (16).
- Laproscopic – Laproscopic surgery uses several smaller cuts and specialized longer tools to remove the prostate. Due to the smaller incisions, this therapy results in less blood loss and recovery time, however, requires highly skilled urologist surgeons (16).
- Robotic-Assisted Laproscopic – The robotic assisted surgery provides the surgeon with much more precision with the surgery tools, however, the skill of the surgeon remains the most important factor in the success of the therapy (16).

1.2.2. 1st generation anti-androgens

For ~35% patients with recurrent PCa after localized therapy, androgen deprivation therapy (ADT) remains the standard of care. The purpose of ADT is to compromise the production of testosterone and DHT in the body by compromising production leutenizing hormone releasing hormone (LHRH) and inhibiting the pituitary-gonadal hormone axis. Taking advantage of feedback loops, LHRH inhibitors can be both antagonistic and agonistic. LHRH antagonists like degarelix inhibit release of leutenizing hormone (LH) and follicle stimulating hormone (FSH) from the pituitary and consequently the production of testosterone from the testis. LHRH agonists like leuprolide function by tricking the LH negative feedback loop and after a temporary testosterone “flare”, the testis stop producing testosterone (17). AR LBD inhibitors like bicalutamide (18), flutamide (19) and nilutamide (20) were initially used to manage the testosterone flare. These molecules function as competitive inhibitors for testosterone and/or DHT in the LBD of AR in order to inhibit its activity. As the most potent/effective of the

three, bicalutamide was investigated in many different scenarios and doses in the clinic with limited success (21, 22). In the late 1990s combination of low dose bicalutamide (50mg/kg) and leuprolide became the mainstay 1st line treatment for most patients with advanced prostate cancer displaying better outcome than leuprolide alone (21).

These treatment modalities can also be used in conjunction with surgical therapies. Neoadjuvant hormone therapy (NHT) as a tool can reduce the tumor burden in an attempt to increase the ratio of organ confined disease prior to surgery (23). While no randomized study has shown improvement in outcomes with the standard 3-month NHT followed by surgery, it is suspected that this strategy could be beneficial to a subset of patients (24).

1.2.3. 2nd generation anti-androgens

Unfortunately, all patients develop resistance to anti-androgens and the progression to Castration Resistant Prostate Cancer (CRPC) is not a question of “if” but “when”. The diagnosis of CRPC occurs under the following scenario: progression of lesions and/or rise of serum PSA in consecutive tests while the patient is on ADT a minimum of 4 weeks and amount of serum testosterone is still within castration range. The average age of CRPC diagnosis is between 70-73 years and 10-20% of men progress to CRPC within 5 years of initial hormone therapy (25). Approximately 90% of CRPC patients exhibit enhanced AR activity and therefore, AR remains the cornerstone of targeted therapy in CRPC. In 2011 and 2012, two breakthrough trials, CUO-AA-301 (26) and AFFIRM (27) led to the approval of anti-androgens abiraterone (Zytga) and enzalutamide (Xtandi) respectively.

The initial approval of abiraterone was gained in patients already progressing on the chemotherapeutic docetaxel, and later the CUO-AA-302 trial (28) gained approval for abiraterone to be used in chemotherapy naïve CRPC. Mechanistically, abiraterone is a CYP17A1 inhibitor that cripples the conversion of pregnenolone to DHT precursor dehydroepiandrosterone, compromising the 5 α -dione pathway and therefore reducing the amount of DHT produced by CRPC patients (29). Abiraterone inhibits both isoforms of CYP17A1, the 17 α -hydroxylase and the 17,20-lyase (30). In 2014, Taplin et al. demonstrated in a phase II clinical trial that relative to ADT (luprolide), addition of abiraterone reduced DHT by an additional 85%, DHEA by 97-98%, and androstenedione (AD) by 77-78% (31). This research prompted the LATITUDE phase III clinical trial, which in 2017 demonstrated that co-administration of abiraterone and ADT in hormone naïve CRPC improved radiographic free survival by 33 months in comparison to 14.8 months in ADT alone patients (32).

Due to its structural similarity to pregnenolone, abiraterone is a substrate for another major steroidogenesis enzyme, 3 β -HSD. Between 2014 and 2016, in a series of elegant papers Sharifi and colleagues demonstrated how abiraterone is metabolized in patients and investigated the biological role of these metabolites (33-35). Their research demonstrated that 3 β -HSD metabolizes abiraterone into D4-abiraterone (D-4A), which displays anti-androgen activity comparable to enzalutamide. Unfortunately, this D4-A metabolite is transient and is converted to 3-keto-5 α -abiraterone by 5 α -reductase, resulting in an AR agonist. Building on this work, clinical investigation of 5 α -reductase inhibitor dutasteride is currently underway (36).

Almost parallel to the development of abiraterone, Dr. Charles Sawyers built upon the structure of anti-androgen bicalutamide and selected a more potent anti-androgen now called enzalutamide (ENZ). ENZ also competes with testosterone and DHT for the LBD pocket of the AR, and treatment with ENZ significantly reduces AR activity both in vitro and in vivo (37). Following a similar path to abiraterone's clinical development, the PREVAIL trial in 2013 led to the approval of ENZ in the pre-chemotherapy landscape (38). Currently, the ARCHES trial is evaluating the efficacy of ENZ in combination with ADT (Luprolide) in hormone therapy naïve CRPC (NCT02677896). It would be reasonable to expect similar results to the LATITUDE trial with abiraterone, cementing the use of these 2nd generation anti-androgens as first line therapy in combination with LHRH agonists/antagonists in CRPC.

1.3. AR driven mechanisms of resistance to hormone therapy

In cancer, whenever a targeted therapy is available for a specific cancer type, the major resistant mechanisms always develop around the original target (39). Similarly, in PCa continued AR signaling is observed in approximately 90% of patients after 1st generation anti-androgens and approximately 60% after treatment with the more powerful 2nd generation anti-androgens (40).

1.3.1. Resistance to 1st line hormone therapy

The AR+ mechanisms of resistance fall into the following categories:

- *AR Amplification and enhancer activation*

Although the number varies, AR amplification can be present in up to 60% of CRPC patients (41). This creates a hypersensitive cell that can continue to proliferate in a low androgen (testosterone) environment. Interestingly however, patients with AR amplifications

in CRPC have better outcomes than patients who do not; the AR amplification may allow the cells to remain differentiated and androgen driven (42). Therefore, it is logical to expect that these tumors retain their AR dependence and remain sensitive to further AR inhibition with more potent anti-androgens.

More recently, mutations in AR ubiquitination pathways have been identified that in essence would mimic genomic amplification and result in significantly higher protein levels of AR. Chief among them is the SPOP mutations which are present in approximately 11% of CRPC patients (43). Furthermore, expression of chaperone proteins that prevent AR degradation like HSP27 also create a scenario of “amplified” AR expression in CRPC (44).

Between June and July 2018, several key publications utilized next generation sequencing (NGS) technology to perform whole genome sequencing on PCa patients and discovered that ~80% of patients have duplications in chromosome X approximately 650k base pairs upstream of the AR. This region serves as an enhancer for the AR and this duplication drastically increases AR expression and promotes resistance to anti-androgens (45).

- *AR Variations and truncations*

Splice variants of AR are a more recent discovery (46). Theoretically, these variants of the AR that lack LBD are constitutively active. The functional importance of these variants is highly debated as they are always accompanied by increased AR expression (47). The predominantly expressed and studied variant in prostate cancer is AR-V7. This variant activates a set of canonical AR target genes but not surprisingly, V7 with its altered structure has a unique set of sequences it binds and activates (48, 49). An even more recent discovery is the genomically truncated versions of AR detected in a surprising amount of patients. These truncations have similar result to the splice variants as they create variants of AR that lack the LBD. However, these changes occur in the genome where the exons encoding the LBD are deleted (50). While their presence is detectable, the importance of splice variants and genomic truncations in promoting PCa progression remains a topic of intense debate.

- *AR mutations*

The first reported AR mutation was discovered in LNCaP cells, a missense mutation in residue 878 that changed a Threonine to and Alanine (T878A). This mutation increased promiscuity of the AR making agonists of progestins, oestrogens and anti-androgens like

Flutamide. Another characterized AR mutation is the L702H mutation. Interestingly, this mutation reduces AR's affinity to DHT, however, it increases binding to cortisol and cortisone by up to 300% (51). This allows these glucocorticoids to activate the AR under ADT conditions and promote growth of PCa. Furthermore, several other LBD mutations have been characterized in CRPC that promote either sensitivity or promiscuity of the AR (L702H, V716M, V731M, W742C, T878S, and H875Y) (52-54). In addition to LBD mutations, N-terminal mutations also occur during CRPC that alter protein-protein interactions of the AR resulting in increased stability and or nuclear localization, including E255K, W435L and many more that have not been functionally characterized (53, 55).

- *Outlaw pathways (Post-translational modifications)*

Historically, the outlaw pathways are signaling cascades that lead to re-activation of the AR through growth factors and/or receptor tyrosine kinase mediated mechanisms. These extrinsic and intrinsic mechanisms all result in varying post-translational modifications of the AR that enhances its function in CRPC. The table below refers to modifications of the AR that have their functional role characterized.

Table 1-2: List of Androgen Receptor post-translational modifications:

<u>Modification</u>	<u>Enzyme responsible</u>	<u>Functional role</u>
<u>Phosphorylation</u>		
S81 (56-58)	CDK1, CDK5, CDK9	Enhance chromatin binding, transcriptional activity and proliferation.
S213, S791 (59, 60)	AKT, PIM1	Promotes localizations and protein stability
T282, S293 (61)	AURKA	Enhances transcriptional activity.
S650 (62)	P38, JNK	Role in nuclear localization.
Y267, Y363 (63, 64)	ACK	Promotes ligand independent activity.
Y534 (65)	SRC	Promotes ligand independent activity.
S515 (66, 67)	CDK7, MAPK	Enhances transcriptional activity but can increase ubiquitination and degradation.
S578 (68, 69)	PKC, PAK6	Enhances transcriptional activity but can increase ubiquitination and degradation.
S308 (70)	CDK11 ^{P58}	Represses transcriptional activity.
S81, S94, S256, S308,	PP2A	Removes phosphorylations and reduces

S424 (71)		AR activity but also reduces ubiquitination and degradation.
S256, S650 (72)	PP1	Removes phosphorylations and reduces AR activity but also reduces ubiquitination and degradation.
<u>Methylation and Acetylation</u>		
K630, K632 (73)	Set9	Methylation - Enhances chromatin interaction.
K639, K632 (74)	p300	Acetylation – Enhances co-activator binding and promotes proliferation.
K618 (75)	ARD	Causes dissociation from HSP90 and promotes nuclear localization.
K639, K632 (76)	SIRT1	De-Acetylation – Inhibits co-activator recruitment.
<u>Ubiquitination</u>		
K845, K847 (77, 78)	MDM2, CHIP	Ubiquitination and proteasomal degradation

- *Altered Steroidogenesis*

Although circulating androgen levels remain low in patients treated with ADT, the intra-tumoral androgens remain very high in these patients at resistance. Several key publications demonstrated that the “backdoor” androgen synthesis pathway produces dihydrotestosterone (DHT) in the tumor (79). Specifically, androgen precursors from the adrenal gland like dehydroepiandrosterone (DHEA) are processed by the cancer cells into androstenedione (AD) by the enzyme 3 β HSD (**Fig. 1.4**) (80). AD is then converted to 5 α -AD or androstenediol by the enzyme 5 α -reductase 3 β HSD17 and 5 α -AD is directly converted to DHT by 3 β HSD17 creating the dominant steroidogenesis pathway in CRPC (80). Additionally, DHT has a 2-3 times higher affinity for the AR as well as a lower k_d and therefore, would activate AR at much lower concentrations (81). Therefore, even small increases in DHT synthesis combined with hypersensitive nature of the AR during CRPC can drastically increase proliferation of PCa cells (82).

Recently, several key mutations have been identified in the steroidogenesis pathway that has important implications for CRPC patients and what treatments they receive moving forward (83, 84). Specifically, point mutation in 3 β HSD (1245A>C) enhanced DHT synthesis

by stabilizing the enzyme and preventing its ubiquitination and subsequent proteasomal degradation (85).

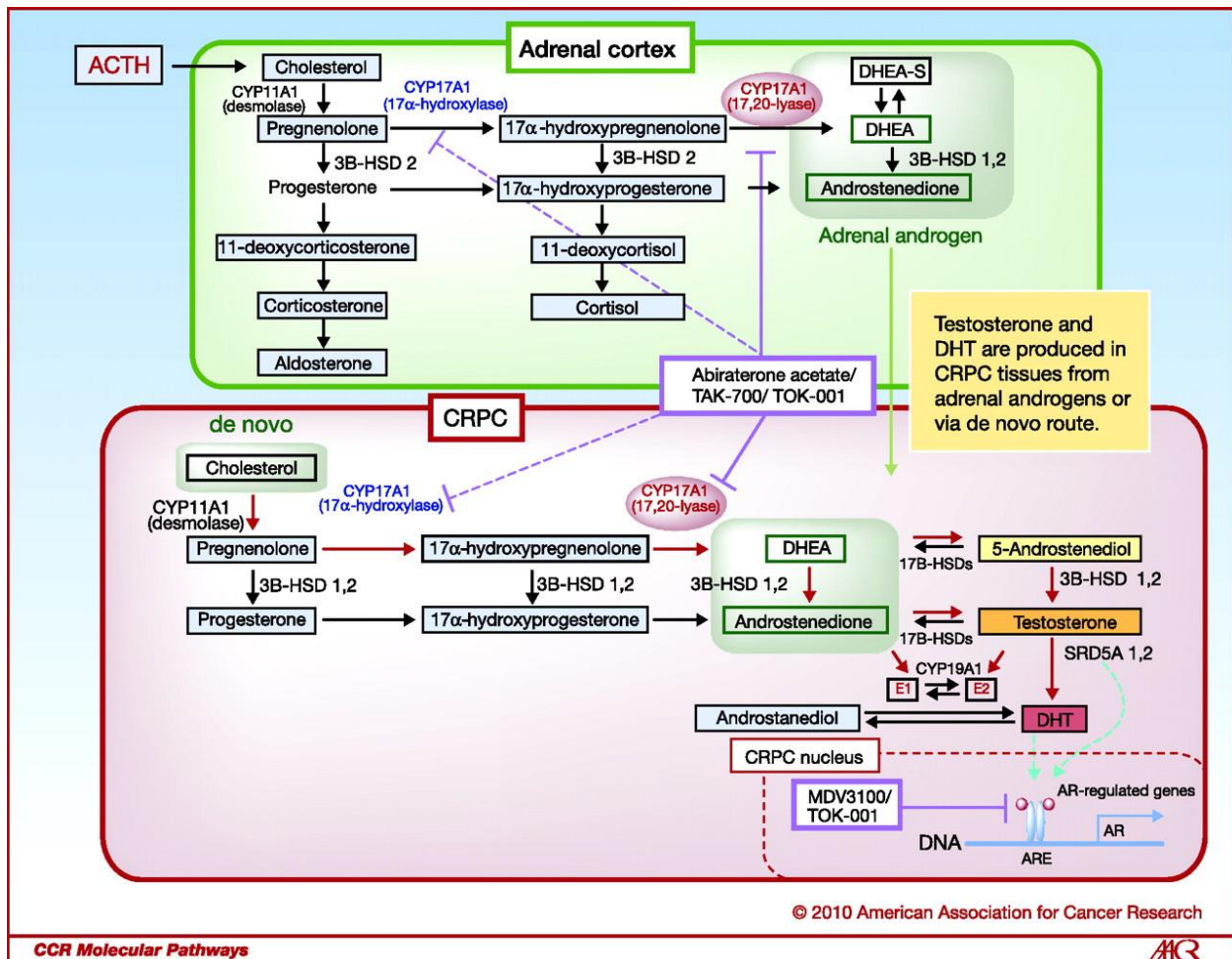


Figure 1.4 - Steroidogenesis pathways in Castration resistant prostate cancer:

Simplified androgen synthesis pathway and inhibitors. Extracted from Yamaoka et al. (2010) (Clinical Cancer Research) with permission from publisher AACR.

- *Co-activators and Co-repressors*

The steroid receptor coactivators (SRC) also known as the p160 family are the first identified co-activators of hormone receptor proteins. This family of proteins contains a protein interaction domain on the N-terminus and transcription activation domains at the C-terminus (86). Binding with the SRC proteins enables recruitment of GATA2, an important activator of AR signaling (87, 88). Combination of promiscuity mutations and binding with SRC co-activators likely enhance AR signaling in CRPC. Overall, over 150 different proteins interact with the AR either activating or inhibiting its activity. For example, interactions with the following proteins can differentially modulate AR cistrome and enhance its activity.

- Chromatin modifiers like EZH2 (89), LSD1 (90), p300 (91), BRD4 (92).
- Transcription factors and activators like NFκB (93), STAT3 (94) and β-catenin (95) are known to promote canonical AR signaling.
- Pioneer factors like FOXA1 (96), GATA2 (88) and HOXB13 (97).

Interestingly, loss of AR-corepressors occurs frequently in PCa. Although they can be accompanied by AR amplification, mutations in co-repressors like NCOR1/2 (~12%), and ZBTB12 (~10%) are expected to markedly increase AR activity during CRPC (41). These repressors function through interaction with the AR N-terminus domain (NTD) and the LBD (98).

1.3.2. Resistance to 2nd generation anti-androgens

A large majority of PCa patients that are resistant to 2nd generation anti-androgens enzalutamide and abiraterone still retain the potential to respond to further inhibition of the AR pathway. Similar to the AR positive mechanisms of resistance observed during CRPC, AR reactivation is observed in approximately 60-65% of patients resistant to enzalutamide and abiraterone (40). Histologically, these patients present with either adenocarcinoma or mixed phenotype and typically observe a rise in PSA as tumor burden increases CRPC (99). This has led to the clinical evaluation of many potential 3rd generation anti-androgens like Galeterone (100), Orteronel (101), VT646 (102), ODM-201 (103) and many more under pre-clinical development.

- *Mutations*

The most common genetic modification in these patients is copy number amplifications (CNA) of the AR, likely retained from exposure to 1st generation anti-androgens. This results in drastically increased expression of the AR and therefore increasing the sensitivity of the cancer cells to gonadal and non-gonadal androgens. Since the AR is the final target for both these therapies, it is no surprise that AR mutations are selected by these treatments, specifically in response to enzalutamide. Korpál et al. in 2013 showed that the F877L mutation confers resistance to enzalutamide as it becomes an agonist for AR activity (104). Utilizing cfDNA technology, Azad et al. detected H875Y mutations in the AR LBD of patients progressing on enzalutamide (105). A follow up study by Lallous et al. in 2015 functionally characterized this mutation as a partial agonist for enzalutamide. Interestingly, this study also demonstrated that the previously identified T878A mutation is also a partial agonist for

enzalutamide, and combination of F877L and T878A or H875Y mutations convert enzalutamide to a full agonist (54).

- *Splice Variants*

In addition to mutations, splice variants of the AR have long been implicated in resistance to anti-androgens. In 2014, Antonarakis et al. assembled the most convincing clinical evidence for the importance of AR-V7 in resistance to both enzalutamide and abiraterone (47). The inherent resistance to enzalutamide of PCa cell line 22RV1 that expresses a high amount of AR-V7 supports this premise (49). These data prompted great interest in development of AR N-terminus inhibitor EPI-001 (106) as well as the newly synthesized AR DBD inhibitor (107). Both inhibitors target domains of AR present in the FL and the V7 version. While convincing, the data implicating AR-V7 as a major form of resistance is somewhat controversial. For example, studies have shown that the presence of AR-V7 is coupled with increased AR-FL mRNA and overexpression of AR-V7 in LNCaP cells did not confer resistance to enzalutamide *in vitro* and *in vivo* (108). Thus, the authors hypothesized that the increased AR-V7 expression is a by-product of increased AR-FL mRNA (108, 109). Supporting evidence for this can be garnered from studies that show that AR-V7 and AR-FL have very different cisome binding regions and V7 may not regulate the same genes that FL does to drive AR+ PCa (110). The failure of AR inhibitor/degrader Galeterone in phase III that selected patients based on their AR-V7 expression is perhaps the most stark piece evidence against the importance of AR-V7 as a targetable mediator of resistance to anti-androgens (NCT02438007). While its importance as a driver of resistance is debatable, the utility of AR-V7 as a predictive biomarker of response to 2nd generation anti-androgens is almost undeniable as patients AR-V7+ patients receiving chemotherapy (Taxanes) have a better prognosis than AR-V7+ patients receiving anti-androgens (111, 112).

- *Truncations*

Apart from alternative splicing of mRNA to produce variants of the AR, recent studies have identified genomic truncations in the AR gene on the X chromosome that delete the region of the genome that codes for the LBD (50). Originally thought to be rare, recent studies have demonstrated these truncations to be more prevalent, but these truncations are subject to the same scrutiny as AR-V7 as they produce a similar product in the end. Interestingly, the presence of the truncated AR was the single most significant factor in predicting resistance to enzalutamide and abiraterone (113). A considerable amount of

research is currently underway with the goal of unmasking the role of AR-V7 as well as the truncated AR versions in enzalutamide and abiraterone resistance.

Lastly, section 1.2.3 mentions the shift of enzalutamide and abiraterone to first line therapy given in combination with LHRH agonist leuprolide. The drastic increase in patient survival in patients receiving abiraterone in combination with ADT (LATITUDE) is likely also occur in the ARCHES trial (enzalutamide + with ADT); moving them both to first line therapy in the future. Historically, CRPC referred to resistance to ADT; however, with this change in the treatment paradigm of PCa, in the future CRPC will also encompass resistance to enzalutamide and abiraterone.

1.4. Cell plasticity driven responses to hormone therapy

All somatic cells in the human body (apart from red blood cells and B-cells) contain all 3.23 billion base-pairs and therefore have equivalent potential. Under perfect conditions, it should theoretically be possible for a terminally differentiated cell to de-differentiate and then re-differentiate into a completely different cell type. The term cell plasticity attempts to define the process of cells re- and de-differentiating in a more succinct manner; focusing on the ability of the cells to “bend like plastic” into any shape the environment requires in order to survive (114). Analogously, once treatment begins, PCa cells find themselves in a cellular environment/state devoid of either androgens or AR activity and need to adapt in order to survive. Therefore, it is important to study their response to anti-androgen therapies in order to characterize any differentiation processes undertaken by the cancer cells for their continued survival.

1.4.1. Epithelial to Mesenchymal transition

One of the major differentiation phenomenon studied in cancer biology is epithelial mesenchymal transition (EMT). This process is the primary suspect for the mechanisms behind dissemination of cancer cells to distant metastatic sites, and one of the defining characteristics of CRPC is the presence of metastasis. Approximately 85% of CRPC patients have metastatic disease while only 4% of primary PCa patients present with metastasis (25). Additionally, approximately 1/3 patients who are diagnosed with CRPC without metastasis develop them within 2 years (25). Finally, metastatic disease is the cause of death in CRPC, therefore studying and understanding it is imperative in order to improve patient survival.

Since its characterization in 1995 (115), EMT has been closely linked to the metastatic process. EMT is loosely defined by a loss of epithelial markers and cell polarity and an augmented invasion and migration. As a key aspect of development, the EMT process endows cells with these enhanced migratory attributes that assist in formation of organs like gastrulation, neural crest formation and even heart development (116). Mechanistically, hallmarks of EMT consist of the loss of epithelial cell adhesion molecules like E-Cadherin (*CDH1*) and ZO-1 (*TJP1*) and a gain of EMT cytoskeletal proteins like Vimentin (*VIM*), N-Cadherin (*CDH2*) and Fibronectin (*FN1*) (117). Furthermore, an increase of matrix metalloproteases (MMP) also occurs during the transition in order to break down the extra-cellular matrix (ECM) and allow for migration of cells. These transformative cytoskeletal and ECM proteins as well as suppression of E-cadherin is controlled by 3 major families of transcription factors, TWIST, ZEB and SNAI families.

Several studies have demonstrated that AR pathway inhibition induces EMT (118, 119). In 2012, Sun et al. demonstrated that androgen deprivation triggered the E-cadherin to N-cadherin switch, suggesting EMT was occurring (119). The authors reported that during androgen deprivation, expression of Zeb1 (*ZEB1*) drove EMT. Furthermore, Kwok et al. showed that Twist1 was upregulated in androgen independent prostate cancer and downregulation of Twist increased E-cadherin expression and reduced cell migration and invasion (120). In 2012, Reiter and colleague conducted one of the more comprehensive studies looking at EMT biomarker N-Cadherin in CRPC. They found N-cad to be upregulated in both primary and metastatic CRPC, and inhibiting N-cadherin with an antibody suppresses EMT and reduces tumor growth and metastasis (121).

Interestingly, it appears as though EMT transcription factors may come into play immediately after castration but prior to resistance. Akamatsu et al. studied a patient derived xenograft (PDX) model's response to castration by sampling tumors overtime for RNA-seq. Their data demonstrated within the first few days after castration, transcription factor Snail (*SNAI1*) was upregulated and family member Slug (*SNAI2*) was downregulated. This is consistent with other study that demonstrated that Slug is an AR-regulated gene (122). Interestingly, Zeb2 (*ZEB2*) (123) and Slug (124) are established AR target genes that could potentially promote EMT processes during CRPC. Altogether, these studies suggest that transcription factors like Snail and Zeb1 promote EMT immediately after castration and during resistance when the AR recovers its activity, TFs like Slug and Zeb2 may continue to promote metastasis.

While it may not be direct, many signaling pathways culminate in regulation of either TWIST, ZEB or SNAI family proteins and promote EMT processes in CRPC. Downstream of

several growth factors like Epithelial Growth Factor (EGF) (125, 126) and Insulin Growth Factor (IGF) (127), kinases like AKT (*PKC*) and ERK (*MAPK*) can regulate the stability of Slug and Snail by inhibiting phosphodegradation activation by GSK3 β (128, 129). These post-translational modifications on the SNAI family are instrumental in regulating their activity as their half-life even in mesenchymal cells is approximately 4 hours (130). Many factors play into this stability, as even the sub-cellular localization of these proteins can limit their vicinity to cytoplasmic proteasome based degradation methods (131). Furthermore, phosphorylation by p21-activated kinase (PAK1) regulates the nuclear translocation and stability of the Snail (132).

Our lab has previously shown that non-receptor tyrosine kinase *LYN* is upregulated in CRPC (133). Research discussed in Chapter 3 of this thesis demonstrates how this increased expression of *LYN* regulates the sub-cellular localization and stability of both Snail and Slug, increases their expression and activity thus promoting metastasis (134). Furthermore, we demonstrate *LYN*'s upregulation and activation of this pathway active in both triple negative breast cancer (TNBC) and muscle invasive bladder cancer (MIBC), the most metastatic and lethal subtypes of their respective cancers.

1.4.2. Emerging clinical subtypes in PCa

Historically, during CRPC only 5-10% of patients presented with AR/PSA low disease, however, as the 2nd generation anti-androgens have become the “go to” treatment option for most patients, the emerging phenotypes of resistance have drastically changed the landscape of CRPC progression. Clinicians noted an increase in the percentage of patients progressing on enzalutamide or abiraterone without a concomitant rise in serum PSA. These patients generally present with an abnormal histology different from traditional adenocarcinoma. These pathologies included the lethal small cell/neuroendocrine prostate cancer (NEPC) observed in approximately 13-14% of patients and a newly characterized Intermediate Atypical Carcinoma (AIC) observed in a striking 28% of patients. The IAC subtype carries a worse prognosis in comparison to resistant patients with adenocarcinoma (99). Further investigation into this new subtype will be illuminating once the initial characterization is published and available for data mining. Relative to the new IAC subtype, NEPC is better characterized and understood. Aside from the unique small cell morphology and positive staining for neuroendocrine (NE) markers, namely chromogranin A (CHGA), neuron specific enolase (NSE), and synaptophysin (SYP), it is often distinguished from prostatic adenocarcinoma by reduced AR activity (135).

More recently, Bluemn et al. and reported that approximately 13% of patients develop NEPC post enzalutamide and abiraterone (40). This number was further corroborated from

Stand UP 2 Cancer data that showed that 17% of patients post enzalutamide and abiraterone develop NEPC (136). Interestingly, Bluemn et al. also stated that ~25% of patients had what they referred to as Double Negative Prostate Cancer (DNPC). In patients DNPC presented with abnormal histology, but the tumors were negative for AR/PSA as well as NEPC markers like CHGA and SYP (17). Transcription factors from the Inhibitor of Differentiation (ID) family were the major regulators of the DNPC phenotype downstream of fibroblast growth factor receptor (FGFR) signaling. It remains to be seen if there are any commonalities between the IAC subtype and the DNPC subtype and how they relate to the terminal NEPC stage.

1.4.3. Neuroendocrine Prostate Cancer

Poorly differentiated neuroendocrine tumors can arise from a variety of different mechanisms. In epithelial cancers genomic and epigenomic alterations can drive this phenotype as the cancer progresses, however, the acquisition of this phenotype as a response to targeted therapy in epithelial cancers has generated a renewed interest. Specifically, the mechanisms behind increased incidence of NEPC has become a major topic of research in PCa. In an effort to understand the biology of NEPC, the cell of origin for this form of PCa is a focus of intense debate as there are two competing hypothesis. The “lurker cell” hypothesis (51) states that the NEPC cells grow out from the sparse neuroendocrine (NE) cells population already present in the prostate. Until recently, this is a reasonable hypothesis as the prevalence of *de novo* NEPC is approximately 1% (137). Furthermore, the presence of tumor cells with NEPC characteristics within well-differentiated adenocarcinomas is well documented and can be interpreted to support this hypothesis (138, 139).

The other major theory in the field states that these tumors arise due to an unexpected yet powerful plasticity of PCa cells as an adaptive response to more potent therapies: enzalutamide and abiraterone. Combined with the detection of typical adenocarcinoma mutations like TMPRSS-ERG fusions and a general lack of gross genomic differences in terminal NEPC tumors, a model of divergent evolution from a common precursor PCa cell is conceivable (2). A similar sequence of events is also observed in lung cancer patients that acquire resistance to EGFR-targeted therapies detour through a plastic state that can lead to small cell lung cancer (SCLC) in 15-20% of patients (140). Recently, several major research papers have demonstrated the remarkable plasticity of PCa cells in response to therapy. This growing body of work favours the plasticity model through a variety of cell fate governing transcription factors (141-144), including BRN2 (POU3F2) which is discussed in chapter 3 and 4 of this thesis (145).

1.4.3.1. Pathology, Markers and history

The WHO has two classifications of “neuroendocrine” cancers. Well-differentiated NE tumors in the lung or gastroenteropancreatic tract are not very aggressive and mostly retain their respective organ’s architectural pattern. These characteristics are similar to normal neuroendocrine cells in the body and secrete neurosecretory proteins like serotonin and chromogranins. Conversely, poorly differentiated NE tumors have a high mitotic index and are characterized by sheets or clusters of small round cells that visually lack cytoplasm, contain a hyperchromatic nuclei that are often disfigured (146). The last known histological subtype is a large cell neuroendocrine, and as evident from the name they maintain their cytoplasm and contain prominent nucleoli.

For the purposes of accurate diagnosis, some NE biomarkers exist to differentiate between low grade and high-grade NE carcinomas. While somatostatin and serotonin can identify low-grade tumors, the utility of biomarkers for high-grade tumors is somewhat limited as they can be present in tumors that lack NE morphology and therefore are not recommended by the WHO as a defining characteristics. While these biomarkers like chromogranin-A (CHGA), synaptophysin (SYP), NCAM1 (CD56) cannot define the disease alone, their presence in an abnormal amount could be foretelling for resistance to targeted therapies (147, 148). Not surprisingly, the expression of these markers is significantly higher in NEPC when compared to CRPC-adenocarcinomas (149) and in combination with pathological data could provide both diagnostic assistance and possible treatment regimens.

1.4.3.2. Consistencies and differences between NEPC and SCLC

These poorly differentiated NE tumors can occur in the lung, prostate, bladder and breast. However, small cell lung cancer (SCLC) and small cell prostate cancer are the only two with significant research into them. There are few differences but considerable similarities between SCLC and NEPC. The mutational rate for SCLC is approximately 7.4 protein-changing mutations per 1 million base pairs, while it is only 1 protein-changing mutation per million base pairs for NEPC. The high mutational burden of SCLC is likely the reason behind the promising efficacy of immune checkpoint inhibitors observed in clinical trials (146). Although there are several clinical trials underway in NEPC with checkpoint inhibitors (NCT02601014, NCT0248935, NCT02787005, NCT02312557, NCT02861573), they will likely require accurate patient selection for mis-match repair (MMR) mutations that result in an increased mutational load for that patient.

Apart from this major difference, the similarities between SCLC and NEPC are substantial. For example, homozygous loss of function mutations or deletions in tumor suppressor genes p53 (TP53) and retinoblastoma 1 (Rb1) is global event across all SCLC patients (150). In NEPC, loss of p53 and Rb1 occurs in approximately 60-70% of patients (2). Furthermore, much of research conducted in NEPC today stems from previous SCLC studies, for example, several of the recent major drivers and targets identified in NEPC have been previously identified in SCLC; most notably nMYC (151, 152), SOX2 (153), EZH2 (154, 155) and SOX11 (156, 157).

1.4.3.3. Drivers and Targets in NEPC

The oldest and most studied model of NEPC comes from the GEM TRAMP mouse model where the SV40 large T-antigen is expressed in the prostate. The SV40 T-antigen inhibits both p53 and Rb1 and upon castration ~15% these mice progress to NEPC characterized by small cell phenotype and expression of NEPC markers like CHGA, SYP and CD56 (158, 159). More recently, a pair of studies explored the effect of prostate specific knockout of p53 and/or Rb1 (Single KO or Double KO). These mice spontaneously developed heterogeneous tumors in their prostate with loss of luminal characteristics (high AR and KRT8) and NE characteristics with high SYP and CHGA (160). Further analysis revealed that both the luminal and NE cancer cells arose from a single clone. Furthermore, the DKO mice were resistant to castration and interestingly, mice with SKO for Rb1 developed loss of function mutations in p53 post castration and progressed to NEPC. Similar to the findings in the TRAMP model, the authors discovered that with the loss of p53 and more specifically Rb1, the activity of Enhancer of Zeste homolog 2 (EZH2) was significantly increased; and inhibition of EZH2 restored sensitivity to AR pathway inhibition in these tumors as well as in cell lines derived from these tumors (160). Simultaneously, Mu et al. also reported plasticity in an *in vitro* LNCaP-AR model with knock-out of both Rb1 and p53 (141). Similar to the GEM model, these authors also noted that KO of these tumor suppressors render the cells resistant to AR pathway inhibition. This *in vitro* model displayed a switch from a luminal AR+ KRT8+ lineage to an AR- KRT5+ NE marker positive basal/NE lineage. The authors reported that sex-determining-region Y box 2 (SOX2) was the transcription factor driving this plasticity and conferred resistance to enzalutamide (141). Overall, the Rb1 and p53 knockout GEM model corroborated previous studies with the TRAMP model, further establishing the importance of p53 and more specifically Rb1 in NEPC.

In 2011, Beltran et al. characterized the first patient dataset of NEPC and identified CNA of Aurora Kinase A (AURKA) and its allosteric binding partner nMYC (135). The data showed

that inhibition with AURKA inhibitor Alisertib reduced tumor proliferation in human NEPC cell line NCI-H660 (135) by creating an unstable nMYC that is promptly degraded (161). In 2016, two major publications tested the transformative properties of nMYC from adenocarcinoma to NEPC, while artificially generated the models in these two papers demonstrated the potential of nMYC as a driver of NEPC. Lee et al. provided convincing evidence showing that nMYC over-expression paired with constitutively active myristoylated AKT converted benign prostate cells to castration resistant tumors with focal NEPC histology (142). Mechanistically, Dardenne et al. demonstrated that nMYC could cooperate with EZH2 in order to drive NEPC specific histone methylation patterns (143). These findings were complemented with patient data that clearly show that NEPC is an epigenetically driven disease with stark increases in expression of genes responsible for histone and DNA methylation (2, 162). On the bases of these studies, clinical trial was established to evaluate the efficacy of nMYC inhibition by targeting AURKA (NCT01799278) in NEPC. While unsuccessful overall, a few patients on the trial responded well to AURKA inhibition warranting further exploration with better patient selection.

1.5. Treatment options: Beyond the AR

1.5.1. Chemotherapies (Taxanes)

Until 2005, treatments for CRPC were palliative. Anti-androgens like bicalutamide provided a minimal survival benefit and was used to control the testosterone “flare” at the beginning of agonistic ADT. However, in 2005 with the completion of the SWOG 9976 (163) and TAX 327 (164) trials, treatment with docetaxel (Taxotere) chemotherapy showed a 3 month survival benefit in CRPC patients. Docetaxel is a well-studied chemotherapeutic agent that disrupts microtubule dynamics, preventing their depolymerisation during mitosis (165). This triggers mitotic catastrophe and results in apoptosis dependent cell death (166). While docetaxel did improve survival, resistance was once again inevitable. Several mechanisms of resistance were attributed to this phenomenon, primary among them was the increased expression of multi-drug resistance protein 1 (MDR1) (167). Additionally, cancer cells were also noted to switch to class III β -tubulin which had much lower binding affinity to Docetaxel (168). In 2007, a semi-synthetic 2nd generation taxane called cabazitaxel (Jevtana) boasted evasion of MDR1 and it was expected to be effective after resistance to docetaxel. In 2010, the TROPIC trial determined that cabazitaxel provided a survival advantage post-docetaxel when compared to the standard of care at that stage, mitoxantrone (169). Interestingly, cabazitaxel failed to demonstrate superiority to docetaxel in chemotherapy naïve CRPC patients at their maximum

clinically doses of 20-25 mg/m² for cabazitaxel and 75 mg/m² for docetaxel (170). In hindsight, this result isn't surprising as the two chemotherapies were equally potent pre-clinical models demonstrated and cabazitaxel only displayed an advantage in Docetaxel resistant models (171) and was equi-potent to docetaxel in chemotherapy naïve setting.

More recently, CHAARTED trial demonstrated a significant survival advantage when docetaxel was used in combination with ADT in hormone naïve metastatic prostate cancer patients (172). Since then, various combinations of taxanes are currently under investigation at different stages of PCa in an effort to find ideal combinations that improve patient survival.

1.5.2. Personalized Therapies (Immunotherapies and PARP inhibitors)

While taxanes and hormone therapy remain the cornerstones of PCa treatment, recent advances in personalized medicine (precise patient selection) have yielded several therapies that demonstrated success in CRPC.

Immunotherapy: The U.S. Food and Drug Administration for treatment (FDA) approved many different therapies of mCRPC between 2010 and 2012. The IMPACT trial in 2010 lead to the approval of Sipuleucel-T (Provenge), the first immunotherapy for minimally symptomatic mCRPC patients (173). Sipuleucel-T is a dendritic cell based vaccine against prostatic acid phosphatase (PAP) (174). While successful, due to the expensive nature of the treatment as well as the approval of other therapies in that timeframe, Sipuleucel-T is rarely used. Several other vaccine type immunotherapies are currently under development for CRPC. Recently, a PSA poxviral-vaccine based immunotherapy called PROSTVAC discontinued the PROSTPECT trial for patients with metastatic CRPC (NCT01322490) based on lack of efficacy in the interim analysis. Other candidates include DNA based vaccine INO-5150 and CD40 inducible dendritic cell vaccine BPX101.

In addition to vaccine-based immunotherapies, checkpoint blockade antibodies are an attractive therapeutic option in PCa. These antibodies function by disrupting the inhibitory interactions between T-cells and cancer cells. While many different proteins are responsible for this, the most studied proteins are, Cytotoxic T-lymphocyte associated protein 4 (CTLA4) and Programmed Death protein 1 (PD-1). With the approval of CTLA-4 antibody Ipilimumab (175) in 2010 followed by the approval of two anti PD-1 antibodies Nivolumab (176) and Pembrolizumab (177) in 2014 for metastatic melanoma, there has been an immense interest in elucidating the optimal clinical scenario where these therapies could benefit PCa patients. For example, pre/post chemotherapy, pre/post 2nd line hormone therapy or in combination with either of the two.

PARP Inhibitors: Building on the treatment strategy from ovarian cancer, in 2015 Mateo et al. investigated the efficacy of Poly-ADP-ribose polymerase 1 (PARP1) inhibitors (PARPi) in PCa (178). In response to DNA damage, PARP1 is activated and recruits proteins that direct DNA damage response (DDR) and activate base excision repair (BER) machinery (179). Inhibition of PARP1 compromises repair of both single-strand and double-strand DNA breaks at replication forks that are generally repaired by tumor suppressor proteins BRCA1 and BRCA2. Therefore, inhibition of PARP1 in tumors that have BRCA1/2 loss leads to accumulation of DNA break and massive cellular toxicity (179). Comprehensive analysis into the TOPARP trial revealed that 14 out of the 16 (total 50 on trial) patients that responded to PARPi harboured homozygous deletions or mutations in 1 or more DDR genes like BRCA1/2, ATM, CHEK2 etc. These results led to a “breakthrough therapy” designation from the FDA. With the recent advances in next generation sequencing, DNA from tumor biopsy and possibly cell-free DNA (cfDNA) will provide DDR gene status and guide patient selection for PARP inhibitors, thus birthing the first precision medicine platform for PCa.

The most striking advantage of both immunotherapies and PARP inhibitors is possibility of their use at any stage of PCa. In addition to CRPC, NEPC patients with BRCA1/2 mutation are expected to respond to PARP inhibitors (180). This sensitivity to PARP inhibitor has the potential to create a more fundamental sub-type within PCa that is independent of histology. Also depending on their clinical success, checkpoint inhibitors combined with optimal patient selection may also yield therapy regimens that provide benefit to patients regardless of AR status or histological sub-types.

1.6. Thesis Hypothesis and Objectives

Androgen receptor plays a central role in PCa progression and remains a crucial driver of resistance to anti-androgens. While it is essential to understand the processes that result in re-activation of the AR, increasing evidence suggests non-AR driven mechanisms of resistance may be more important than previously thought. The work presented in this thesis largely focuses on these AR independent mechanisms of resistance, namely the hijacking of cell plasticity mechanisms that alter PCa cell identity thus making them resistant to AR pathway inhibitors.

Chapter 3: Building upon the previous work done in the lab on the increased expression of *LYN* tyrosine kinase in metastatic CRPC as PCa tumors become resistant to 1st generation anti-androgens, we hypothesized that this increased *LYN* expression enhances the metastatic

capability of PCa cells. Our goal was to determine whether *LYN* expression can promote a transition from epithelial to mesenchymal phenotype and delineate the molecular mechanisms behind this process.

Chapter 4: As the treatment landscape of PCa shifted to use of 2nd generation anti-androgens, the prevalence of NEPC increased and we also hypothesized that AR-pathway suppression may trigger NE-differentiation as a mechanism of resistance. Utilizing a model of resistance to enzalutamide that captures this NE-differentiation our objective was to identify, understand and target molecular mechanisms behind this process.

Chapter 5: Results in Chapter 4 implicate neuronal transcription factor BRN2 in NE-differentiation and demonstrate its role in growth and survival of NEPC. Therefore, we hypothesized that targeting BRN2 with small molecule inhibitors may provide an effective strategy to help treat NEPC. The objective for this chapter was to design and implement effective selection criteria for BRN2 inhibitors and utilize these molecules as tool compounds to gain further insight into BRN2's role in maintenance of NEPC phenotype and survival.

2. Chapter 2: Materials and Methods

2.1. Generation of ENZ-resistant xenografts and cell lines:

Chapter 4 and 5: Detailed procedure for generation of CRPC and ENZ^R tumors and cell lines is found in our previously published report (181). In summary, 1×10^6 LNCaP cells in matrigel were injected subcutaneously into flanks of 6-8 week old athymic male nude mice (LNCaP SQ) and body weight, tumor growth and serum PSA was measured weekly. Once serum PSA reached 50-75 ng/ml, mice were surgically castrated (Cx). Upon recurrence of PSA to pre-castration levels, mice were randomized into 2 treatment groups and received either vehicle control or 10 mg/kg ENZ daily by oral gavage (Tx). Body weight, tumor growth and serum PSA was monitored weekly until vehicle control treated CRPC, or tumors that recurred in the 10 mg/kg ENZ treatment group (1^o ENZ^R) grew to the experimental endpoint. Select primary ENZR (1^o ENZ^R) tumors were excised at the experimental endpoint and tumor sections were allografted subcutaneously into bilateral flanks of castrated 8-10 week old athymic nude mice, which were dosed daily with 10 mg/kg ENZ from day of tumor transplant and mice were monitored for growth of transplanted tumors, body weight and serum PSA (ENZ^RT1). Serial transplant of select ENZ^RT1 tumors was repeated for a second and third time (ENZ^RT2 and ENZ^RT3) as above into castrated mice dosed daily with 10 mg/kg ENZ. In total, 35 ENZ^R tumors were generated over 3 serial transplant generations from 4 out of 10 primary PSA⁺ ENZ^R tumors. Cell lines were generated from primary CRPC as well as primary and T1-3 transplanted ENZ^R tumors. Specific cell lines used in chapter 2 and 3 are derived from CRPC, primary ENZ^R (1^o ENZ^R) and transplanted ENZ^R (ENZ^RT1-3) tumors are listed as “tumor derived cell lines” in Figure 4.1.

2.2. Human PCa specimens for RNA-Seq and immunohistochemistry (IHC):

Chapter 4 and 5: RNA-seq was performed on samples from Weill Cornell College of Medicine: Beltran 2016 (phs000909.v.p1 – cBioportal) (2)= 68 adenocarcinoma, 34 CRPC-Adeno and 15 CRPC-NE; Beltran 2011 (phs000310 .v.p1 – cBioportal) =30 Adeno and 7 NEPC (1). Tumors were classified by the following criteria based on histomorphology (1, 2): Adeno = usual prostate adenocarcinoma without neuroendocrine differentiation (from radical prostatectomy), CRPC = tumor obtained from CRPC adenocarcinoma metastasis without neuroendocrine differentiation and NEPC = either of the following categories, adenocarcinoma with > 20%, neuroendocrine differentiation, small cell carcinoma, large cell neuroendocrine

carcinoma, or mixed small cell carcinoma – adenocarcinoma. For IHC, prostate cancer specimens were obtained from the Vancouver Prostate Centre Tissue Bank and were classified as above (Adeno n=93, CRPC n=30, NEPC n=11). Tissue microarrays of duplicate 1 mm cores were constructed manually (Beecher Instruments). Samples were from radical prostatectomy or transurethral resection of prostate. Immunohistochemical staining was conducted as previously described (182) using the Ventana DiscoverXT Autostainer (Ventana Medical System) with enzyme labeled biotin streptavidin system and a solvent-resistant DAB Map kit by using 1/150 concentration of BRN2 and (Abcam) and 1/25 concentrations of CGA and AR (Sigma) antibodies. Specimens were graded from 0 to +3 intensity by visual scoring, representing negative-heavy staining. Automated quantitative image analysis was conducted using pro-plusimage software. Scoring was conducted at 200x magnification.

2.3. Cell culture

Chapter 3: Unless noted otherwise cells were maintained in complete media: RPMI-1640 (Hyclone) + 10% FBS for LNCaP, BT549, T47D, +Insulin (1 µg/ml) for BT549, DMEM (Hyclone) + 10% FBS for UC-13 and UC-13luc cells, Keratinocyte Serum Free Medium (Gibco) with BPE and EGF for RWPE-2.

Chapter 4 and 5: PC-3, NCIH660 and LAPC-4 cells were obtained from the ATCC in 2013. LNCaP cells were kindly provided by Dr. Leland W. K. Chung (Emory University) and authenticated in January 2013. CRPC and ENZ^R cell lines were generated from LNCaP cells (181), tested and authenticated by whole-genome and whole-transcriptome sequencing (Illumina Genome Analyzer IIx, 2012). Cells were maintained in RPMI-1640 (LNCaP derived and PC3) or IMDM (LAPC4), containing 10% FBS, 100 U/mL penicillin-G, 100 mg/mL streptomycin (all Hyclone), +/-10 µM ENZ (Haoyuan Chemexpress) or DMSO (Sigma-Aldrich) vehicle (for ENZ^R vs. CRPC, PC-3 did not receive ENZ). Where indicated, CRPC or LAPC-4 cells induced to a NE phenotype were cultured in RPMI-1640, 10% FBS, 100 U/mL penicillin-G, 100 mg/mL streptomycin, +10 µM ENZ for 7 days prior to downstream analysis.

2.4. Cell line transfections and treatments

siRNA - Seeded cells were transfected with 10 nM of siLYN (*Santa Cruz Bio* - sc29393 and sc156047), 10 nM of siPAK1 (*Santa Cruz Bio* – sc29700) with Oligofectamine (*Invitrogen* - 12252-011) in OPTI-MEM (*Gibco*) media using manufacturer's protocol. shRNA – shLYN plasmid (*Santa Cruz Bio* - sc29393SH) 6 µg was transfected with X-tremeGENE 9 (*Sigma* –

6365779001) using manufacturer's protocol. Plasmid – LYN wild-type, constitutively active, kinase dead and empty vector plasmids were generously provided by Dr Yamaguchi (Department of Molecular Cell Biology, Chiba University, Chiba, Japan). 6 µg was transfected using TransIT-2020 (Mirus - MIR #5400). Selleckchem - Bafetinib (S1369). Millipore - MG132 (#474791), Cycloheximide (#239765).

Chapter 4 and 5: CRPC or ENZR cells were seeded at a density of 10^6 cells/ 10 ml complete media in 10 cm tissue culture dishes (Corning Life Sciences) 18-24 hours prior to transfection with siRNA, sh-RNA, plasmid overexpression or DNA aptamer. siRNA- Cells were transfected with 10 nM BRN2#1 or control siRNA (Santa Cruz Biotechnology), 10 nM of BRN2#2 and siSOX2 (Thermo) using Oligofectamine 3000 (Invitrogen) and OPTI-MEM media (Gibco). After 18 hours, cells were re-transfected. After 4 hours, OPTI-MEM media was replaced with complete media and cells were harvested after 48 hours. shRNA- The same protocol as siRNA was used for sh-BRN2 transfections using sh-BRN2 or control sh-RNA (Santa Cruz Biotechnology) and successfully transfected clones were selected and expanded in complete media containing 10 µg/ml Puromycin.

Overexpression- 1 µg SOX2 plasmid (Addgene, #16353) or 8 µg BRN2 plasmid (Addgene #19711) were transfected using Mirus T20/20 and OPTI-MEM media (Invitrogen) according to manufacturer's instructions. After 18-24 hours, OPTI-MEM media was replaced with complete media +/- 10 µM ENZ and cells were harvested after 7 days or at indicated time points. For 7 day experiments, CRPC cells were re-transfected on day 4. siRNA/overexpression- Cells were plasmid transfected with Mirus T20/20 on day 1 and the following day transfected with siRNA with Oligofectamine 3000. After 18-24 hours cells were re-transfected with siRNA and OPTI-MEM was replaced with complete media +/- 10 µM ENZ and harvested 48 hours later (total 5 days).

BRN2 Aptamer- Indicated doses of BRN2-ARE aptamer were transfected into cells using Oligofectamine 3000. After 18 hours cells were transfected for a second time for 4 hours. This was repeated on day 4 and cells were either in OPTI-MEM or in complete media + 10 µM ENZ. 42D^{ENZ} cells were transfected with the aptamer and after 18 hours transfected a 2nd time. Following this they were exposed to R1881 for 48 hours and samples were harvested.

Generation of BRN2 CRISPR Knockout cells- Cells were transfected with 500 ng GeneArt Platinum Cas9 nuclease (Thermo) and 125 ng gRNA using Lipofectamine CRISPRMAX (Thermo). The targeting gRNA sequence 5'-GCTGTAGTGGTTAGACGCTG-3' was used to edit

exon 1 of the POU3F2 locus. At 72 hours post-transfection, cells were harvested for analysis of genome modification efficiency using the GeneArt Genomic Cleavage Detection Kit (Thermo) with the forward primer 5'-AAATCAAAGGGCGCGGCC-3' and reverse primer 5'-GCCGCCGCCGTGGGACAG-3'. Sanger sequencing assessed ten individual clones for indels at the POU3F2 locus.

Generation of doxycycline inducible eSpCas9 stable cell lines: Doxycycline inducible eSpCas9 in a piggybac vector (Vectorbuilder). pHypbase vector containing the piggybac transposase was provided by the Sanger Institute. 4 µg of pPb_eSpCas9 and 4 µg of pHypbase were transfected into 42D^{ENZ}R cells using Mirus T20/20 overnight. Cells were allowed to grow RPMI +FBS media for 2 days prior to Puromycin selection at 1 µg/mL concentration for 1 week.

BRN2 gRNA transfection: gRNA purified from GeneArt kit was transfected into 42D^{ENZ}R cells stably expressing doxycycline inducible eSpCas9. During and post transfection, 100 nM of doxycycline was present in the media. Cells were harvested 4 days later for analysis by WB.

2.5. Proliferation, invasion and migration assays

Chapter 3: Migration Assay: Transfected cells were trypsinized and plated in 6 well plates at 250,000 cells per well. At approximately 100% confluence, cells were exposed to 10 µg/ml Mitomycin (*Sigma*) for 2 hours prior to scratch to arrest proliferation and isolate migration as the only source of wound closure. Images were taken at indicated time points using Axioplan II microscope (*Zeiss*).

Invasion Assay: Transfected cells were trypsinized and 25,000 cells were run through BioCoat Matrigel coated Transwell inserts with 8 µm pore size (*BD Biosciences*) as per manufacturer's protocol.

Chapter 4: Proliferation Assay: WST-1 (Promega) or Crystal Violet staining was used to assess cell growth according to the manufacturer's protocol. 1,000 cells were seeded in 96 well plates in complete media and absorbance at 450 nm for WST1 and 590 nm for crystal violet was measured after 72 hours.

Migration Assay: Cell migration was assessed in a wound-healing assay. Cells were plated on Essen ImageLock 96-well plates (Essen Instruments), incubated for 2 hours with mitomycin (10 µg/ml) prior to wound scratching with a wound maker (Essen Instruments) 24 hours after plating. Wound confluence was monitored with Incucyte Zoom Live-Cell Imaging System and

software (Essen Instruments). Wound closure was measured every six hours for 24 hours by comparing the mean relative wound density of three replicates.

Invasion Assay: Invasion was assessed by the invasion of 2.5×10^4 cells through BioCoat Matrigel-coated Transwell inserts with 8 μ m pore size (BD Biosciences). After 24 h, the Transwell insert was removed and fixed for 10 min in 100% methanol (Sigma-Aldrich) at -20° C and mounted on glass cover slips with Vectashield Mounting Media with DAPI (Vector Laboratories). Filters were imaged using Zeiss Axioplan II microscope (Zeiss) and cells invaded in membrane were quantified.

Chapter 5: Proliferation Assay: Cells were seeded in 96 well plates (7000 per well for 42D^{ENZ}R and 5000 per well for 16D^{CRPC} cells) in RPMI media with 10% FBS, treated for 72 hours. Fixed in 1% Glutaraldehyde and stained with Crystal Violet. Sorenson solution dissolved the Crystal Violet and plates were read at 590 nm.

2.6. Gene expression profiling

Chapter 4 and 5: RNA-seq- Specimens were prepared for RNA sequencing (RNA-seq) using TruSeq RNA Library Preparation Kit v2 and transcriptome sequencing was performed using Illumina HiSeq 2000 (Illumina Inc.) or HiSeq 2500 (human tumors) according to standard protocols. Sequence data mapping and processing was performed as previously described (183), except normalization was performed using reads per million. Quantification of gene expression was performed via RSEQtools using GENCODE v19 as reference gene annotation set. Expression levels (RPKM) were estimated by counting all nucleotides mapped to the gene and normalized by the total number of mapped nucleotides (per million) and the gene length (per kilobase). Sequencing of the AR ligand binding domain was performed exactly as previously described (105). To assess global differences in gene expression in microarray and RNA sequencing data, multidimensional scaling to analyse differences between cell line gene expression data was performed using the Principal Coordinate Analysis (PCoA) tool in XLSTAT software (Addinsoft®).

Micro-array- Differential expression profiling was performed on 16D^{CRPC}, 42F^{ENZ}R and 16D^{CRPC} cells with BRN2 over-expression. Total RNA was extracted using TRIzol® and the RNA quality was measured using Agilent 2100 bioanalyzer (Agilent, Santa Clara, CA). Samples were prepared following Agilent's One-Color Microarray-Based Gene Expression Analysis Low Input Quick Amp Labeling v6.0. An input of 100 ng of total RNA was used to generate Cyanine-3 labeled cRNA. Samples were then hybridized on Agilent SurePrint G3 Human GE 8x60K

Microarray (AMDID 028004) and arrays were scanned with the Agilent DNA Microarray Scanner at a 3 μ m scan resolution. Data was processed with Agilent Feature Extraction 11.0.1.1. and processed signal was quantile normalized with Agilent GeneSpring 12.0.

RNA quality control as well as gene profiling was done in the Laboratory for Advanced Genome Analysis at Vancouver Prostate Centre, Vancouver, British Columbia, Canada.

2.7. Western blotting (WB)

Chapter 3, 4 and 5: RIPA lysis buffer (Thermo Fisher) was mixed with protease and phosphatase inhibitors and was used to lyse total proteins as previously described (44).

2.8. Subcellular fractionation

Chapter 3 and 5: Cytoplasmic, membrane, nuclear and chromatin fractions were isolated using the Subcellular Protein Fractionation Kit for Cultured Cells (Thermo Fisher) using manufacturer's instructions.

2.9. Immunoprecipitation

Chapter 3 and 4: Immunoprecipitation (IP) was performed using ImmunoCruz™ IP/WB Optima B System (Santa Cruz) based on the manufacturer's guideline. 2 μ g of primary antibody, or immunoglobulin G (IgG) was used for immunoprecipitation and control respectively. Blots were incubated overnight at 4° C with designated primary antibodies at 1:1000 dilution, unless noted otherwise. Proteins were visualized using the Odyssey system (Li-Cor Biosciences) and densitometric analysis was performed using ImageJ software (National Institutes of Health, USA).

2.10. Reagents and antibodies

Chapter 3: Primary antibodies were used at 1/1000 dilution: Cell Signaling - LYN (#2796), Slug (#9585), Snail (#3879), E-cadherin (#3195), VAV1 (#4657), PAK1 (#2602). BD Biosciences – Fibronectin (610077), E-cadherin (610181). Abcam – pLYNY396 (ab40660), pVAV1Y174 (ab76225), ZO-1 (ab59720). Millipore – pPAK1S204 (#09-257), RAC1 (#05-389). Santa Cruz Bio – Vimentin (sc5565), LYN (sc7274).

Chapter 4 and 5: Primary Antibodies were used at 1/1000 dilution: Cell Signaling – BRN2, AR, PSA. Dako – ENO2. Santa Cruz – SYP, CHGA. Millipore – SOX2. Active Motif – EZH2, BD Biosciences – ASCL1

Secondary antibodies (Licor) were used at 1/5000 dilution

2.11. Immunofluorescence

Chapter 3: Transfected cells were plated at 50,000 cells per well in 12 well plates with cover slips, 24 h later cells were fixed with 4% paraformaldehyde and permeablized with 100% cold methanol. Cells were blocked with 3% BSA and Slug, Snail, E-cadherin, ZO-1 and LYN antibodies were used at 1/50 dilution. Secondary antibodies Alexaflour 488 (green) and 594 (red) were used at 1/500 dilution. Cells were mounted using Vectashield Mounting Media with DAPI (Vector Labs). Images were taken using the 780 LSM Confocal Microscope (Zeiss).

2.12. Quantitative real time PCR (qRT-PCR)

Chapter 3, 4 and 5: RNA was extracted from cells using TRIzol reagent (*Life Technology*). cDNA was created using reverse transcriptase MMLV and random hexamers (*Invitrogen*) from 2 µg mRNA. Real-time PCR amplification of cDNA was performed using SybrGreen ROX Master Mix (Roche Applied Science). Gene expression was normalized to GAPDH and β-Actin levels with 3 experimental replicates.

2.13. Luciferase assay

Chapter 4: CRPC and ENZ-resistant cells were plated in six-well plates (2×10^4 cells / cm²) and transfected with a BRN2 luciferase reporter (courtesy of Dr. Goding, Ludwig Institute for Cancer Research, Oxford, UK) (184) or Renilla (Promega) using T20/20 (Mirus). At 24 h post-transfection, cells were incubated with or without 10 nM R1881 for 24 hours and luciferase activities were measured using a Dual-Luciferase Reporter Assay System (Promega) and a Tecan Infinite® 200 PRO microplate luminometer (Tecan). BRN2 luciferase activities were corrected by the corresponding Renilla luciferase activities.

Chapter 5: BRN2 luciferase reporter cassette was cloned into piggybac backbone vector and stable 42D^{ENZ^R} BRN2-luc cells were created by co-transfection of BRN2-luc with pHypbase plasmid (Sanger Institute) followed by selection with 20 µg/mL of Blasticidin. 42D^{ENZ^R} BRN2-luc cells were plated in 24 well plates at 100,000 cells per well. The following day the cells were treated with 10 µM of different BRN2 inhibitors. 24 hours and luciferase activities were measured using a Dual-Luciferase Reporter Assay System (Promega) and a Tecan Infinite® 200 PRO microplate luminometer (Tecan). The reduction of luciferase activity was validated by WB for luciferase protein in the positive hits.

2.14. Chromatin immunoprecipitation (ChIP)

Chapter 4: Cells treated with or without 1 nM R1881 for 24 hours were cross-linked with paraformaldehyde (Sigma-Aldrich) and sonicated (Covaris sonicator) to shear DNA. ChIP assay was performed using ChIP Assay Kit (Magnetic Agarose Beads) according to the manufacturer's protocol (Millipore) and antibodies against AR (N20; Santa Cruz), SOX2 (Millipore) and BRN2 (Cell Signaling). Negative control primers were designed for the regions approximately 1600 bp upstream and 1800 bp downstream of the ARE 8733bp upstream of BRN2 TSS using Primer Express 3 (Thermo Fisher). Negative control regions were selected to be far enough away from the target site based on the fragment lengths upto 1000 bp during sonication of genomic DNA.

Sequential Chromatin Immunoprecipitation (Re-ChIP)- Assay was performed via Re-ChIP-IT® kit (Active Motif Inc., Japan), based on the manufacturer's protocol using antibody against BRN2 (Cell Signaling) and SOX2 (Millipore). IgG was used as negative control for antibodies and negative control primers for each binding site were designed as listed in Supplemental Experimental Procedures. Using Primer Express 3 (Thermo Fisher), primers were designed around BRN2/SOX2 consensus binding elements approximately 7500 bp upstream of NES start codon and 35000 bp downstream of RFX4 start codon. Negative control primers were approximately 5400 bp upstream of NES start codon and 38000 bp downstream of RFX4 start codon. Negative control regions were selected to be far enough away from the target site based on the fragment lengths upto 1000 bp during sonication of genomic DNA and also have a lack of OCT binding motifs.

Chapter 5: 42D^{ENZR} cells were treated with 20 µM of BRN2i for 9 hours prior to fixing and lysis. Cells were sonicated using Covaris sonicator at high setting for 3 minutes. ChIP was conducted using Millipore MagnaChip kit as per manufacturer's instruction. BRN2 (Cell signaling) antibody was used at 1:100 dilution on 100 µL of lysate. qRT-PCR was used to analyze data as % input. Primers were designed for intron 1 of PEG10 and downstream enhancer region of SOX2.

2.15. Animal studies

Chapter 3: Ultra-sound guided orthotopic injection delivered UC13-luc shCtrl and shLYN cells as previously described (185). Mice were euthanized at ≤15% weight loss after a luciferin injection of 150 mg/kg D-luciferin (Caliper Life Sciences). IVIS200 Imaging System (Caliper Life Sciences) was used to take image of metastasis after cystectomy. Metastatic spread was visualized based on bioluminescence. Tumors with bioluminescence ≥105 photons and were

excised and counted. All animal procedures were conducted according to the guidelines of the Canadian Council on Animal Care.

Zebrafish Embryo: BT549 cells with or without siRNA *LYN* were stained with Vybrant CM-Dil (Invitrogen) as per manufacturer's protocol. Cells were grown to confluence and trypsinized with EDTA. Cells were then washed with RPMI 1640 (Gibco). Cells were washed once in PBS, and suspended in RPMI for injection into embryos. Casper Fish™⁶⁴ embryos were raised in E3 media at 28.5° C until 48 h post-fertilization; prior to injection, embryos were dechorionated and anesthetized in 200 µg/mL tricaine (Ethyl 3-aminobenzoate methanesulfonate salt, Sigma, A5040), and then placed in 10 cm petri dish coated with 1.5% agarose, in addition to a few drops of 6% Ficoll PM (Sigma, F4375) containing 200 µg/mL tricaine for better healing after injection. A microinjector (INJECT+MATIC) was used to load the cell suspension into a pulled capillary needle for embryo injection. Approximately 100-150 BT549 cells were injected into the yolk sac of each embryo. Following injection, embryos were kept at 35°C for the duration of the experiments. Around 15-20 fish were anesthetized and visualized using Axioplan II microscope (Zeiss) at 24 and 48 h time intervals. Visible and individual dots outside the yolk sac were counted per fish.

Chapter 4: 42^{FENZ^R} sh-BRN2 and sh-CTR ENZ^R cells were injected into castrated male athymic mice (Harlan Sprague-Dawley) under pressure of daily oral 10 mg/kg ENZ. Tumors were monitored for growth and blood was drawn for PSA screening weekly as previously described (181). When tumors reached 1000 mm³ or greater than 10% animal body weight, tumors were harvested and processed for RNA analysis by qRT-PCR. All animal procedures were conducted according to the guidelines of the Canadian Council on Animal Care.

Chapter 5: Three male Nu/Nu mice (body weight 25-30 g) were purchased and caged individually at the day of experiment. Each mouse was given IP dose (10 mg/kg) of drug formulation in a volume of approximately 100 µl. Blood was collected by tail vein bleed (~70 µl per time point per mouse) in different indicated time. Blood samples were centrifuged at 10000 rpm, at 4° C for 5min. The serum sample are subjected to LC-MS/MS analysis to get the concentration of BRN2 inhibitor (Cpd. 18-51) in the blood in ng/mL concentration.

2.16. Zymography

Chapter 3: **Zymography:** After serum starvation, cells were incubated in fresh serum free RPMI with for 24h prior to and media was collected and concentrated using Amicon centricon-10 concentrators (EMD Millipore, Billerica, MA). Samples were resolved on 10% non-denaturing

polyacrylamide gel containing 1 mg/ml of porcine gelatin (Bio-Rad). Staining, de-staining and imaging was done as previously described (125).

2.17. In vitro kinase assay

Chapter 4: *In vitro Kinase Assay*- Recombinant protein kinase PAK1 [10-50 nM] employed in the substrate profiling process was cloned, expressed and purified using proprietary methods at *Kinexus*. The SNAI2 peptides [S251], [S251A], [S247A/S251A/S254A] were synthesized at *Kinexus* and the [γ -³³P]-ATP was purchased from *PerkinElmer*. The assay was conducted using *Kinexus*' proprietary protocol.

2.18. RAC1 Activity assay

Chapter 3: *Millipore* (#17-283) performed according to manufacturer's instructions. In short, cells were lysed and immunoprecipitation was done using magnetic beads fused with p21 binding domain of PAK1 to pull out active levels of RAC1. The precipitate was then run on SDS page gel for western blot analysis.

2.19. Drug Affinity Responsive Target Stability (DARTS)

Chapter 5: Cells were lysed in NP40 lysis buffer (1% NP-40, 150mM Sodium Chloride, 50mM Tris-HCL @ pH 8.0) containing protease and phosphatase inhibitors (Roche). 600 μ L of lysis supernatant at a concentration ranging from 4-6 μ g/ μ L is split into two 300 μ L tubes. Tube 1 is incubated with DMSO while the 2nd tube is incubated in 10 μ M concentration of small molecule for 1 hour. Pronase diluted in 1xTNC buffer (10x TNC = 500 μ L 1 M Tris-HCl pH 8.0, 100 μ L 5 M sodium chloride, and 100 μ L 1 M calcium chloride with 300 μ L ultrapure water) (186) to 1:100 and serially diluted further to 1:1000, 1:5000 etc. concentrations is added into separate tubes. Following this, 30 μ L of cell lysate from DMSO and small molecule tubes are added into each Pronase dilution for 30 minutes. Samples are boiled and analysed by WB.

2.20. BioLayer Interferometry

Chapter 5: Avidin-tagged DNA-binding domain of BRN2 was biotinylated by biotin ligase produced by pBirACm transformed BL21 cells. Bacteria were grown overnight in culture, and diluted to 0.1 OD the next morning in media containing biocytin. At OD of 0.6, cells were stimulated with 250 nM of IPTG for 3 hours and collected. BRN2 was purified with Ni-nTA beads using buffers and conditions previously described (187). Purified and biotinylated BRN2-DBD was bound to super-streptavidin sensors in assay buffer (188). Compounds were diluted 2-fold down from 50 μ M to 1.3 μ M. Data was quantified using OctetRED (ForteBio) apparatus.

2.21. Microsomal Stability

Chapter 5: Conducted by Sai Life Sciences using their proprietary protocol.

2.22. Analysis of publically available databases

Two publically available databases were used in this study:

CBioportal for Cancer Genomics- This website allows the researcher to visualize, download and analyze large-scale cancer studies such as The Cancer Genome Atlas (TCGA) studies for different cancers (189). TCGA provisional studies (2015) for prostate adenocarcinoma, invasive Breast Cancer and Bladder. Other data sets include

The UCSC Xena Genome Browser (<http://genome.ucsc.edu/>)- This website is developed and maintained at the University of California Santa Cruz (UCSC) not only makes large-scale studies available for further analysis but also allows the researcher to visualize and analyze his/her data in the context of larger datasets (190). Xena software was used to visualize the clinical correlation between mRNA expression of *LYN* and following EMT genes, Vimentin (VIM), N-Cadherin (CDH2) and Fibronectin (FN1).

2.23. Statistical analyses

Data are representatives of three independent experiments and are expressed as mean \pm standard error of the mean (SEM). P-values were calculated using Student *t*-test to compare control and treated groups and p-values less than 0.05 were considered statistically significant (* $P < 0.05$; ** $P < 0.001$; *** $P < 0.001$).

3. Chapter 3: *Targeting LYN regulates Snail family shuttling and inhibits metastasis*

3.1. Background

3.1.1. Src Family Kinase – *LYN*

Since its discovery in 1979, research into the “proto-oncogene” Src has lead the field of non-receptor tyrosine kinases (191). The Src family of kinases (SFK) has 11 members that contain a Kinase domain, a SH2 domain and a SH3 domain (192). Combined, these SFKs play a major role in the cellular events of different biological systems, ranging from the immune system (193) to the nervous system (194). Due to their pleiotropic nature, it is no surprise that aberrant activation of SFKs is associated with carcinogenesis and tumor progression. Aside from their fundamental roles in cell proliferation, survival and angiogenesis, SFKs enhance cell migration and invasion across different cancers. Increased migratory and invasive attributes of cells in cancer occurs through a process called Epithelial-Mesenchymal Transition (EMT) which is considered crucial for metastasis (116). Metastasis is the sequential process whereby cells gain enhanced abilities to penetrate the basement membrane, intravasate into blood/lymphatic vessels, survive in the vasculature, extravasate to secondary sites, and adapt to new host environments (195). The colonization and tumor growth at the distant site is dictated by conflicting pressures like proliferation, dormancy, angiogenesis and apoptosis; all these pathways, like EMT, are regularly modulated by SFKs (196).

LYN kinase is a member of the Src family of kinases. Consistent with the other members of the family, *LYN* consists of a kinase domain, an SH2, an SH3 domain and a unique N-terminal region. It is active when phosphorylated at Y397 and inactivated when phosphorylated at Y508 (197). The inactive form is created when the C-terminus phosphorylation creates a binding site for its own SH2 domain. This intramolecular interaction closes the protein and blocks the kinase domain, thus shutting down *LYN* activity (197). The chief culprit for this inactivating phosphorylation is C-terminal Src kinase (CSK), and Y508 can be de-phosphorylated by phosphatases such as SHP-2 (198) and CD45 (199), leading to activation of the kinase. Interestingly, SHP-1 and SHP-2 can also de-phosphorylate Y397 in the kinase domain and abolish the kinase activity of *LYN* (200). *LYN*'s activity is modulated downstream of many receptor proteins like GM-CSF receptor (201), c-KIT (202), EGFR (203) as well as Integrins

(204). In turn, *LYN* can activate or inhibit a number of signalling molecules through tyrosine phosphorylation for example, FAK (205), STAT5 (206), ras-GAP (207) and PI3K (208).

Structurally, *LYN* also has two splice variants that differ by 20 amino acids at the N-terminus and generate 53kDa and 56kDa isoforms. These isoforms can also drastically change *LYN*'s function as demonstrated by Huang et al.; phosphorylation on Y32 occurs downstream of EGFR signaling and mediates DNA replication through MCM7 activity in human cancers (209). The presence or absence of these important regulatory elements between these isoforms exhibits potential for versatility in *LYN*'s functions between different cell types.

3.1.2. Roles of *LYN* in cancer

Although genetically modified models (GEM) of hyperactive *LYN* did not provide evidence of *LYN* initiating neoplasia, there is mounting evidence that it plays a role in regulating and maintaining cancer biology in both solid and liquid cancers (197). For example, several reports have demonstrated the crucial role of *LYN* in BCR-Abl induced Chronic Myeloid Leukemia (CML) (210, 211). BCR-Abl and *LYN* can cross phosphorylate each other, enhancing their respective signaling pathways (212, 213). Interestingly, patients that develop resistance to CML therapy Imatinib, display significantly higher levels of *LYN* expression and ablation of *LYN* from these cells induces strong apoptosis (214). Coincidentally, small molecule inhibitors developed for Imatinib resistant CML like Bafetinib (215) and Ponatinib (216) are also potent inhibitors of *LYN*. In addition to CML, *LYN* promotes progression of B-Non Hodgkins Lymphomas (B-NHL) through activation of STAT3 (217). *LYN* also activates the AKT pathway downstream of the B-cell receptor in B-cell chronic lymphocytic leukaemia (B-CLL) (218). A unique incident with *LYN* has been described in Acute Myeloid Leukaemia (AML), whereby fusion of Tel (ETV6) and *LYN* activates STAT5 independently from JAK2 promoting proliferation (206). Altogether, these studies show the *LYN* activity is intimately involved with oncogenic signaling cascades in Leukaemia/Lymphoma, and inhibiting *LYN* has potential for treatment of certain types of liquid cancers.

While few kinases are genetically altered in solid cancers, their activity is commonly enhanced. In particular, there is increasing evidence that *LYN* is associated with metastasis and thus may promote EMT (219). For example, we have recently reported increased expression of *LYN* in metastatic castration-resistant prostate cancer (mCRPC) (133). In addition to prostate, *LYN* has been implicated in other cancers, including breast (220), colon (221) and glioblastoma (222). *LYN* regulates cellular events, like proliferation and survival, in multiple cancer types

(197) and targeting *LYN* in Ewing's Sarcoma reduces metastatic potential (223). Higher *LYN* protein expression has been implicitly linked to highly aggressive Triple Negative Breast Cancer (TNBC), whereby 46% of TNBC cases were *LYN*(+). Also, 79% of *LYN*(+) patients were TNBC and *LYN* expression was linked to reduced patient survival (224). In this study, *LYN* knock-down using siRNA in TNBC cell lines reduced cell migration and invasion. With the availability of a well-tolerated and clinically active inhibitor, Bafetinib (225), targeting *LYN* presents as a viable strategy. Therefore, the underlying mechanism by which *LYN* modulates metastasis warrants exploration.

3.2. Introduction

The gain of mesenchymal markers Vimentin and Fibronectin with a concomitant loss of E-cadherin are hallmarks of EMT. Central to this process is an increase in transcription factors of the SNAIL family, which lead to transcriptional repression of E-cadherin and start the transformation to a mesenchymal phenotype (226). In this study, we provide mechanistic insight into how *LYN* regulates EMT in prostate cancer (PCa), breast cancer (BrCa) and bladder cancer (BICa). In vitro and in vivo studies showed *LYN* promotes EMT via initiating the VAV-RAC1-PAK1 signal cascade; this leads to protein localization and stability of the SNAIL transcription factors Slug and Snail, upregulation of EMT-related genes, invasion and metastasis. Furthermore, we established the importance of *LYN* in human metastatic cancer, demonstrating that *LYN* expression across multiple tumor types is, i) increased in metastatic tumors and primary tumors that eventually metastasize, ii) negatively correlates with E-cadherin expression, iii) positively correlates with the expression of EMT markers Vimentin and Fibronectin. Our results suggest that *LYN* is a major upstream regulator of Slug and Snail, two central transcription factors that control EMT across multiple cancer types; thus specific targeting of *LYN* may be a rational therapeutic approach to prevent or treat metastatic disease.

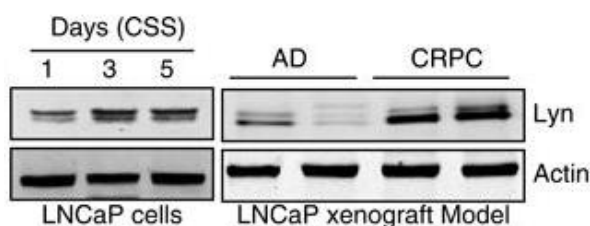


Figure 3.1 - *LYN* expression induced by androgen deprivation:

LNCaP cells cultured in CSS over time (left panel), and LNCaP xenografts before castration (AD) or after progression to CRPC in xenografts (right panel)

The critical importance of this research to prostate cancer treatment resistance comes from two pieces of data from Zardan et al. (133). *LYN* expression is induced under androgen deprivation conditions and consolidated at castration resistance (**Fig. 3.1**). A possible interpretation of this data would suggest that *LYN* gets up-regulated in

response to treatment and helps confer resistance to ADT. Importantly, the expression of *LYN* remains increased into CRPC which is almost always metastatic.

3.3. Results

3.3.1. *LYN* mRNA expression correlates with cancer metastasis and E-cadherin expression.

To investigate the relevance of *LYN* to tumor spread in human cancers, we analyzed *LYN* expression in PCa across published data sets (<http://www.oncomine.org/>). We found that *LYN* was significantly upregulated in PCa metastases compared to primary tumors across 5 different cohorts (**Fig. 3.2**) (227-231). This clinical data further implicates *LYN* in the metastatic process of PCa.

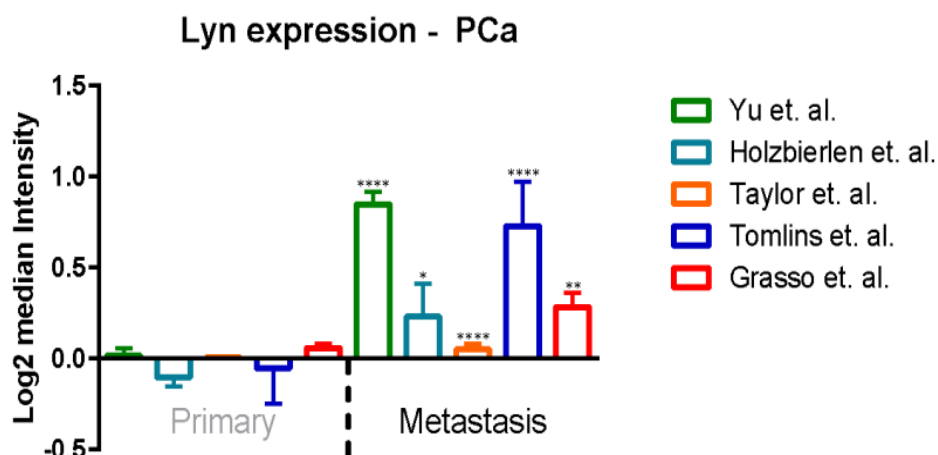
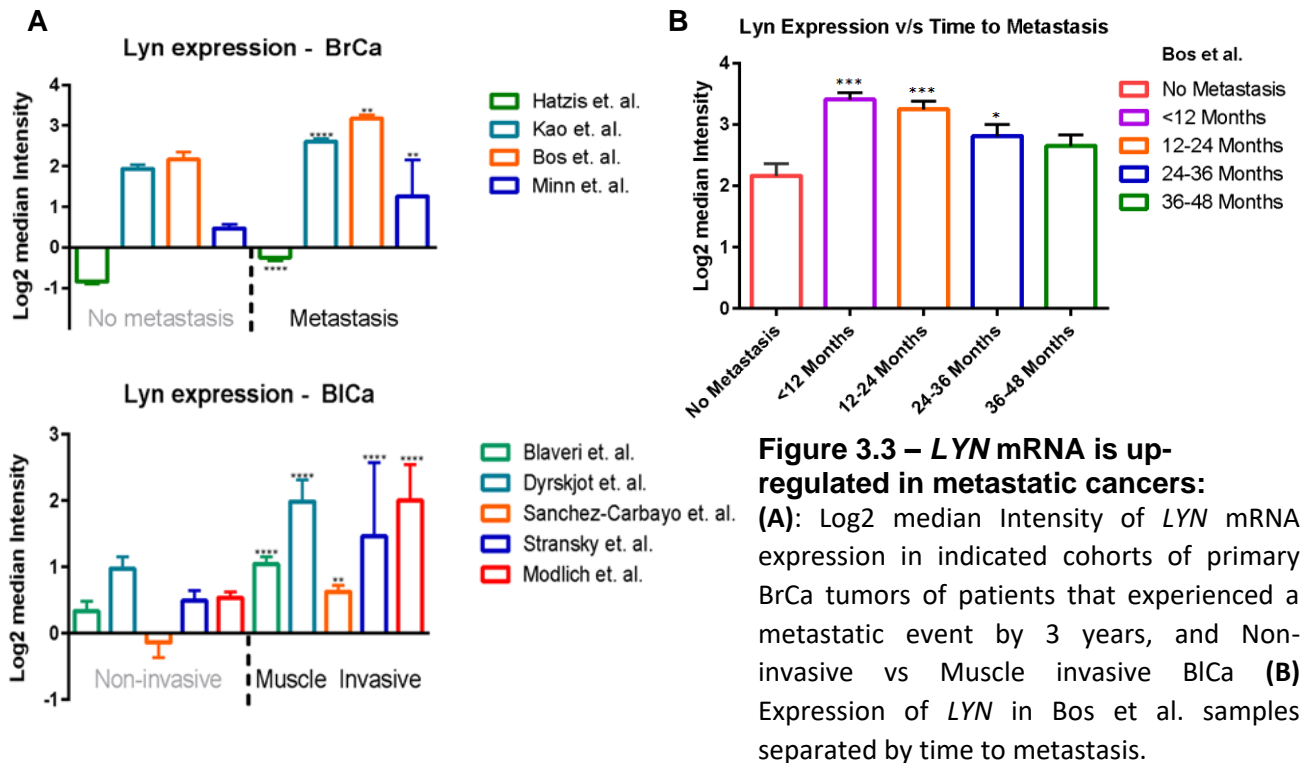


Figure 3.2 - *LYN* expression vs. Metastasis:

Log2 median Intensity of *LYN* mRNA expression compared between indicated cohorts of PCa tumor samples from primary tumor and metastasis.

Interestingly, we discovered a similar trend in other cancers; whereby *LYN* expression is upregulated in metastatic forms of the disease. In 4 cohorts of BrCa patients, *LYN* was significantly upregulated in the primary tumor in patients that experienced a metastatic event in less than 3 years compared to tumors that did not metastasize (**Fig. 3.3 A**) (232-235). Surprisingly, the study from Bos et al. contained temporal data and further analysis revealed that *LYN*'s expression was highest in primary tumors that metastasized within 12 months of diagnosis, and the expression decreased in patients that experienced a metastatic event later (**Fig. 3.3 B**). *LYN* expression was also significantly upregulated in 5 different cohorts of primary muscle invasive Bladder Cancer (BICa) compared to superficial BICa (**Fig. 3.3 A**) (236-240). Together, these human data strongly implicate *LYN* in promoting metastasis of multiple tumor types and implicate it as a potential target to prevent disease progression.



To decipher *LYN*'s role in EMT, we examined a possible link between *LYN* and E-cadherin, a major epithelial cell-adhesion protein and a *de facto* tumor suppressor (241). Analysis of gene expression of *LYN* and E-cadherin (*CDH1*) in multiple patient tumor samples using the *in silico* transcriptomics database (<http://ist.medisapiens.com/>) showed an inverse relationship between the two genes across multiple tumor types (statistically significant cancers identified in the legend **Fig. 3.4 A**). To further establish the link between E-Cadherin and *LYN* expression at the protein level, we examined the E-Cadherin Reverse phase protein array

(RPPA – dot blot assay for protein expression in patient samples) in tumors with ± 1 z-score vs. unaltered *LYN* expression in TCGA datasets from the cBioportal repository (189). Statistically significant up- or down-regulation of E-cadherin protein expression was observed in prostate, breast and bladder tumors with low and high *LYN* expression respectively, compared to unaltered (**Fig. 3.4 B**).

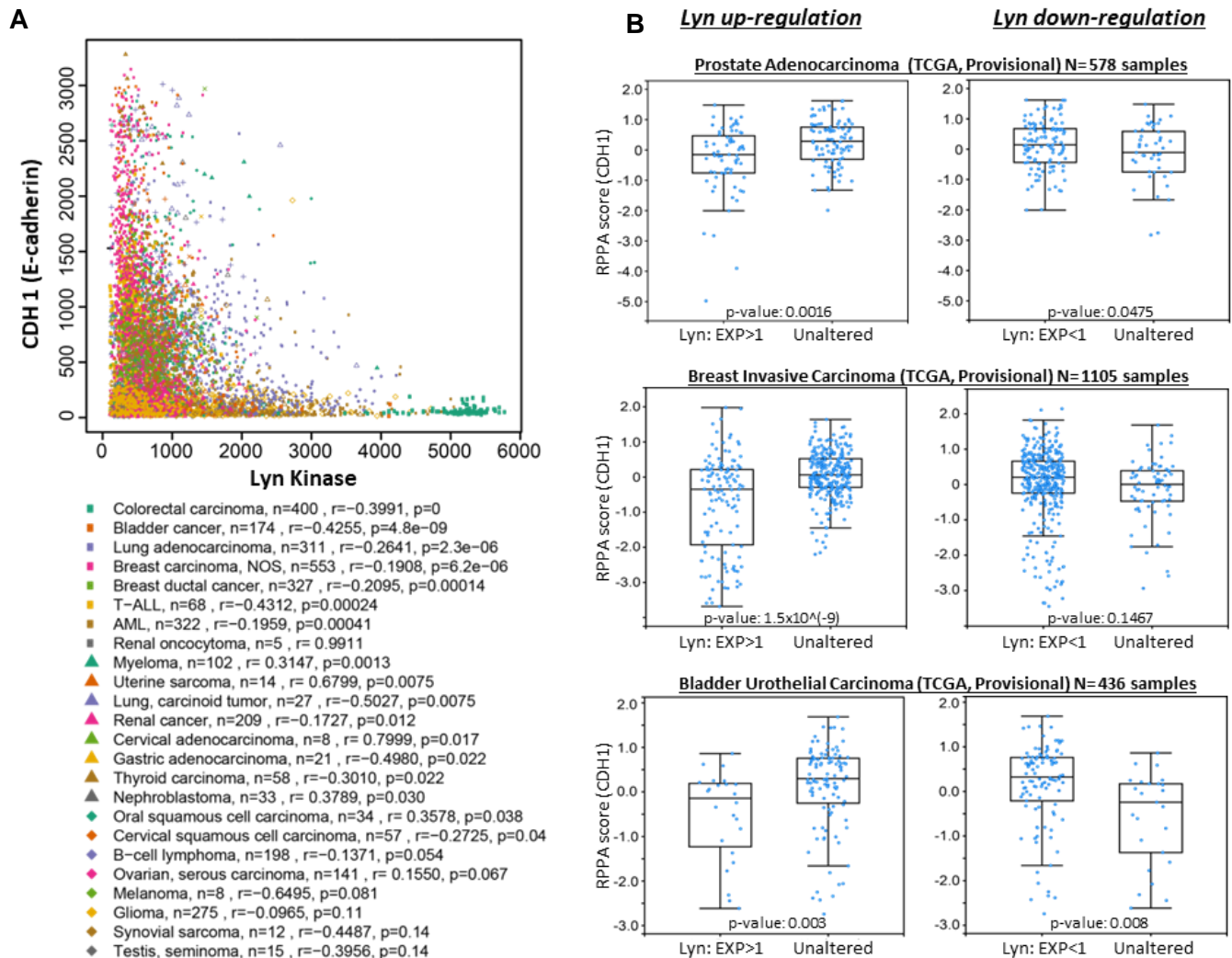


Figure 3.4 - *LYN* expression vs E-Cadherin:

(A) Affymetrix analysis of patient mRNA expression comparing *LYN* vs E-Cadherin (n= 8575, from 175 different tissue types) from <http://ist.medisapiens.com>. (B) Prostate Cancer, BrCa and BlCa TCGA Provisional data sets from www.cbioportal.com. The graphs show RPPA score of E-cadherin (CDH1) in tumours with *LYN* mRNA up or down-regulated by 1 standard deviation (z-score) vs unaltered *LYN* mRNA levels.

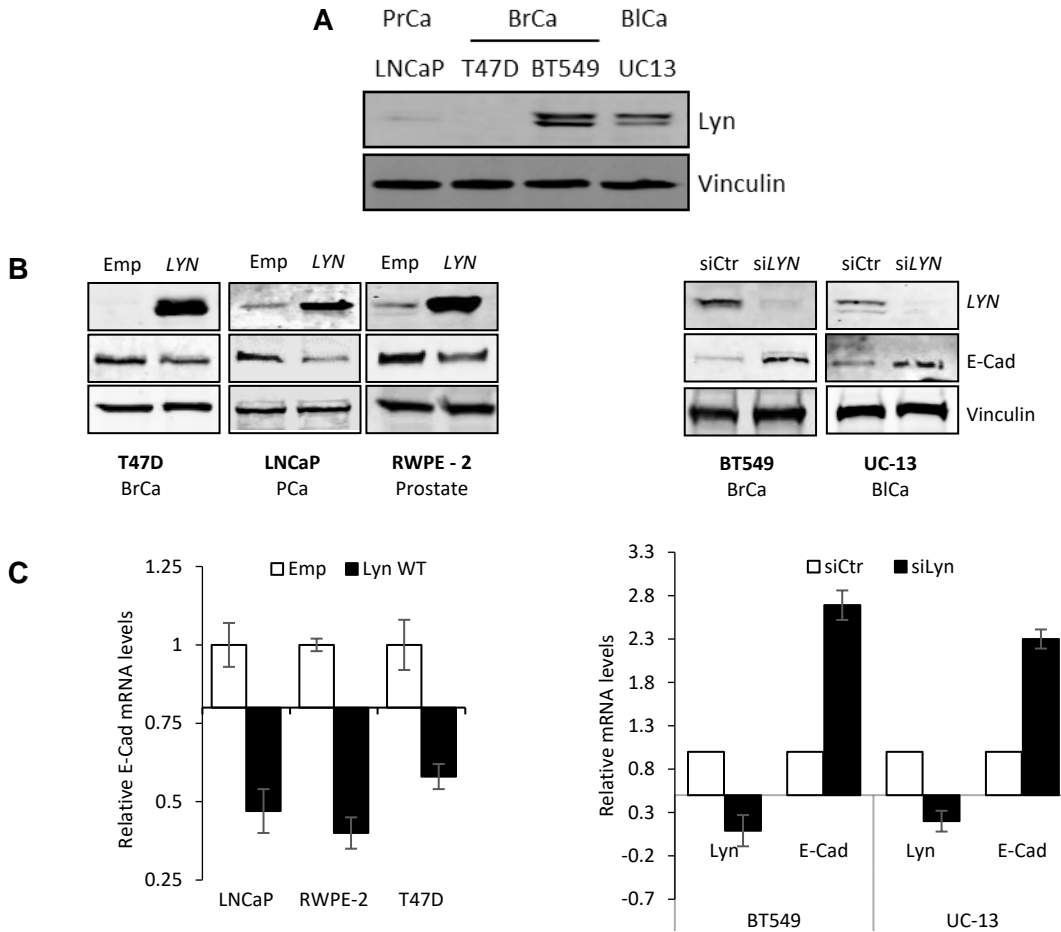


Figure 3.5 – *LYN* modulates E-Cadherin *in vitro*:

(A) Levels of *LYN* Kinase in LNCaP, T47D, BT549 and UC13 cells **(B-C)** Western Blot analysis and relative mRNA expression of *LYN* and E-cadherin with over-expression and siRNA knockdown of *LYN*. Graphs represent pooled data from 3 independent experiments.

To validate the patient data *in vitro*, we modulated *LYN* expression in PCa, BrCa and BICa cell lines, inducing expression in primarily epithelial cell lines with low levels of endogenous *LYN* and using siRNA knockdown in more mesenchymal cell lines with high levels of *LYN* (**Fig. 3.5 A**). We first transiently over-expressed wild-type (WT) *LYN* in PCa LNCaP cells, K-Ras transformed prostate epithelial RWPE-2 cells, and in epithelial-like T47D BrCa cells. In all three cell lines, *LYN* over-expression suppressed E-cadherin at both mRNA and protein levels (**Fig. 3.5 B**). By contrast, knockdown of *LYN* by siRNA increased E-cadherin mRNA and protein levels in mesenchymal-like BT549 (BrCa) and UC-13 (BICa) cell lines (**Fig. 3.5 C**). Collectively, these data suggest that modulating *LYN* expression affects levels of E-cadherin inversely in cancer cells *in vitro*, and in human tumors.

3.3.2. *LYN* expression and activity modulates Epithelial and Mesenchymal cell states

Accompanied by loss of E-cadherin expression, ectopically induced expression of *LYN* decreases cell-cell contact (cobblestone structures), E-cadherin and ZO-1 expression and vice versa for knockdown of *LYN* (**Fig. 3.6**).

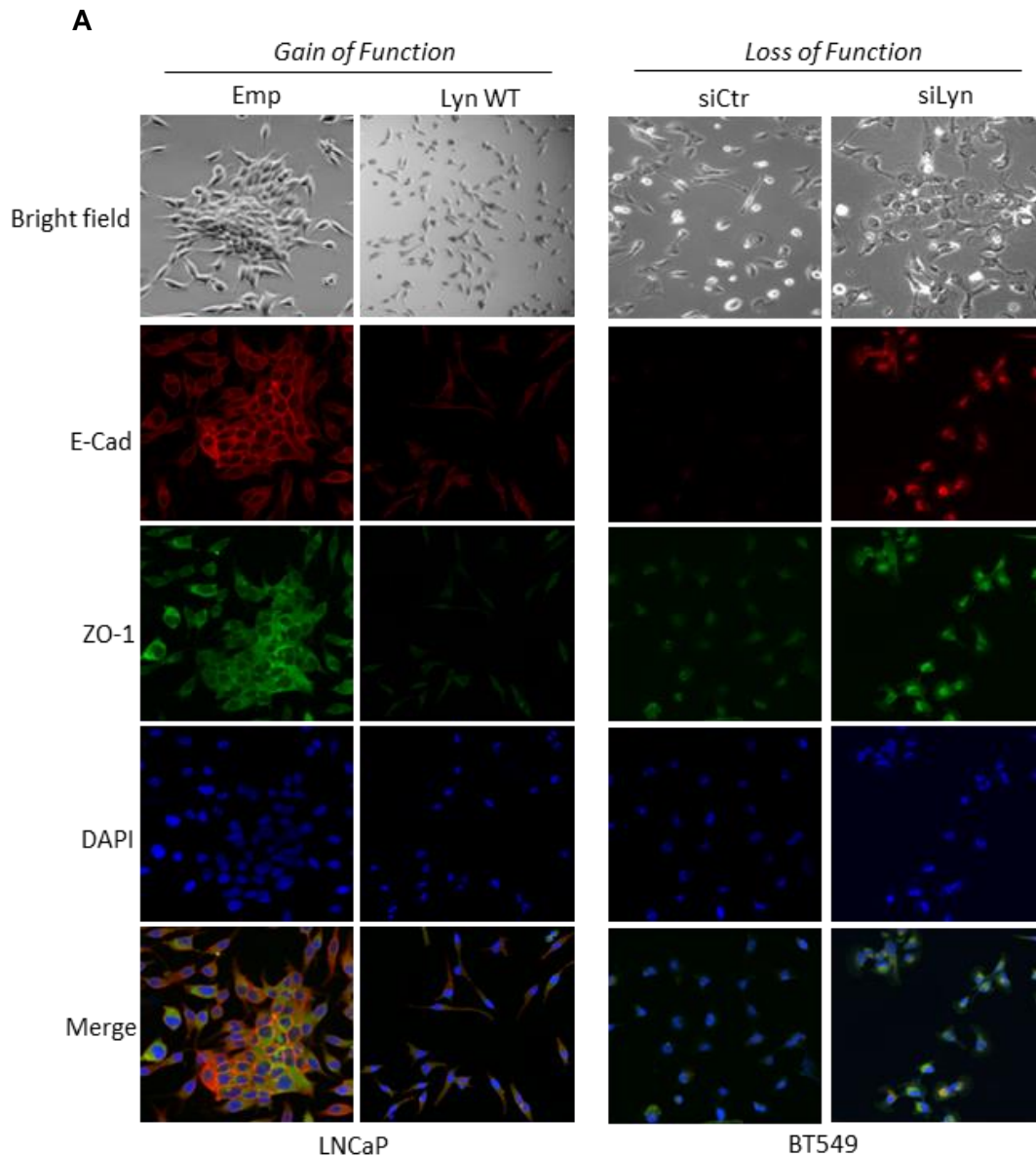


Figure 3.6 – *LYN* kinase regulates EMT phenotype:

Bright-field and immunofluorescence imaging with E-cad in Red and ZO-1 in green of **(left)** LNCaP cells treated with Empty or *LYN* WT plasmid and **(right)** BT549 treated with siRNA control or *LYN*.

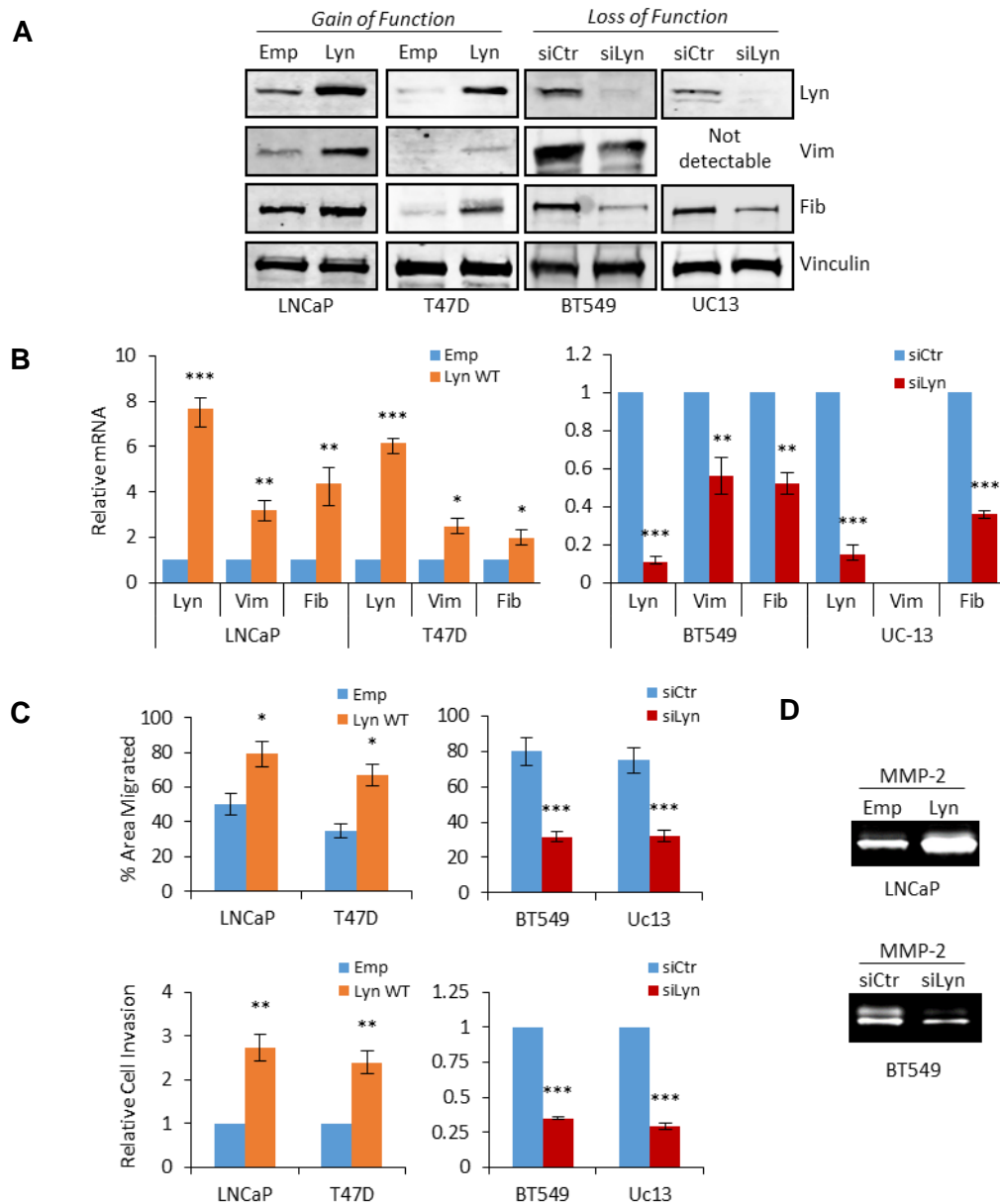


Figure 3.7 – *LYN* expression regulates EMT markers and cell migration and invasion:

(A and B): Analysis of indicated genes with over-expression *LYN* and si RNA knock-down of *LYN*. **(A)** Western Blot **(B)** Relative mRNA expression, graphs represent pooled data from 3 independent experiments. **(C)** LNCaP and T47D cells transfected with Empty or *LYN* WT plasmid, BT549 and UC-13 cells transfected with siRNA *LYN*: *Top half* - Percent area migration from time zero assessed in scratch assay in after 48h for LNCaP and T47D, 9h for BT549 cells and 18h for UC-13 cells. *Bottom half* – Relative number of cells migrated through Matrigel Boyden chamber after 24h. **(D)** Zymography assay measuring MMP2 activity in LNCaP transfected with *LYN* WT and BT549 cells treated with si*LYN*.

Accordingly, overexpression of WT *LYN* in PCa (LNCaP) or epithelial-like BrCa (T47D) cells induced a significant increase of the mesenchymal markers Vimentin and Fibronectin at the protein and mRNA level compared to cells transfected with empty vector (**Fig. 3.7 B&C**). Reciprocally, *LYN* knockdown by siRNA induced a mesenchymal-to-epithelial transition (MET)

in cancer cells. Silencing *LYN* in mesenchymal-like BT549 (BrCa) and UCM-UC13 (BICa) lines caused a marked increase in E-cadherin, as well as decreases of Vimentin and Fibronectin at both protein and mRNA levels compared to control (**Fig. 3.7 B&C**). Invasion and migration were also significantly increased in WT *LYN* expressing cells compared to empty vector control (**Fig. 3.7 C**) while knockdown decreased cell migration and invasion compared to control (**Fig. 3.7 C**). *LYN* expression also modulated MMP activity as knockdown reduced while over-expression increased MMP-2 activity as shown by Zymography assay (**Fig. 3.7 D**).

Data-mining of the TCGA cohorts for PCa, BrCa and BICa further corroborated our *in vitro* data as patients with higher *LYN* mRNA exhibited an increase of EMT markers Vimentin (*VIM*) in BrCa and BICa, Fibronectin (*FN1*) in PCa and BICa and N-Cadherin (*CDH2*) somewhat weakly in BICa while the patients with decreased *LYN* displayed lower expression of all markers(**Fig. 3.8**).

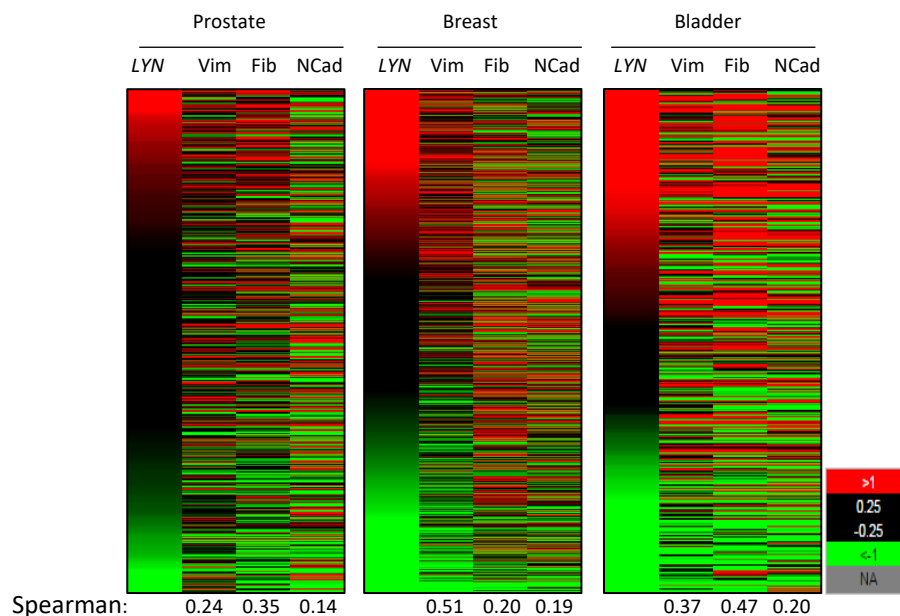


Figure 3.8 – *LYN* mRNA correlates with EMT markers in patients:

Heat map of TCGA data showing gene expression of Vimentin, Fibronectin and N-Cadherin in human PCa, BrCa and BICa patients stratified by their *LYN* expression (<http://xena.ucsc.edu>).

As a kinase, *LYN* functions primarily by phosphorylating downstream effectors. To investigate whether the kinase activity of *LYN* is required for regulating epithelial and mesenchymal cell states, constitutively active (CA) and kinase dead (KD) mutants of *LYN* (242) were transfected into LNCaP cells. Compared to *LYN* WT (**Fig. 3.6**) and *LYN* CA, cells expressing *LYN* KD retained their cell-cell contact, E-cadherin and ZO-1 expression (**Fig. 3.9 A**) while inhibition in BT549 cells using the *LYN* inhibitor Bafetinib (243) was accompanied by an

increase in cell-cell contact, E-cadherin and ZO-1 (**Fig. 3.9**). With the increased activity of *LYN* as shown by the levels of p-*LYN*, our results showed that overexpression of *LYN* CA further increased Fibronectin and Vimentin expression and decreased E-Cadherin expression, while in *LYN* KD expressing cells, these markers remained equivalent to empty vector control (**Fig. 3.10 A&B**). Conversely, we found that Bafetinib treatment of BT549 cells significantly upregulated E-cadherin and decreased Vimentin and Fibronectin expression compared to control treated cells (**Fig. 3.10 A&B**). Lastly, *LYN* CA cells showed significantly increased cell migration and invasion compared to *LYN* WT, KD or empty vector controls, whereas Bafetinib treatment significantly reduced migration and invasion (**Fig. 3.10 C&D**). Together these data support that *LYN* expression and activity regulate EMT, cell migration and invasion.

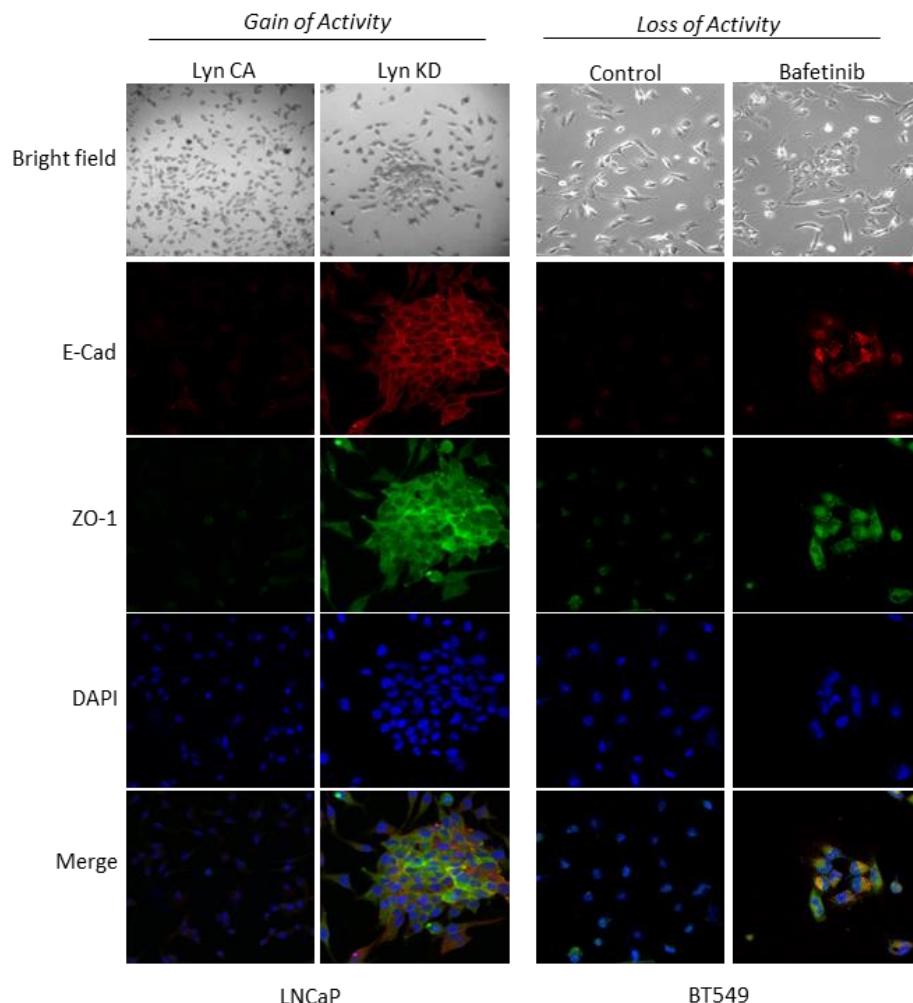


Figure 3.9 – *LYN*'s kinase activity is required for EMT:

Bright-field and immunofluorescence imaging with E-cad (Red) and ZO-1 (green) in LNCaP cells treated with *LYN* CA or *LYN* KD plasmid (*left*) and BT549 treated with 1 μ M Bafetinib (*right*) for 24h.

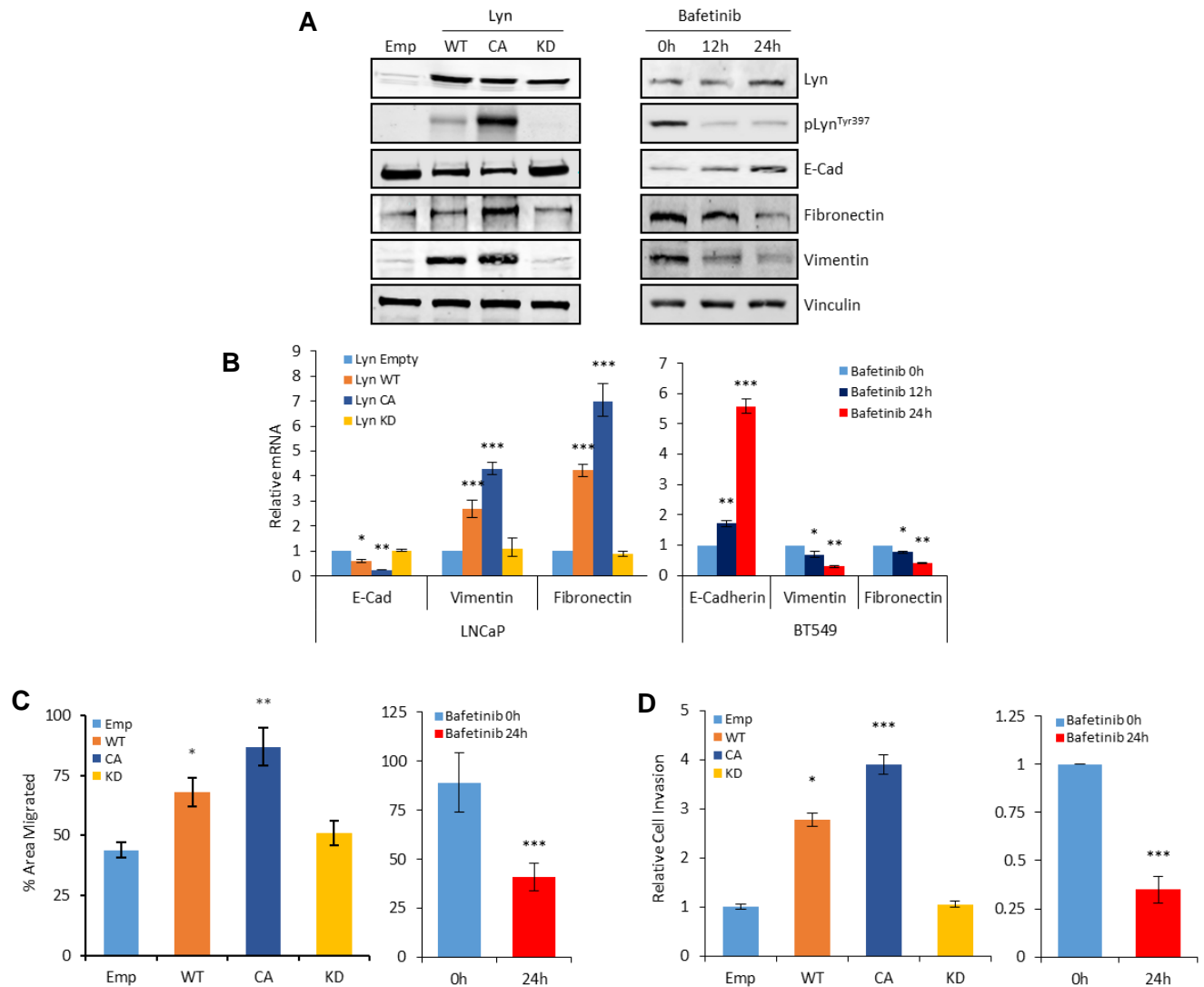


Figure 3.10 - Kinase activity of *LYN* is responsible for EMT:

(A and B): Analysis of indicated genes after transfection of *LYN* WT, CA and KD mutants in LNCaP (*left*) or 1 μ M Bafetinib treatment in BT549 (*right*) for 24h. **(A)** Western Blot **(B)** Relative mRNA expression, graphs represent pooled data from 3 independent experiments. **(C and D)** LNCaP cells transfected with Empty or *LYN* WT, CA and KD plasmids and BT549 treated with 1 μ M Bafetinib: **(C)** Percent area migration from time zero assessed in one dimensional scratch assay in after 48h for LNCaP and 9h for BT549 cells. **(D)** Relative number of cells migrated through Matrigel Boyden chamber after 24h.

3.3.3. *LYN* regulates E-Cadherin through *SNAI* family proteins

Our results indicated that modulating *LYN* expression and activity resulted in regulation of E-cadherin at both protein and mRNA levels, suggesting *LYN* may alter transcriptional control of E-cadherin. To test this hypothesis, we investigated the relationship between *LYN* and E-cadherin transcriptional repressors. Knockdown of *LYN* by siRNA reduced protein expression of Slug (*SNAI2*) and Snail (*SNAI1*) in BT549 and UC13 cells (**Fig. 3.11 A**) which was validated using different *LYN* siRNA (**Fig. 3.11 C**). This trend was also observed in an *in vivo* model of *LYN* loss-of-function; prostatic and bladder tissue from *LYN* knockout mice (244) showed reduced expression of Slug and Snail compared to tissue from WT animals (**Fig. 3.11 B**). In a combination experiment, over-expressing WT *LYN* following siRNA knockdown rescued the levels of Slug and Snail (**Fig. 3.11 D**).

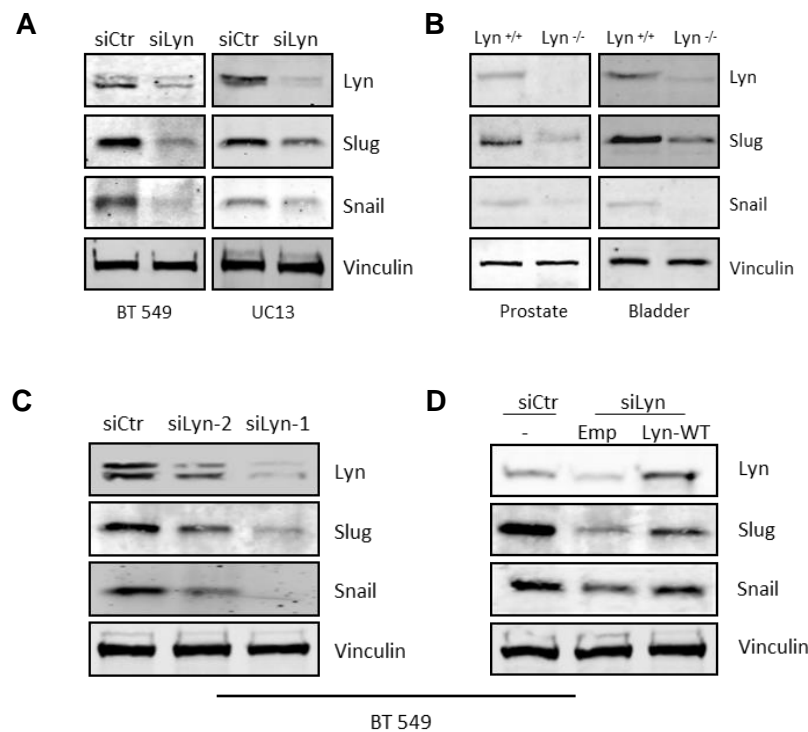


Figure 3.11 - Targeting *LYN* kinase reduces expression of EMT factors Slug and Snail
(A-D) Western Blot analysis of indicated proteins **(A)** in BT549 and UC13 cells transfected with *LYN* siRNA, **(B)** in prostate and bladder tissue from *LYN*^{+/+} and *LYN*^{-/-} transgenic mice, **(C)** BT549 of cells treated with different *LYN* siRNAs, **(D)** BT549 cells treated with *LYN* siRNA ± *LYN* WT plasmid.

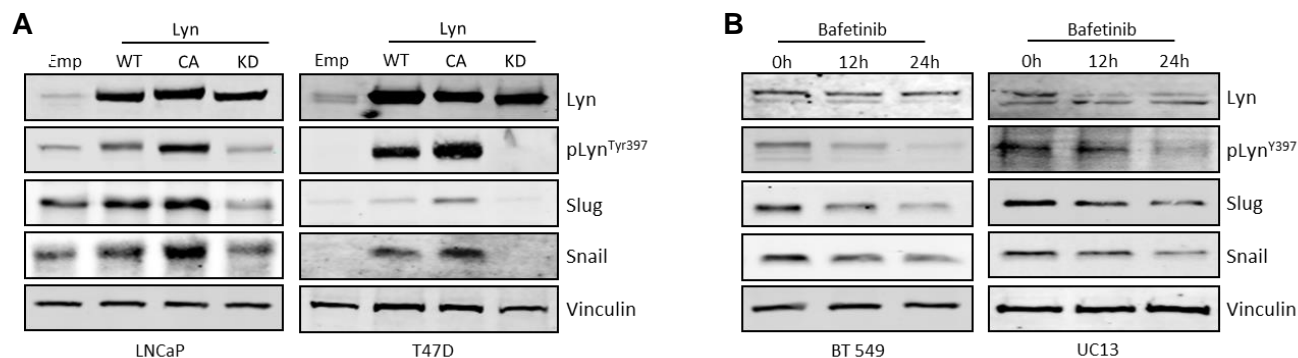


Figure 3.12 - *LYN* kinase activity modulates protein levels of Slug and Snail:

(A-B): Western Blot analysis on indicated genes in **(A)** LNCaP and T47D cells transfected with *LYN* WT, CA and KD mutants and **(B)** BT549 and UC13 cells treated with 1 μ M Bafetinib for 12 and 24 hours.

Conversely, overexpression of WT *LYN* increased protein expression of both Slug and Snail and this increase was enhanced with *LYN* CA, but not *LYN* KD compared empty vector control in LNCaP cells and T47D cells (**Fig. 3.12 A**). This result was further supported by Bafetinib treatment, which decreased Slug and Snail protein expression in BT549 cells and UC13 cells (**Fig. 3.12 B**). Interestingly, *LYN*'s regulation of Slug and Snail protein was not reflected at mRNA level in these experiments (**Fig. 3.13**) suggesting a post-translational modification.

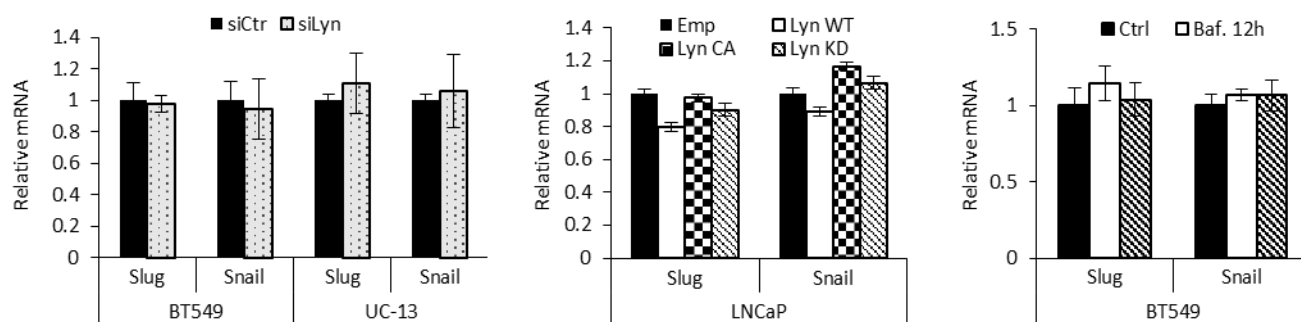


Figure 3.13 - Targeting *LYN* does not alter Slug and Snail mRNA:

Relative mRNA expression of Slug and Snail in experiments from 3-11 and 3-12.

Reflective of our results showing changes in protein, but not mRNA, levels of Slug and Snail after modulating *LYN* expression and activity; RPPA analysis of the BrCa TCGA cohort (245) revealed significant Slug (SNAI2) upregulation in patients with higher *LYN* expression (**Fig. 3.14**). Collectively, our data demonstrate a positive relationship between *LYN* expression and activity and the SNAI family factors Slug and Snail, in PCa, BrCa and BICa.

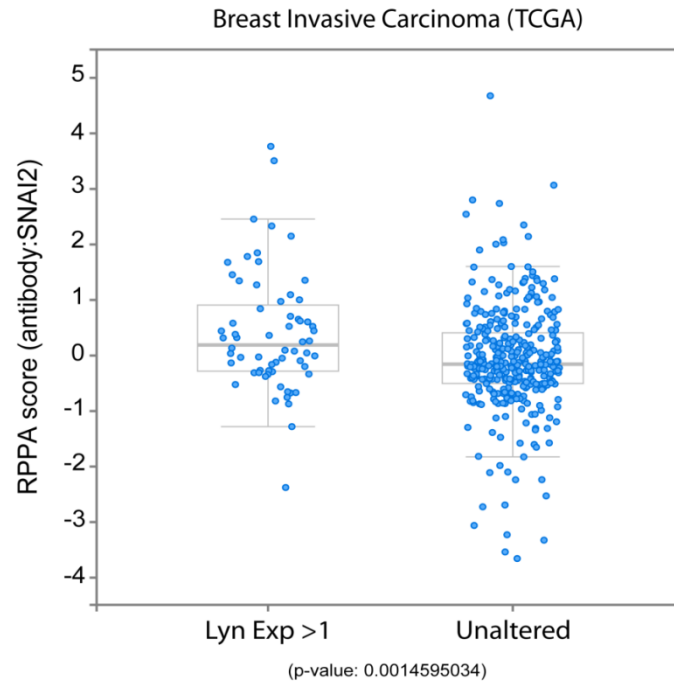


Figure 3.14 – Slug expression is higher in patients with high expression of *LYN*.

RPPA score of Slug (SNAI2) in tumours with *LYN* mRNA up-regulated by 1 standard deviation (z-score) vs unaltered *LYN* mRNA levels.

3.3.4. *LYN* kinase expression regulates Slug and Snail stability

To investigate how *LYN* of Slug and Snail at the protein level, we investigated the effects of *LYN* expression and activity on the rate of Slug and Snail degradation using Cycloheximide (CHX) to block de novo protein synthesis. Interestingly, we found that by 4 hours, Slug and Snail protein levels were almost completely degraded in empty vector control samples (**Fig. 3.15**). By contrast, the rate of degradation of both Slug and Snail was reduced after *LYN* overexpression, with WT *LYN* expressing cells showing sustained protein expression at both 2 and 4 hours post-CHX treatment compared to control (**Fig. 3.15**). Reciprocally, reducing *LYN* expression by siRNA treatment, or activity with Bafetinib, increased the rate of Slug and Snail degradation compared to their controls, with both treatments causing Slug and Snail protein levels to be at negligible levels by 2 hours (**Fig. 3.15**). These results showed that *LYN* expression and activity are required to regulate the stability of Slug and Snail at the protein level.

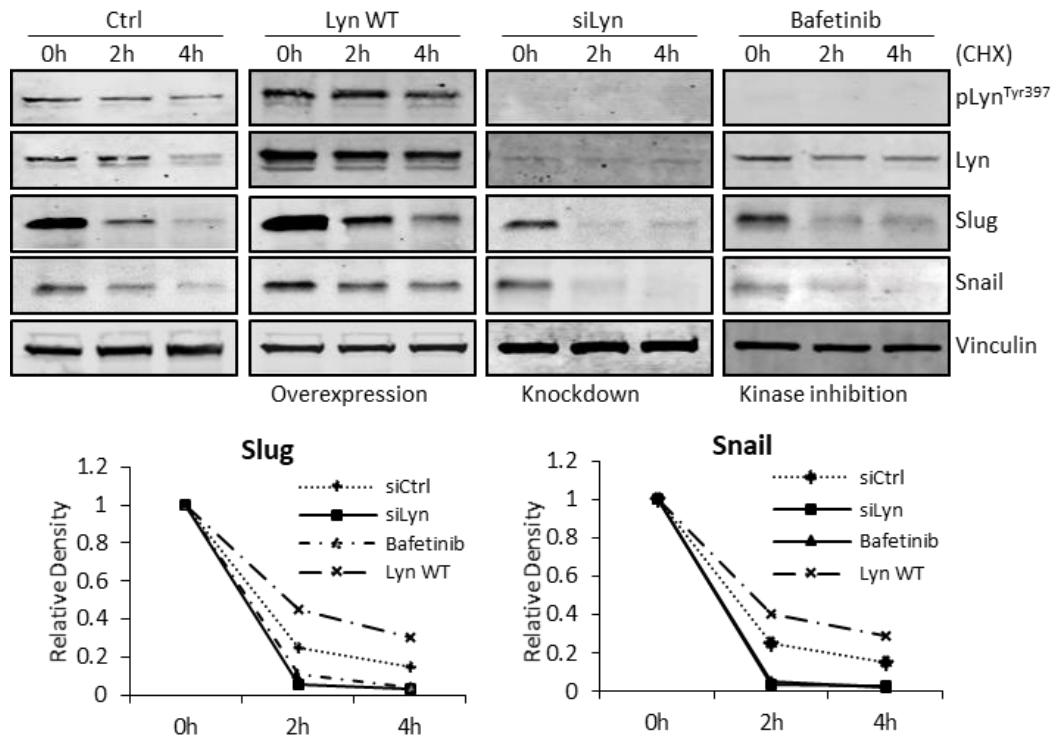


Figure 3.15 - *LYN* expression modulates Slug and Snail protein stability:

BT549 cells transfected with control plasmid, *LYN* WT, *LYN* siRNA or treated with 1 μ M of Bafetinib +/- 10 μ M Cyclohexamide for 2 and 4 hours prior to extraction. Vinculin was used as a loading control and densitometry (bottom graphs) was performed to quantify band intensities of the WB (graph quantification: n=1).

Since Snail and Slug have been reported to be degraded via the proteasome (246), we investigated the role of *LYN* in regulating Slug and Snail proteasomal degradation. To do so, cells were treated with *LYN* siRNA or Bafetinib with or without the proteasome inhibitor MG132. Our data revealed that in *LYN* siRNA cells treated with MG132, there was less accumulation of Slug and Snail compared to control siRNA cells (**Fig. 3.16 A**). Their degradation was further investigated by adding 2.5 μ M of Bafetinib and MG132 simultaneously for 8 hours. This experiment again illustrates the decrease of Slug and Snail after *LYN* inhibition using Bafetinib, however, when MG132 is added together with Bafetinib there is no decrease of Slug or Snail (**Fig. 3.16 A**) as protein degradation is induced by Bafetinib and inhibited by MG132 simultaneously. Slug/Snail degradation via the proteasome requires ubiquitination, therefore, we examined ubiquitinated levels of Slug and found that in *LYN* CA overexpressing in the presence of MG132 failed to accumulate ubiquitinated Slug, while Bafetinib treatment induced its ubiquitination (**Fig. 3.16 B**). Together, these data illustrate that *LYN* kinase expression and activity prevents SNAIL family protein proteasomal degradation and increases their stability.

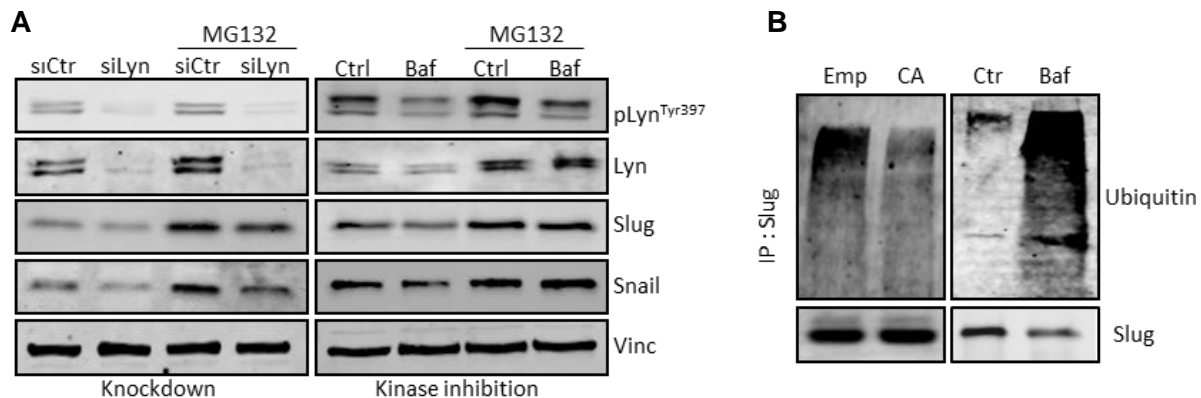


Figure 3.16 - *LYN* expression and activity regulates Slug and Snail ubiquitination and degradation via proteasome

(A) Western Blot analysis of BT549 cells transfected with *LYN* siRNA for 40 hours and then treated with 10 μ M MG132 8 h prior to extraction. *Right Panel* – cells treated with 2.5 μ M of Bafetinib and 10 μ M MG132 both for 8 hours prior to extraction. **(B)** Immunoprecipitation of Slug followed by immunoblot for Ubiquitin in BT549 cells transfected with WT *LYN* or treated with 1 μ M of Bafetinib. Cells were treated with 10 μ M MG132 8 hours prior to extraction.

3.3.5. *LYN* kinase activates the VAV1-RAC1-PAK1 pathway translocating Slug and Snail to the nucleus

Cytosolic localization and sequential proteasomal degradation of Slug and Snail can be initiated by their phosphorylation by GSK3 β , thus preventing transcription of their target genes that promote EMT (247). As our results showed *LYN* prevents Slug and Snail degradation by the proteasome, we explored whether *LYN* affects GSK-3 β activation. Our data revealed that neither *LYN* overexpression (WT or CA) nor inhibition (with Bafetinib) affected levels of the inhibitory phosphorylation of GSK3 β at Ser9 (248, 249) (**Fig. 3.17 A**). Despite having no effect on pGSK-3 β , however, *LYN* activity modulated Snail and Slug nuclear translocation. Immunofluorescence analysis showed that Slug and Snail (**Fig. 3.17 B**) accumulated in the nucleus in WT *LYN* transfected LNCaP cells, and this effect was enhanced with *LYN* CA transfection, while there was no detectable change with the KD mutant.

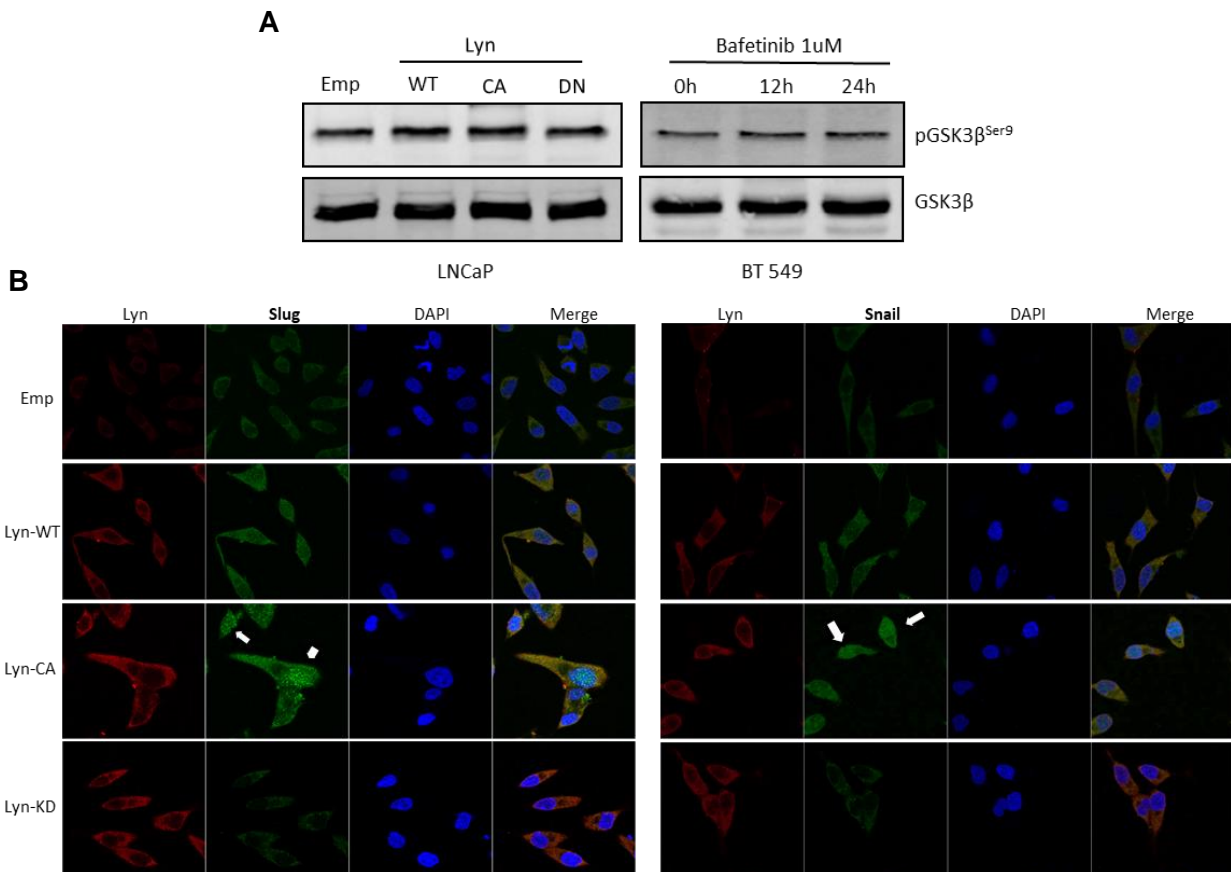


Figure 3-17 - *LYN* expression and activity promotes Slug and Snail nuclear localization

(A) Expression of GSK3 β in LNCaP cells transfected with *LYN* WT, CA and KD mutants and BT549 cells treated with 1 μ M Bafetinib for 24h. **(B)** Immunofluorescence imaging with *LYN* in Red and Slug (left) and Snail (right) in green of LNCaP cells transfected with *LYN* WT, CA and KD mutants. Arrows point to strong nuclear localization.

The signal intensity and cellular localization of Slug and Snail in under these conditions was also quantified (**Fig. 3.18**).

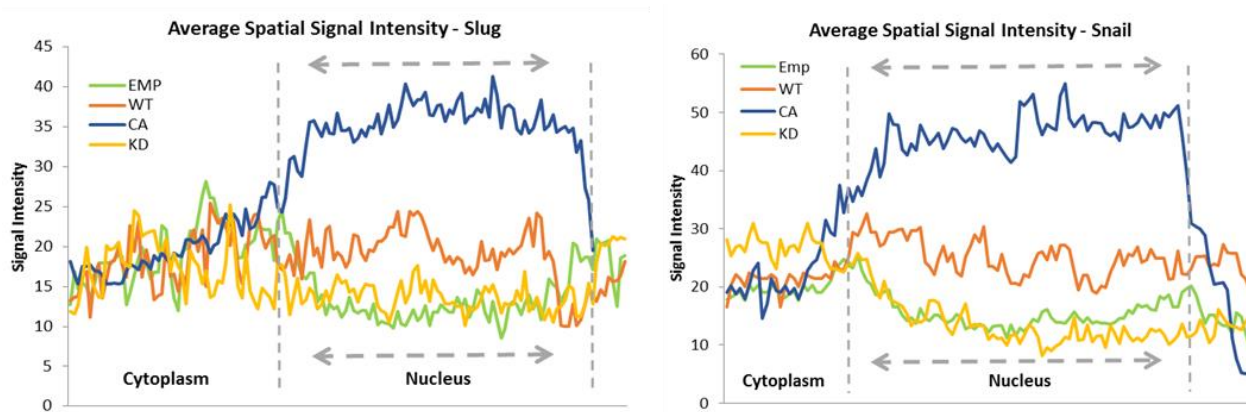


Figure 3.18 - Slug and Snail nuclear intensity in response to *LYN* mutant transfection: Quantification of the average signal intensity of Slug and Snail from Figure 5A and S2B using Zeiss Zen software (black edition).

Reciprocally, treatment of mesenchymal BT549 cells for 24 hours with 1 μ M Bafetinib and MG132 for 8 hours to prevent degradation, illustrates a clear cytoplasmic localization of Slug and Snail (**Fig. 3.19 A**) when *LYN* activity was inhibited compared to Bafetinib untreated cells. These results were corroborated by a fractionation assay, showing that upon inhibition of *LYN* activity by Bafetinib, Slug and Snail expression in the cytoplasmic fraction was higher than in untreated cells (**Fig.3.19 B**).

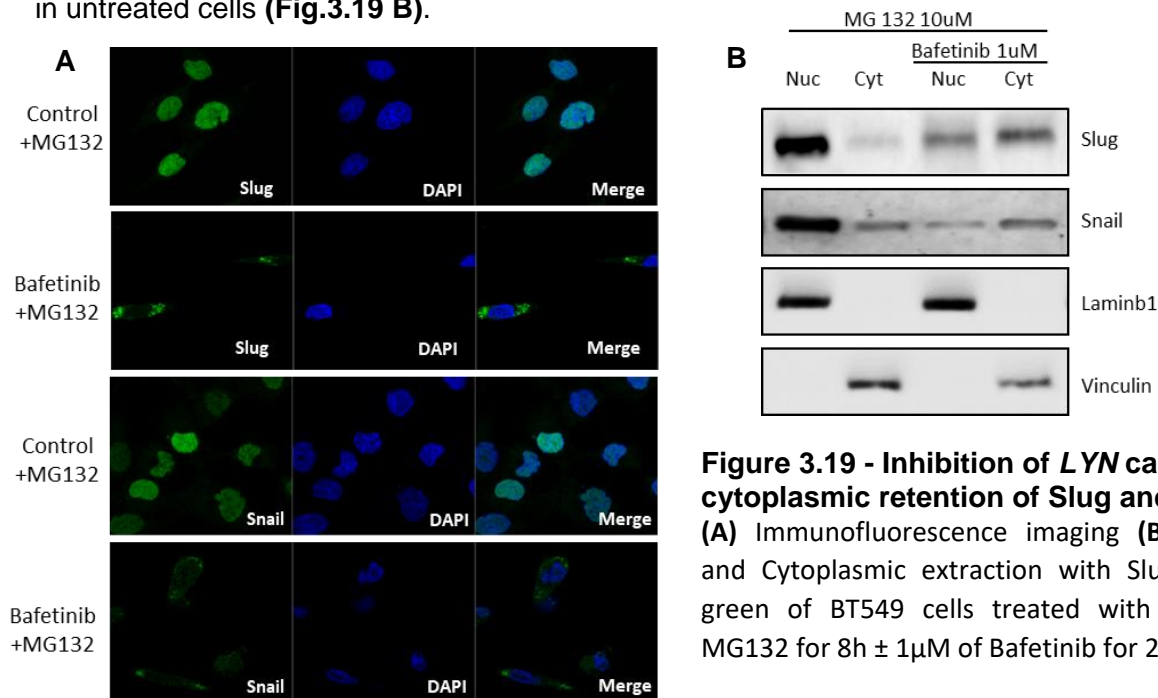


Figure 3.19 - Inhibition of *LYN* causes cytoplasmic retention of Slug and Snail: (A) Immunofluorescence imaging (B) Nuclear and Cytoplasmic extraction with Slug/Snail in green of BT549 cells treated with 10 μ M of MG132 for 8h \pm 1 μ M of Bafetinib for 24h.

In addition to canonical GSK-3 β signaling, p21 Activated kinase (PAK1) has been reported to regulate the cellular localization of Snail (132) by phosphorylating and increasing its nuclear translocation. First assessing the effect of PAK1 knockdown on Slug and Snail expression, we found that, similar to what we observed with *LYN* knockdown (**Fig. 3.11**), targeting PAK1 with siRNA reduced Slug and Snail protein levels (**Fig. 3.20**).

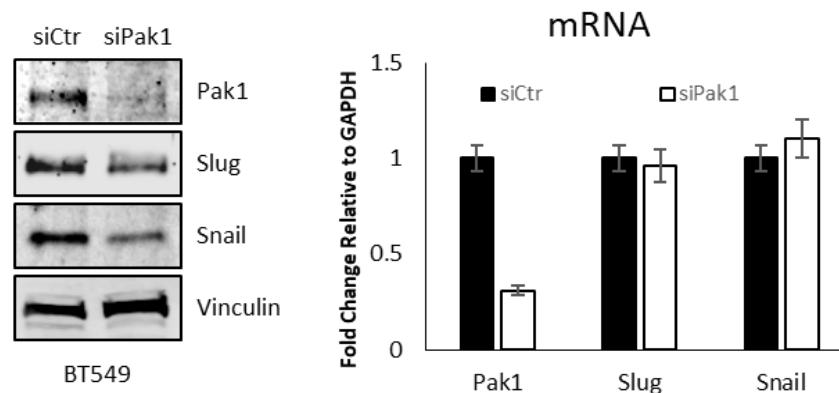


Figure 3.20 - PAK1 regulates protein levels of Slug and Snail:

Relative mRNA expression and Western Blot analysis of indicated genes in BT549 cells treated with siRNA PAK1.

We then interrogated if PAK1 can bind and phosphorylate Slug. Our immunoprecipitation experiment revealed that PAK1 and Slug form a complex and this complex is reduced after Bafetinib treatment in BT549 cells while this interaction is enhanced when LNCaP cells are transfected with CA *LYN* vs KD *LYN* (**Fig. 3.21**).

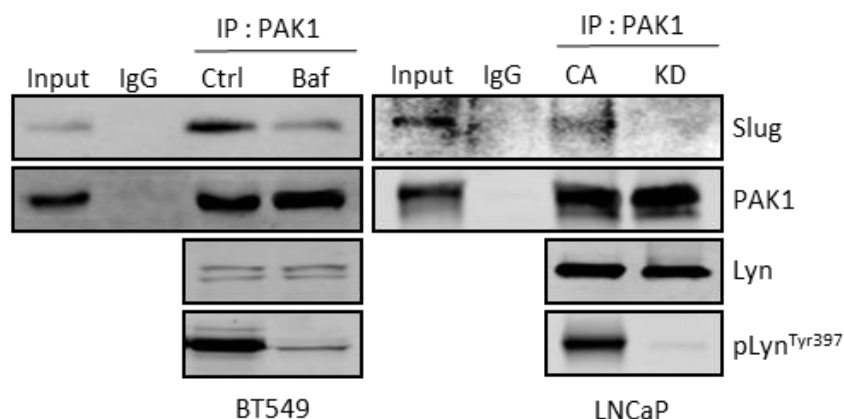


Figure 3.21 - *LYN* activity alters interaction between PAK1 and Slug:

Immunoprecipitation of PAK1 followed by immunoblot for Slug in BT549 cells treated with 1 μ M of Bafetinib for 24h and LNCaP cells transfected with *LYN* CA and KD mutants.

In addition, we found that Slug harbors a Pak consensus phosphorylation domain at Serine 251 (**Fig. 3.22, top**) and, in a kinase assay, PAK1 phosphorylated Slug at this residue while the mutant peptides exhibit significantly less signal from PAK1 phosphorylation (**Fig. 3.22, bottom**). These results show for the first time that in addition to Snail, (132) PAK1 binds and phosphorylates Slug and this effect can be regulated by *LYN* activity.

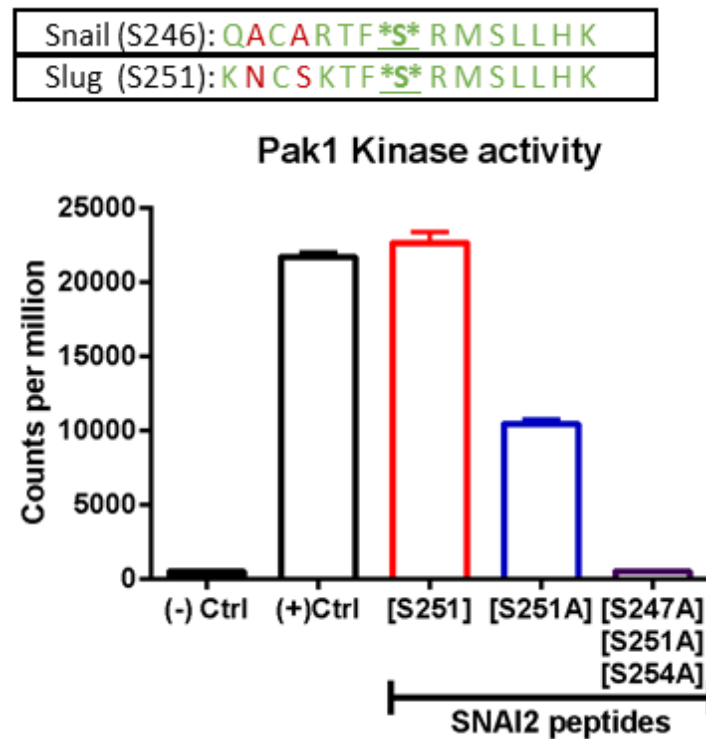


Figure 3.22 - PAK1 phosphorylates Slug at similar consensus domain as Snail: Schematic of amino acid sequence of Snail at Ser246 aligned with the sequence of Slug at S251. *Bottom Panel* – in vitro kinase assay of control PAK1 consensus sequence compared with a synthesized the Slug S251 peptide from the schematic.

PAK1 is heavily regulated by the RAC1 GTPase (250) and in hematopoietic cells *LYN* can modulate the activity of RAC1 through its GTP exchange factor VAV1 via direct tyrosine phosphorylation (251). However, a role for *LYN* in epithelial regulation of VAV has not been described. We therefore hypothesized that *LYN* phosphorylation of VAV1 activates PAK1 to phosphorylate Slug and Snail, leading to their nuclear translocation. Consistent with this hypothesis, we observed that PAK1 Ser204 phosphorylation, Tyr174 VAV1 phosphorylation, and active RAC1, measured by the RAC1-GTP assay, were increased in LNCaP cells expressing WT *LYN* or the CA *LYN* mutant compared to empty or KD transfected controls (**Fig. 3.23**). Reciprocally, knockdown of *LYN* expression by siRNA and inhibition of *LYN* activity by Bafetinib in mesenchymal BT549 cells reversed these effects on PAK1 and VAV1 phosphorylation and Rac-1 GTP (**Fig. 3.23**).

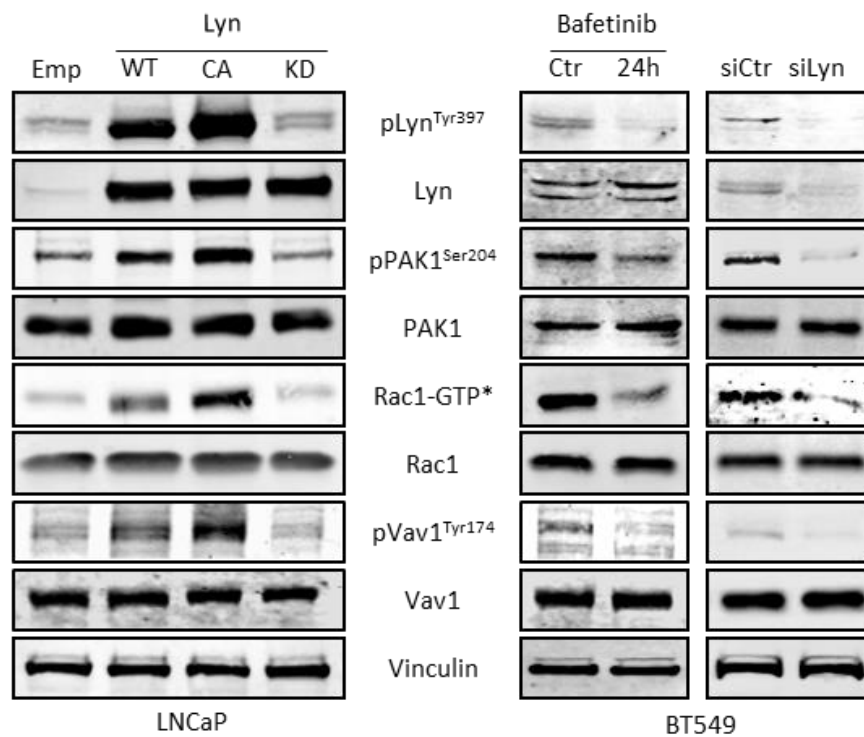


Figure 3.23 - *LYN* activity regulates VAV-RAC1-PAK1 signaling pathway: Western Blot analysis of indicated gene products in LNCaP cells transfected with *LYN* WT, CA and KD mutants and BT549 cells treated with 1 μ M of Bafetinib and transfected with *LYN* siRNA. *WB for RAC1-GTP from RAC1-GTP assay.

These results implicated *LYN* in activating the VAV1-RAC1-PAK1 pathway, however whether PAK1 was the primary mediator of Slug and Snail levels downstream of *LYN* remained unclear. To assess the requirement for PAK1 in the *LYN*-dependent control of Slug and Snail, we over-expressed *LYN* WT, CA and KD mutants in LNCaP cells while knocking down PAK1 by siRNA. Indeed, we found that PAK1 knockdown abrogated the accumulation of both Slug and Snail that is observed after overexpression of WT or CA *LYN* (**Fig. 3.24**), indicating that PAK1 is required for *LYN*-mediated effects on Slug and Snail. Overall, our *in vitro* data reveal for the first time a novel mechanism by which the *LYN* kinase activates the VAV1-RAC1-PAK1 pathway (**Fig. 3.25**) in epithelial tumor cells, which promotes nuclear translocation of SNAI family proteins to initiate transcription of EMT genes and repress E-Cadherin.

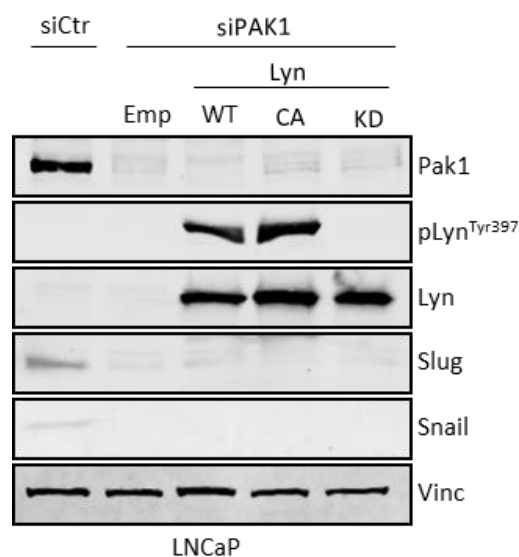


Figure 3.24 - PAK1 is required for *LYN* to stabilize expression of Slug and Snail:

Western Blot analysis of indicated genes in LNCaP cells transfected with *LYN* WT, CA and KD mutants simultaneously treated with siRNA PAK1.

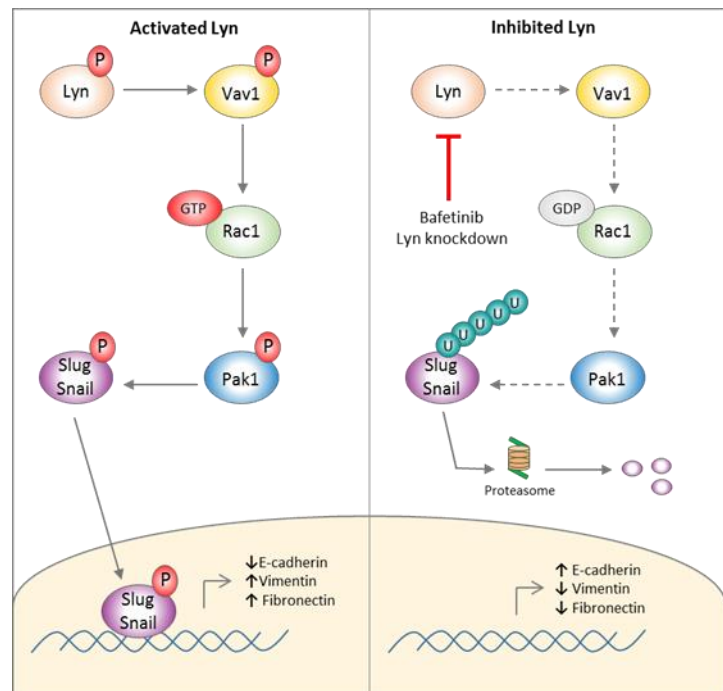


Figure 3.25 - Proposed model of *LYN*'s regulation of Slug, Snail and EMT

3.3.6. *LYN* kinase facilitates metastasis in vivo.

To show the requirement for *LYN* in promoting tumor metastasis *in vivo*, we modulated *LYN* function and expression and assessed BrCa and BlCa metastasis. First, using a well-established zebrafish model where cell migration and invasion through the yolk sac are quantified (252), BT549 cells were injected into the yolk sac of 2 day-old dechorionated zebrafish embryos and cell migration/invasion into the fish was quantified. After 24 hours control fish had significant cell migration to the tail region (**Fig. 3.26**).

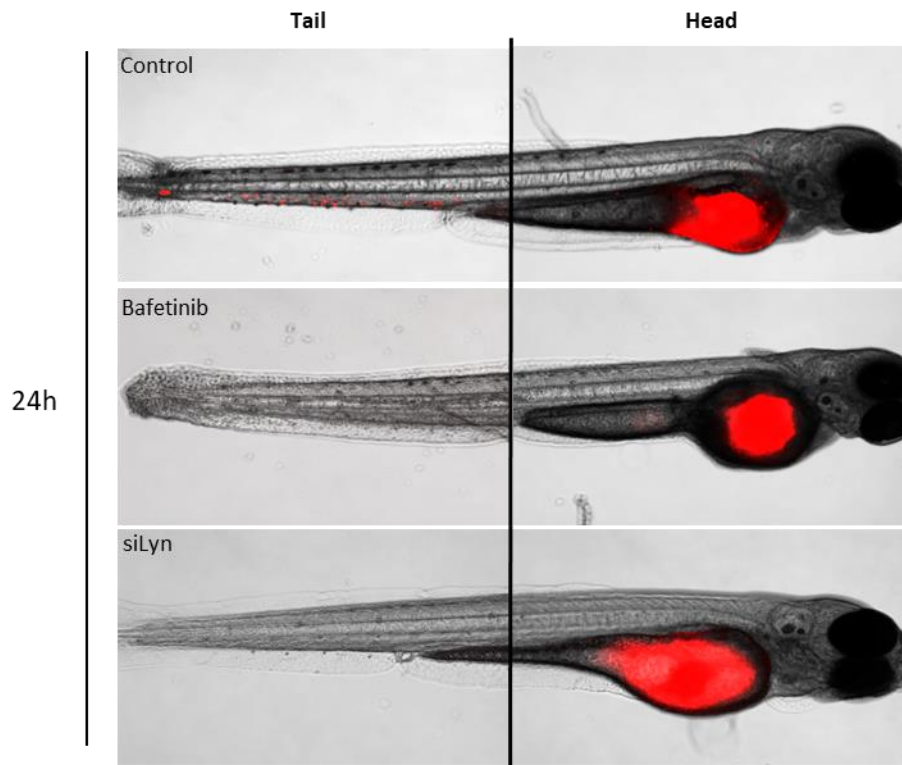


Figure 3.26 - Inhibition of *LYN* reduces in vivo cell migration and invasion:

Representative image illustrating overlay of Bright-field and fluorescent live images of the head and tail of embryos at 24h shown (n = 15–20 embryos). Embryos were treated with 5 μ M of Bafetinib for the duration of the experiment.

This effect became more drastic at 48 hours (**Fig 3-27**). By contrast, embryos injected with siLYN treated BT549 cells or Bafetinib treated embryos showed only low-moderate numbers of cells migrated at both twenty-four (**Fig 3.26**) and 48 hours (**Fig 3.27**).

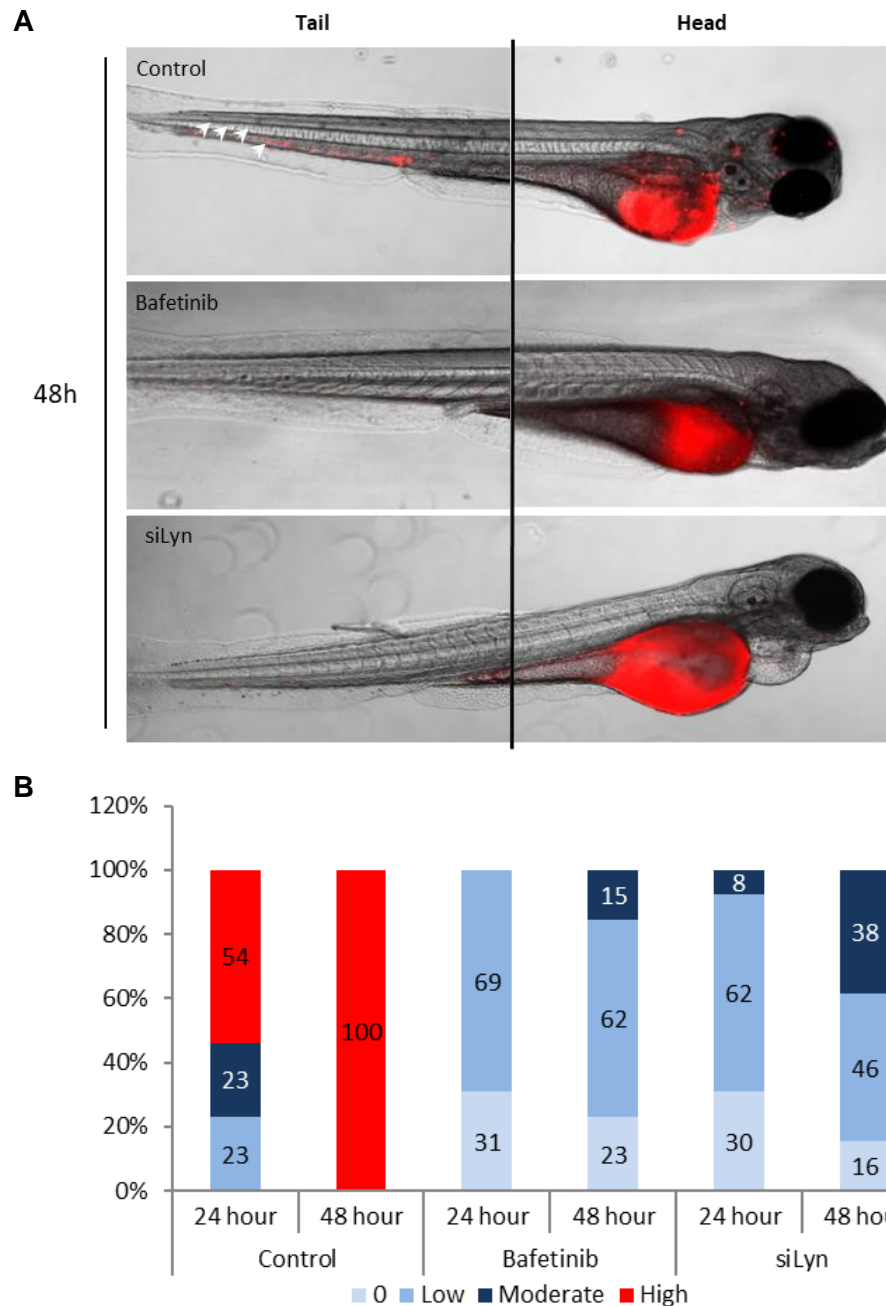


Figure 3.27 - Inhibition of *LYN* reduces *in vivo* cell migration and invasion:

(A and B) BT549 cells \pm siLYN were labeled with Vybrant Cm-Dil and injected into 48-hr post-fertilization casper zebrafish embryos. **(A)** Overlay of Bright-field and fluorescent live images of the head and tail of embryos at 48h shown (n = 15–20 embryos). Embryos were treated with 5 μ M of Bafetinib for the duration of the experiment. **(B)** Migration/Invasion of BT549 cells to regions outside the yolk sac where **Low = 1-20, Moderate = 21-40 and High = >40 cells.**

Moreover, the control fish also had a much lower survival rate when compared to the treatment arms (**Fig 3.28**) as the cancer cells seem to clog-up the blood vessels in the embryo.

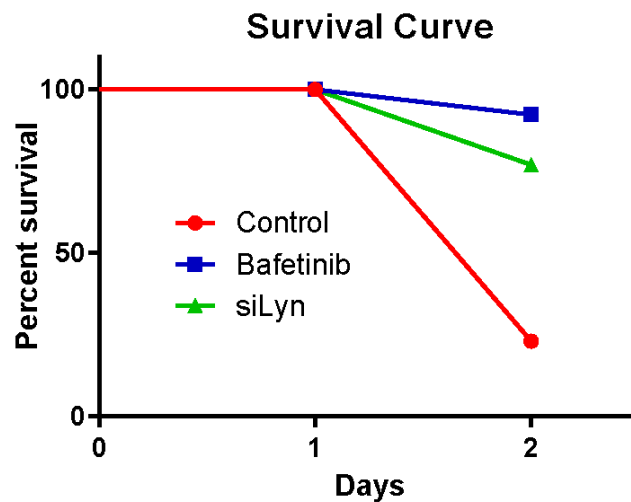


Figure 3.28 - Inhibition of *LYN* reduced metastasis induced embryo mortality:
Survival Curve for Zebrafish in each arm of the experiment from Figure 3-26 and 3-27

Second, we used an *in vivo* orthotopic BICa model with highly invasive UC-13 cells, which have been shown to metastasize from the primary tumor site *in vivo* (185). UC-13 luciferase expressing BICa cells transfected with sh-control or sh-*LYN* were tested for their expression of EMT markers, SNAI proteins and invasion and migration capacity *in vitro* (**Fig. 3.29**).

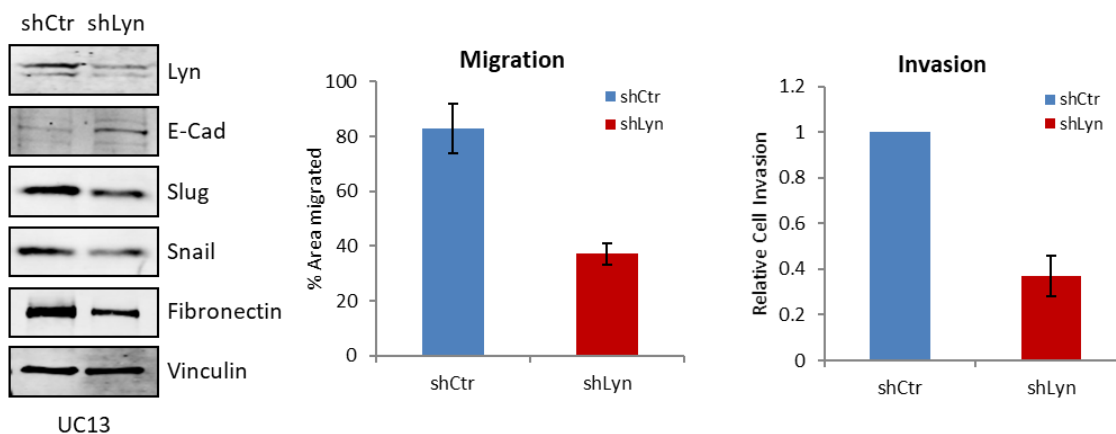


Figure 3.29 - Stable K/O of *LYN* reduces EMT in UC13 BICa cells:

UC-13 cells transfected with *LYN* shRNA: *Left Panel* - Western Blot analysis of indicated genes. *Middle Panel* - Percent area migration from time zero assessed in one dimensional 18h for UC-13 cells. *Right Panel* - Relative number of cells migrated through Matrigel Boyden chamber after 24h.

These cells were then implanted orthotopically into the bladder of female nude mice and tumor growth was monitored by IVIS imaging over 5 weeks. We observed no significant difference in the average bioluminescence or weight of primary bladder tumors formed by sh-*LYN* UC-13 cells vs. sh-control (**Fig. 3.30 A-C**).

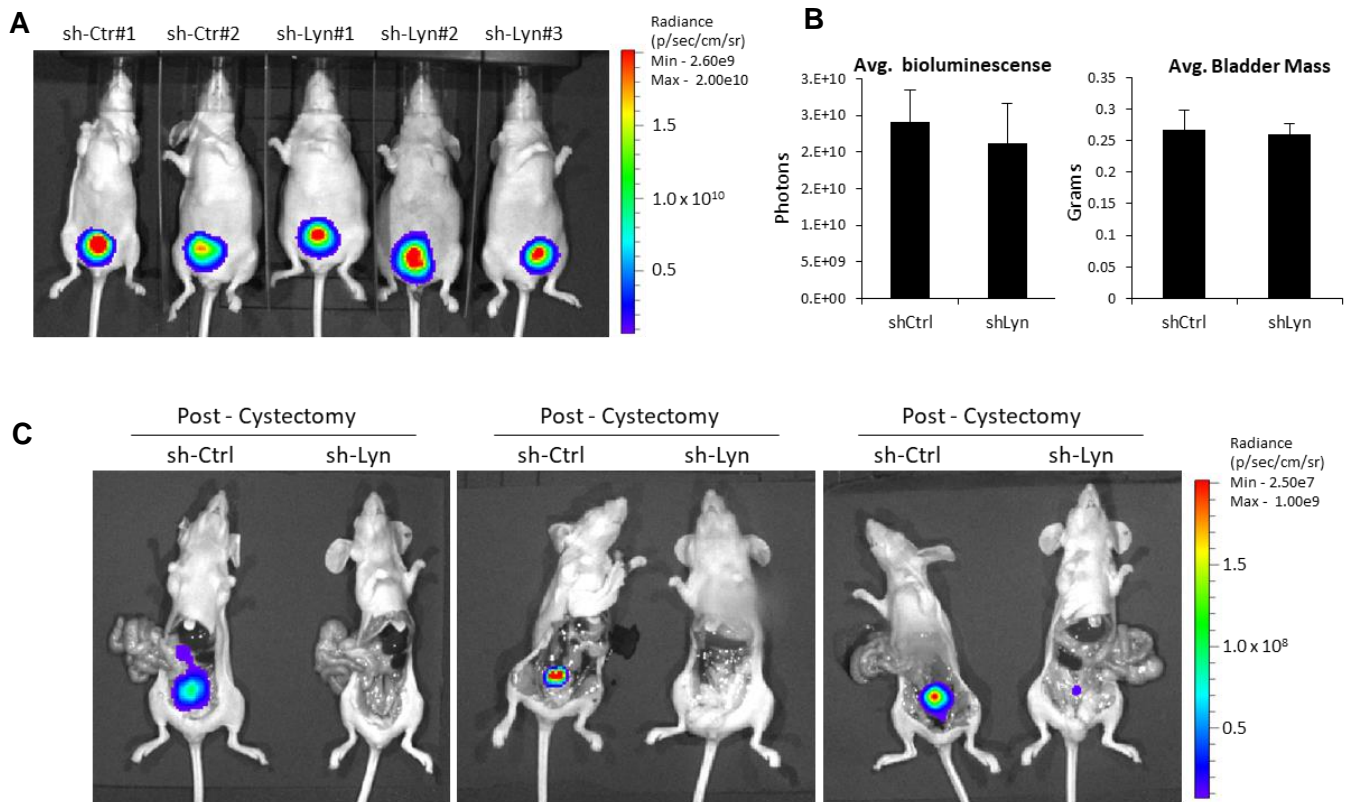


Figure 3-30 - Targeting *LYN* reduces in vivo metastasis in orthotopic BICa model:

(A) Bioluminescence from orthotopic bladder xenograft of UC13-luciferase cells transfected with shCtrl (n=10) and sh*LYN* (n=7): Representative image of the 17 mice (*Left Panel*), (B) average bioluminescence (*Middle Panel*) and average bladder mass (*Right Panel*). (C) Representative images showing metastatic dissemination via bioluminescence of shCtrl and sh*LYN* cells from the primary tumor (*TopPanel*) and average Bioluminescence of the abdomen post-cystectomy (*Bottom left*). Representative image of macroscopic metastasis of shCtrl and sh*LYN* cells from the primary tumor (*Bottom middle*) and average macroscopic metastasis per mouse, shCtrl (n=10) and sh*LYN* (n=7) (*Bottom right*).

However, upon removal of the primary tumor and re-imaging to identify tumors in metastatic sites, we found a significant reduction in bioluminescence from metastases (**Fig. 3.31**) as well as macroscopic metastases in sh-*LYN* tumor bearing mice compared to control (**Fig. 3.31**).

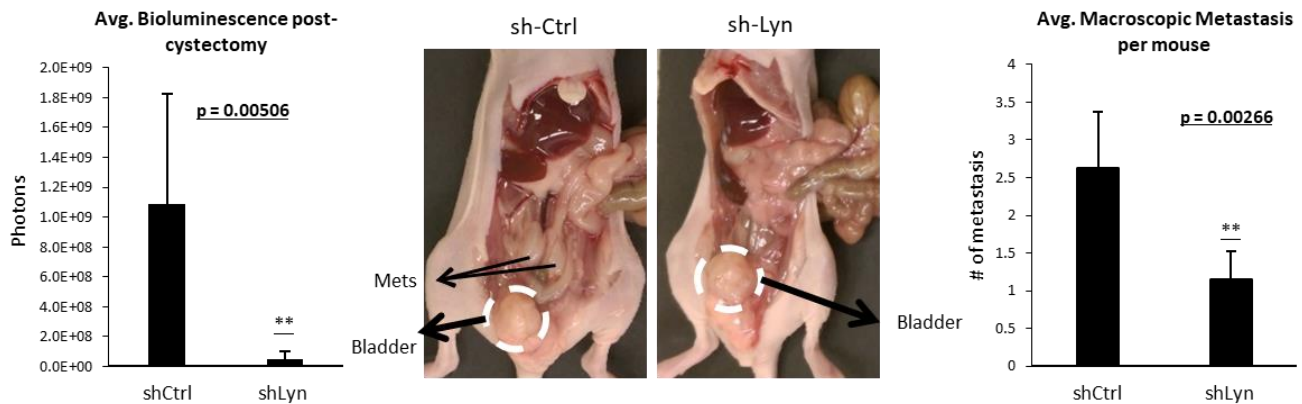


Figure 3.31 - Targeting *LYN* reduces in vivo metastasis in orthotopic BICa model:

Average Bioluminescence of the abdomen post-cystectomy (*left*). Representative image of macroscopic metastasis of shCtrl and sh*LYN* cells from the primary tumor (*middle*) and average macroscopic metastasis per mouse, shCtrl (n=10) and sh*LYN* (n=7) (*right*).

Interestingly, WB analysis of the tumors revealed that the primary tumors maintained their *LYN* K/O; however, metastatic tumors from the sh*LYN* arm recovered their levels of *LYN* (**Figure 3.32**). Additionally, these metastatic tumors recovered their levels of Slug and Fibronectin, lost their E-cadherin and showed no significant difference in their expression of Ki67 (**Figure 3.32**). Taken together, our results show that targeting *LYN* can diminish the metastatic capability of primary tumors.

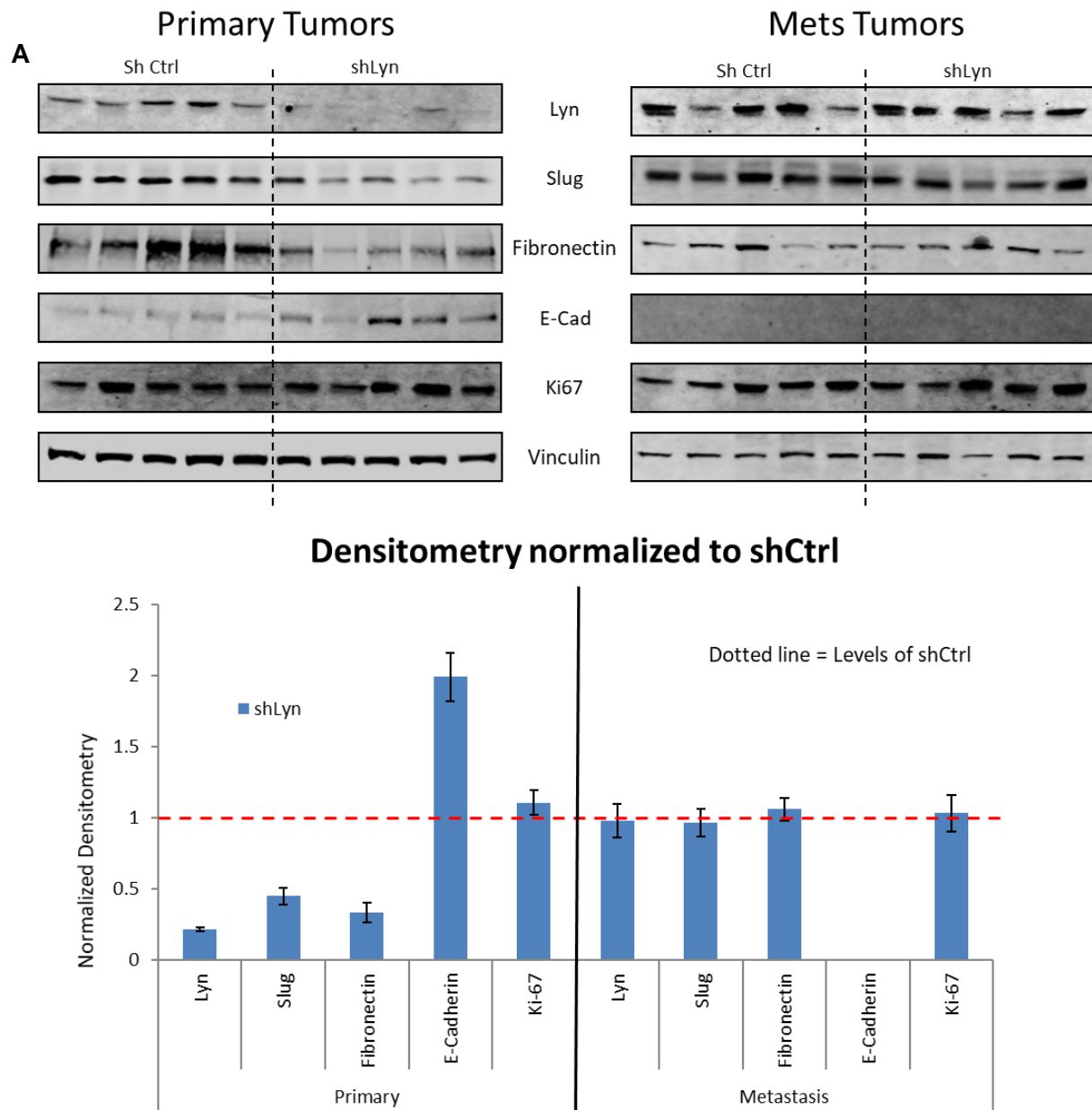


Figure 3.32 - *LYN* expression is recovered at metastasis:

(A) Frozen primary tumor samples and metastatic tumor samples) were lysed with T-PER lysis buffer. The lysed samples were subject to Western Blot analysis. **(B)** Average densitometry for both the primary and the metastatic tumors were normalized to the average shCtrl signal for each antibody. Signal was calculated using ImageJ software.

3.4. Discussion

Metastasis is the cause of approximately 90% of cancer related deaths (253). Epithelial-Mesenchymal Transition (EMT) and Mesenchymal-Epithelial Transition (MET) are transient physiological events that are central for tumor metastasis, however identifying a clinically relevant and targetable mechanism that controls these dynamic processes has been elusive. One potential candidate is the *LYN* tyrosine kinase, which we demonstrate is a central upstream regulator of several different potent metastasis inducers; RAC1, PAK1, Slug and Snail. We show for the first time that *LYN* regulation of VAV1 in cancers activates the RAC1-PAK1 kinase cascade to stabilize Slug and Snail, allowing them to initiate transcription of EMT genes. Our mechanism of EMT regulation by *LYN* is supported in human cancer data showing mutually exclusive expression of *LYN* and E-Cadherin, and our results showing the requirement for *LYN* in supporting metastasis *in vivo* is mirrored across multiple cohorts of prostate, breast and bladder cancers. This work underscores the role of *LYN* in promoting tumor progression and highlights it as a therapeutic target for advanced disease.

Multiple studies have shown an association between increased *LYN* kinase expression and poor outcomes in cancer (197) or a mesenchymal phenotype in cancer cell lines (223, 224, 254), however, a well-defined relationship between *LYN* expression and human tumor metastasis, or the mechanisms governing metastasis, such as EMT, have not been explored. Using variety of *LYN* gain and loss of function experiments in *in vitro* models of PCa, BrCa and BICa, we are the first to show *LYN* controls EMT by stabilizing the E-Cadherin repressors Slug and Snail, and the transcription of EMT associated proteins. Accordingly, elevated *LYN* expression and kinase activity enhanced the migration and invasion of cells *in vitro*, and *LYN* was required for metastasis of BICa *in vivo*. Our *in vivo* data are further supported by a recent studies showing reduced metastasis in spontaneous TRAMP PCa (255) and TNBC (256) *in vivo* models after *LYN* knockout or inhibition. More importantly however, they are supported by data from multiple human tumors showing significantly higher *LYN* expression is found in metastatic PCa, BrCa and BICa tumors, and that *LYN* expression correlates with expression of Vimentin, Fibronectin and N-Cadherin in these cancers.

Like all Src family members, *LYN* has a kinase domain along with two protein interaction domains, a SH2 and a SH3 domain(197). Several reports have implicated *LYN* as a mediator for protein stability. This can occur through its kinase activity (213), as well as its protein interaction SH3 domain (257). Using mutant *LYN* expression (CA or KD) as well as a more selective *LYN* inhibitor, Bafetinib, we were able to show that *LYN* kinase activity and not the

SH3 domain is regulates expression of SNAI transcription factors; specifically, we discovered *LYN* controls Slug and Snail expression post-translationally, by preventing their ubiquitination and proteasomal degradation. These results support previous data showing drastic changes in protein, but non mRNA, expression of Slug and Snail proteins, underscoring their potentially unstable nature and the importance of protein-protein interactions that modulate their degradation (130, 258). Among these are phosphorylation events of Slug/Snail at the phosphodegradon, mediated by GSK3 β (247, 259), phosphodegradon-independent ubiquitination by both the FBXL14 ubiquitin ligase (260) as well as the p53WT and MDM2 ubiquitin ligase complex (261),. Importantly however, ubiquitin-ligase dependent mechanisms of Slug and Snail degradation require their cytoplasmic localization and p-GSK3 β was not altered with *LYN* over-expression and inhibition. These results suggested that *LYN*-dependent control of Slug and Snail stability was through alternative mechanisms.

Indeed, we found that *LYN* kinase activity indirectly triggers a signaling cascade concluding in the phosphorylation and activation of PAK1, which is known to shuttle Snail to the nucleus upon phosphorylation at S246 (132). Not surprisingly therefore, PAK1 and its upstream regulator, the RAC1-GTPase, are both well established modulators of cell migration, invasion and metastasis (262, 263) and PAK1 is consistently upregulated in invasive human BrCa tumors (264). Based on reports showing *LYN* can activate the RAC1-GTPase GTP exchange factor VAV1 by phosphorylation (265), we hypothesized that *LYN* may be a key upstream regulator of the VAV1-RAC1-PAK1 to Slug/Snail cascade. Consistent with this hypothesis, we found silencing PAK1 reduces Slug and Snail at protein and not mRNA levels, and that the increase of Slug and Snail from *LYN* over-expression is abrogated if PAK1 is silenced. Importantly, we explain the effect of PAK1 on Slug by showing for the first time phosphorylation on Slug at S251 by PAK1 and its interaction with Slug. Moreover, we showed that *LYN* was required for activation of VAV1 as well as the RAC1-GTPase. While a role for *LYN* in activating VAV1 has been established in platelets (265), macrophages (266) and lymphocytes (267), it has not been shown in solid cancers, nor linked to downstream mechanisms by which EMT may be regulated. Therefore, our results illustrate a novel role for the *LYN* kinase in regulating the VAV1-RAC1-PAK1 pathway to modulate the sub-cellular localization and stability of the SNAI family transcription factors, which initiates EMT.

Our work has established the clinical relevance of *LYN* in tumor metastasis as well as delineated the mechanism by which *LYN* kinase modulates EMT in models of multiple human cancers, suggesting *LYN* may be a rational therapeutic target, not only in treatment refractory leukemia, where Bafetinib (INNO-406) has shown efficacy (225), but also in epithelial cancers.

In particular, our data supports the use of *LYN* specific inhibitors in cancer patients with solid tumors to prevent metastasis. Analysis of phase II trials in hormone refractory prostate cancer and advanced glioblastoma (NCT01234740, NCT01215799) will indicate whether *LYN* inhibition prevented disease spread in advanced cancer patients. It is likely that multiple pathways simultaneously drive tumor metastasis; however, with the advent of personalized medicine and advanced genomics, pre-identification of metastasis effectors like *LYN* allows us to be better prepared for implementing successful combination treatment regimens in an attempt improve patient survival.

4. Chapter 4: *The master neural transcription factor BRN2 is an Androgen Receptor-suppressed driver of neuroendocrine differentiation in Prostate Cancer*

4.1. Background

4.1.1. POU family transcription factor: BRN2

All POU family transcription factors contain a POU_S domain followed by a POU_H domain with each containing their own helix-turn-helix motif (HTH) that recognizes DNA (268). As a family, these proteins are ubiquitously expressed and different family members play important roles in guiding development of different organs. While the POU domains are highly conserved between the family members, the linker region between the two domains is highly variable and flexible. This creates variability between the two domains and differentiates the DNA binding capabilities of the POU family members. The binding element for POU family members is a palindromic Oct factor recognition element (PORE) comprised of slightly variable palindromic repeat of the basal Oct factor sequence 5' – ATGC(A/T)AAT – 3' (269). The POU_S domain recognizes the “ATGC” sequence while the “AAAT” sequence binds to the POU_H domain. Since each POU domain retains independent DNA binding capabilities, these two halves of the octamer sequence bind in several different orientations (**Figure 4.1**).

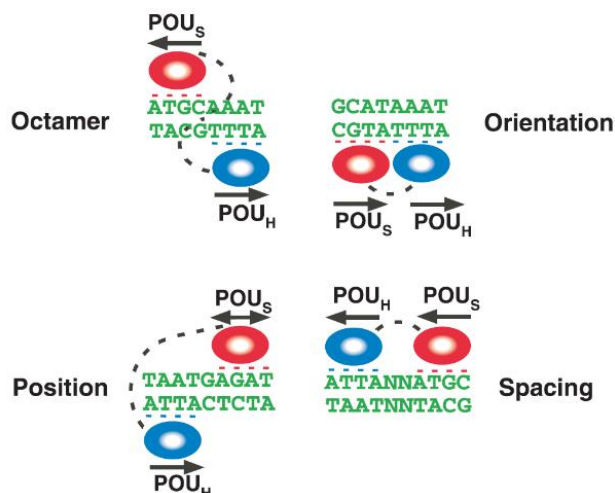


Figure 4.1 - Binding orientation of POU domains:

Binding of the POU_S and POU_H domains across the sense and anti-sense strands of DNA in several different orientations. Extracted from Cook et al. 2008 (Pigment Cell & Melanoma Research) with permission from publisher Wiley.

The flexibility of the linker region permits use of More PORE sites (MORE) that contain extra base pairs between the recognition half-sites, thus adding another layer of complexity to

the binding elements POU proteins recognize (270, 271). In addition to these three recognition elements, BRN2 aka N-Oct-3 also recognizes N-Oct-3 recognition elements (NORE) (**Figure 1.5**). This element allows for non-cooperative dimerization between two BRN2 proteins and the POU_S domains overlap binding on both strands of DNA at a recognition site (272).

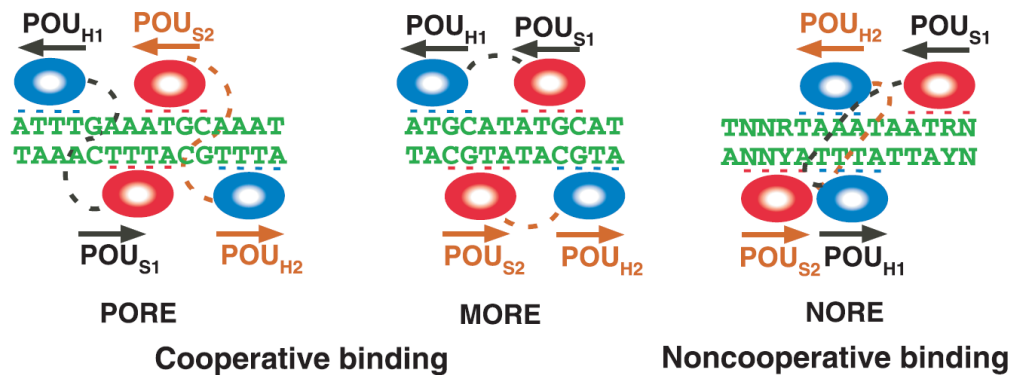


Figure 4.2 - Binding orientation of PORE, MORE and NORE sites with POU domains:

Reported binding orientations of BRN2 dimers. Extracted from Cook et al. 2008 (Pigment Cell & Melanoma Research) with permission from publisher Wiley.

In 2013, Ladato et al. published one of the first studies that comprehensively characterized BRN2's DNA binding capabilities. The authors examined how BRN2 and SOX2 co-operate to govern differentiation from embryonic stem cells (ESC) to neural progenitor cells (NPC) (273). The authors found that ectopic expression of BRN2 in ESCs was sufficient to alter SOX2 cistrome away from its ESC binding with partner OCT4 (*POU5F1*). Furthermore, Urban et al. conducted an in-depth analysis of BRN2 binding to these three elements and discovered that unsurprisingly, BRN2 binding partners modulate differential binding to these elements (274). The authors discovered that in addition to SOX2, BRN2 also co-operates with Zic1 in mouse ESCs to regulate crucial genes for neuronal differentiation. This publication further confirmed that in ESCs BRN2 primarily recognizes the basal Octamer, MORE and NORE motifs (274). The repertoire of binding elements combined with the differential expression of POU family members and their binding partners provides exquisite control over cell lineages both in normal cells as well as in cancers.

4.1.2. Induced Neuronal differentiation

Following the pioneering work from Dr. Shinya Yamanaka, the capacity of terminally differentiated cells to reprogram to a different lineage is a very active area of research (275). This reprogramming is expected to aid in treatments of several diseases and understanding the relevance of these processes in cancers may bear unexpected fruit. For neuronal

reprogramming, Wernig and colleagues from Stanford reported that ectopic introduction of a combination of 3 transcription factors BRN2, ASCL1 and MYTL1 (BAM) could efficiently convert mouse embryonic fibroblasts (MEF) into induced neurons (iN) (276). More recently, this experiment was repeated with dCAS9-VPR64 fusion protein and guide RNA (gRNA) that allows for activation of endogenous BAM factors to convert fibroblasts to iN (277). The specific functions of these proteins within this cocktail is an active area of exploration since the initial characterization in 2011 (276). A follow-up paper from Dr. Wernig's lab demonstrated that ASCL1 expression is sufficient to begin differentiation of fibroblasts into iN and they hypothesized that BRN2 and MYTL1 likely just increase the efficiency of the differentiation (278, 279). Wapinski et al. in 2017 validated some of the results by establishing ASCL1 as a pioneer factor with the ability to bind to and open up closed regions of the chromatin (280). A significantly more detailed analysis at a single cell level revealed that while ASCL1 is important to initiate differentiation to iN, unchecked the cells will end up in a myocyte lineage, and BRN2 is crucial in maintenance of the neuronal lineage initiated by ASCL1 (281). Moreover, BRN2 and ASCL1 also co-occupy genomic loci containing important neuronal differentiation and cell proliferation genes. Cooperative binding between these proteins likely initiates differentiation and restricts cell cycle (282).

Independent of chronology, the many papers exploring this field can be summarized as the following:

- ASCL1 is the pioneer factor that alters chromatin dynamics to favour neuronal differentiation.
- Left unchecked, ASCL1 based differentiation ends in a myocyte lineage.
- Co-expression of BRN2 maintains neuronal pathways and suppresses myocyte lineage.
- BAM cocktail remains ideal for inducing neurons from mice embryonic fibroblasts.

It is important to note that these experiments are on mice embryonic fibroblast cells, and not in human embryonic cells. The neuronal development process is very different in humans, for example the neural progenitor population during corticogenesis is expanded to allow for the much larger cerebral neocortex that defines human beings and their mental capacity (283). The maturation process of the neurons is tightly controlled and Karakhanyan et al. demonstrated that in addition to the suppression of REST, BRN2 expression combined with knockdown of mRNA binding protein PTBP2 can create functional mature neurons from human embryonic fibroblasts (284). Additionally, the induction of neurogenic program by micro-RNA 124 is

significantly more efficient in combination of BRN2 over-expression (285). The lack of requirement for ASCL1 in differentiation of human neurons identifies an interesting discrepancy that requires further investigation; however, the research consolidates the role of BRN2 in neuronal differentiation of human cells.

4.1.3. Roles of BRN2 in other cancers

While the variability in binding sequences and binding partners hints at different phenotypic results, across several cancers, the over-arching role of BRN2 is surprisingly consistent. BRN2 expression allows differentiated epithelial cells to climb up the differentiation ladder to a more primitive “plastic” state. Considerable evidence exists in both melanoma (286, 287) and glioblastoma (288, 289) that BRN2 expression promotes a slow proliferating cancer stem cell or tumor initiating cell phenotype.

Many studies have validated the inverse relationship between BRN2 and Melanogenesis Associated Transcription Factor (MITF) as a possible driving force of “phenotype switching” observed in heterogeneous melanoma tumors (290). The current model states that melanoma cells switch between a proliferative state driven by MITF and an invasive state driven by BRN2 (286). The invasive state of these cancer cells is accompanied by reduced proliferation and increased tumor initiating capacity. Numerous studies have demonstrated that while knockdown of BRN2 doesn’t affect melanoma cell proliferation, it severely reduces their ability to metastasize and initiate tumors (291, 292). Similar to BRN2, slow-cycling melanoma cells express higher levels of histone demethylase JARID1B. Knockdown of JARID1B initially switches cells to a higher proliferative state, but drastically reduces their tumor initiating capacity *in vivo* (293). While they both may serve as a driver of this plastic melanocyte state, the relationship between BRN2 and JARID1B is yet to be elucidated.

Due to its involvement in neuronal differentiation, the importance of BRN2 in glioblastoma was not entirely surprising. Through a series of elegant experiments, in 2014 Suva et al. demonstrated that BRN2 was part of a 4 necessary transcription factors (SOX2, OLIG2 and SALL2) to maintain CD133⁺ glioblastoma stem cells that had potent tumor initiating capabilities (289). The authors showed that while BRN2 and or SOX2 can enrich the stem cell population, the combination of these 4 TF created an over 50% population of CD133⁺ cells that retained tumor initiating capacity *in vivo* with as little as 50 cells (289). Furthermore, while BRN2 has not been explicitly studied in other brain related cancers, it is highly expressed in Medulloblastoma, Glioma and Neuroblastoma (**Figure 4.3**). Interestingly, data from Figure 4.3 also shows high expression of BRN2 in several small cell cancers like Ewing’s Sarcoma, SCLC

and the previously mentioned Medulloblastoma and Neuroblastoma. Several previous studies have shown that BRN2 is highly expressed in SCLC, where it acts upstream of other key regulators of neural programming and is required for aggressive tumor growth (294, 295). BRN2 is also among the top differentially expressed genes between Osteosarcoma and EWS-FLI fusion Ewing's Sarcoma (296). More detailed studies are required for understanding the role of BRN2 in these small/blue cell cancers, and in Ch2 and Ch3 of this thesis, our work explores the essential role of BRN2 in small cell/neuroendocrine prostate cancer (145).

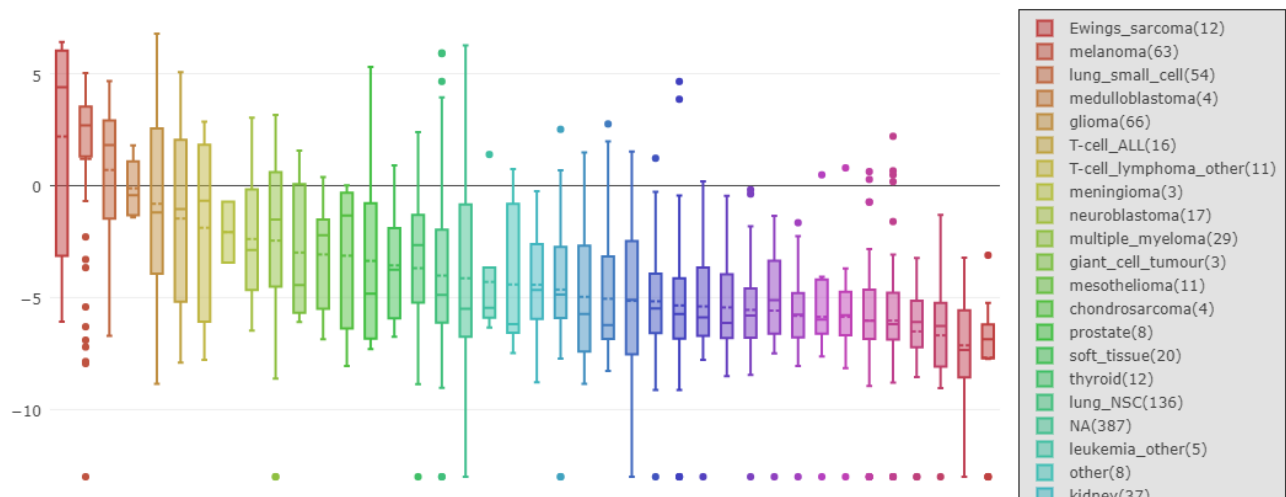


Figure 4.3 - BRN2 expression in other cancers:
Expression of BRN2 in cancer cell lines from the CCLE database.

4.2. Introduction

Progression from primary prostate cancer (PCa) to advanced metastatic disease is heavily dependent on the androgen receptor (AR), which fuels tumor survival. In men where treatments for localized prostate tumors have failed, or in those who present with metastatic disease, androgen deprivation therapies (ADT) are used to deplete circulating androgens to abrogate AR signalling and prevent disease progression. Eventually however, PCa recurs after first-line ADT as castration resistant prostate cancer (CRPC). Despite low levels of serum androgens in men with CRPC, reactivation of the AR occurs; thus it remains central to tumor cell survival, proliferation and metastatic spread. Thus, targeting the AR is a cornerstone therapeutic intervention in CRPC patients and AR pathway inhibitors (ARPIs) that further prevent AR activation, such as enzalutamide (ENZ), have become mainstays in the PCa treatment landscape (297). Despite being a potent ARPI, the treatment benefits of ENZ are short lived in CRPC patients and resistance rapidly occurs (27).

ENZ resistant (ENZ^R) CRPC represents a significant clinical challenge due not only to the lack of third-line treatment options to prevent AR driven tumor progression, but also because it can be a precursor to rapidly progressing and lethal neuroendocrine prostate cancer (NEPC). Although NEPC rarely arises de-novo, it is increasingly defined as a variant of highly ARPI-resistant CRPC (99, 298). Aside from the unique small cell morphology and positive staining for neuroendocrine (NE) markers that characterize NEPC, it is often distinguished from prostatic adenocarcinoma by reduced AR expression or activity (299). Clinical presentation of NEPC reflects this shift away from reliance on the AR, as patients typically present with low circulating levels of prostate specific antigen (PSA) despite high metastatic burden in soft tissues, and are refractory to APIs (298). Importantly, it has been reported that under the strong selective pressure of potent APIs like ENZ, these “non-AR driven” prostate cancers, which include NEPC, may constitute up to 25% of advanced, drug resistant CRPC cases (300). Not surprisingly therefore, the incidence of NEPC has significantly increased in recent years (301), coinciding with the widespread clinical use of APIs.

A number of molecular mechanisms likely facilitate the progression of CRPC to NEPC. These include loss of tumor suppressors like RB1 (302, 303) and p53 (304), amplification of n-Myc (1), mitotic deregulation through AURKA (1) and PEG10 (122), epigenetic controls such as REST (305-307) and EZH2 (1, 308) and splicing factors like SSRM4 (306, 309). Importantly, the AR plays a crucial, albeit still mechanistically unclear, role in NEPC. Reports over many years have highlighted how ADT (310, 311) or loss of AR promotes the NE differentiation of prostate cancer cells (reviewed in (178)); as such, many genes associated with a NE phenotype, including ARG2 (312), hASH-1 (313) and REST (307, 314) are controlled by the AR. Although this evidence underscores an inverse correlation between AR expression and/or activity and molecular events leading to NEPC, the mechanisms by which the AR directly influence the induction of a NEPC phenotype from CRPC under the selective pressure of APIs like ENZ remain elusive.

Answering such questions requires a model of API resistant CRPC that recapitulates the trans-differentiation of adenocarcinoma to NEPC that occurs in patients. Herein, we present an in vivo derived model of ENZ^R, which is different to others (92, 315, 316), and underscores the emergence of tumors with heterogeneous mechanisms of resistance to ENZ over multiple transplanted generations. These include the natural acquisition of known AR mutations found in ENZ^R patients (104, 105, 316, 317) and the transdifferentiation of NEPC-like tumors through an AR⁺ state, without the manipulation of oncogenes typically used to establish NEPC in murine PCa models (142, 318, 319). Using this model and human PCa patient data, we show that a

master regulator of neuronal differentiation, the POU-domain transcription factor BRN2 (POU3F2) (320), is directly transcriptionally repressed by the AR, is required for the expression of terminal NE markers and aggressive growth of ENZ^R CRPC, and is highly expressed in human NEPC and metastatic CRPC with low circulating PSA. Beyond suppressing BRN2 expression and activity, we also show that the AR inhibits BRN2 regulation of SOX2, another transcription factor associated with NEPC. These results suggest that relief of AR-mediated suppression of BRN2 is a consequence of ENZ treatment in CRPC that may facilitate the progression of NEPC, especially in men with “non-AR driven” disease.

4.2.1. Emergence of AR-driven and non- driven tumors in ENZ^R CRPC

To model ENZ resistant (ENZ^R) disease, we developed cell lines from LNCaP-CRPC and ENZ^R LNCaP-CRPC xenograft tumors. LNCaP cells were used to establish subcutaneous tumors in intact male athymic nude mice and upon tumor growth and rising PSA, mice were castrated. Once tumors recurred (CRPC) mice were treated with vehicle or 10mg/kg ENZ daily and monitored for tumor growth (Fig. 4.4A).

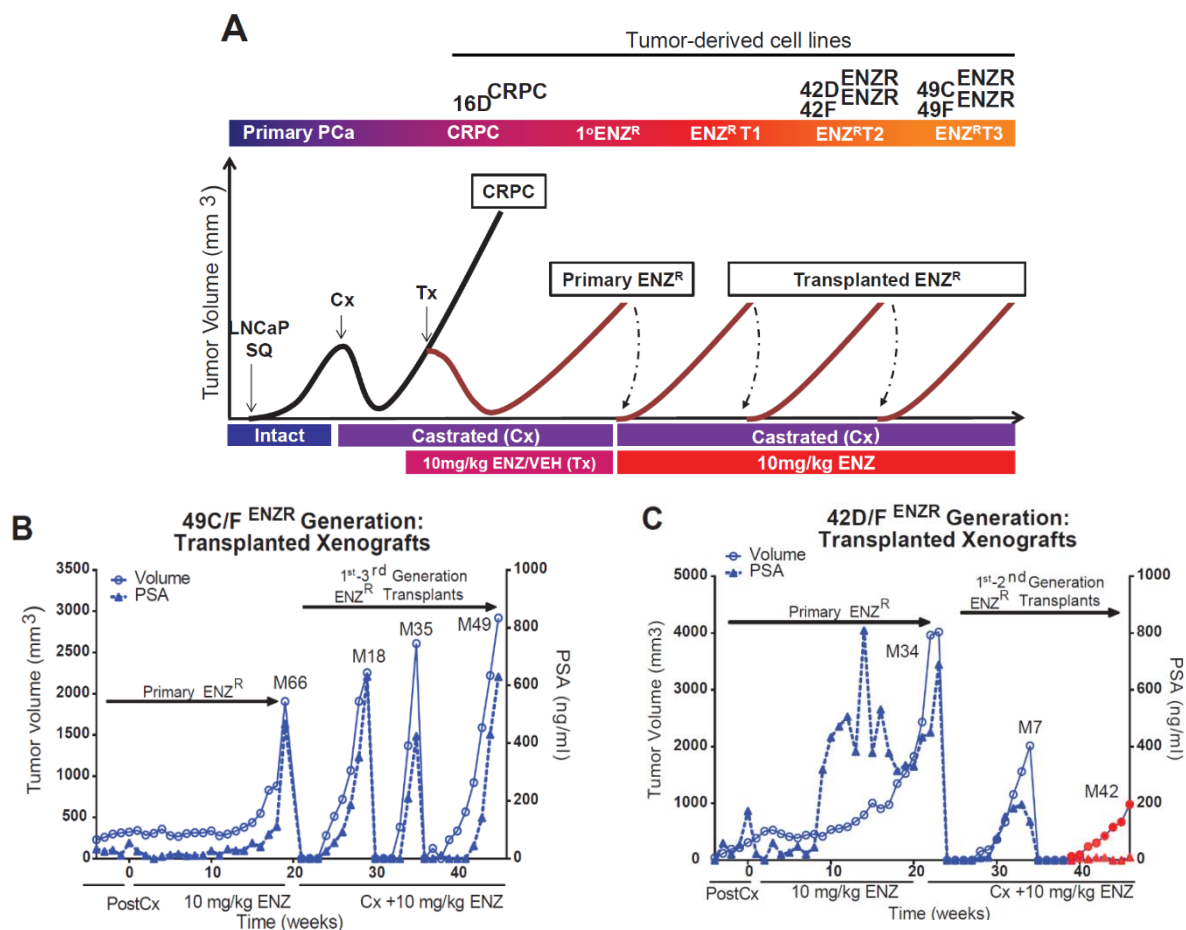


Figure 4.4 - Generation of ENZR Xenografts and Cell Lines:

1x10⁶ LNCaP cells in matrigel were injected subcutaneously into flanks of 6-8 week old athymic male nude mice (LNCaP SQ) and body weight, tumor growth and serum PSA was measured weekly. Once serum PSA reached 50-75ng/ml, mice were surgically castrated (Cx). Upon recurrence of PSA to pre-castration levels, mice were randomized into 2 treatment groups and received either vehicle control or 10mg/kg ENZ daily by oral gavage (Tx). Body weight, tumor growth and serum PSA was monitored weekly until vehicle control treated CRPC, or tumors that recurred in the 10mg/kg ENZ treatment group (1^o ENZ^R) grew to the experimental endpoint. Select primary ENZR (1^o ENZ^R) tumors were excised at the experimental endpoint and tumor sections were allografted subcutaneously into bilateral flanks of castrated 8-10 week old athymic nude mice, which were dosed daily with 10mg/kg ENZ from day of tumor transplant and mice were monitored for growth of transplanted tumors, body weight and serum PSA (ENZ^RT1). Serial transplant of select ENZ^RT1 tumors was repeated for a second and third time (ENZ^RT2 and ENZ^RT3) as above into castrated mice dosed daily with 10mg/kg ENZ. In total, 35 ENZ^R tumors were generated over 3 serial transplant generations from 4 out of 10 primary PSA⁺ ENZ^R tumors. Cell lines were generated from primary CRPC as well as primary and T1-3 transplanted ENZ^R tumors. Specific cell lines used in the manuscript derived from CRPC, primary ENZ^R (1^o ENZ^R) and transplanted ENZ^R (ENZ^RT1-3) tumors are listed as “tumor derived cell lines” in the schematic. Each cell line shown is representative of one line derived from one select tumor at each stage of transplantation. **(B-C)** Growth of exact primary and transplanted tumors grown in individual mice (M66, M18, M35, etc.) that gave rise to **(B)** 49C and 49F ENZ^R cells and **(C)** 42C and 42F ENZ^R cells are shown. Tumors that grew as PSA⁺ are shown as blue lines, PSA⁻ are shown as red (in C, only the tumor in M42 and source of 42D/F cells was PSA⁻). In cell line nomenclature, numbers correspond to mouse number in which transplanted tumors were grown, letters denote the clone.

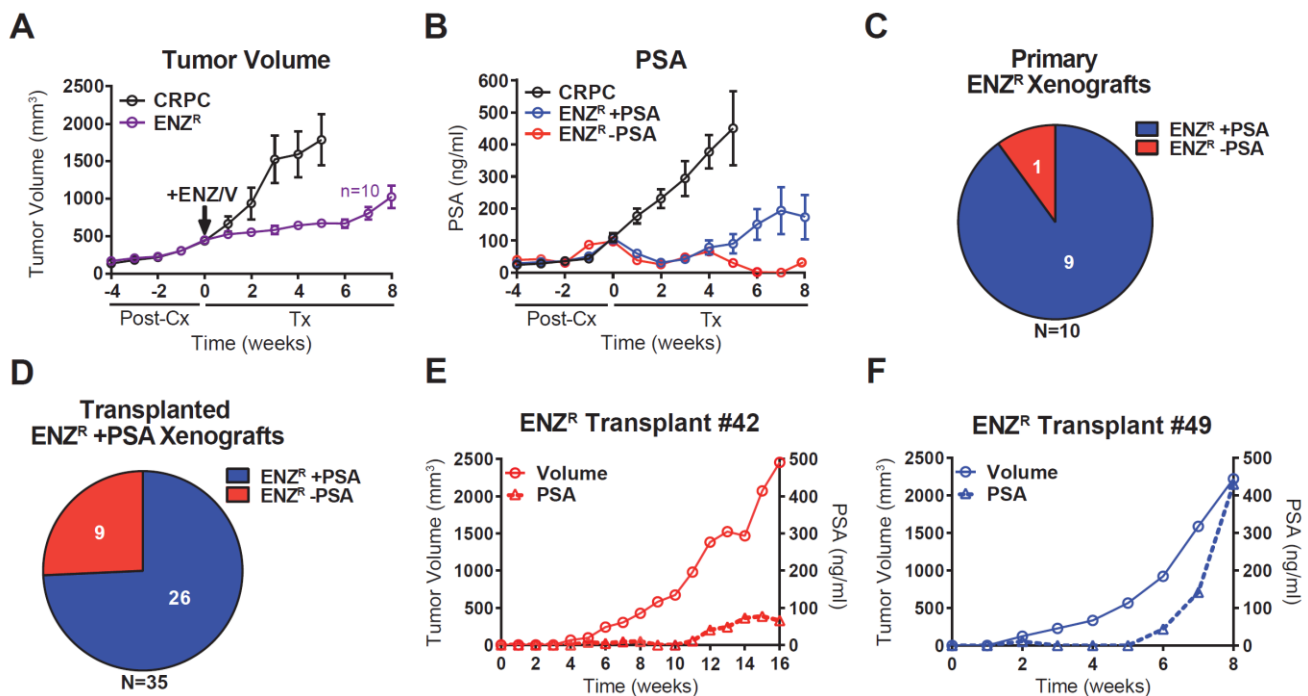


Figure 4.5 - Emergence of AR-driven and non-driven phenotypes in an in vivo model of ENZR CRPC:

(A-B) 1×10^6 LNCaP cells were used to establish primary and castration-resistant prostate cancer subcutaneous xenografts in male athymic nude mice. Graphs show tumor volume and corresponding serum PSA levels of tumors from 4 weeks post-castration. Time 0 represents time at which serum PSA levels reached pre-castration levels and start of treatment with vehicle (V, n=10) or 10mg/kg ENZ (ENZ, n=10). (A) Volumes of 10 vehicle treated CRPC (black line) and 10 ENZ treated (ENZ^R) (purple line) tumors. (B) Black line shows average serum PSA of vehicle treated mice, Blue line represents average serum PSA of 9 out of 10 tumors that recurred in the presence of ENZ (ENZ^R+ PSA) and red line represents average serum PSA of remaining 1 tumor that recurred in the presence of ENZ (ENZ^R- PSA) (n=10 total, represented in purple line from A). (C-D) Fraction of total (C) primary, or (D) transplanted, ENZ^R xenografts that recurred with (blue) or without (red) parallel rise in serum PSA (ENZ^R+/-PSA). (E-F) Tumor volume and serum PSA levels for individual transplanted ENZ^R xenografts (#42 and #49) used to derive ENZ^R cell line clones 42D and 42F or 49C and 49F, respectively.

While ENZ treatment did slow tumor growth compared to vehicle control, it did not prevent tumor recurrence (Fig. 4.5A) and the majority of (9 out of 10, 90%) ENZ treated CRPC tumors increased in tumor volume with concomitant rise in PSA (Fig. 4.5B). Importantly however, PSA was not required for tumor recurrence as observed in one mouse (Fig. 4.5B-C). PSA⁺ CRPC tumors that grew in the presence of ENZ were serially transplanted into castrated male mice treated with 10mg/kg ENZ to establish ENZ^R tumors (Fig. 4.4 A). Similar to the primary CRPC parental xenografts that recurred in the presence of ENZ, the majority (26 out of 35, 74.3%) of transplanted tumors showed increasing volume associated with rising PSA (Fig. 4.5 C). However, over the course of serial transplantation, primary PSA⁺ ENZ^R xenografts also

gave rise to 9 serially transplanted tumors out of 35 (25.7%) that grew without rise in PSA (**Fig. 4.5 D**).

Cell lines were derived from vehicle treated CRPC (referred to as 16D^{CRPC}) and multiple transplanted ENZ^R tumors (referred to as 42D^{ENZ^R}, 42F^{ENZ^R}, 49C^{ENZ^R}, 49F^{ENZ^R}, etc.) and were screened for protein expression of AR and PSA. Reflecting in vivo data, the established cell lines displayed heterogeneous expression of PSA, yet all retained expression of the AR (**Fig. 4.6 A**). Importantly, 42D^{ENZ^R} and 42F^{ENZ^R} cell lines derived from PSA negative tumors (**Fig. 4.4 E, 4.6 C**) remained PSA negative in vitro (**Fig. 4.6 A**), whereas 49C^{ENZ^R} and 49F^{ENZ^R} cells derived from PSA positive tumors (**Fig. 4.4 F, 4.6 C**) retained PSA expression (**Fig. 4.6 A**). Accordingly, sequencing the ligand binding domain (LBD) of the AR revealed the presence of the F878L AR activating mutation in PSA⁺ 49C^{ENZ^R} and 49F^{ENZ^R} cells but not in PSA⁻ 42D^{ENZ^R} and 42F^{ENZ^R} cells (**Fig. 4.6 B**). Emergence of this mutation in only PSA⁺ ENZ^R cells supports previous results showing this alteration mediates resistance to ENZ (104, 105, 316, 317) and suggest that it may be one mechanism by which the AR is reactivated specifically in this subset of ENZ^R cells.

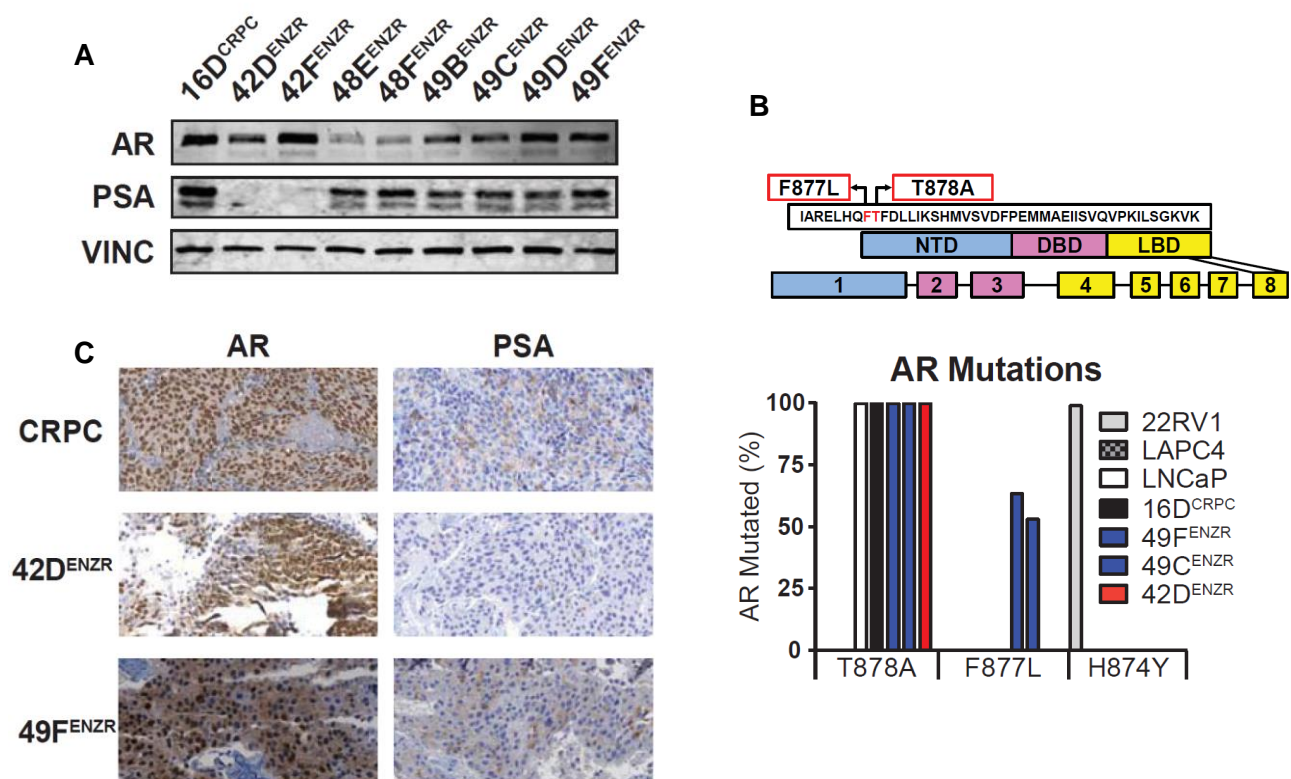
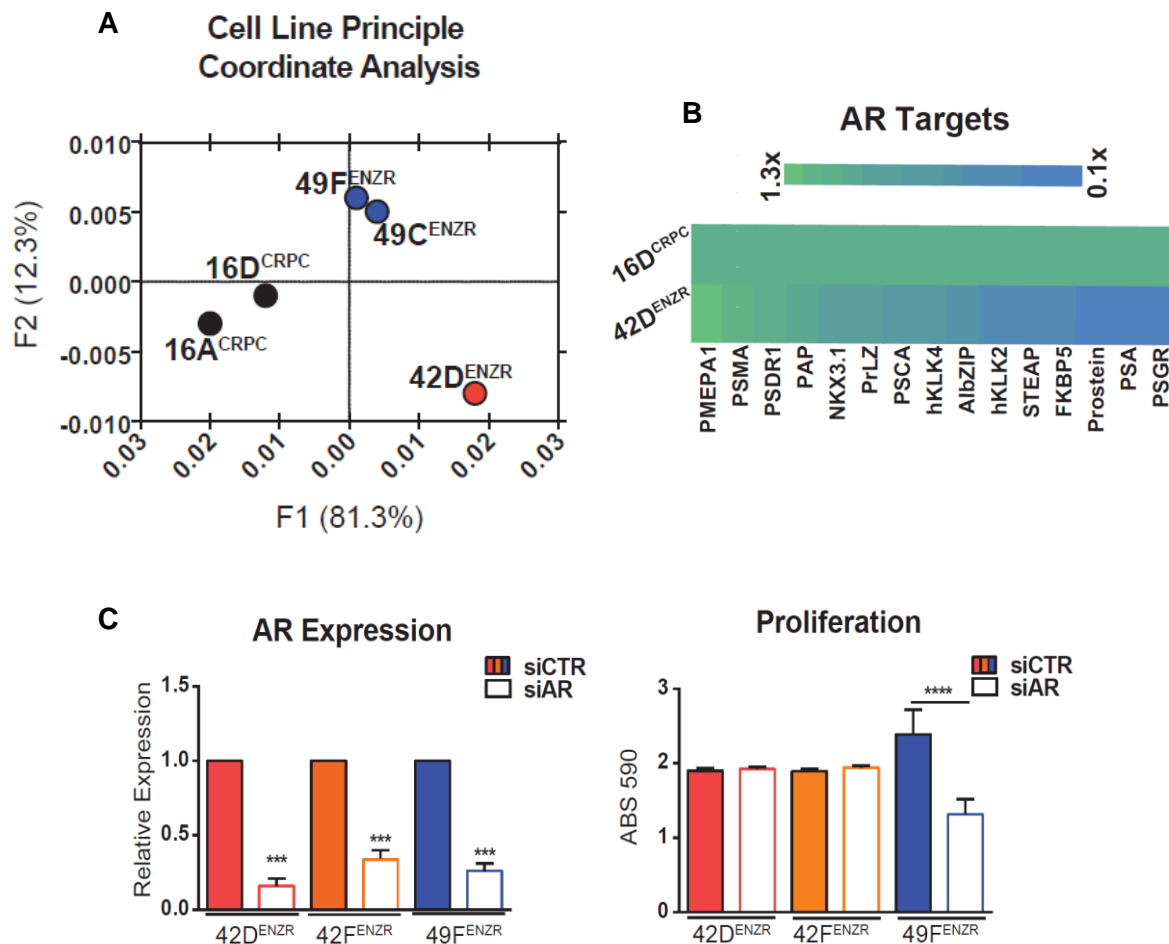


Figure 4.6 - AR status in ENZ^R cell lines:

(A) Protein expression of AR, PSA and VINC in CRPC and ENZ^R cell lines. **(B)** Percent AR mutations in 22RV1, LAPC4, LNCaP, CRPC and ENZ^R cell lines. **(C)** Immunohistochemistry staining of xenograft tumors from Mouse 16, 42 and 49 for AR and PSA.

Mounting evidence suggests that “non-AR driven” phenotypes of PCa can emerge under the selective pressure of potent APIs like ENZ. Importantly, “non-AR driven” tumors are not necessarily negative for AR expression, in fact many retain AR but show reduced AR activity (2). Accordingly, our model of ENZ^R showed approximately 25% of serially transplanted tumors may be non-AR driven (**Fig. 4.5 D**), which is a similar distribution to that seen in clinical reports (300, 321). RNA-seq and microarray analysis (**Fig. 4.7 A, D**) of PSA⁻ ENZ^R cells indicated that these cells exhibited divergence in global RNA expression on principle coordinate analysis from either CRPC or PSA⁺ (“AR-driven”) cells and displayed reduction not only in PSA (*KLK3*), but in many classical AR-regulated genes compared to 16D^{CRPC} cells (**Fig. 4.7 B, E**). Underscoring the AR dependency of AR-driven vs. non-AR driven ENZ^R phenotypes, targeting AR using siRNA significantly reduced cell proliferation in 49F^{ENZ^R} cells, while no effect was observed in 42D^{ENZ^R} and 42F^{ENZ^R} cells (**Fig. 4.7 C**). These data suggest that emergence of ENZ resistance does not require AR re-activation.



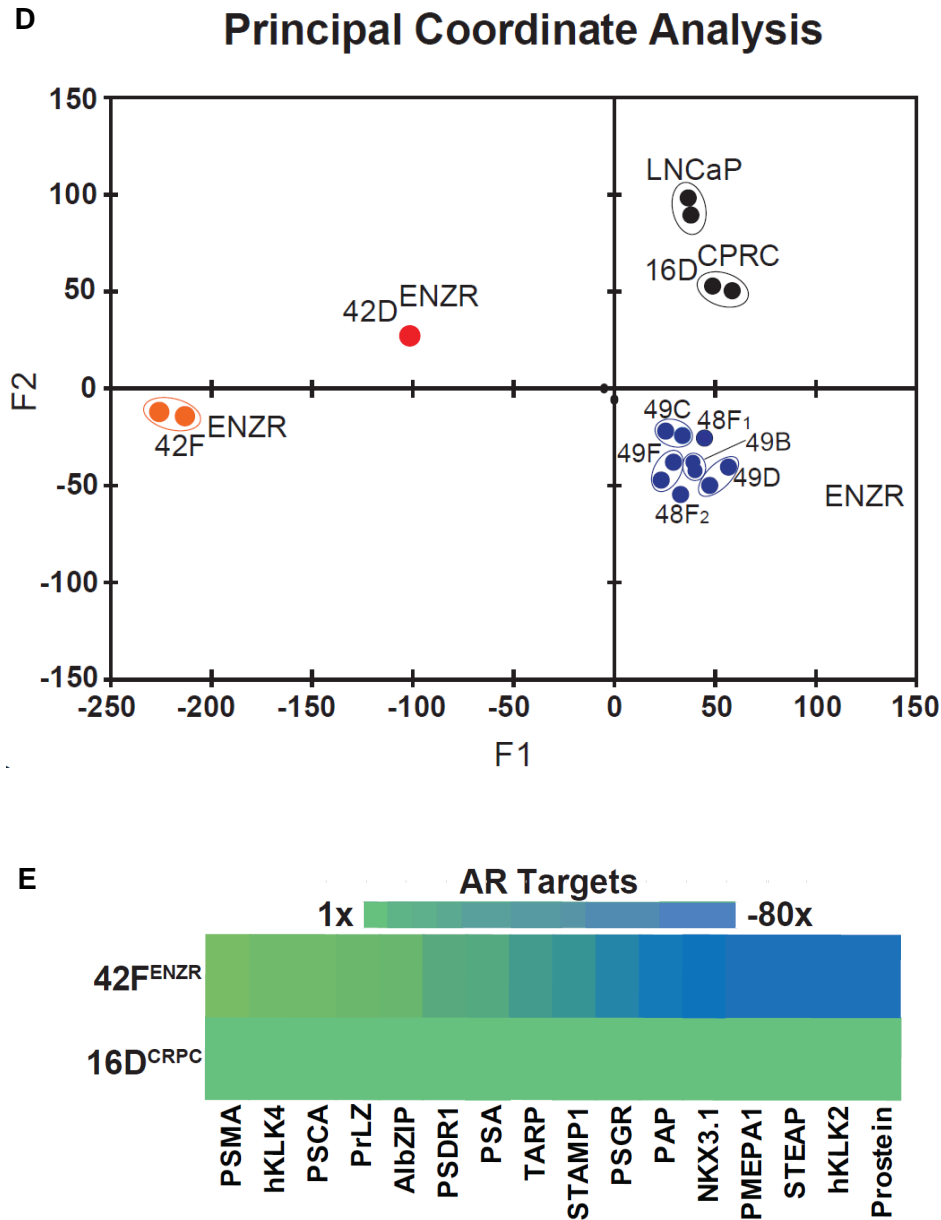


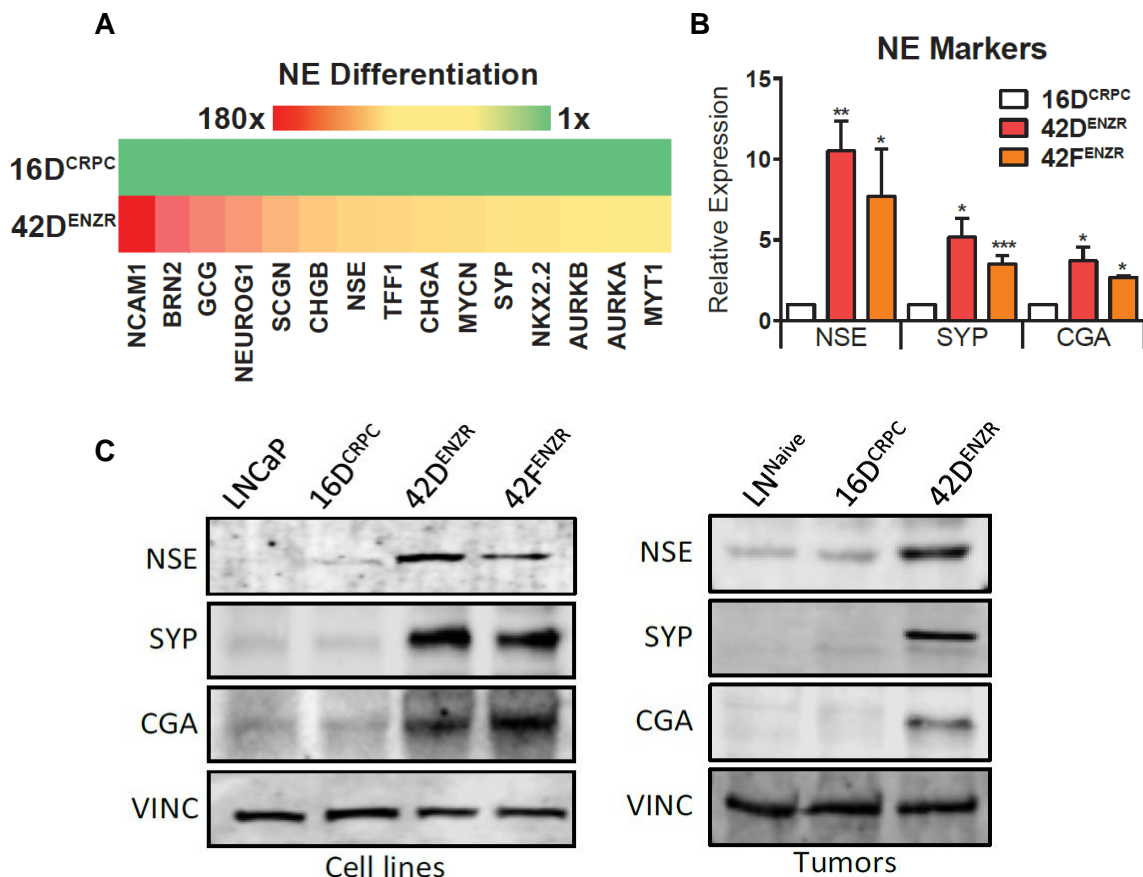
Figure 4.7 - 42D^{ENZR} cells are AR non-driven:

(A) Differences in global RNA expression was determined using multidimensional principle coordinate analysis of RNA sequencing data from CRPC and ENZ^R cell lines. **(B)** Heat map showing fold increase in RNA sequencing reads per million of AR target genes in 42D^{ENZR} cells compared to 16D^{CRPC} (=1). **(C)** Proliferation of “non-AR driven” 42D and 42F^{ENZR} vs. “AR-driven” 49F^{ENZR} 72 hours after seeding in the presence of AR knockdown (siAR) compared to control (siCTR) measured by absorbance. **(D)** Differences in global gene expression were determined using multidimensional principle coordinate analysis of gene profiling data from CRPC and ENZ^R cell lines. **(E)** Heat map showing fold increase in gene expression profiling analysis of AR target genes in 42D^{ENZR} cells compared to 16D^{CRPC} (=1).

4.3. Results

4.3.1. The neural transcription factor BRN2 is highly expressed in NE-like ENZ^R and in human NEPC

Our data analysis revealed that 42D^{ENZ^R} and 42F^{ENZ^R} cells exhibited reduced expression of classical AR target genes. Additionally, 42D^{ENZ^R} and 42F^{ENZ^R} cells showed increased expression of canonical transcription factors and markers associated with neuronal development and NEPC (299), such as neuron specific enolase (NSE), synaptophysin (SYP), chromagranin A (CGA, gene code CHGA) and neural cell adhesion marker 1 (NCAM1) (**Fig. 4.8 A**). The increased expression of each of these terminal NE markers was validated at the mRNA (**Fig. 4.8 B, D**) and protein level (**Fig. 4.8 C**) in 42D^{ENZ^R} and 42F^{ENZ^R} cell lines and in tumors compared to CRPC controls. Significantly increased surface expression of NCAM1 on 42D^{ENZ^R} and 42F^{ENZ^R} cells compared to 16D^{CRPC} cells was confirmed by flow cytometry (**Fig. 4.8 E**). Importantly, 42D^{ENZ^R} cells were also enriched with NEPC score genes and have reduced expression of AR score genes (**Fig. 4.8 F**).



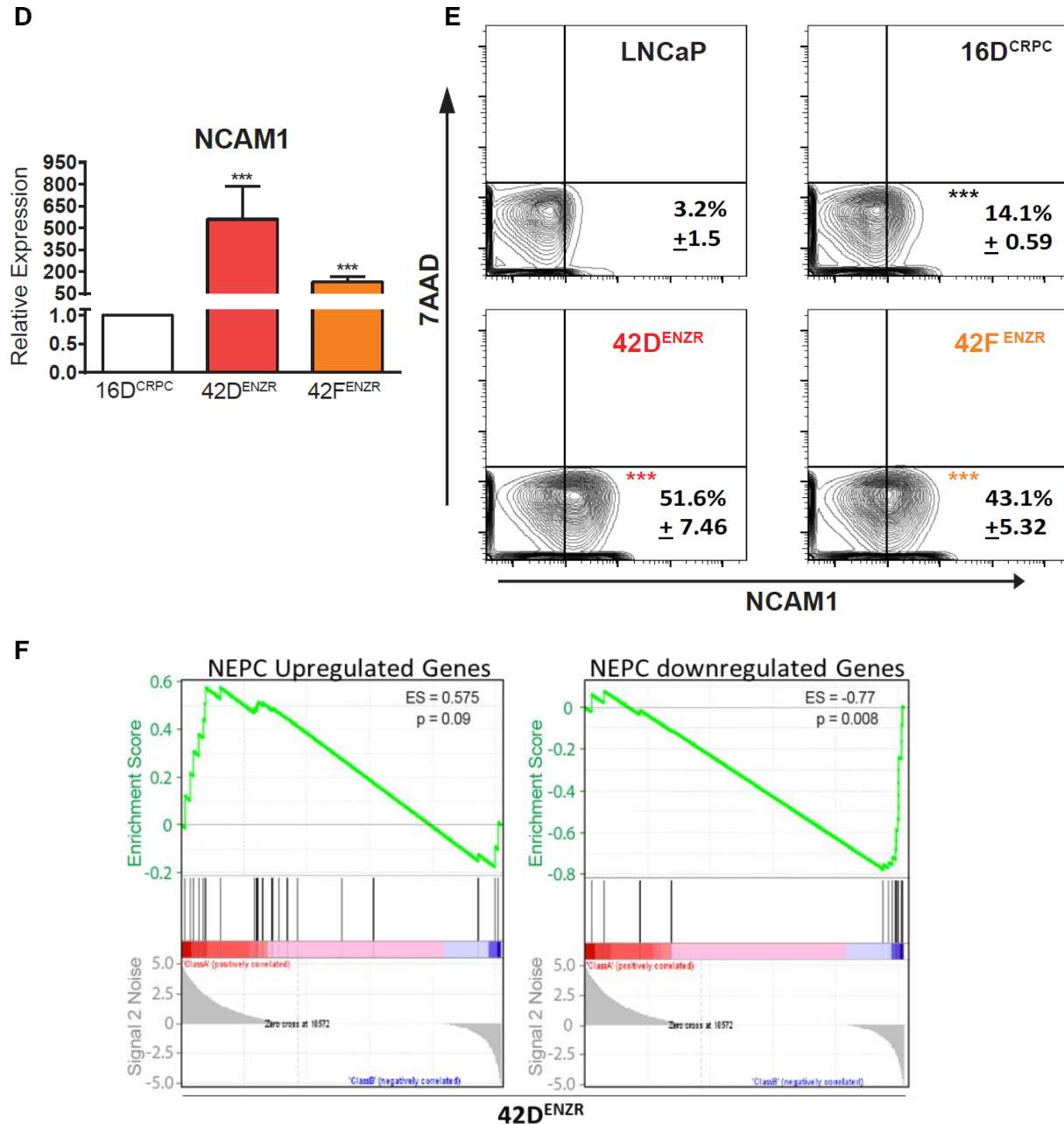
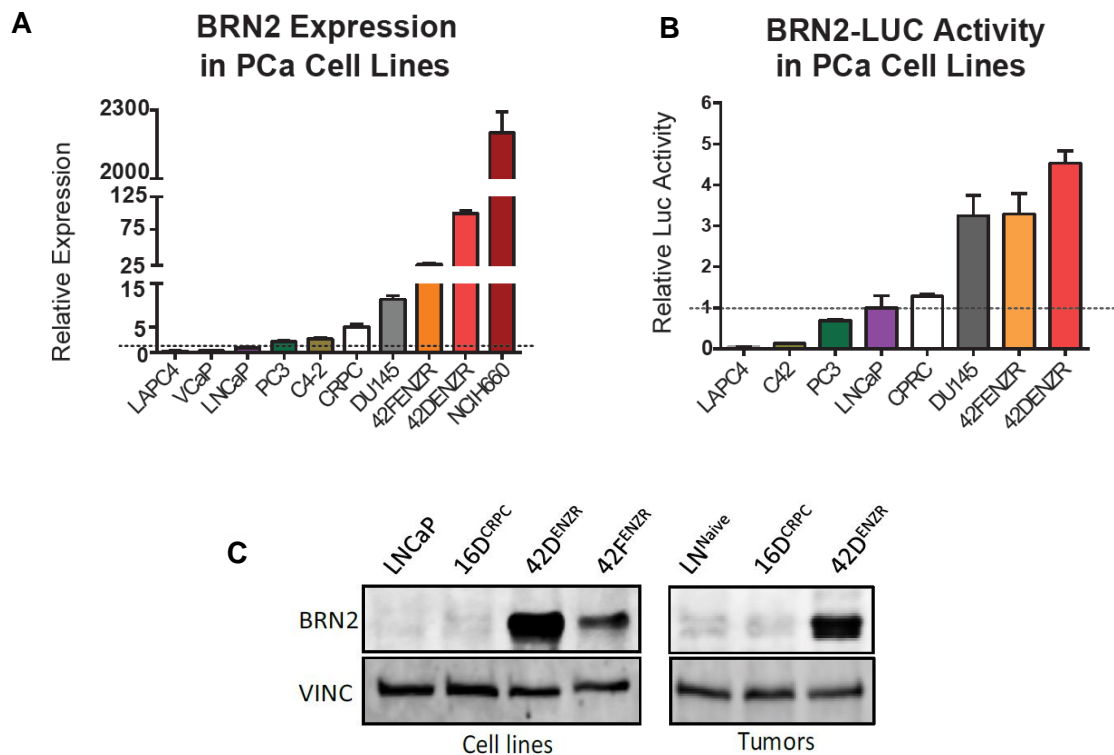


Figure 4.8 - AR non-driven ENZR cells display a NE differentiation signature:

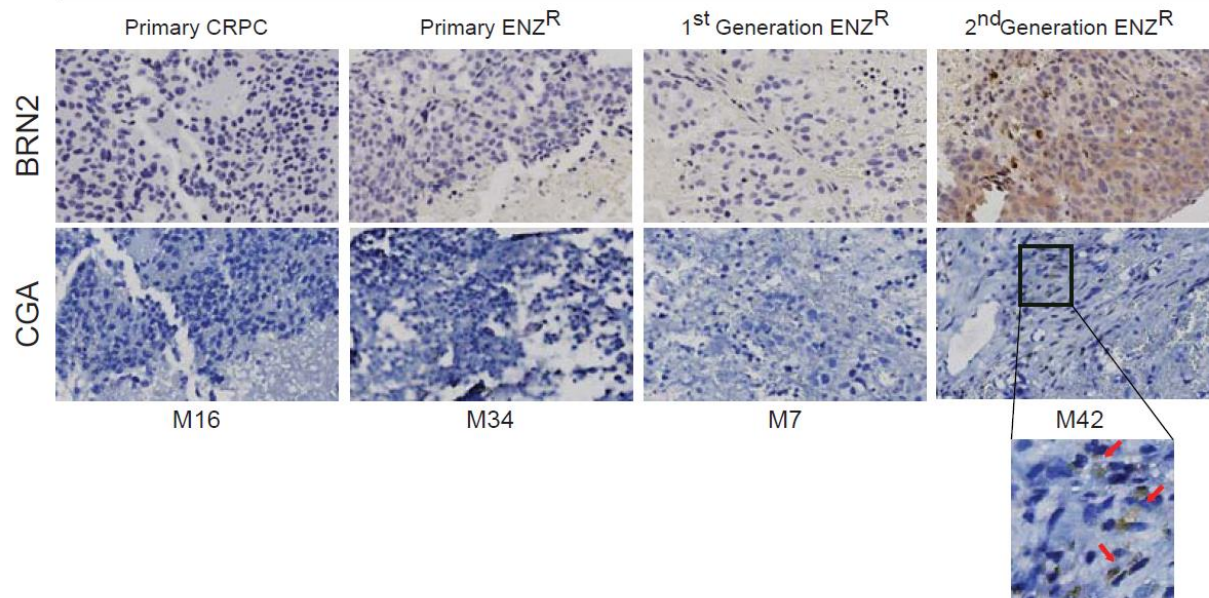
(A) Heat map showing fold increase in reads per million of genes involved in NE differentiation in 42D^{ENZR} cells compared to 16D^{CRPC} (=1). (B) Relative mRNA expression of NSE, SYP, CGA (C) Protein expression of CGA, NSE, SYP and VINC in LNCaP, 16D^{CRPC}, 42D^{ENZR} and 42F^{ENZR} cells and tumors. (D) Relative mRNA expression of NCAM1 in 42D^{ENZR} and 42F^{ENZR} cells compared to 16D^{CRPC} (=1). (E) Frequency of live (7AAD⁻) NCAM1⁺ in LNCaP, 16D^{CRPC}, 42D^{ENZR} and 42F^{ENZR} cells. (F) Gene set enrichment analysis comparing 16D and 42D RNA-seq data for NEPC gene signatures.

Importantly, we found the neural POU-domain transcription factor BRN2 was strongly upregulated in our RNA sequencing data in 42D^{ENZ^R} vs. 16D^{CRPC} cells (**Fig. 4.9A**). Across multiple PCa cell lines, BRN2 mRNA expression was highest in the NEPC tumor derived NCIH660 cell line and second highest in 42D^{ENZ^R} and 42F^{ENZ^R} cells. These data were reflected in serially transplanted xenografts that gave rise to 42D^{ENZ^R} and 42F^{ENZ^R} cells but not primary CRPC tumors (**Fig. 4.9 D-top**). These ENZ^R cells showed the highest BRN2 activity (**Fig. 4.9 B**) and increased BRN2 expression was validated at the protein level by western blot (**Fig. 4.9 C**) and IHC (**Fig. S2C**) in 42D^{ENZ^R} and 42F^{ENZ^R} cells and tumors compared to 16D^{CRPC}. In addition to NCIH660 and our ENZ^R cell lines, BRN2 expression was also increased in NE-like TRAMP+ transgenic prostate tumors (159, 322), where it positively correlated with the expression of NSE, SYP and CGA (**Fig. 4.9 D-bottom**). These data suggest that, non-AR driven models of ENZ^R display NE characteristics which may be supported by the expression of BRN2.

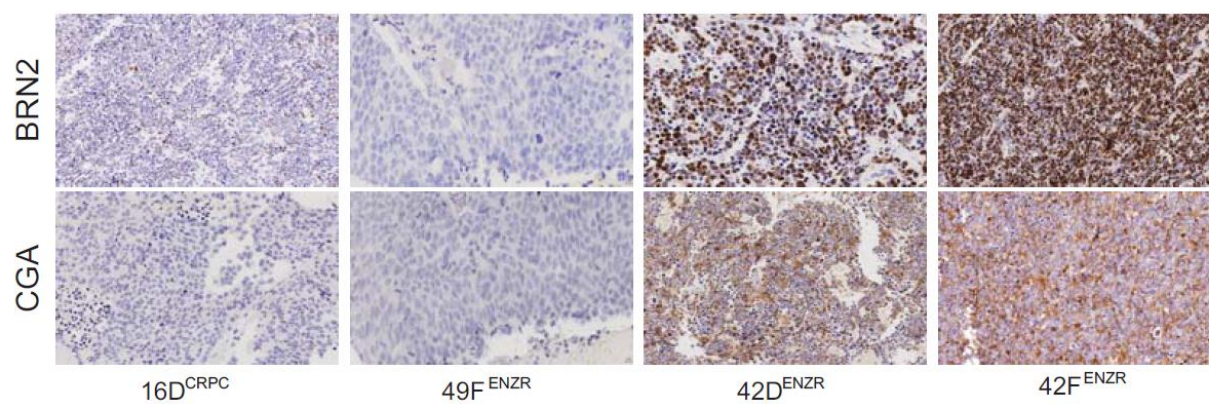


D

42D/F^{ENZ^R} Serial transplanted tumors

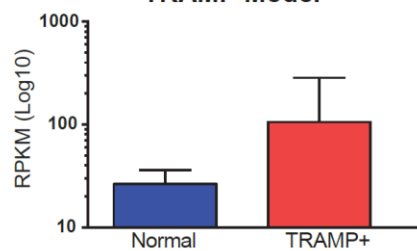


Cell line xenografts



E

BRN2 Expression in TRAMP Model



F

BRN2 v. NE Markers in TRAMP+ Prostates

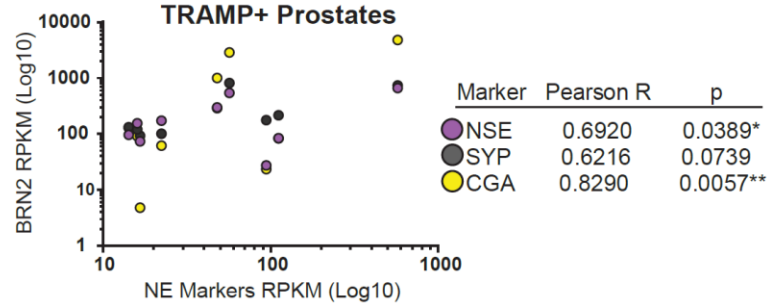
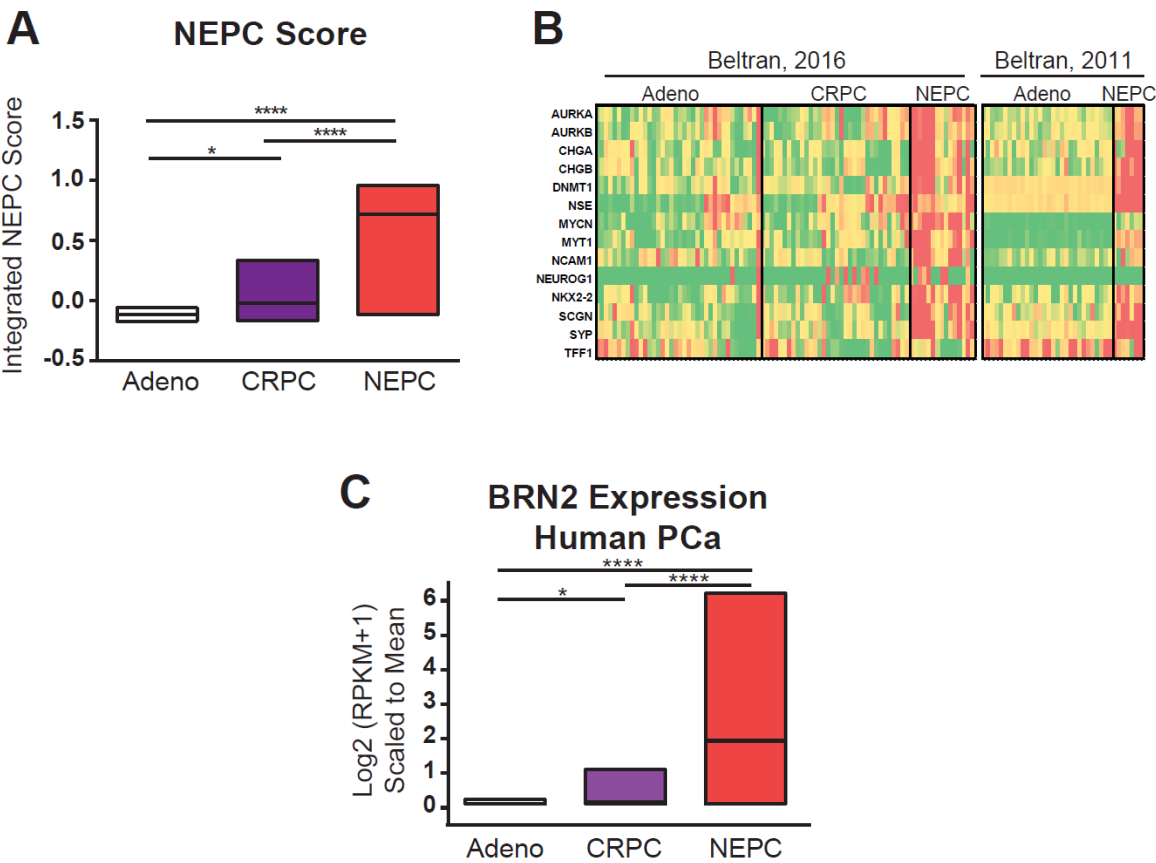


Figure 4.9 - AR non-driven ENZR cells have increased levels of the neural transcription factor BRN2.

(A) Relative mRNA expression of BRN2 in PCa cell lines compared to LNCaP (=1), representative data is shown. **(B)** Relative activity of luciferase under the control of BRN2 48 hours post-transfection in PCa cells compared to LNCaP (=1). Luciferase activity of BRN2 is normalized to Renilla, representative data are shown. **(C)** Protein expression of BRN2 and NEPC markers (VINC loading control) in CRPC and ENZR cell lines and tumors. **(D)** Representative IHC staining of BRN2 and CGA in *(top)* serially transplanted tumors which gave rise to 42D^{ENZR} and 42F^{ENZR} and in *(bottom)* cell line xenografts. **(E)** RPKM score of BRN2 in prostate tumors or tissue isolated from TRAMP+ transgenic mice compared to normal. **(F)** Pearson score of NSE, SYP and CGA compared to BRN2 in TRAMP+ prostates.

To investigate the clinical relevance of BRN2 in human NEPC, we assessed BRN2 expression in RNA sequencing data from prostatic hormone naive adenocarcinoma, castration resistant adenocarcinoma (CRPC) and NEPC patient tumors (Beltran cohorts, 2016 (2) and 2011 (1)). In NEPC tumors, characterized by a high NEPC score and upregulation of canonical NE genes (**Fig. 4.10 A-B**), BRN2 expression was significantly increased compared to CRPC or adenocarcinoma (**Fig. 4.10 C**). Beyond this gene expression profile, NEPC is often associated with low AR activity; in these patient tumors the AR activity score was significantly lower than adenocarcinoma or CRPC (**Fig. 4.10 D-E**).



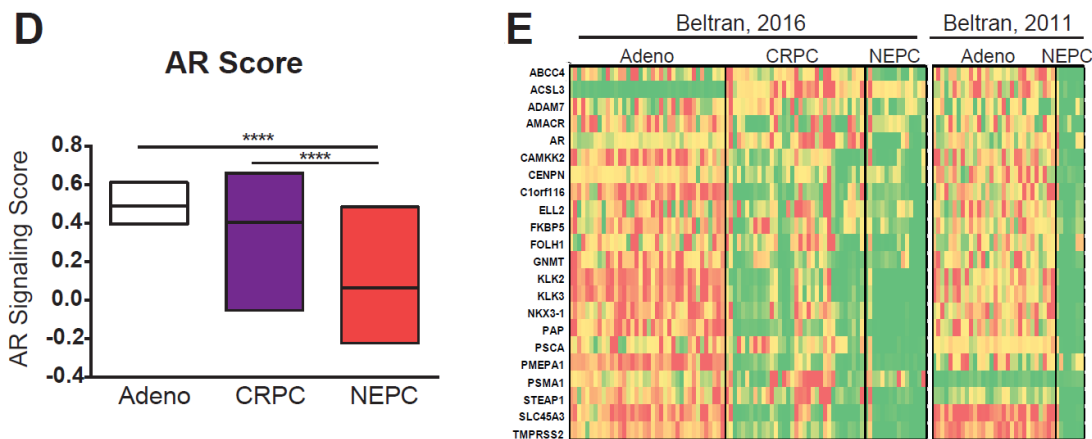


Figure 4.10 - BRN2 is highly expressed in human NEPC:

(A) NEPC score, (B) Heat map of neuroendocrine associated genes, (C) BRN2 expression (line at mean), (D) AR Score (1) and (E) Heat map of AR regulated genes in RNA sequencing data, obtained from two cohorts (1, 2) of Adeno (n=98), CRPC (n=32) and NEPC (n=21) patients.

These data are in accordance with our observation in a human CRPC PDX which transdifferentiated to NEPC in castrated mice (182). In this model we found BRN2 expression was highly upregulated in transdifferentiated NEPC vs. adenocarcinoma (**Fig. 4.11**).

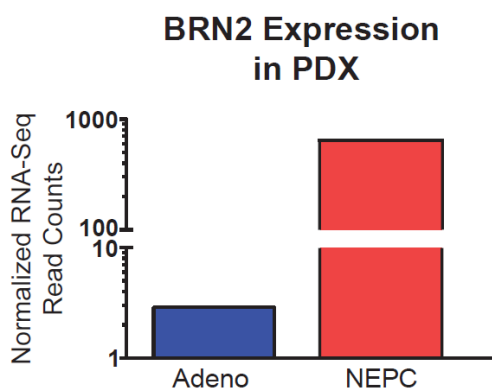


Figure 4.11 - BRN2 is increased in NEPC transdifferentiation model:

BRN2 expression in patient-derived prostatic adenocarcinoma xenografts (Adeno) and terminally transdifferentiated NEPC tumors (NEPC) based on RNA sequencing.

Increased BRN2 expression in NEPC was also observed by IHC staining (**Fig. 4.12**). Importantly, IHC analysis of not only human NEPC but also CRPC and adenocarcinoma supported the inverse correlation between BRN2 and AR (Pearson $R = -0.144$, $p = 0.0043$) and positive correlations with CGA (Pearson $R = 0.2686$, $p < 0.0001$) and SYP (Pearson $R = 0.2709$, $p < 0.0001$).

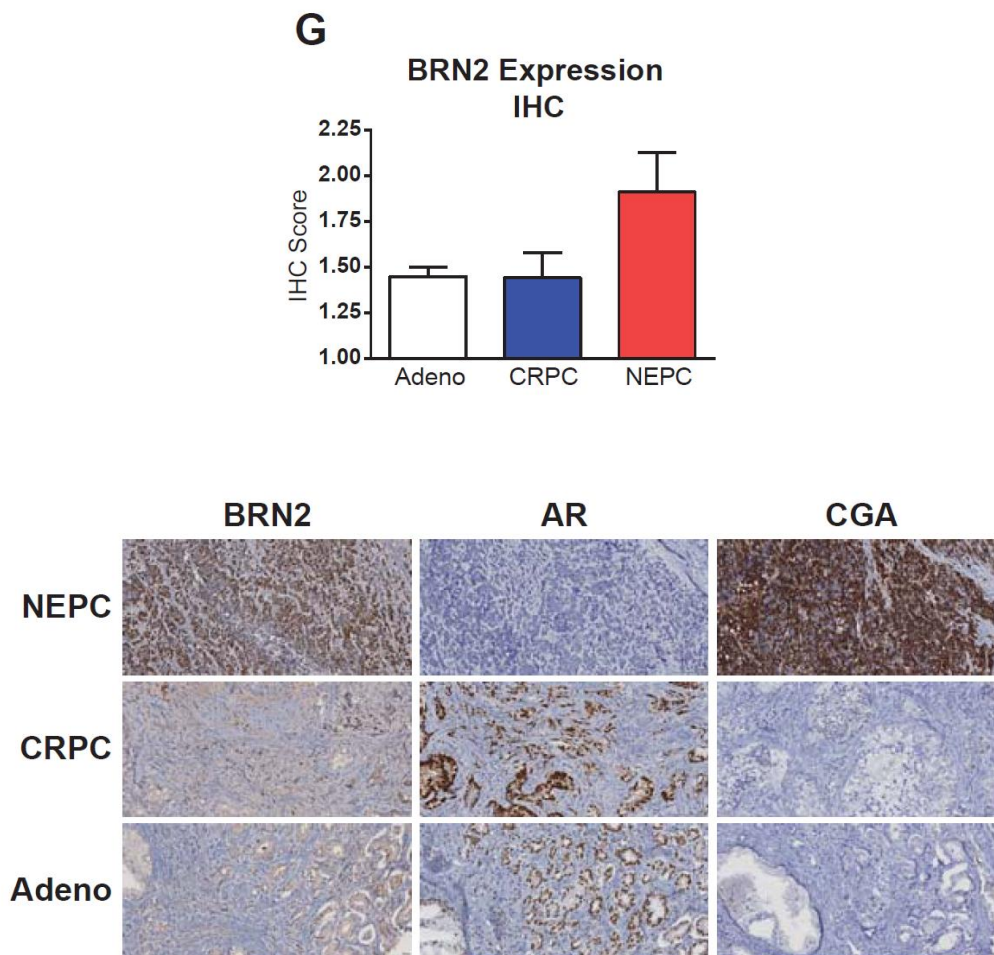


Figure 4.12 - BRN2 protein expression in human NEPC:

IHC score for BRN2 protein expression in adenocarcinoma (Adeno, n=93), CRPC (n=30) and neuroendocrine prostate cancer (NEPC, n=11). Representative IHC for AR, BRN2 and CGA in Adeno, CRPC and NEPC tumors.

Furthermore, in patients, BRN2 was more highly expressed in metastatic CRPC than localized adenocarcinoma (231) (**Fig. 4.13 A**) and in metastatic than primary PCa (229) (**Fig. 4.13 B**). Finally, expression of BRN2 positively correlated with the NE associated genes CGA, CGB, SYP and MYCN (229) (**Fig. 4.13 C**). These data show for the first time that BRN2 expression is strongly associated with severity of disease in PCa, especially a NE phenotype, and that it is inversely correlated with AR activity.

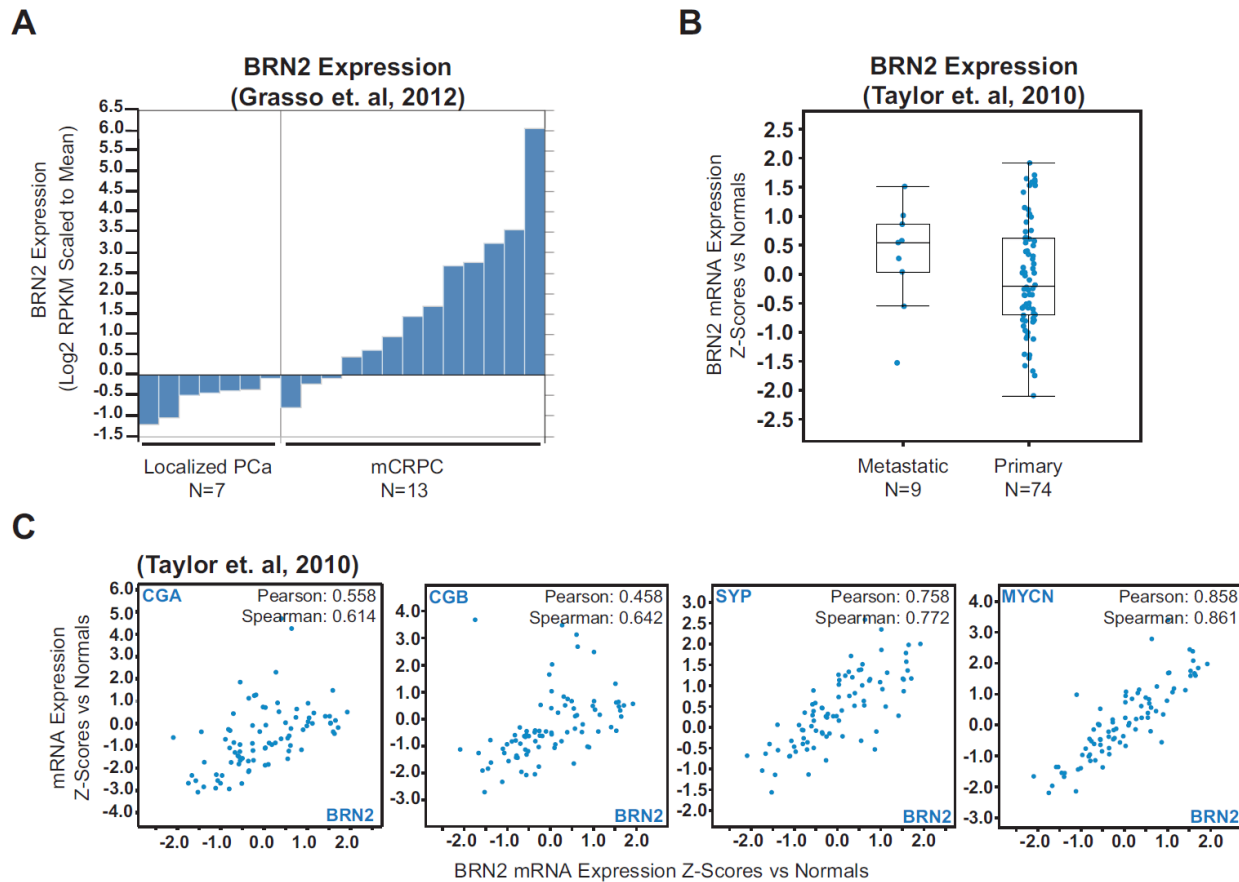


Figure 4.13 - BRN2 expression is higher in metastatic prostate cancer and correlates with NEPC markers:

(A) Waterfall plot of BRN2 mRNA expression in prostatic adenocarcinoma or CRPC tumors from the Grasso data set. **(B-C)** BRN2 mRNA expression in metastatic vs. primary PCa **(B)** and correlation between BRN2 and CGA, CGB, SYP and nMYC mRNA z scores **(C)** from the Taylor data set, analyzed using cBioportal.

4.3.2. BRN2 is inversely correlated with AR expression and activity

Our observations in both NEPC patient tumors and our ENZ^R model, lead us to test the hypothesis that inhibition of the classical AR pathway increases the expression of BRN2. In accordance with our in vitro model where we observed PSA⁻ cell lines express BRN2, analysis of the CRPC samples in Grasso et al. (231) as well as the prostate adenocarcinoma TCGA data showed an inverse correlation between BRN2 and serum PSA (**Fig. 4.14 A**). This trend was mirrored by immunohistochemistry analysis of a TMA of both CRPC specimens as well as treatment-naïve adenocarcinoma, where we found a significant inverse correlation between BRN2 staining intensity and circulating PSA levels in primary and CRPC patients. Moreover, BRN2 staining intensity significantly increased in progression from primary PCa to CRPC only in patients with low levels of circulating PSA (**Fig. 4.14 B**).

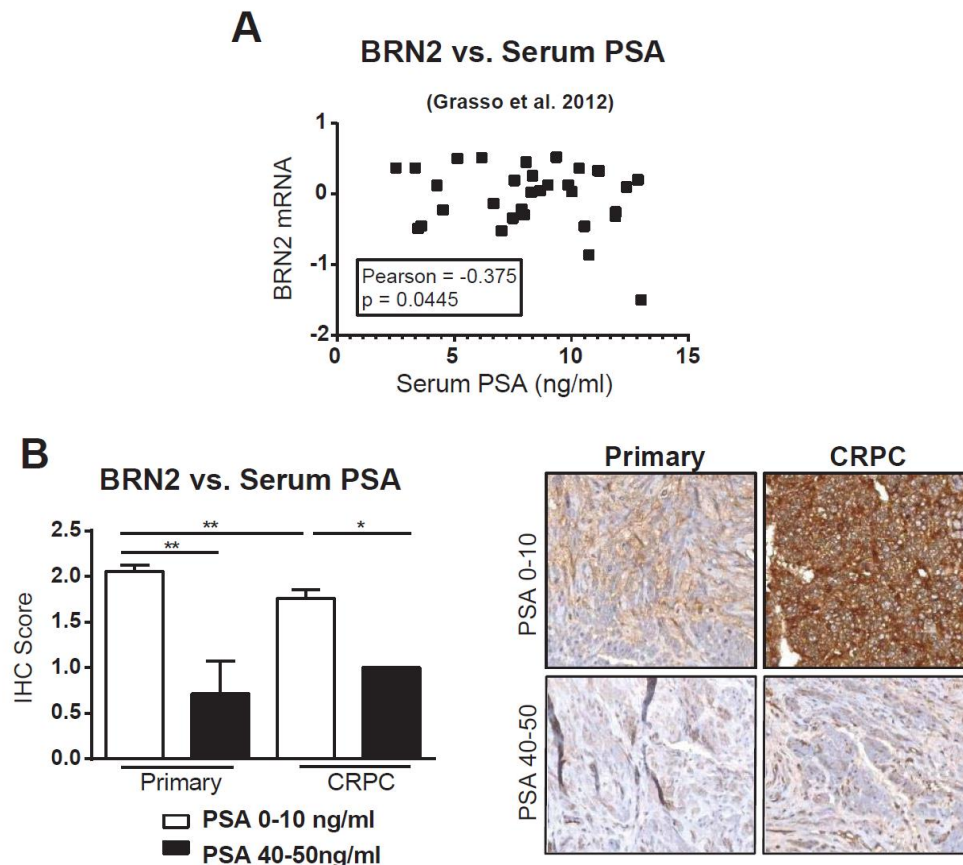


Figure 4.14 - BRN2 expression is negatively correlated to AR activity:

(A) BRN2 expression in CRPC tumors vs. patient serum PSA in Grasso dataset. **(B)** IHC score as well as representative TMA samples for BRN2 protein expression in radical prostatectomy (Primary) or TURP (CRPC) specimens from patients with circulating levels of PSA between 0-10 ng/ml or 40-50 ng/ml. Primary PCa PSA 0-10 n=26, Primary PCa PSA 40-50 n=7, CRPC PSA 0-10 n=22, CRPC PSA 40-50 n=2.

In vitro studies further indicated that suppression of AR signaling regulates BRN2. Data obtained from our AR-driven, PSA positive ENZ^R cell lines showed that compared to 16D^{CRPC}, they did not upregulate BRN2 or markers of NE differentiation in RNA sequencing data (**Fig. 4.15 A, C**), at the mRNA or protein level by western blot (**Fig. 4.15 B**), and showed significant reduction in BRN2 activity (**Fig. 4.15 C**). Serially transplanted tumors that gave rise to 49F cells (**Fig. 4.4 B**) were also negative for BRN2 and CGA (**Fig. 4.15 D**).

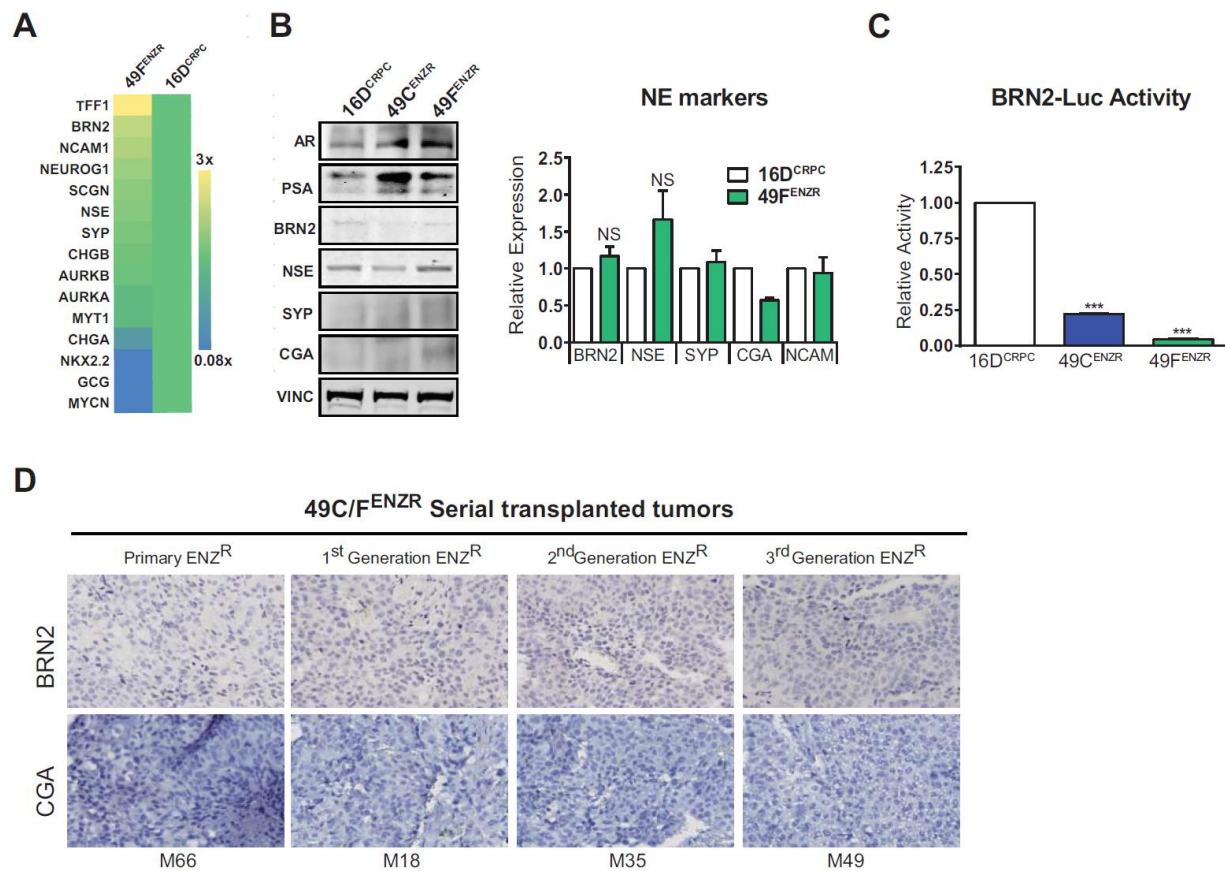
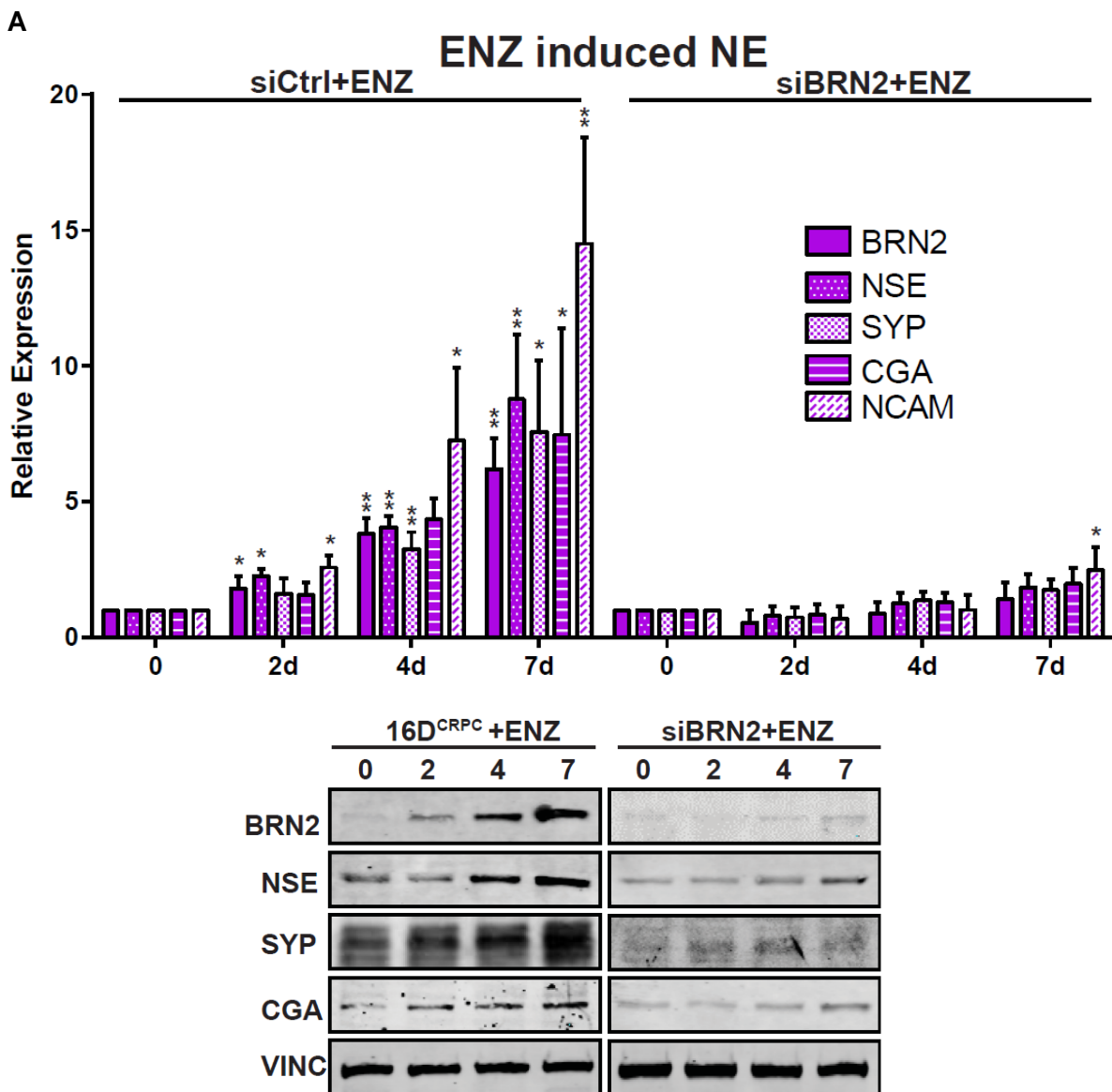


Figure 4.15 - ENZ^R cells with high AR activity do not display higher BRN2 or NEPC marker expression:

(A) Heat map showing fold increase in RNA sequencing reads per million of BRN2 and NE differentiation genes in 49F^{ENZ^R} cells compared to 16D^{CRPC} (=1). (B) Protein expression of AR, BRN2, CGA, NSE, PSA, SYP and VINC in 16D^{CRPC}, 49C^{ENZ^R} and 49F^{ENZ^R} and relative mRNA expression of BRN2 and NE markers in 16D^{CRPC} vs. 49F^{ENZ^R}. (C) Relative activity of BRN2-luciferase reporter (normalized to Renilla) assessed 48 hours post-transfection in 49C^{ENZ^R} and 49F^{ENZ^R} cells compared to 16D^{CRPC} (=1). (D) Representative IHC staining of BRN2 and CGA in serially transplanted tumors which gave rise to 49F^{ENZ^R} and 49C^{ENZ^R}.

Notably, in 16D^{CRPC} cells BRN2 protein expression was increased after 2 days of ENZ treatment, which was followed by increased expression of the terminal NE markers CGA, NSE and SYP over 7 days of ENZ treatment (**Fig. 4.16 A**). Importantly, siRNA-mediated silencing of BRN2 over the course of ENZ treatment prevented the ENZ induced upregulation of NE markers in 16D^{CRPC} cells (**Fig. 4.16 A**) and in LAPC4 cells (**Fig. 4.16 D**). Similarly, deletion of BRN2 by CRISPR/Cas9 gene editing (**Fig. 4.16 B**) or stable knockdown by sh-RNA (**Fig. 4.16 C**) in 16D^{CRPC} cells prevented ENZ-induced upregulation of NEPC markers, further confirming BRN2 is a prerequisite for terminal NE marker expression.



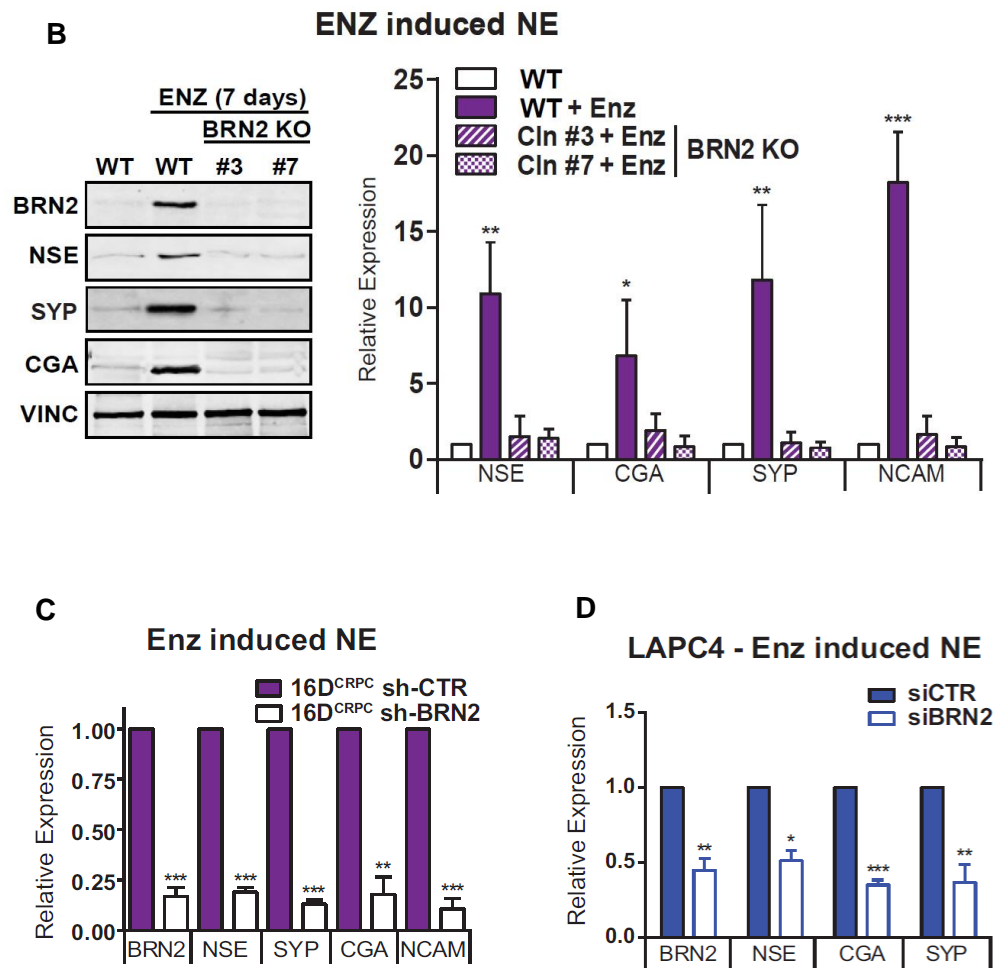
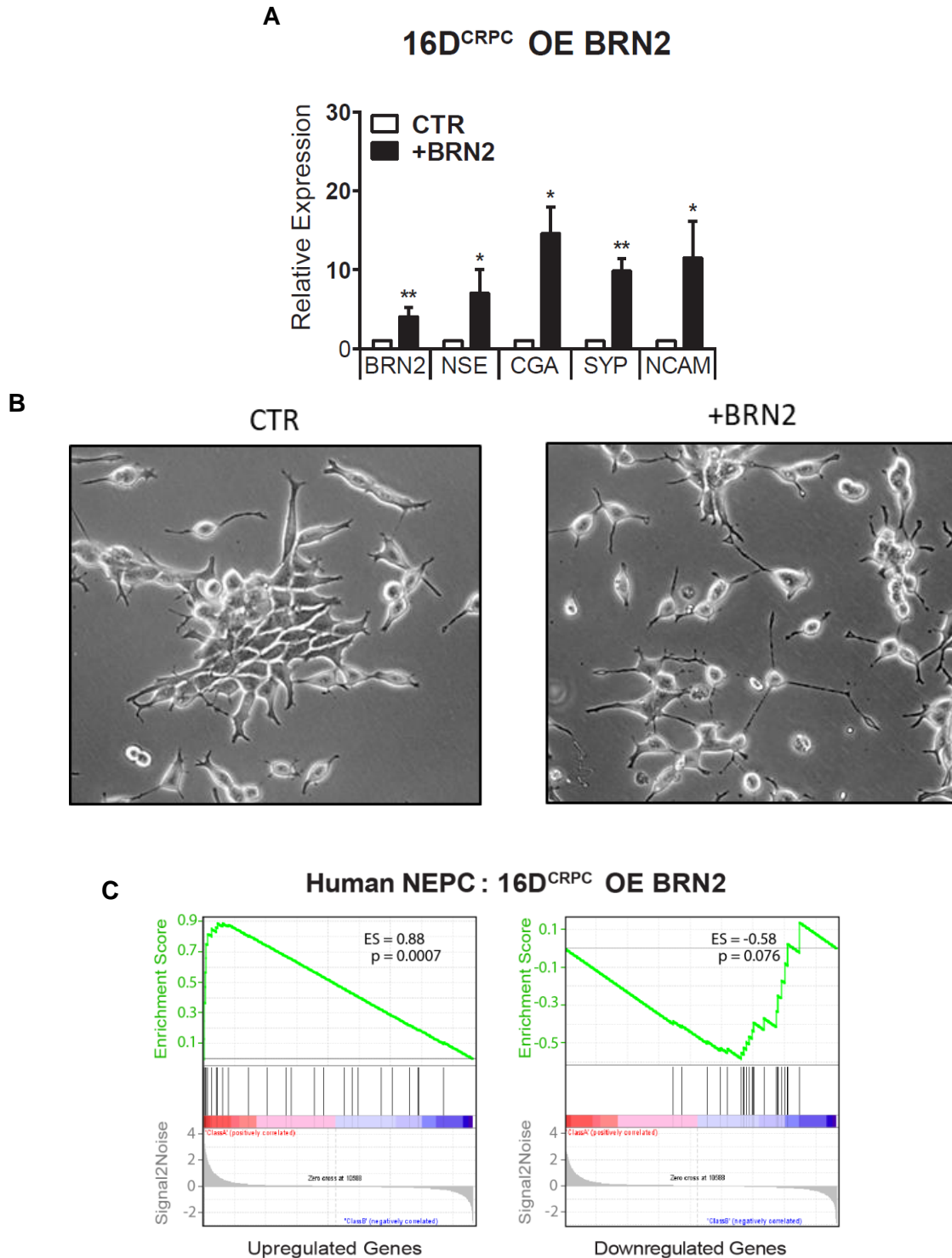


Figure 4.16 - Knockout of BRN2 prevents ENZ induced NE differentiation:

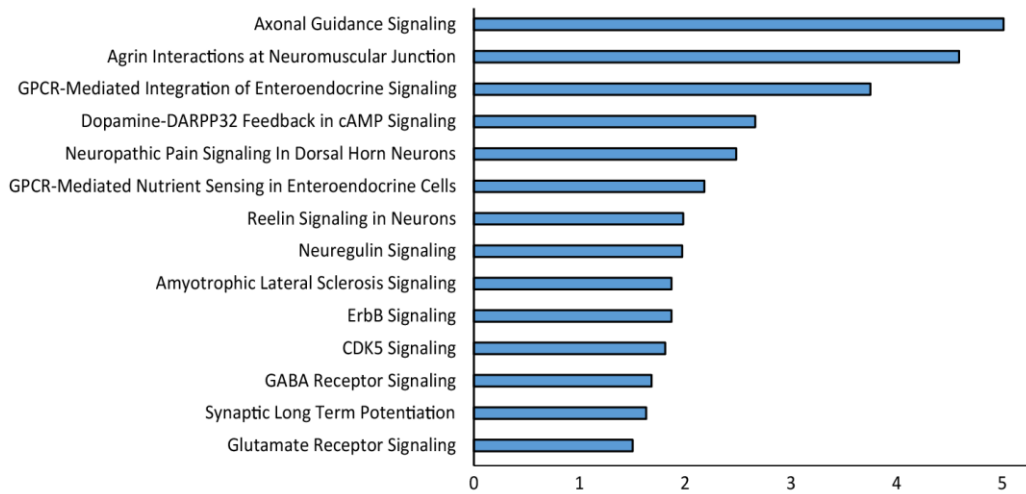
(A) Protein and relative mRNA expression of BRN2, SYP, NSE, CGA, and VINC in siScr and siBRN2 16D^{CRPC} cells treated +/- 10 μ M ENZ for 2, 4 or 7 days. (B) Protein and relative mRNA expression of BRN2, SYP, NSE, CGA, and VINC in different clones of 16D^{CRPC} harboring BRN2 CRISPR knockout (BRN2 KO) +/- 10 μ M ENZ for 7 days compared to wild type 16D^{CRPC} cells (WT). mRNA expression of BRN2 in 16D^{CRPC} WT was set to 1. (C & D) Relative mRNA expression of BRN2 and NE markers in (C) 16D^{CRPC} cells with stable knockdown of BRN2 (sh-BRN2) and (D) LAPC-4 transfected with BRN2 siRNA (siBRN2) that were treated with 10 μ M ENZ compared to ENZ treated siCTR (siCTR=1) or empty vector transfected (sh-CTR=1).

Reciprocally, transient overexpression of BRN2 in 16D^{CRPC} cells was sufficient to induce expression of NSE, CGA, SYP and NCAM1 (**Fig. 4.17 A, B**). Overexpression also triggered NE morphology in the 16D cells as well as enriched for a NEPC gene signature and neuronal associated pathways in BRN2 overexpressing 16D^{CRPC} cells (**Fig. 4.17 C, D**).



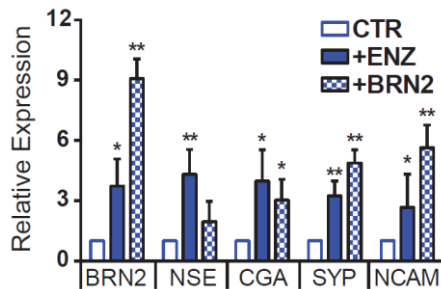
D

IPA analysis : 16D^{CRPC} OE BRN2



E

LAPC 4 + ENZ or BRN2



F

49F^{ENZ}R OE BRN2

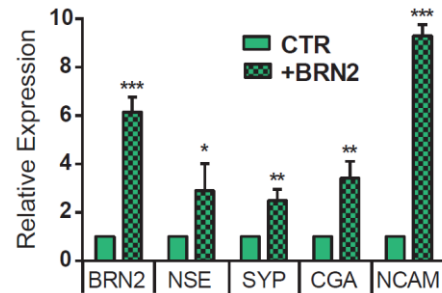


Figure 4.17 - BRN2 overexpression induces NE differentiation:

(A-D) Series of experiments in 16D^{CRPC} cells transfected with BRN2 overexpression vector (+BRN2). (A) Relative mRNA expression of BRN2 and NE markers. (B) Bright field microscopy demonstrating morphology changes. (C) Gene set enrichment analysis of NEPC signature from Beltran et al. 2016 on gene-expression profiling of BRN2 OE cells (D) Ingenuity pathway analysis from gene-expression profiling. X-axis is $-\log(p\text{-value})$ (E-F) Relative mRNA expression of BRN2 and NE markers in (E) LAPC-4 cells treated with 10 μM ENZ or overexpressing BRN2 (+BRN2) and (F) 49F^{ENZ}R cells overexpressing BRN2 (+BRN2) compared to control vector transfected (CTR=1).

Moreover, the effect of BRN2 overexpression on NE markers was enhanced with ENZ treatment of 16D^{CRPC} cells (**Fig. 4.18 A**). Importantly, overexpression of BRN2 in 16D^{CRPC} cells (**Fig. 4.18 B**), but also AR-driven 49F^{ENZ} cells (**Fig. 4.18 B**) reciprocally downregulated AR target gene expression, which was associated with significantly reduced sensitivity to ENZ in both cell lines (**Fig. 4.18 D, E**). Together, these results suggest that the suppression of classical AR signaling with ENZ treatment induces the NE phenotype in CRPC cells and this process driven by BRN2 leads to ENZ-resistance.

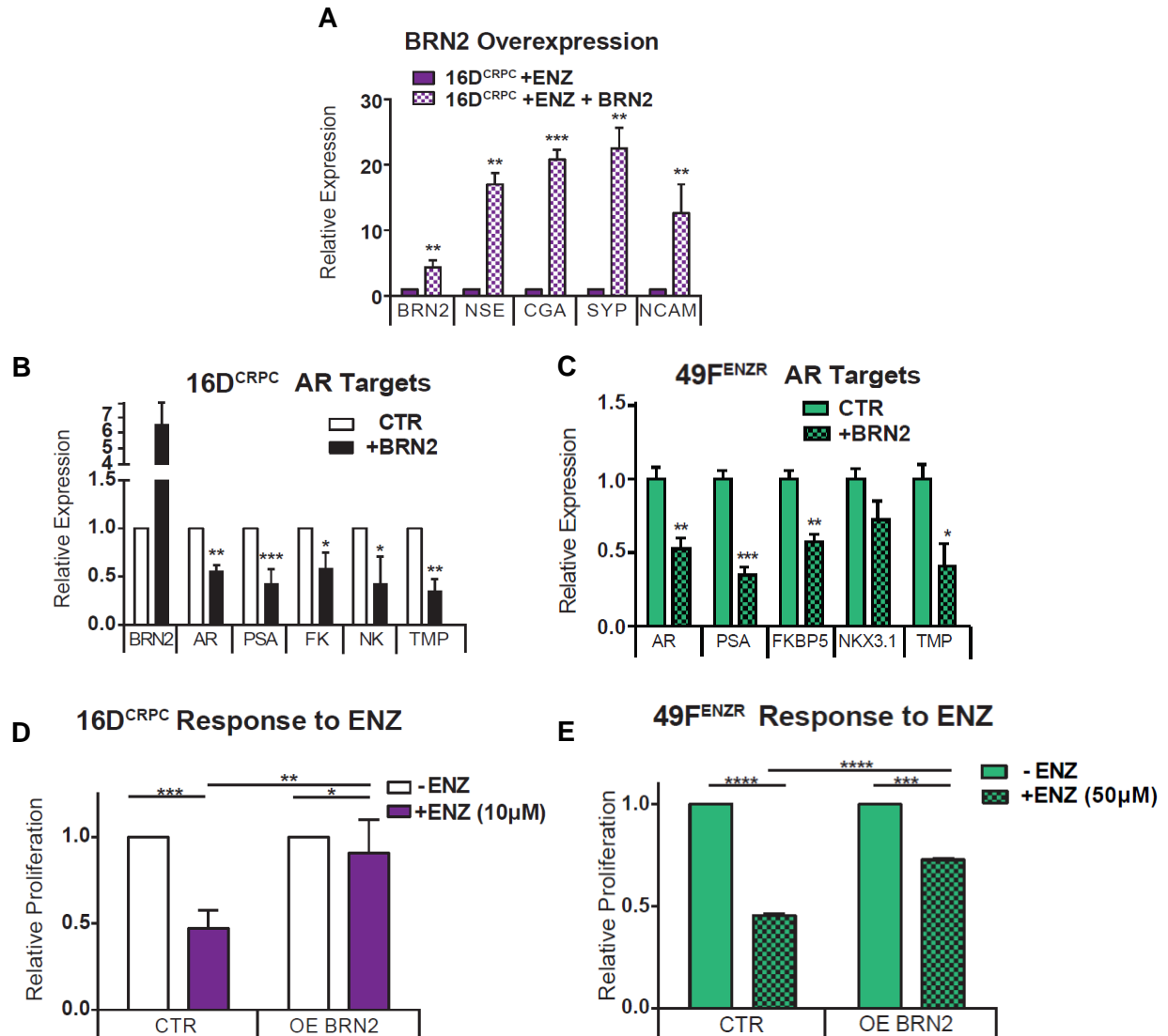


Figure 4.18 - BRN2 overexpression enhances NE differentiation, suppresses AR pathway and confers resistance to enzalutamide:

(A) Relative mRNA expression of BRN2 and NE markers in 16D^{CRPC} cells with overexpression of BRN2, treated with 10μM ENZ for 7 days compared to control vector treated (CRPC+ENZ=1). (B-C) Relative mRNA expression of AR and AR target genes in 16D^{CRPC} and 49F^{ENZ} cells over-expressing BRN2 and (D-E) growth response of 16D^{CRPC} and 49F^{ENZ} cells overexpressing BRN2 exposed to 10μM of ENZ after 72 hours.

4.3.3. Androgen Receptor directly represses BRN2 expression

To address AR regulation of BRN2 in CRPC, we assessed the effects of synthetic androgen (R1881) stimulation of AR on BRN2 activity and expression. We found that R1881 significantly reduced BRN2 reporter activity in 42F^{ENZ}R (Fig. 4.19 A), 42D^{ENZ}R (Fig. 4.19 B) and in 16D^{CRPC} cells (Fig. 4.19 C). The expression of BRN2 mRNA was also reduced by R1881 in multiple cell lines (Fig. 4.20 A, B, C) and was accompanied by a reduction in terminal NE markers (4.20 A, B, C).

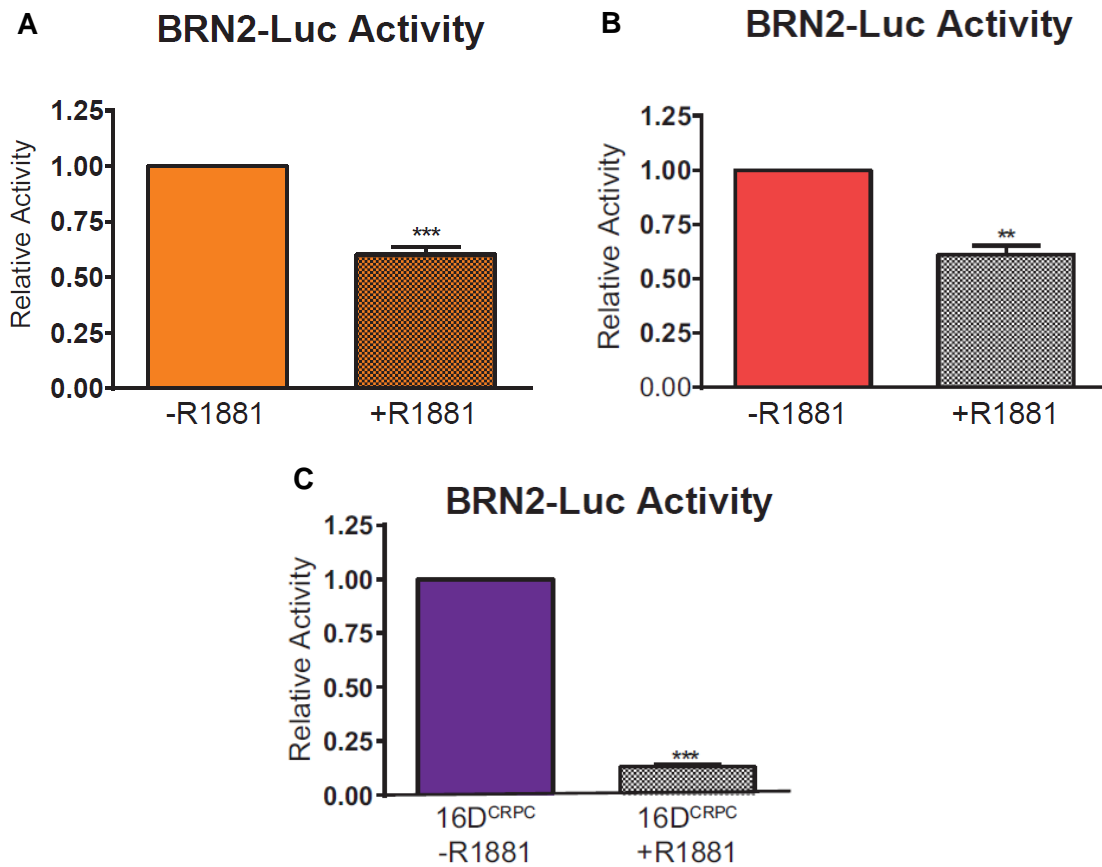


Figure 4.19 - Reactivation of AR suppresses BRN2 activity:

(A-C) BRN2-luciferase reporter activity in (A) 42F^{ENZ}R, (B) 42D^{ENZ}R and (C) 16D^{CRPC} cells treated with 1nM of synthetic androgen R1881 for 48 hours.

Importantly, the R1881 dependent reduction of NE markers was rescued by BRN2 overexpression, suggesting it is an important upstream androgen regulated transcription factor responsible for NE marker expression (**Fig. 4.20 A, B, C**).

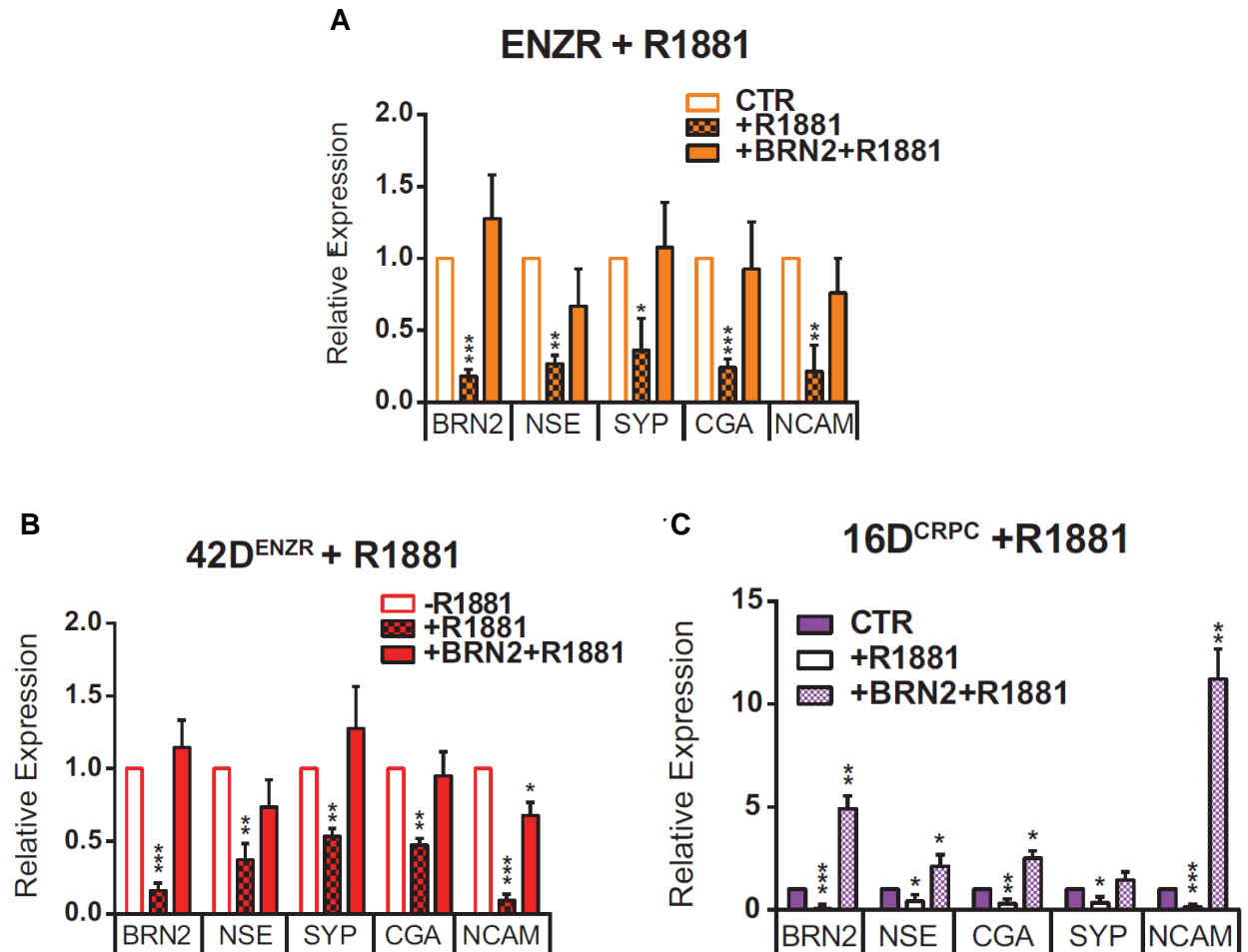


Figure 4.20 - Exogenous expression of BRN2 rescue NEPC gene expression:

(A-C) Relative mRNA expression of BRN2 and NE markers in (A) 42F^{ENZR}, (B) 42D^{ENZR} and (C) 16D^{ENZR} cells overexpressing BRN2 treated with 10nM R1881 for 24 hours compared to control cells (=1).

Indeed, we identified an androgen response element (ARE) 8,733bp upstream of the BRN2 transcriptional start site, and chromatin immunoprecipitation showed that stimulation with R1881 significantly increased AR occupancy at this ARE compared to androgen-deprived conditions (**Fig. 4.21 A, B**). To address the effect of AR binding specifically to BRN2 at this ARE, a 20bp DNA aptamer, which physically inhibits binding of other molecules to its complementary sequence (323), was designed to prevent AR binding at the ARE in the BRN2

enhancer region (**Fig. 4.21 C**) and the effects of R1881 on BRN2 and NE marker expression was assessed. The reduction of BRN2 (**Fig. 4.21 D**) and NE marker (**Fig. 4.22 A**) expression by R1881 treatment in ENZ^R cells could be rescued in a dose dependent fashion by introduction of the BRN2 ARE aptamer (ARE^{Ap}). No effects of aptamer treatment were seen on other AR dependent genes such as PSA, FKBP5 and TMPRSS2, indicating the specific effects of aptamer treatment on AR binding to BRN2 (**Fig. 4.22 B**). In addition, treatment of 16D^{CRPC} cells with the BRN2 ARE^{Ap} increased expression of BRN2 and NE markers to similar levels as ENZ (**Fig. 4.22 C**). Taken together, these results indicate that BRN2 is negatively regulated by AR activation in both ENZ^R cells and 16D^{CRPC} cells under the pressure of ENZ.

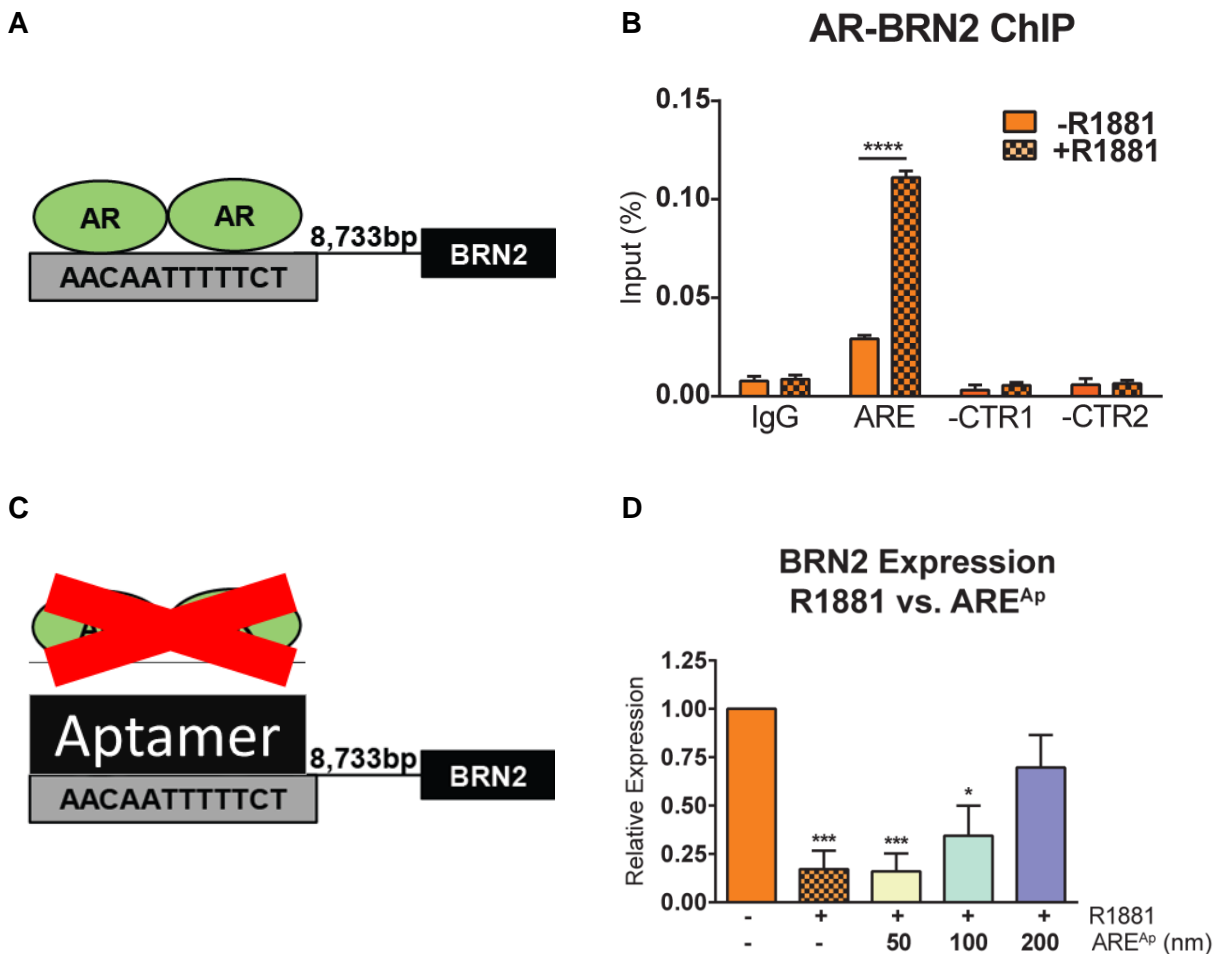


Figure 4.21 - Active Androgen Receptor binds to BRN2 upstream enhancer:

(A) Schematic of Androgen Response Element (ARE) upstream of BRN2 transcription start site. **(B)** Chromatin immunoprecipitation showing AR binding to the enhancer region of BRN2 in 42F^{ENZ^R} cells treated +/-10nM R1881 for 24 hours. **(C)** Schematic of anti-ARE aptamer designed to disrupt AR recruitment to the BRN2 enhancer upstream of BRN2 transcription start site. **(D)** Relative mRNA expression of BRN2 in 42F^{ENZ^R} cells treated with 10 μ M R1881 +/- increasing doses of BRN2-ARE^{Ap} for 48 hours compared to control treated cells (=1)

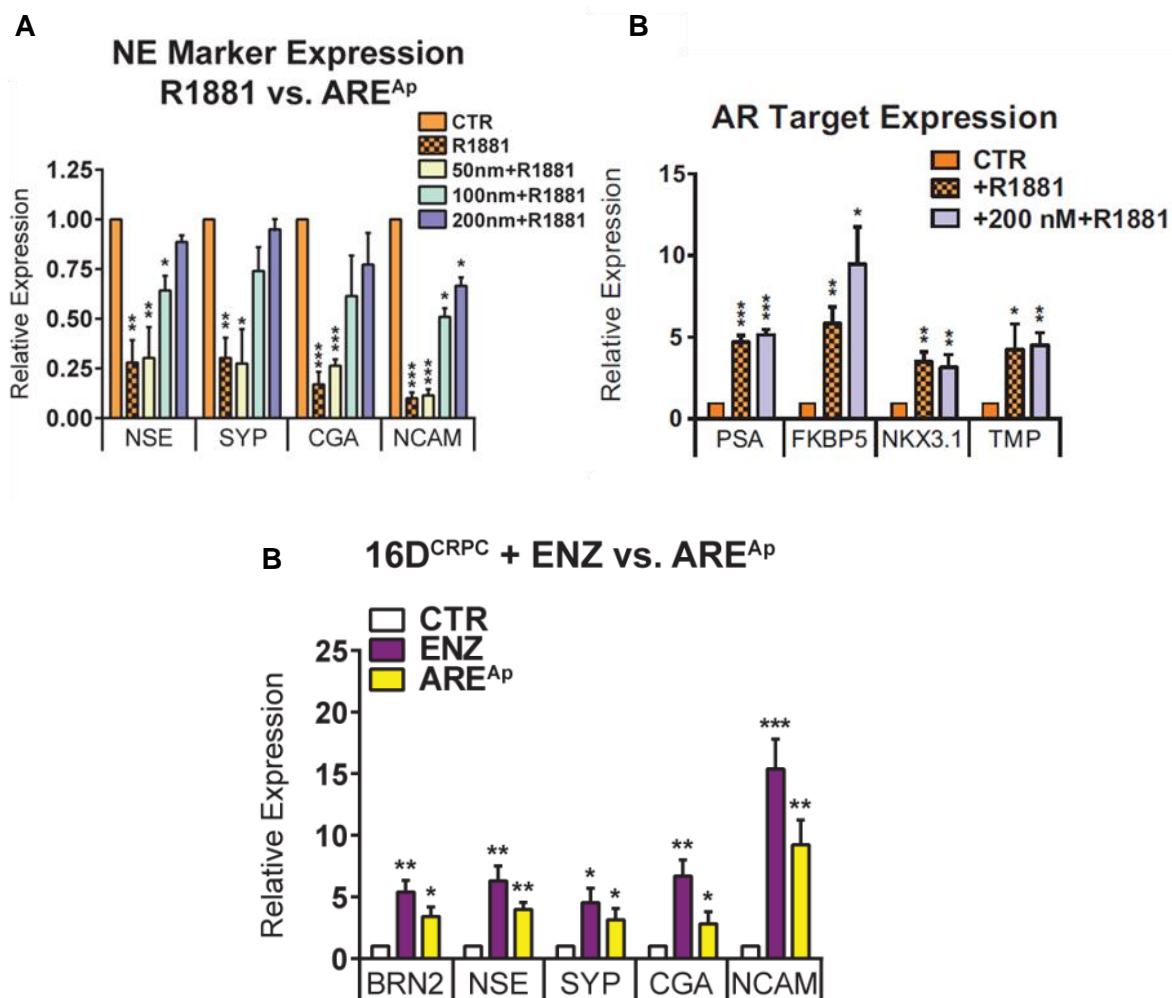


Figure 4.22 - Inhibiting AR recruitment to BRN2 enhancer induces BRN2 and NE differentiation:

(A-B) Relative mRNA expression of **(A)** NE markers and **(B)** AR target genes in 42F^{ENZ} cells treated with 10 μ M R1881 +/- increasing doses of BRN2-ARE^{Ap} for 48 hours compared to control treated cells (=1). **(C)** Comparison of 16D^{CRPC} cells treated with 10nM ENZ +/- 100nM of BRN2-ARE^{Ap} for 7 days compared to control treated cells (=1).

4.3.4. BRN2 and AR regulate SOX2 expression in NEPC

As in neural development, multiple transcription factors may enhance a NE phenotype in PCa. One candidate that has been implicated in human NEPC (324) and cooperates with BRN2 in neural cells (325) is SOX2. Indeed, SOX2 was significantly upregulated in human NEPC compared to adenocarcinoma or CRPC (**Fig. 4.23 A**) as well as in NEPC PDX model (**Fig. 4.23 B**), and was positively correlated with BRN2 expression in metastatic PCa (231) (**Fig. 4.23 C**). Like BRN2, SOX2 expression was highly expressed in NCIH660 cells, as well as 42D^{ENZR} and 42F^{ENZR} cells compared to other PCa lines (**Fig. 4.23 D**).

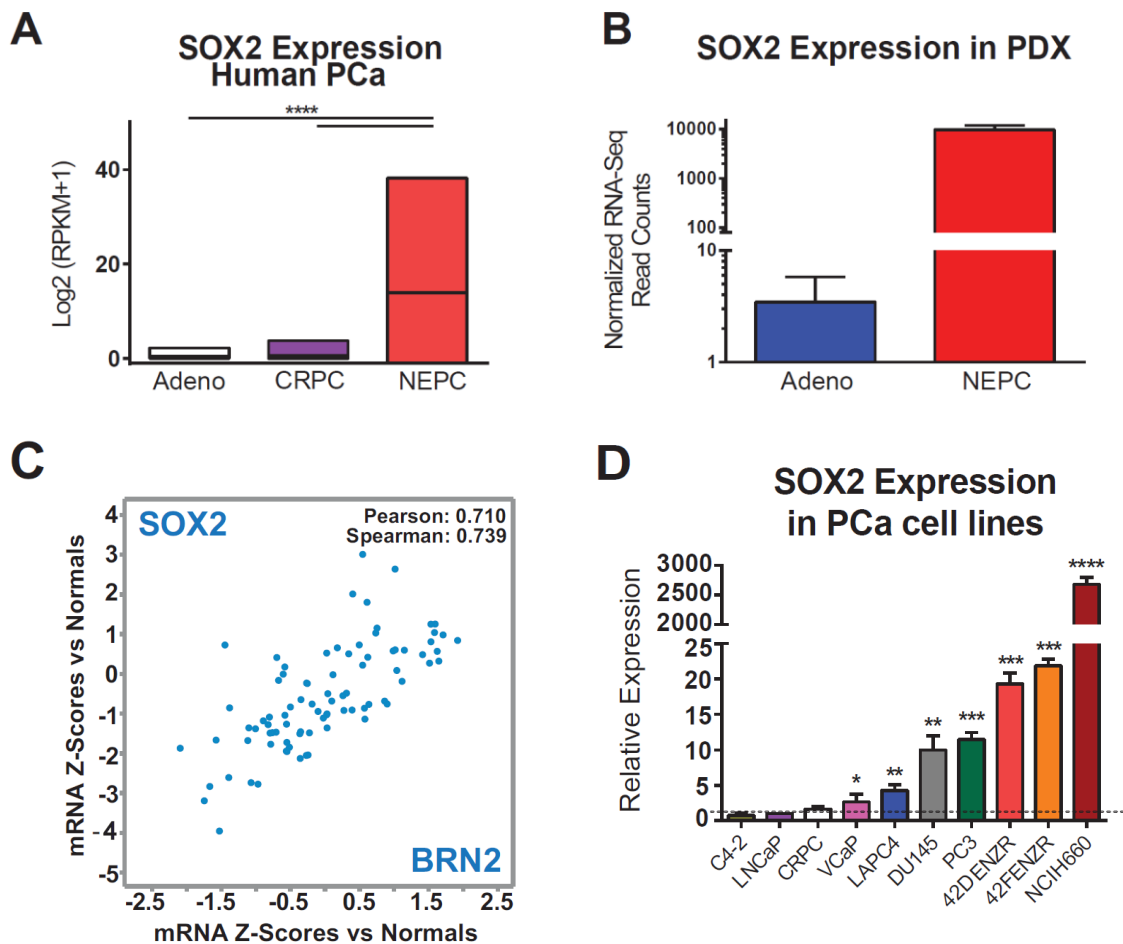


Figure 4.23 - SOX2 is upregulated in human NEPC:

(A) SOX2 expression in human prostatic adenocarcinoma (Adeno, n=68), CRPC (n=32) and NEPC tumors (n=21). (B) SOX2 expression in patient-derived prostatic adenocarcinoma xenografts (Adeno) and terminally transdifferentiated NEPC tumors (NEPC) based on RNA sequencing. (C) Relative mRNA expression of SOX2 across different prostate cancer cell lines compared to LNCaP as control (=1). (D) **Left:** Heat map of SOX2-BRN2 co-bound neural progenitor cell (NPC) gene targets in NEPC, Adeno and CRPC tumors in two cohorts.

In addition, genes co-bound and co-regulated by both BRN2 and SOX2 identified in neural progenitor cells (NPCs) (273) were also enriched in NEPC patients (**Fig. 4.24 A-left**) and in 42D^{ENZR} compared to 16D^{CRPC} cells (**Fig. 4.24 A-right**). Co-regulation of these genes may be mediated by BRN2-SOX2 protein-protein interaction, which we confirmed by co-immunoprecipitation of BRN2 and SOX2 in 42D^{ENZR} and 42F^{ENZR} cells (**Fig. 4.24 B**), and Re-ChIP experiments showing BRN2 and SOX2 co-occupy enhancer regions of NES and RFX4 in 42D^{ENZR} (**Fig. 4.24 C**). These results showed that BRN2 and SOX2 can physically interact in PCa cells and supported further investigation into the hypothesis that these two transcription factors may work in concert to promote NEPC.

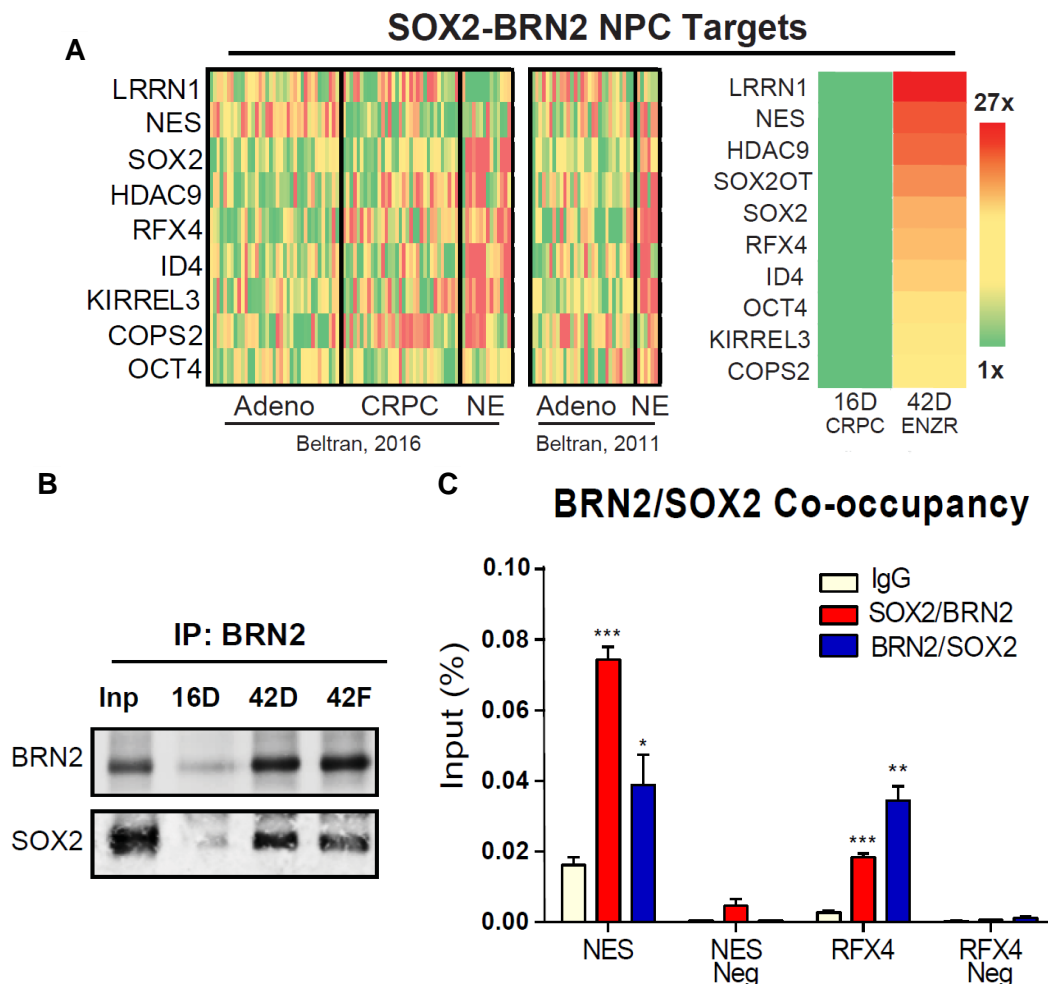


Figure 4.24 - SOX2 co-operates with BRN2 to drive sub-set of NE differentiation genes:

(A) Heat map of fold increase in reads per million of genes identified as co-bound by SOX2 and BRN2 in NPCs in 42D^{ENZR} cells compared to 16D^{CRPC} (=1). **(B)** SOX2-BRN2 protein interaction shown by immunoprecipitation of BRN2 and western blot for SOX2 in 16D^{CRPC}, 42D^{ENZR} and 42F^{ENZR} cells. **(C)** Quantitative Re-ChIP analysis for the enhancer region of NES and RFX4 in 42D^{ENZR} cells using anti-BRN2 and anti-SOX2 antibodies with indicated sequential order (BRN2/SOX2, Blue or SOX2/BRN2, Red). IgG was used as antibody control while sequences outside of the enhancer regions were designed for the specificity of the binding.

Similar to BRN2, SOX2 is also negatively regulated by the AR (326). Consistently, we found that SOX2 expression was induced by ENZ treatment in 16D^{CRPC} and LAPC4 cells (**Fig. 4.25 A**), whereas R1881 reduced SOX2 expression (**Fig. 4.25 B**). Beyond the AR however, it remains unclear what regulates SOX2 expression in PCa and whether BRN2 is involved. We found that SOX2 mRNA levels were reduced after BRN2 knockdown in ENZ^R (**Fig. 4.25 C**), PC3, NCIH660 and ENZ treated LAPC4 cells (**Fig. 4.26 A, B, C**). While overexpression of BRN2 in 16D^{CRPC} (**Fig. 4.26 D**), PC3, LAPC4 or 49F^{ENZ^R} cells (**Fig. 4.26 E**) markedly increased SOX2; data that is in accordance with previous studies showing that BRN2 is required for SOX2 activity in neural development (327). Moreover, R1881 dependent suppression of SOX2 could be rescued in ENZ^R cells by the addition of our BRN2 ARE aptamer (**Fig. 4.26 F**), further supporting our data that BRN2 is AR suppressed and regulates SOX2 expression.

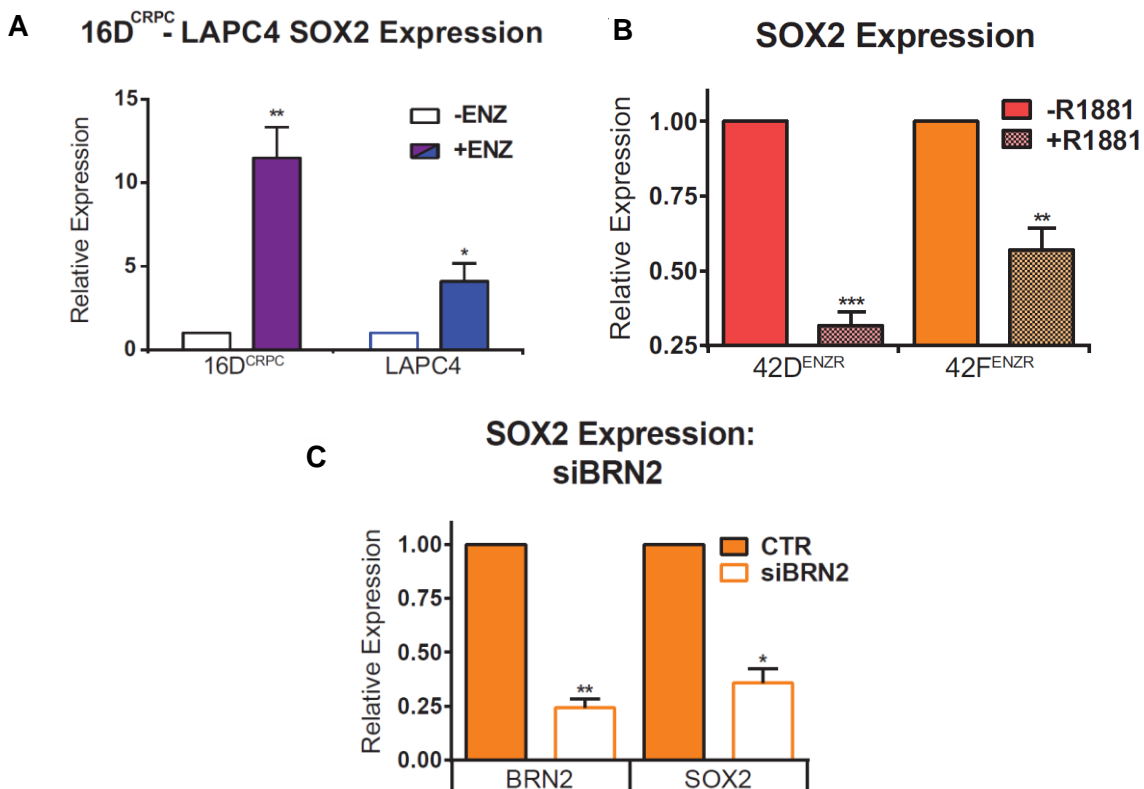


Figure 4.25 - AR negatively regulates SOX2 expression in PCa:

(A) Relative mRNA expression of SOX2 in 16D^{CRPC} and LAPC-4 cells treated with 10 μ M ENZ for 7 days compared to control treated cells (=1). (B) Relative mRNA expression of SOX2 in 42D^{ENZ^R} and 42F^{ENZ^R} cells treated + R1881 for 24 hours compared to -R1881 (=1). (C) Relative mRNA expression of BRN2 and SOX2 in 42F^{ENZ^R} transfected with siBRN2 compared to siCTR transfected cells (=1).

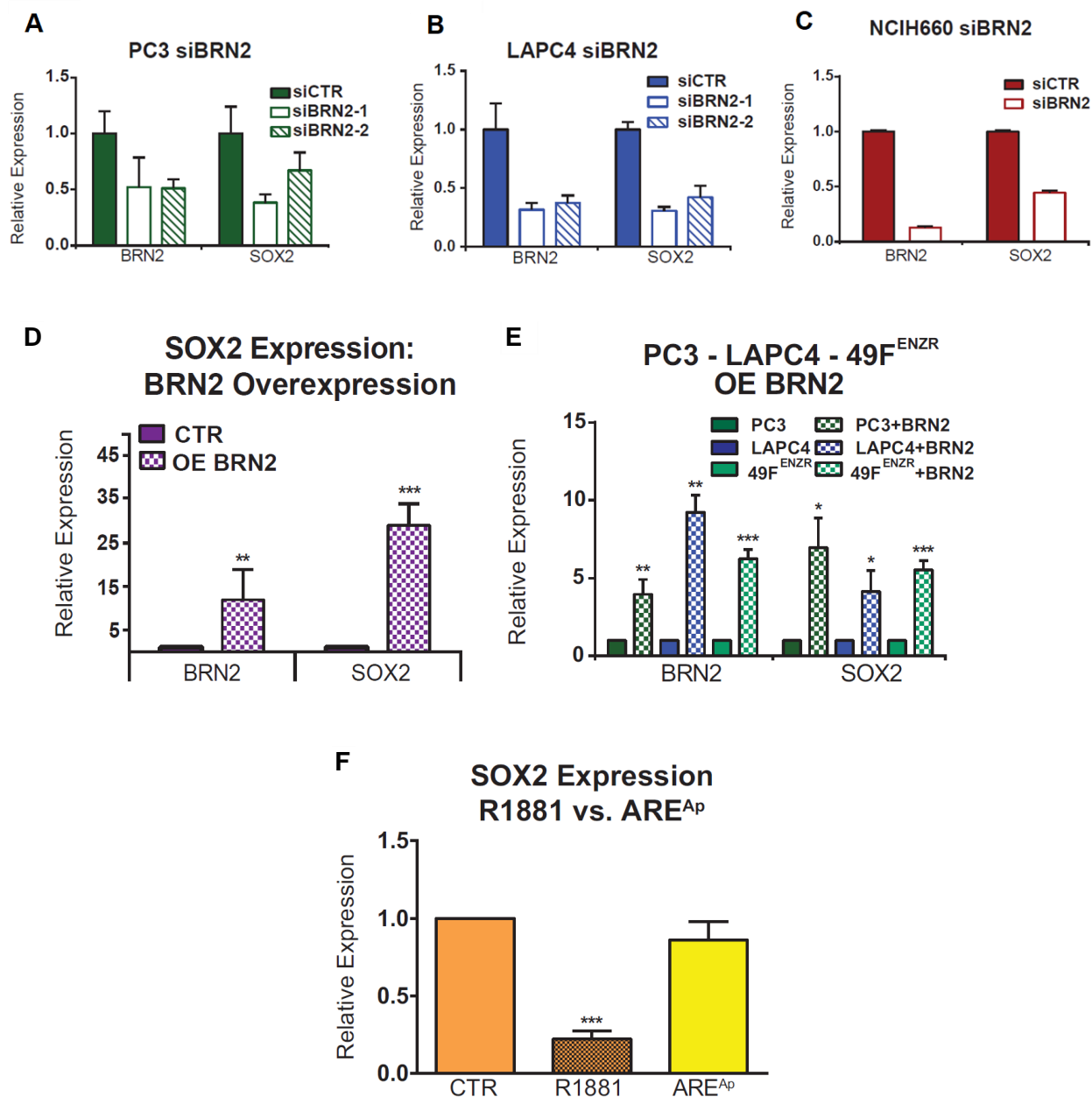
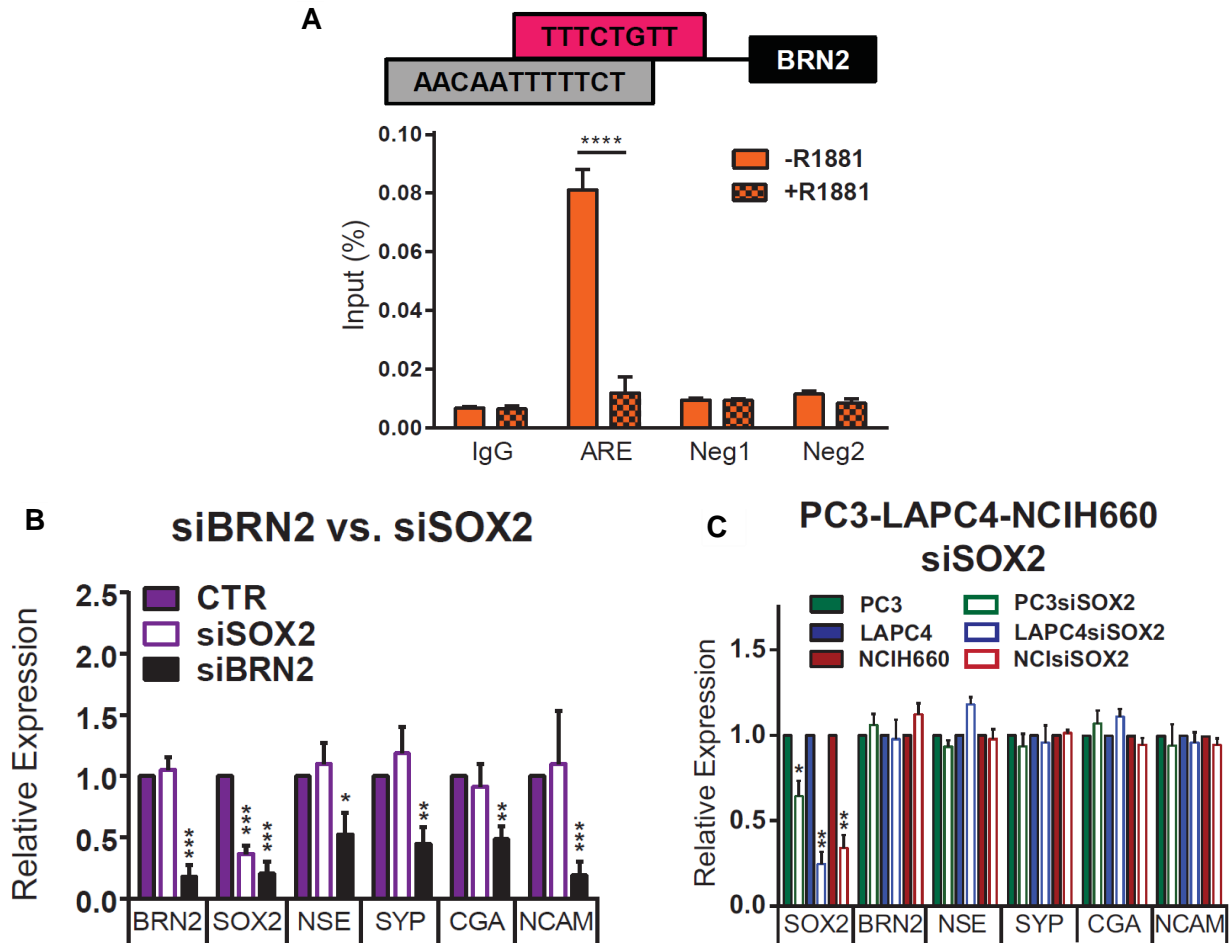


Figure 4.26 - BRN2 positively regulates SOX2 expression:

(A-C) Relative mRNA expression of SOX2, BRN2 and/or NE markers in (A) PC-3 cells, (B) LAPC-4 cells or (C) NCIH660 cells transfected with different BRN2 siRNAs. (D) Relative mRNA expression of BRN2 and SOX2 in 16D^{CRPC} cells overexpressing BRN2 (OE BRN2) compared to control vector (CTR=1). (E) Relative mRNA expression of SOX2 in PC-3, LAPC-4 and 49F^{ENZR} cells transfected with BRN2 overexpression vector. (F) 42F^{ENZR} cells treated with 10nM R1881 +/- 200nM BRN2-ARE^{Ap} for 48 hours

To investigate whether SOX2 may reciprocally regulate BRN2, we examined the enhancer region of BRN2 for potential SOX binding sites. Strikingly, we found a canonical SOX binding motif (273) that overlapped with the ARE in BRN2 (**Fig. 4.27 A**). ChIP was used to validate binding of SOX2 to the same region as the AR upstream of BRN2 in ENZ^R cells in androgen deprived vs. stimulated conditions, and we found that SOX2 was able to bind this site in the absence, but not presence of R1881 (**Fig. 4.27 A**). Interestingly however, we found that neither knockdown nor overexpression of SOX2 altered mRNA expression of BRN2 in ENZ treated 16D^{CRPC} (**Fig. 4.27 B, D, F**), NCIH660, PC3 or ENZ treated LAPC4 cells (**Fig. 4.27 C, E, G**). These results suggest a unidirectional regulation of SOX2 by BRN2 and not vice versa, and show that SOX2 binding to the BRN2 enhancer is regulated by AR.



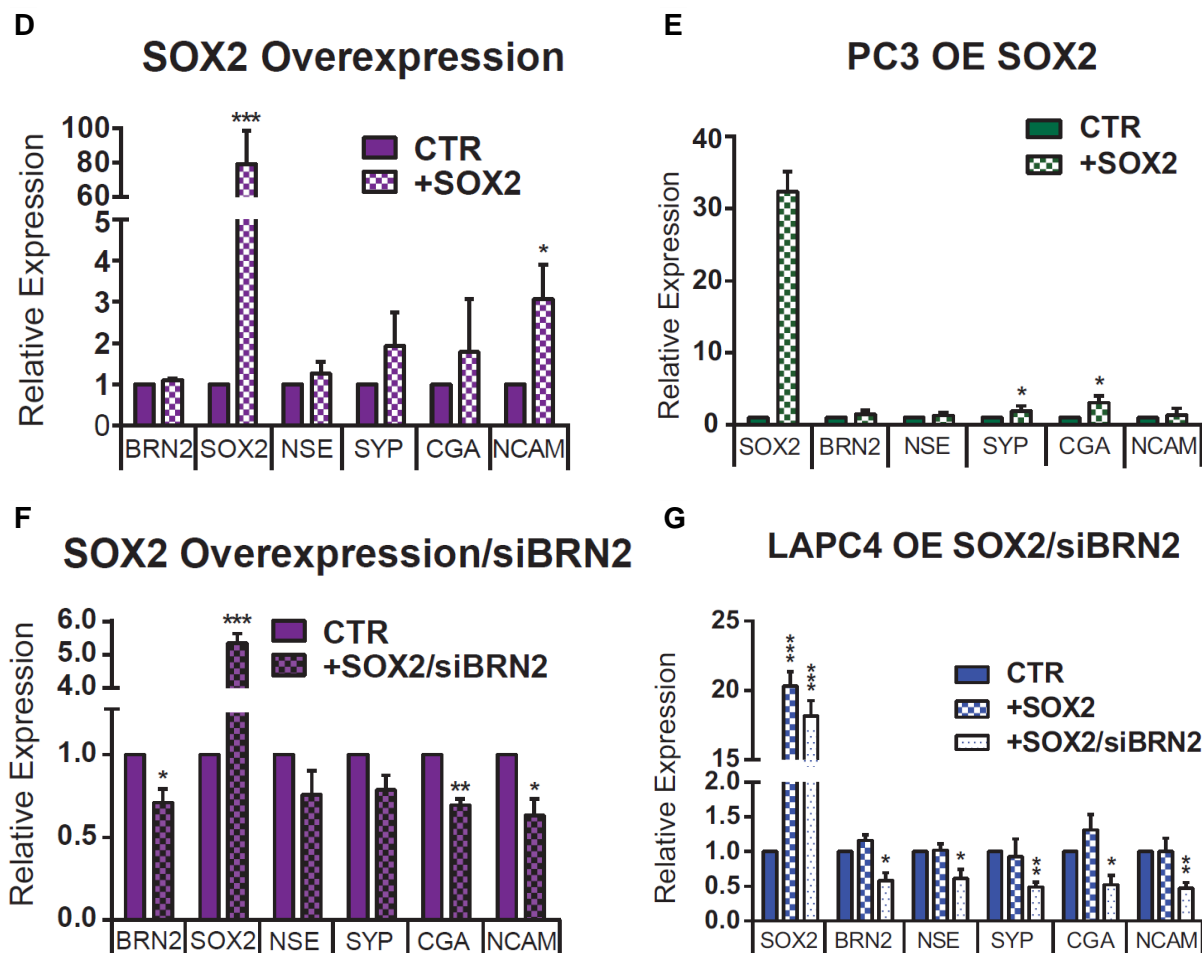


Figure 4.27 - SOX2 does not regulate BRN2 and NEPC differentiation:

(A) Chromatin immunoprecipitation showing SOX2 binding to the enhancer region of BRN2 in 42F^{ENZ^R} cells treated with 10nM R1881 for 24 hours compared to control treated cells (=1). **(B)** Relative mRNA expression of BRN2, SOX2 and NE markers in 42D^{ENZ^R} cells transfected with (siSOX2, siBRN2 or siCTR); **(C)** Relative mRNA expression of SOX2 and NE markers in PC3, Enz treated LAPC4 and NCIH660 cells transfected with (siSOX2 or siCTR). **(D-E)** Relative mRNA expression of **(D)** 16D^{CRPC} and **(E)** PC3 cells with overexpression of SOX2. **(F-L)** SOX2 overexpression vector + siBRN2 (OE SOX2/siBRN2) or CTR vector. Post-transfection, 16D^{CRPC} and LAPC4 cells were cultured in the presence of 10μM ENZ and harvested 5 days later for analysis

4.3.5. BRN2 is required for NE marker expression and aggressive growth of ENZR cells in vitro and in vivo.

Our data suggested that BRN2 contributes to ENZ resistance and is a master regulator of ENZ induced NE differentiation in CRPC. Confirming the requirement for BRN2 in supporting a NE phenotype across multiple cell lines, we found transient targeting of BRN2 reduced mRNA levels of NSE, SYP, CGA and NCAM1 in 42D^{ENZ}, 42F^{ENZ}, PC-3 and ENZ treated LAPC-4 cells (**Fig. 4.28 A-D**) and NCIH660 (**Fig. 4.29 A**). Similar results were observed in stable shBRN2 knockdown 42F^{ENZ} cells (**Fig. 4.29 D**).

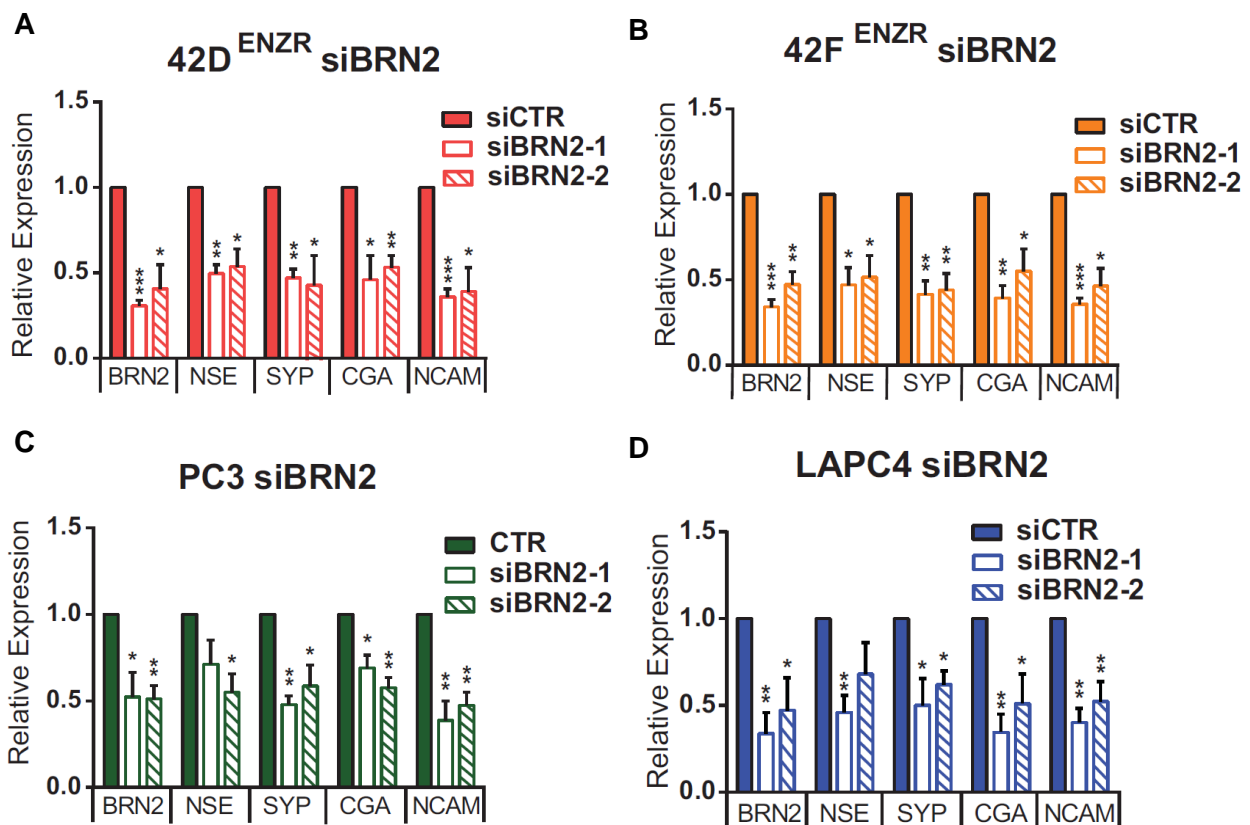


Figure 4.28 - Silencing BRN2 reduces NEPC marker expression:

(A-D) Relative mRNA expression of BRN2 and NE markers in (A) 42D^{ENZ}, (B) 42F^{ENZ}, (C) PC3 and (D) ENZ treated LAPC-4 cells transfected with two different BRN2 siRNA (siBRN2) compared to control (siCTR=1).

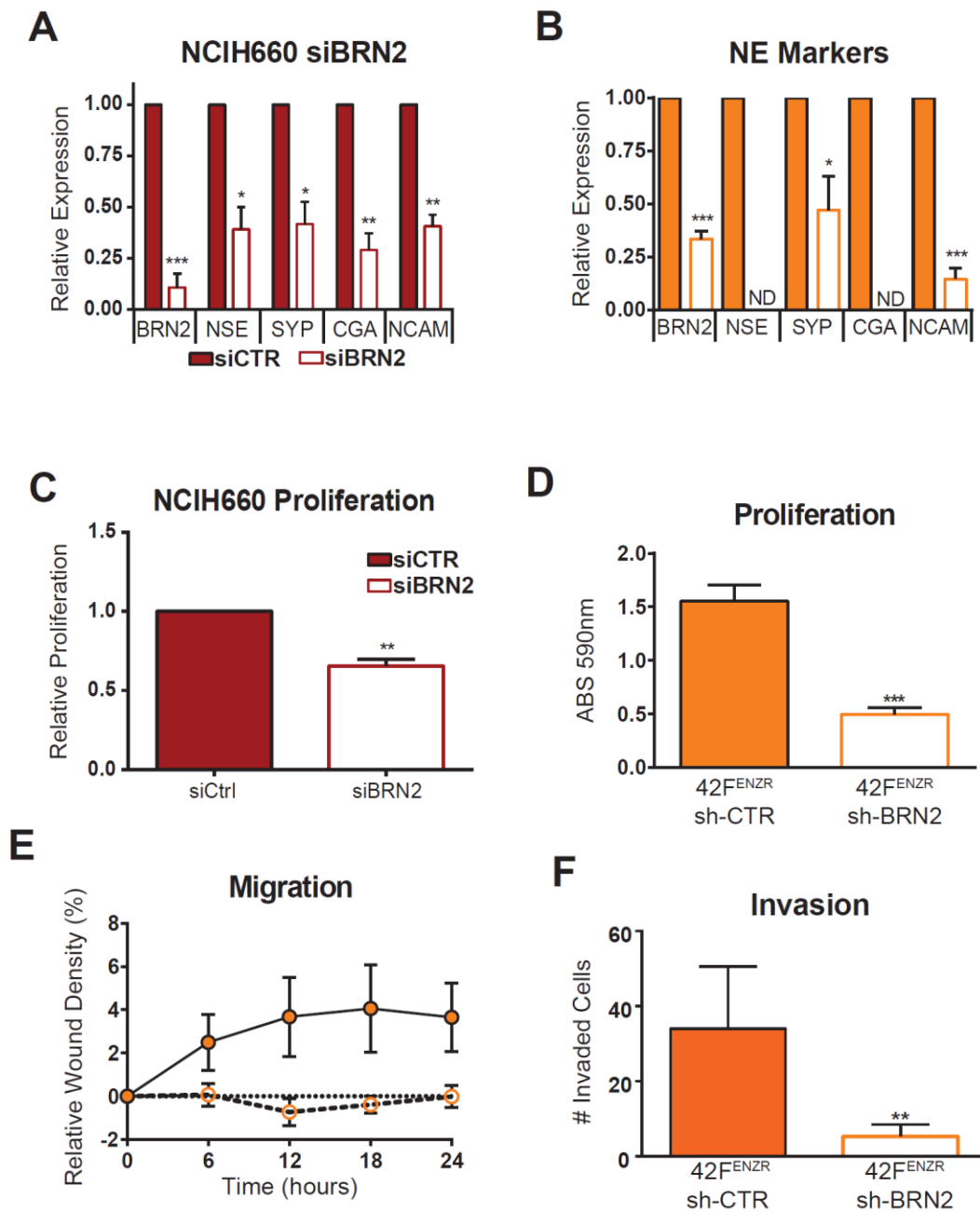


Figure 4.29 - Inhibition of BRN2 reduces cell proliferation, migration and invasion:

(A & B) Relative mRNA expression of BRN2 and NE markers in (A) NCIH660 cells transfected with BRN2 siRNA (siBRN2) compared to control (siCTR=1) and (B) 42F^{ENZR} cells with stable BRN2 knockdown (sh-BRN2) compared to control transfected cells (sh-CTR) (=1). (C) Relative proliferation, 72 hours after seeding in NCIH660 cells transfected with BRN2 siRNA (siBRN2) compared to control (siCTR=1). (D-F) Relative proliferation (D), Relative wound density in one dimensional scratch assay (E) and number of cells migrated through matrigel boyden chamber (F) in 42F^{ENZR} cells with stable BRN2 knockdown (sh-BRN2) compared to control transfected cells (sh-CTR) (=1).

In addition to the expression of terminal NE markers, we questioned whether BRN2 may be important in regulating the aggressive biology of NEPC. Therefore, we investigated the effects of BRN2 knockdown on cellular proliferation, migration and invasion *in vitro*. BRN2 knockdown significantly reduced proliferation in both siBRN2 NCIH660 cells and sh-BRN2 42F^{ENZ^R} cells (**Fig. 4.29 C-D**), and prevented wound closure in a one-dimensional scratch assay (**Fig. 4.29 E**), as well as the capacity of sh-BRN2 42F^{ENZ^R} cells compared to sh-control cells to migrate through a matrigel-coated Boyden chamber (**Fig. 4.29 F**).

The reduced proliferative capacity of sh-BRN2 cells *in vitro* was translated *in vivo*; sh-BRN2 42F^{ENZ^R} subcutaneous tumors grown in castrated mice under the pressure of ENZ were smaller than sh-control tumors (**Fig. 4.30 A**) and these tumors had reduced expression of BRN2 and terminal NE markers (**Fig. 4.30 B**), indicating that this NEPC signature was associated with more aggressive growth. These *in vitro* and *in vivo* results indicate that ENZ-induced NE differentiation is mediated by BRN2, which can be targeted to reduce invasiveness and tumor proliferation both in ENZ^R and in CRPC.

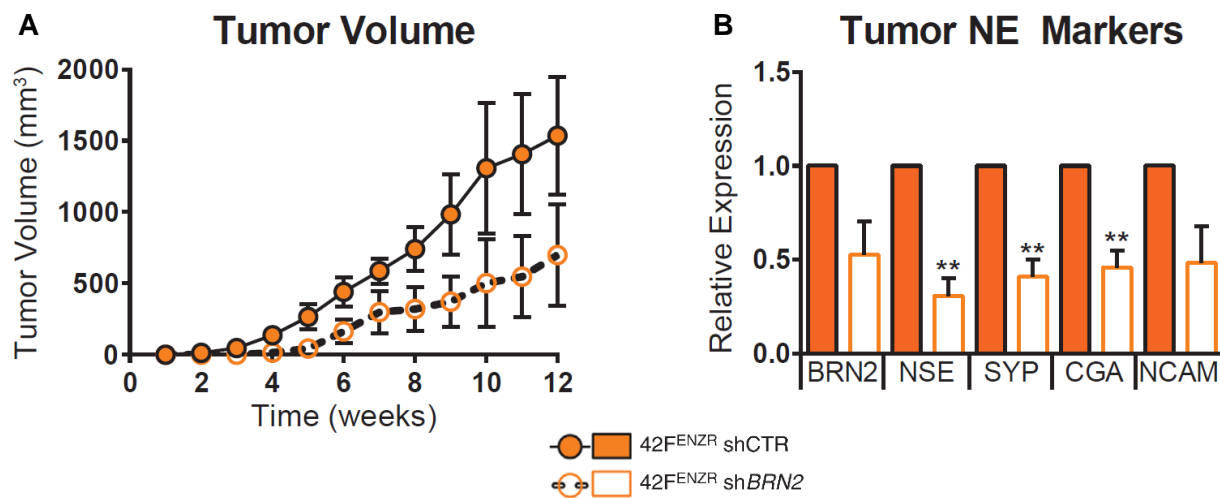


Figure 4.30 - Stable knockout of BRN2 reduces tumor volume and NEPC markers:

(A) Tumor volume of 42F^{ENZ^R} sh-CTR and 42F^{ENZ^R} sh-BRN2 xenografts grown *in vivo* (n=10). **(B)** Relative mRNA expression of BRN2 and NE markers in 42F^{ENZ^R} sh-BRN2 vs. sh-CTR xenografts (=1) harvested at 12 weeks post-inoculation. Graph represents pooled data from 6 sh-BRN2 and 6 sh-CTR tumors.

4.4. Discussion.

Clinical evidence suggests that the repercussion of potent AR suppression with APIs for a subset of CRPC patients is the development of highly lethal NEPC tumors (178). Our work reveals several novel findings with implications for patients with CRPC and NEPC. First and foremost, we identify the master neural transcription factor BRN2 as a central and clinically relevant driver of NE marker expression in advanced PCa. Utilizing a “non-AR driven” *in vivo* derived model of ENZ^R and ENZ treated CRPC, we identified BRN2 as a direct target suppressed by the AR that is both sufficient and required for NE differentiation in PCa and mediates resistance to ENZ. Secondly, our data show for the first time the BRN2 dependent regulation of SOX2 in PCa, and the importance of BRN2 over SOX2 in promoting NEPC. Lastly, our data reveal a striking overlap of AR and SOX binding motifs in the enhancer region of BRN2 that allow the AR to competitively inhibit the interaction between SOX2 and the BRN2 enhancer. These *in vitro*, *in vivo* and human studies highlight BRN2 as a key driver of NE differentiation that may indicate progression towards a non-AR driven or NE phenotype in PCa patients. Moreover, they suggest that relieving AR suppression of BRN2 could be a central mechanism driving NE differentiation, making BRN2 a strong potential therapeutic target for the treatment and/or prevention of NEPC.

BRN2 is a POU-domain transcription factor well-described in developmental biology, where it plays an essential role in neural cell differentiation (320). In addition, BRN2 is highly expressed in NE small cell lung cancer (SCLC), where it acts upstream of other key regulators of neural programming (294) and is required for aggressive tumor growth (295). Complimenting these reports, BRN2 was a highly expressed master neural transcription factor identified in RNA sequencing of our AR non-driven ENZ^R cell lines, making it our top candidate for a potential driver of ENZ induced NE differentiation in PCa. Indeed, we found BRN2 was not only sufficient to increase terminal markers of NE differentiation in CRPC, but was also required for their expression in CRPC cells exposed to ENZ, in ENZ^R cell lines and in bona fide NEPC NCIH660 cells. Importantly, inhibiting BRN2 expression and concomitant reduction in NE markers in both ENZ^R and CRPC cells functionally led to significantly reduced proliferation, migration, invasion as well as decreased ENZ^R tumor growth *in vivo* and increased resistance to ENZ *in vitro*. These data mirror other reports showing the requirement for BRN2 in SCLC (295, 328) as well as in melanoma, where it is required for invasion and migration (329-331). Importantly, we are the first to identify BRN2 as a major regulator of NE differentiation in a model of castration and ENZ resistant PCa and in terminally differentiated NEPC cell lines.

Data from human specimens brought clinical relevance to BRN2 in aggressive PCa tumors, including NEPC. RNA sequencing data from patient cohorts showed that BRN2 was most highly expressed in clinically defined NEPC tumors compared to adenocarcinomas. Importantly however, BRN2 was identified in CRPC specimens as well, indicating that BRN2 is not a specific marker of NEPC, but rather may indicate potential towards disease progression, especially in a setting of androgen deprivation. This was in accordance with our data showing BRN2 is inducible in CRPC cells under the pressure of ENZ and supported our hypothesis that it is an androgen suppressed gene. Indeed, we found BRN2 was most highly expressed in primary adenocarcinoma or CRPC tissue from patients with low levels of circulating PSA, and BRN2 expression significantly increased from progression to CRPC only in patients with low PSA levels. Publically available data mirrored this inverse correlation between high BRN2 expression and low circulating PSA, and further underscored the association between BRN2 and the potential for NE-like disease, as it positively correlated with SYP and CGA expression.

Human data implicating AR control of BRN2 were complemented by mechanistic studies using ENZ^R cell lines, which showed BRN2 is suppressed by the AR through ligand-dependent binding to an ARE in the enhancer region of BRN2. AR binding to this site resulted in reduced levels of not only NE markers but also SOX2, which we also found highly expressed in human NEPC. SOX2 is a well-defined transcription factor that supports the proliferation and invasiveness of prostate cancer (326, 332-334), is associated with NEPC (324), and is required for the function and maintenance of NPCs (335). Importantly however, SOX2 can only drive a neural development program by cooperating with other master transcription factors, especially POU family members (325). In particular, BRN2 and SOX2 co-bind upstream of many genes with central roles in neural cell fate and function (273, 336). Moreover, BRN2 is a key regulator of SOX2 activity in NPCs, a function that is highly evolutionarily conserved (327, 336). Despite extensive research into this “pou-sox code” in neural development, how SOX2 is regulated in PCa is largely unexplored. Our study shows for the first time that BRN2 is required for SOX2 expression in both CRPC cells treated with ENZ as well as ENZ^R cells. The regulation of SOX2 by AR may be compounded by direct enhancer binding (326) and via AR dependent suppression of BRN2. Indeed, as we found for BRN2, SOX2 it is more highly expressed in AR negative than positive PCa cell lines (324), and is higher in NEPC and metastatic CRPC than in adenocarcinoma (324, 326, 337). Altogether, these data suggest that the link between SOX2 and progression to AR-independent CRPC or NEPC may be a result of increased BRN2 expression.

Our results showing BRN2 control of SOX2 also shed light on the importance of BRN2 over SOX2 in driving a NE differentiation in PCa cells. Although SOX2 is present in NE tumors of not only the prostate (324) but lung (338, 339) and skin (340), these studies have not shown a direct requirement of SOX2 in supporting this phenotype. Our results suggest that while SOX2 overexpression alone in CRPC cells can marginally increase CGA, NSE, SYP and NCAM1 expression, SOX2 requires the presence of BRN2 to do so. The hypothesis that BRN2 and SOX2 work together to drive a neural program in CRPC cells is further supported by our data showing direct BRN2/SOX2 protein-protein interaction at the enhancer region of neuronal genes leading to their increase in ENZ^R cells; which is in accordance with previously reported ChIP-seq analysis (273). Importantly however, while BRN2 and SOX2 can both bind upstream of each other in NPCs (273), the controlling signals as well as the consequences of these binding events remain unclear. Intriguingly, our observation that SOX2 bound to a canonical SOX motif that overlapped with the ARE in the enhancer region of BRN2 suggests that the AR may play an important role in controlling SOX protein DNA binding in PCa cells. While the consequence of this inhibition of SOX2 binding to the BRN2 enhancer in the presence of androgen remains unclear, it may be that this interaction supports the two factors coordinating to drive downstream neural gene expression.

While our study focuses on the role of SOX2 and BRN2 in the context of ENZ-resistance, in 2017, Mu et al. interrogated the relevance of SOX2 upregulation in PCa cells upon loss of tumor suppressors RB1 and TP53 and its relationship with luminal and basal PCa lineages (141). The authors were able to demonstrate that SOX2 regulates levels of basal KRT5, KRT14 and p63, thus triggering a luminal to basal switch in LNCaP/AR cells. Consistent with our data, they also observed a nominal increase in NE markers upon SOX2 overexpression in LNCaP/AR cells. Moreover, the inhibition of SOX2 in p53 and Rb1 knockout cells slightly reduced the expression of NE markers. Interestingly, upregulation of SOX2 was also observed in the DNPC population characterized by Bluemn et al (40) which lack NE marker expression and it has been characterized to promote CRPC progression (341). Altogether, these data suggest SOX2 functions as a mediator of different mechanisms of PCa disease progression to different phenotypes likely through its ability to bind to and functionally co-operate with a variety of transcription factors (342, 343).

Although multiple pathways likely converge to drive emergence of NEPC, understanding the contribution of the AR to this disease is critical for better implementation of current API therapies and novel drug design. Together, data from our human cohorts and in vitro

mechanistic analysis strongly implicate BRN2 as an androgen suppressed transcription factor that plays a significant role in the progression of PCa from adenocarcinoma to NEPC, making it a potentially attractive and novel therapeutic target.

5. Chapter 5: *Development and Characterization of small molecule inhibitors for BRN2 as a treatment strategy for NEPC*

5.1. Introduction and *in silico* background

The constant pressure on CRPC tumors by androgen receptor pathway inhibitors (ARPIs), most notably enzalutamide (ENZ) and abiraterone (Abi), selects for ENZ (ENZR) or Abi (AbiR) resistant cells that are less dependent on AR for growth and survival, thereby shifting the natural history of this classically AR-driven disease to an AR indifferent phenotype (298). Up to 25% of ARPI-resistant CRPC patients develop lineage plasticity changes associated with low AR signaling including intermediate and terminally differentiated neuroendocrine prostate cancer (NEPC), for which only limited palliative treatments exist (300, 344, 345). The lack of innovative therapies for ENZ-resistant tumors, in particular those exhibiting neuroendocrine features, stems from our limited molecular understanding of this deadly disease. Hence, to understand the molecular mechanisms that facilitate the trajectory from adenocarcinoma to highly aggressive and lethal NEPC, our lab developed a pre-clinical model of ENZR that captures both AR-driven as well as the AR-indifferent NEPC-like phenotype. Using this model we have been successful in identifying potentially untapped, novel therapeutic targets for the NEPC subset of CRPC patients. In particular, RNA-seq transcriptional profiling identified the neural POU-domain transcription factor BRN2 as strongly upregulated in ENZR NEPC-like tumors and cell lines (145), which was complemented by parallel findings in NEPC patient datasets. Further functional studies, both *in vitro* and *in vivo*, confirmed that BRN2 expression is an absolute requirement for the emergence and maintenance of NEPC phenotype. Based on the data shown in Chapter 4 (145), we have discovered BRN2 as a central and targetable driver of NEPC in ENZR CRPC that warrants further pre-clinical evaluation.

5.1.1. *In silico* modeling of BRN2

BRN2 is a transcription factor (TF) and targeting TFs can be highly effective in treating particular malignancies as has been seen with the success of targeting the AR in prostate cancer. However, unlike AR, most TFs do not harbor a ligand-binding domain (LBD) and inhibitors cannot be designed by studying the natural ligand. Historically, these TFs lacking an LBD are considered difficult to target. However, recent advances in x-ray crystallography and

modern drug discovery approaches shed more light on targeting DNA binding domains of TF as a promising strategy (346, 347).

Since the crystal structure (a common prerequisite for *in silico* drug discovery) of human BRN2 has not been resolved, we built its structure using a homology modeling approach (348). Structurally, the POU domain of BRN2 consists of two subdomains, a C-terminal homeodomain (POU^H) and N-terminal POU-specific region (POU^S) separated by a short non-conserved linker. Based on the sequence homology and crystal structure of other POU-domain proteins (Pit1, Oct1 and BRN5), we developed a BRN2 structure (**Fig. 5.1A**). The flexible loop that connects POU^H and POU^S domains was further refined by Loop Modeler module in MOE software. The quality of the developed BRN2 structure was assessed using Ramachandran plot (**Fig. 5.1B**) and 100 nano-seconds (ns) molecular dynamic (MD) simulations using AMBER (**Fig. 5.1C**) (349). During MD simulations different conformations of BRN2 were explored and their respective stability was assessed by the root mean squared deviation (RMSD) between the initial conformation and each snapshot during MD simulations. The most stable and thermodynamically favorable conformation was established after 35ns simulation time (**Fig 5.1C**). This protein conformation was extracted and its active site was identified using Site Finder module implemented in MOE. We observed that BRN2 does not attain a stable conformation until the protein is allowed to fold for at least 35 ns in conditions simulating the cellular environment, suggesting that our model is likely more robust than a previously described homology model using a 20 ns simulation (350) and provides the optimal confirmation of BRN2.

While BRN2 lacks traditional targeting motifs like a LBD, our modelling identified a potential pocket in the DNA-binding domain (DBD) that could be used to inhibit BRN2 function. As such, four million small-molecules from ZINC database v15 (351) were docked into the DBD pocket of our hBRN2 model structure using Glide (352) and FRED (353) programs. RMSD values were calculated between the docking poses generated by Glide and FRED to identify the most consistent binding orientation of the compounds. Only molecules with poses having RMSD values below 2.0 Å were selected for further analysis. Furthermore, the selected ligands were subjected to additional on-site scoring using the LigX program and the pKi predicting module of the MOE. The 5,000 compounds that consistently demonstrated high predicted binding affinities were selected for visual inspection to exclude compounds containing reactive or toxic groups such as aldehyde and alkyl halide groups. Based on chemical diversity and availability, 62 chemicals were purchased from commercial vendors as a first step of drug testing.

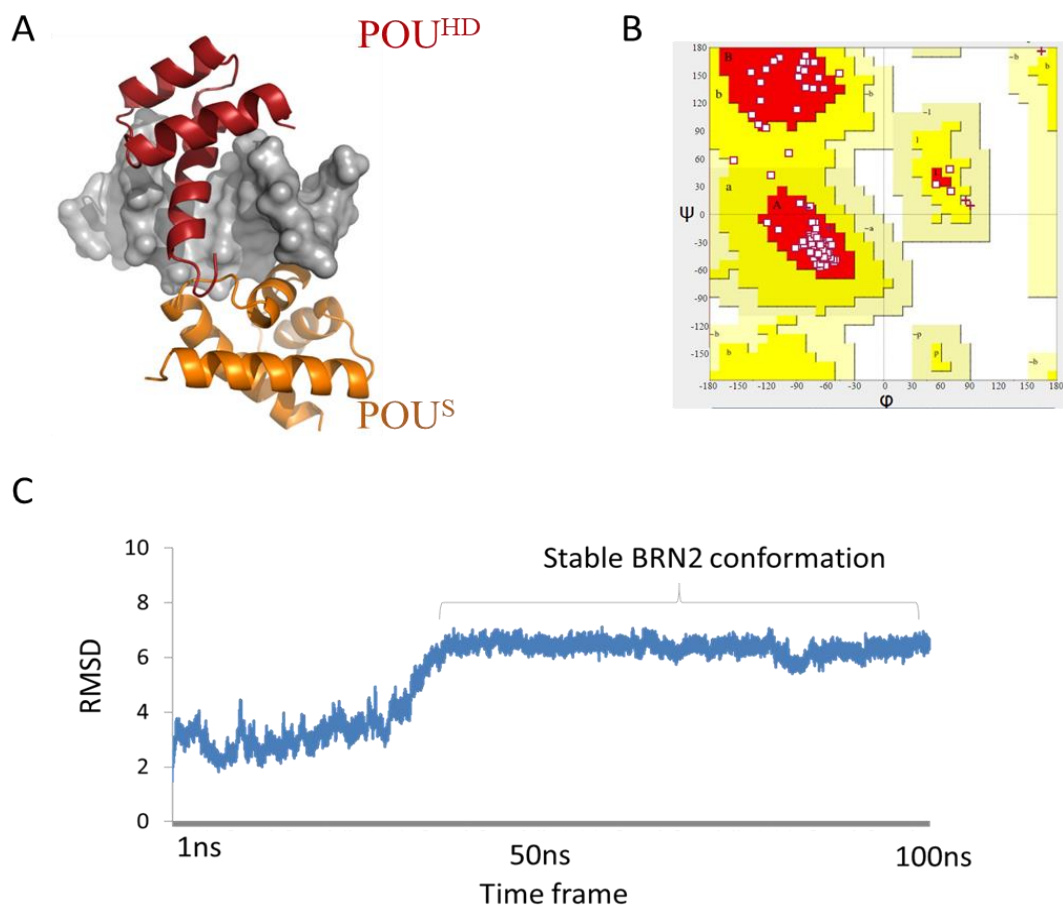


Figure 5.1 - Structural information of the BRN2 protein:

A) Modeled structure of the human BRN2, built using Modeler v9.16. POU^{HD} and POU^S domains are shown in red and orange color, respectively. DNA is shown as grey surface. Loop region is not shown for clarity. **B)** Ramachandran plot showing the structural quality of the developed protein. It should be noted that all the residues except Ser538 fall under allowed region (yellow boundary) confirming high quality of the generated structure. **C)** Root mean square deviation (RMSD) plot generated based on 100ns-molecular dynamic simulations. The RMSD plot shows that conformation of the protein changes significantly after 35ns. However, protein attains stability and maintains its structural integrity throughout remaining simulation time.

5.2. Results

5.2.1. Exclusion Criteria for hits from *in silico* screening

Sixty-two compounds were evaluated *in vitro* in a step-wise manner based on the following **selection/exclusion criteria**:

1. Repression of BRN2 transcription activity using luciferase reporter
2. Affinity to BRN2.
3. Selectivity to BRN2^{hi} (42D^{ENZR}) vs. BRN2^{neg/lo} (16D^{CRPC}) cell lines
4. Repression of bona fide direct BRN2 transcriptional target (SOX2) and NEPC markers (NCAM1 and CHGA)

Criterion #1: The compounds were evaluated for their ability to inhibit BRN2 transcriptional activity using BRN2^{hi} 42D^{ENZR} cells. In short, 42D^{ENZR} cells stably expressing a BRN2 reporter cassette were treated for 24 hours and compounds that inhibited luciferase activity greater than 75% at 10 μ M passed criterion 1 (**Figure. 5.2**) and progressed to the 2nd step in the pipeline. The dotted line represents 50% inhibition while the red line represents 75% inhibition. At the first step, compounds 7,8,18,39,40 and 62 displayed enough inhibition of BRN2 transcriptional activity to progress to the Criterion #2.

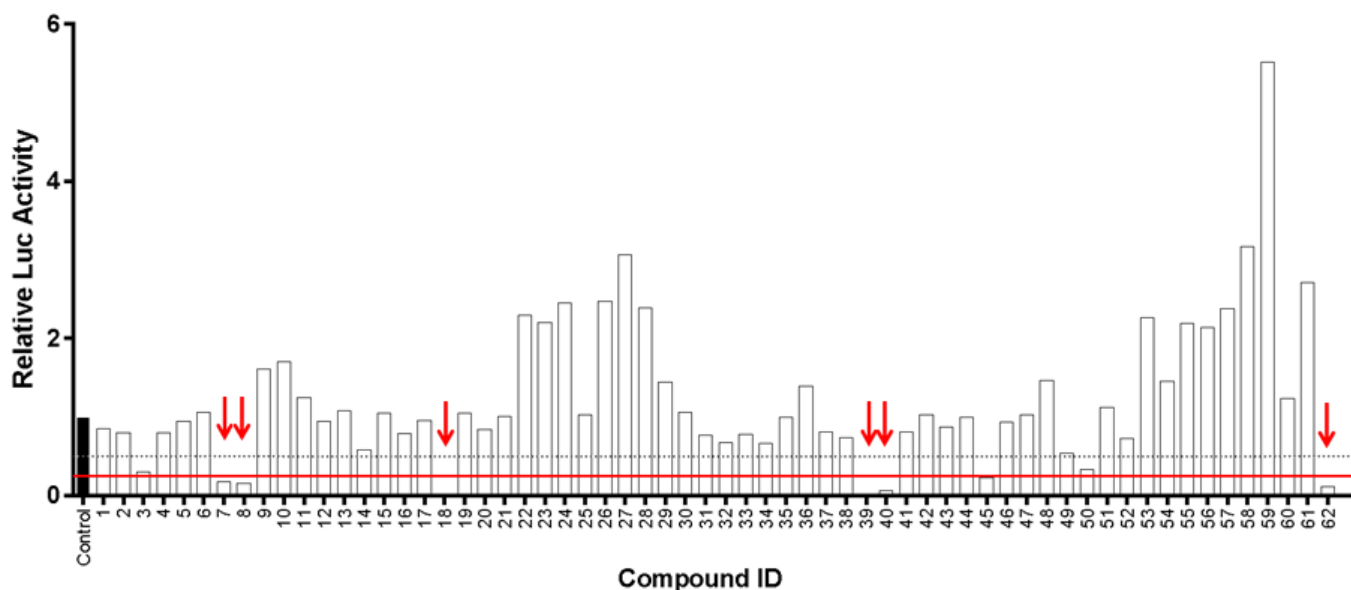


Figure 5.2 - Inhibition of BRN2 transcriptional activity:

Effect of BRN2 small inhibitors on BRN2 transcriptional activity: 42D^{ENZR} cells were transfected with BRN2-Luc plasmid and treated with 10 μ M BRN2 inhibitors and luciferase activity and activity was performed.

Criterion #2: The 2nd selection step provides a yes/no answer for whether the compounds that cleared criterion #1 directly interact with BRN2 protein. This was done using an in-cell assay called the Drug Affinity Responsive Target Stability (DARTS) assay. This assay relies on the protection against proteolysis conferred on the target protein by interaction with a small molecule. Cell lysate from 42D cells is incubated with either DMSO or 3 μ M of one of the compounds. Approximately 1 hour after, the lysate is exposed to increasing doses of the protease Pronase for precisely 30 minutes. The reaction is halted and the lysate is run on an SDS gel and the amount of BRN2 left in the lysate is measured via Western Blot. **Figure 5.3** displays the results of the DARTS assay with the compounds from the 1st selection step. Comparing each “- +” pair at 10⁻⁴ and 10⁻³ concentrations of Pronase shows differences in the amount of BRN2 left over after 30 minutes. Importantly, this difference is attributed to the protection BRN2 gains from the proteolysis process due to the binding of the inhibitors shown with compounds 7, 18 and 39 and not by compounds 8 and 40.

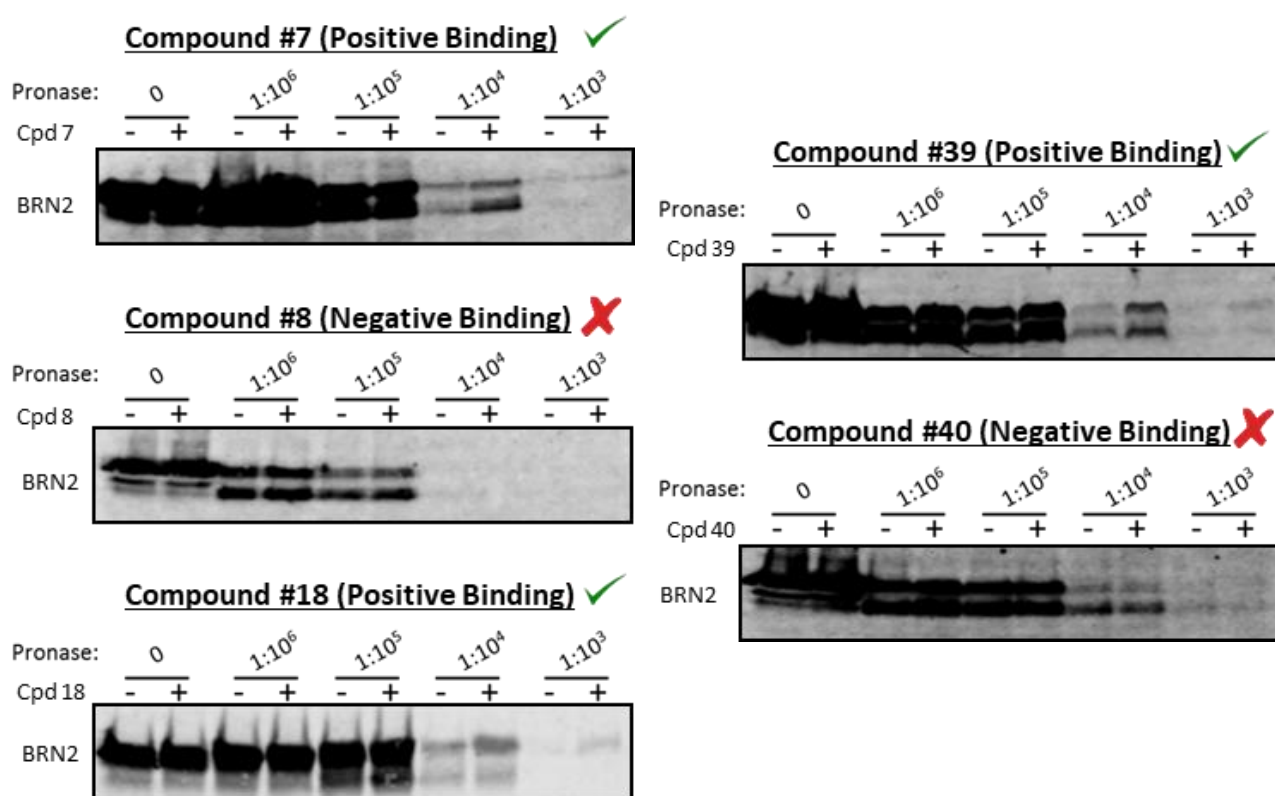


Figure 5.3 - DARTS assay:

BRN2 using DARTS assay: Cell lysate was incubated with BRN2 inhibitors in the presence or absence of Pronase.

Criterion #3: The 3rd crucial yet simple step excludes molecules with off target effects. The 3 molecules that exhibit direct binding to BRN2 were subsequently assessed for activity by cell proliferation using BRN2^{hi} (42D^{ENZR}) and BRN2^{neg/lo} (16D^{CRPC}) cell lines (**Fig. 5.4 - Criterion #3**). All compounds were found to have anti-cancer activity in NEPC cells however only Cpd.7 and Cpd.18 inhibit cell growth in 42D^{ENZR} without any effect on 16D^{CRPC}, while compound 39 failed the criteria as it had off-target anti-proliferative effect on 16D^{CRPC} cells (**Fig. 5.4 – Criterion #3**).

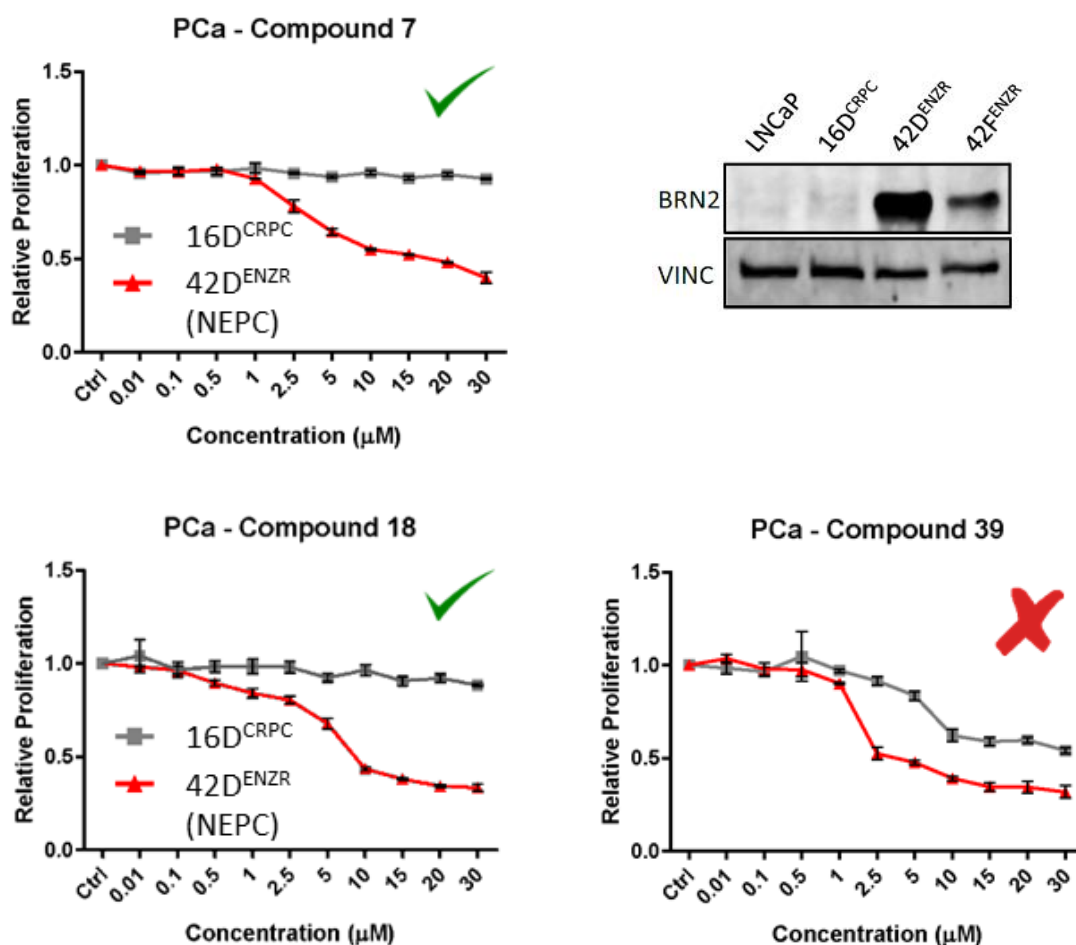


Figure 5.4 - Cell proliferation:

Cell proliferation: NEPC-like cells 42D^{ENZR} and 16D^{CRPC} were treated with different concentrations of BRN2 inhibitors for 72 hours and cell proliferation was performed

Criterion #4: The last criterion measures downstream effects of BRN2 inhibition. For this step, we evaluate whether the compounds can inhibit gene expression of BRN2 target SOX2 as well as NEPC markers NCAM1 and CHGA. Both Cpd.7 and Cpd.18 were found to decrease expression of BRN2 dependent gene SOX2 and NE markers NCAM1 and CHGA in 42D^{ENZR} cells (**Fig. 5.5 – Criterion #4**), thus passing the selection criteria of our full pipeline.

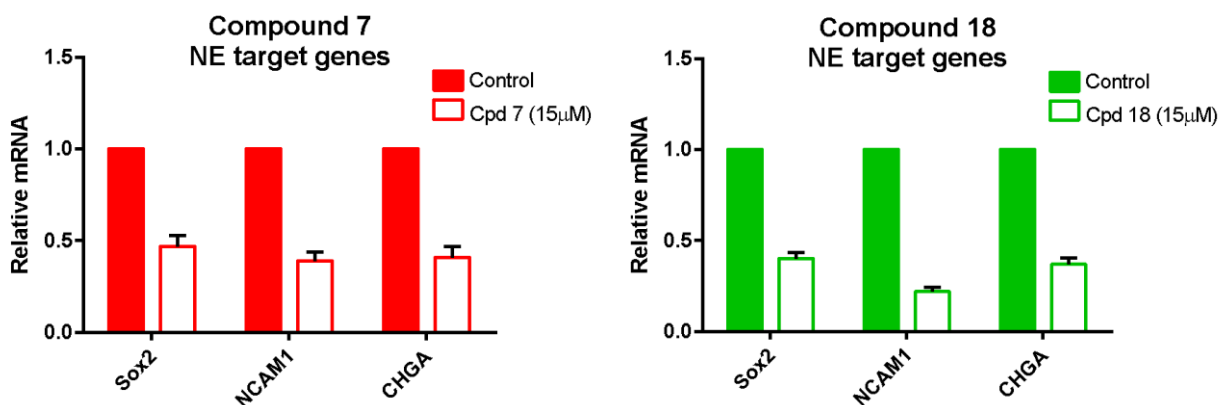


Figure 5.5 - Compounds inhibit BRN2 targets and NEPC markers:

42D^{ENZR} cells were treated with 10μM of BRN2 inhibitors for 48 hours and expression of Sox2, NCAM and CHGA was evaluated using qRT-PCR.

5.2.2. Compounds 7 and 18 directly bind to BRN2 DNA binding domain

In order to confirm that both Cpds 7 and 18 bind directly to BRN2 we utilized BioLayer Interferometry to detect interaction with the DNA binding domain of BRN2. Amino acids 264-440 of BRN2 containing the POU^S, the linker region and POU^H domain was cloned into the pET vector using Polymerase Incomplete Primer Extension (PIPE) cloning (354). In short, primers for the BRN2 insert and the pET vector were designed with matching overhangs with the C-terminus overhang containing the His-tag (**Fig. 5.6**). The PCR products transformed into BL21 cells post digestion with restriction enzyme *Dpn1*.

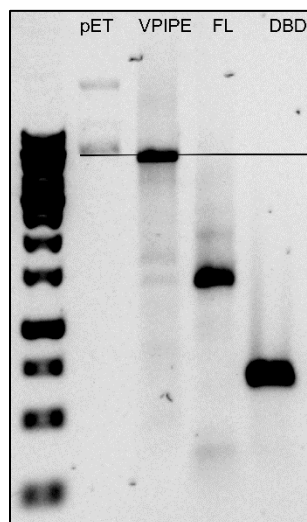


Figure 5.6 - PIPE cloning of BRN2-DBD in pET vector:

Agarose gel displaying the amplicons of the Vector and the two inserts, BRN2 full length (FL) and DBD inserts.

The finished vector containing an Avidin tag at the N-terminus and a His-tag at the C-terminus was co-transformed into bacteria with a pBirACm biotin ligase plasmid. The BRN2-DBD was purified using Ni-nTA affinity chromatography and buffers previously described (187). The purified protein was immobilized on a streptavidin biosensor and the interaction between BRN2 and the two compounds was measured in real time through an interference pattern generated on the Octet system as previously described (188). **Figure 5.7** demonstrates that both compounds 7 and 18 reversibly bind to the DBD of BRN2. This is demonstrated by the loss of signal after 60 seconds as the biosensor is removed from buffer containing the compounds and washed. Furthermore, the increased signal is dose dependent manner, going from 1 μ M (red line) to 50 μ M (teal line).

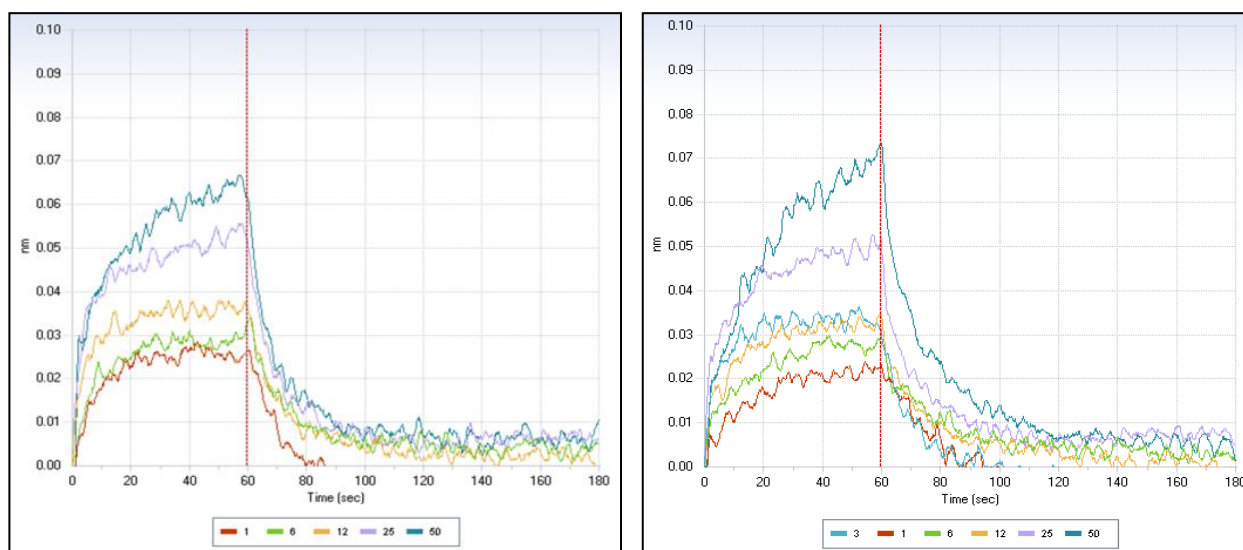


Figure 5.7 - BioLayer Interferometry:

BRN2i Cpd. 7 and 18 binding to purified DNA binding domain of BRN2 quantified using BLI assay.

Combined with the data from the exclusion pipeline, these experiments demonstrate that Compounds 7 and 18 function as BRN2 inhibitors (BRN2i) that bind within the DNA binding domain of BRN2 and inhibit its activity and growth promoting effects.

5.2.3. BRN2 inhibitors disrupt DNA binding

For the purposes of inhibiting BRN2 activity, the initial goal was to design inhibitors for the DNA-binding domain. While Figure 5.6 shows that the two compounds possess the capability to bind to the DBD of BRN2, it does not show evidence that this interaction inhibits BRN2's ability to bind to DNA. To address this, 42D^{ENZ}R cells were subject to sub-cellular

fractionation after short-term (6h) treatment with different BRN2 inhibitors. **Figure 5.8** demonstrates that these compounds work by inhibiting the interaction between BRN2 and the chromatin. Unsurprisingly, most of the BRN2 is detected in the nuclear fraction while the cytoplasmic is relatively empty. Importantly, consistent with our hypothesis that these compounds inhibit DNA binding, the amount of BRN2 detected in the chromatin bound fraction decreases dramatically once the cells are treated with 20μM of Cpd. 7, 18 and derivative 18₁₄ compared to control. HSP90 and Histone H3 are controls for each sub-cellular fraction.

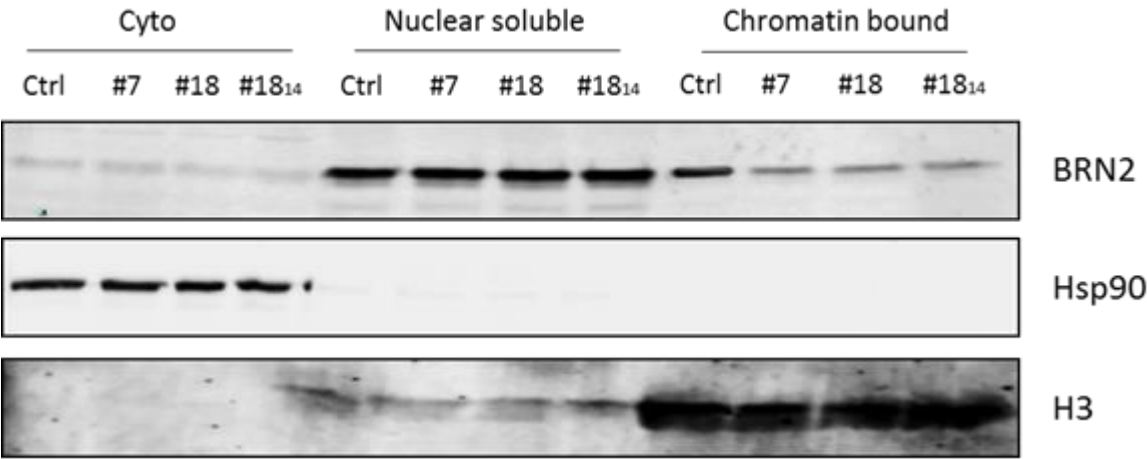


Figure 5.8 – Sub-cellular Fractionation:
 42D^{ENZR} cells were treated with BRN2i at a dose of 20μM for 6 hours prior to cell lysate. Following lysis and fractionation assay, lysate analyzed by WB for indicated genes.

In further support of this hypothesis, ChIP was conducted with BRN2 antibody in 42D^{ENZR} cells ± 20μM of Cpd. 18 for 6 hours. The data showed a marked reduction in BRN2 recruited to specific regions around the SOX2 and PEG10 genomic loci (**Figure 5.9**); originally extracted from ChIP-seq done in Glioblastoma (289). Altogether, these two experiments greatly support the hypothesis that the BRN2i function by interfering with the BRN2 and DNA interaction, thus abolishing its’ transcriptional activity.

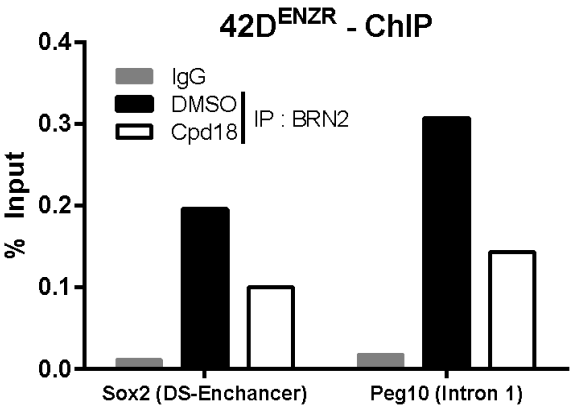


Figure 5.9 - BRN2 Chromatin Immunoprecipitation:
 42D^{ENZR} cells were treated with BRN2i at 20μM for 6 hours were lysed and sonicated. DMSO and Cpd18 treated cells were immunoprecipitated with BRN2 antibody with IgG as control. Extracted DNA was amplified with qRT-PCR for regions of Peg10 and Sox2. Data was analyzed with % Input method.

5.2.4. Pathways downstream of BRN2 inhibition

The previous results chapter examined the role of BRN2 specifically relative to NE differentiation and NEPC markers (SYP, CHGA and NCAM1). The downstream response of cellular pathways to BRN2 inhibition was studied by conducting a gene profiling of 42D^{ENZR} cells treated with BRN2 inhibitors for 48 hours (**Figure 5.10**). Interestingly, the data revealed greater than 50% reduction of major NEPC drivers previously identified: SOX2 (141), PEG10 (122), AURKA (135), EZH2 (2, 160), ASCL1 (313) and SOX11 (144). In addition to the drivers and NEPC markers (Fig. 5.7), surprisingly we observed reduced expression of many of the epigenetic regulators that have been implicated in progression of NEPC like DNMT1, SUV39H1, DNMT3B, CBX1, CBX2, CBX3 and CBX5 (162).

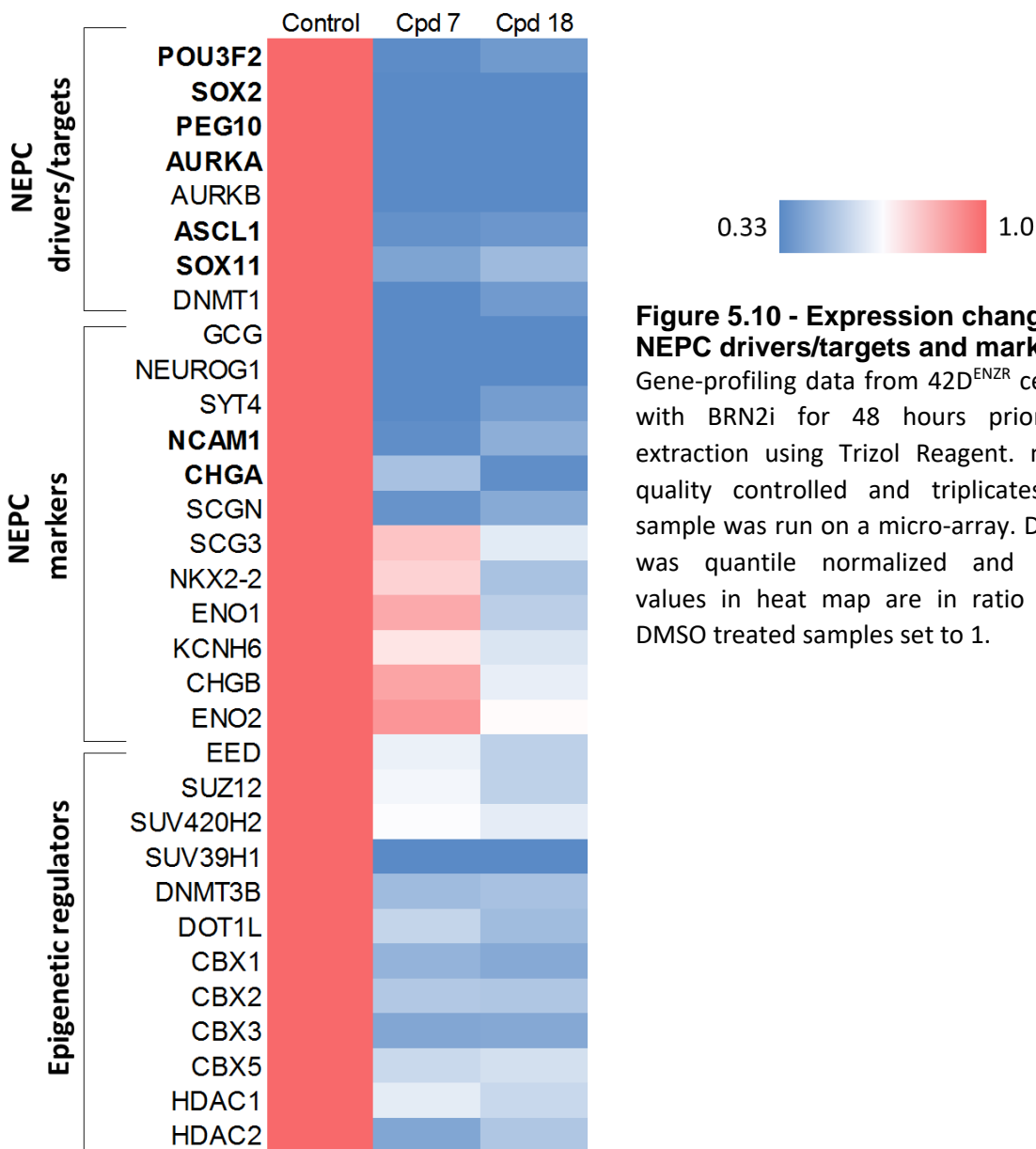


Figure 5.10 - Expression changes in NEPC drivers/targets and markers: Gene-profiling data from 42D^{ENZR} cells treated with BRN2i for 48 hours prior to RNA extraction using Trizol Reagent. mRNA was quality controlled and triplicates of each sample was run on a micro-array. Data output was quantile normalized and expression values in heat map are in ratio to 42D^{ENZR} DMSO treated samples set to 1.

One of the more interesting discoveries from the micro-array we found was that the compounds also down-regulated BRN2 itself. This phenomenon has been alluded to several times in publications. In 2014, Suva et al. discovered that the over-expression plasmid they utilized for BRN2 was in fact hyper-methylated and the BRN2 mRNA in the cells contained the 3' UTR region suggesting that the exogenous expression eventually triggered endogenous BRN2. Moreover, ChIP-seq data from Urban et al. also showed evidence of BRN2 binding in its own promoter, creating a feed-forward loop for its expression. Utilizing our molecules as a tool, we demonstrate that Cpd. 18 reduces BRN2 expression in a dose dependent manner (**Figure 5.11 - left**). Furthermore, once BRN2 expression is triggered in 16D^{CRPC} cells for 24 hours with Doxycycline, its expression is maintained for up to 7 days once the Dox has been removed from the media. Altogether, this data greatly supports the hypothesis that BRN2 regulates its own expression (**Figure 5.11 - right**).

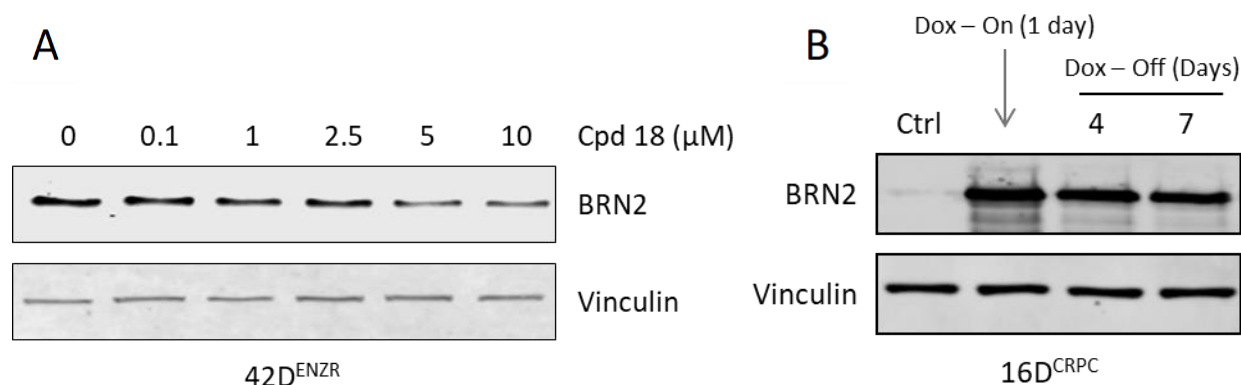


Figure 5.11 - BRN2 autoregulation:

(A) 42D^{ENZR} cells treated with increasing doses of Cpd. 18 for 48 hours. Lysate was collected and protein expression analyzed by WB. **(B)** 16D^{CRPC} cells transfected with Doxycycline inducible BRN2. Cells were stimulated with 1ng/mL of Doxycycline for 24 hours and then removed. Samples were collected for WB analysis at indicated time points.

The downstream effects of BRN2 inhibition were further validated in human NEPC cell lines, NCI-H660. We found that Cpd 7 and 18 not only reduced cell proliferation, but also downregulated expression of a majority of the genes previously studied in Results Chapter 2 and identified in the gene profiling. **Figure 5.12** shows that inhibition of BRN2 in terminal NEPC cells (NCI-H660) also reduces expression of important NEPC drivers like SOX2, ASCL1, PEG10 and n-Myc.

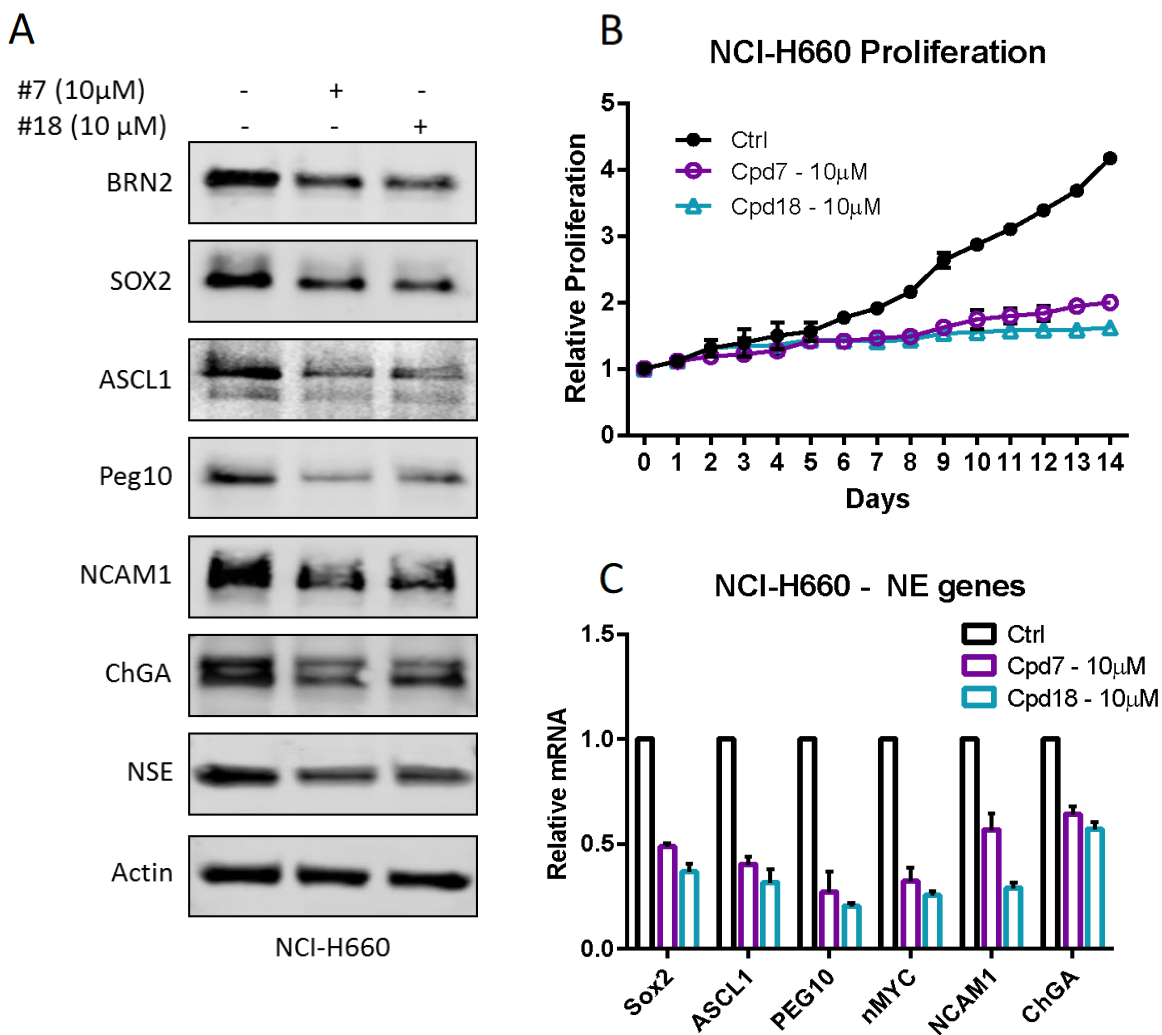


Figure 5.12 - BRN2i reduce NEPC cell proliferation and expression of NEPC drivers and markers:

(A-C) NCI-H660 cells were treated with 10 μ M of BRN2 inhibitors Cpd. 7 and 18 (A) for cell proliferation measured using Incucyte ZOOM, (B-C) for 7 days and cells were extracted for (B) WB analysis of indicated genes and (C) qRT-PCR analysis for indicated genes.

One of the major consistencies in NEPC is the loss of Rb1. While the mRNA levels of Rb1 isn't altered in 42D^{ENZR} cells, Rb1 is hyper-phosphorylated and non-functional (355), thus mimicking the conditions observed in patients (**Figure 5.13A-B**). Therefore, it is no surprise that these cells are enriched for the Rb1 loss signature (**Figure 5.13C**). Interestingly, while analyzing the micro-array, we discovered that treatment with the BRN2 inhibitors completely reverses the Rb1 loss signature (**Figure 5.13D**).

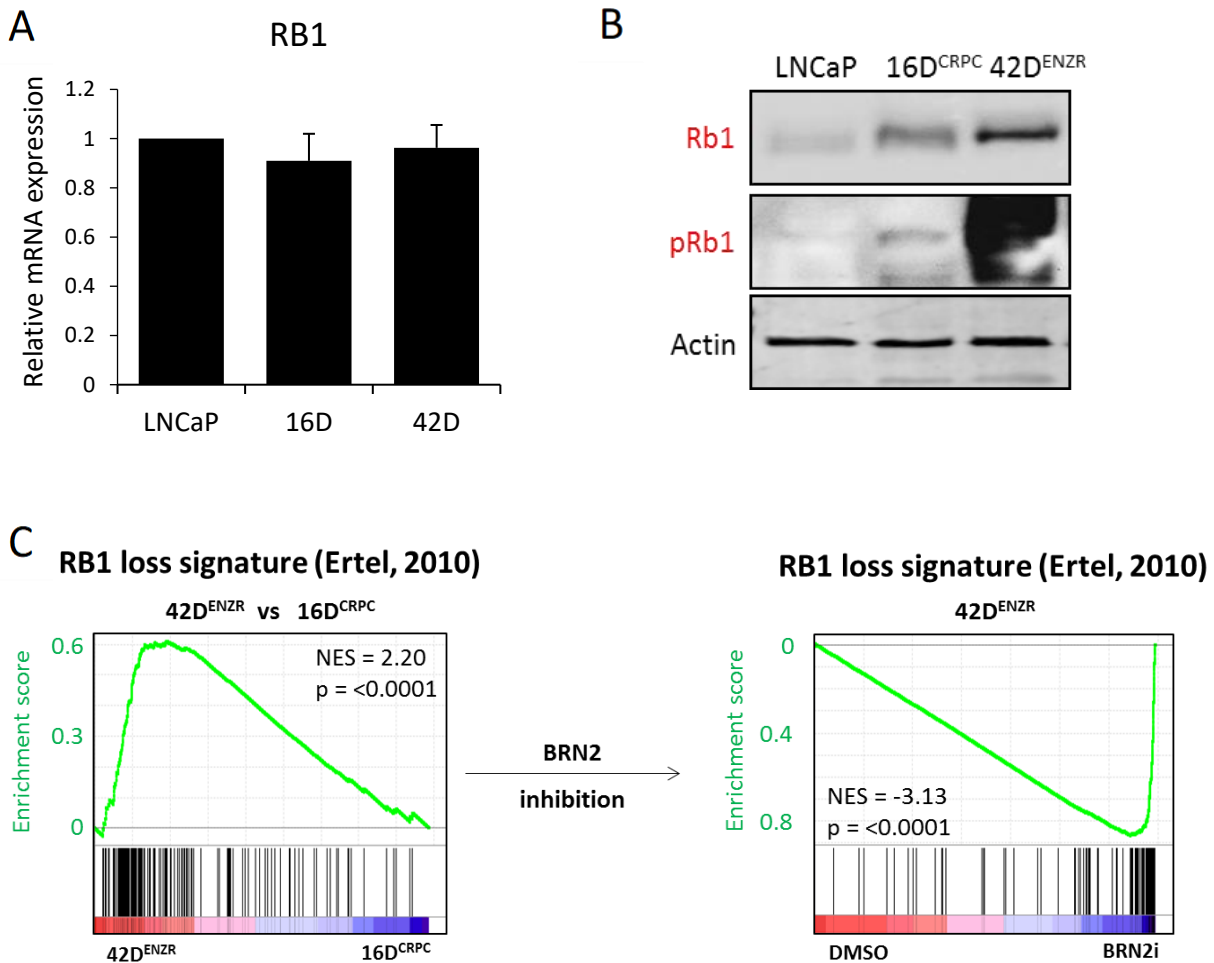


Figure 5.13 - Rb1 status in ENZR cells relative to BRN2

(A) qRT-PCR of Rb1 mRNA levels in LNCaP, 16D^{CRPC} and 42D^{ENZR} cells with LNCaP set as control (=1). (B) Western Blot analysis of protein levels of Rb1, pRb1 (Thr 821/826) and Actin as control. (C) GSEA analysis of Rb1 loss signature enrichment in 42D^{ENZR} cells. (D) GSEA analysis of Rb1 loss signature downregulated after treatment with BRN2i (combined analysis of expression data from Cpd7 and Cpd 18).

This striking reduction in the Rb1 loss signature, essentially the E2F1 signature prompted an examination of the cell cycle in response to BRN2 inhibition. E2F1 signaling is crucial for transition from Growth phase 1 (G₁) to DNA Synthesis (S) phase of the cell cycle (356). Consistent with this, we found that BRN2 inhibition caused powerful G₁ arrest and as approximately 90% of the cells are at this phase. Although not as potent, siRNA treatment with BRN2 showed a similar trend (**Figure 5.13**).

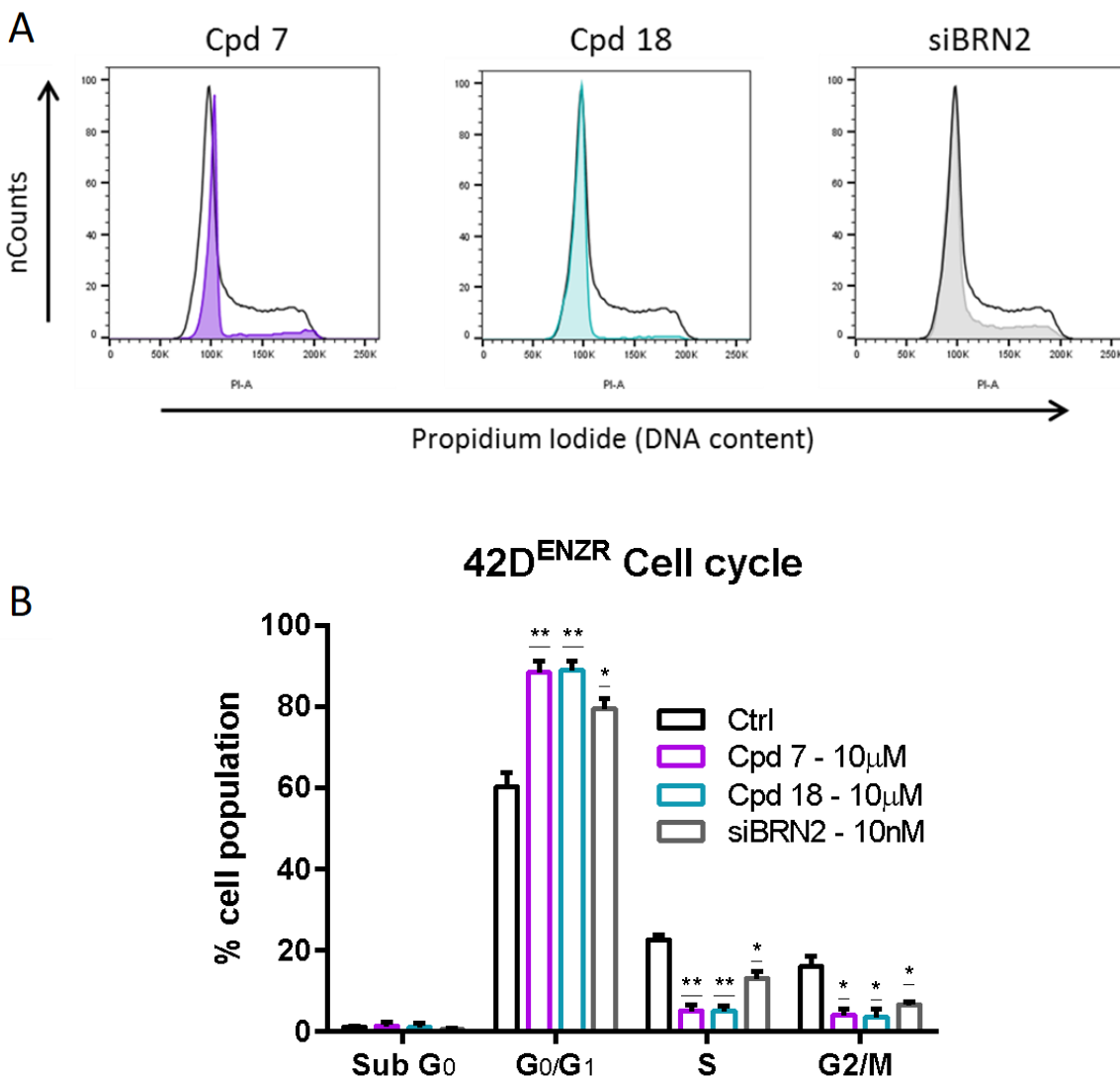


Figure 5.14 - Cell cycle changes in response to BRN2 inhibition:

(A) Flow Cytometry analysis of Propidium Iodide staining vs counts in 42D^{ENZR} cells treated with BRN2i and siBRN2 for 48 hours. Cells were trypsinized, fixed and stained with PI. **(B)** Cell populations analyzed via FlowJo indicate cell cycle stages between the different treatments. Data presented is pooled from 3 independent experiments.

While the propidium iodide (PI) staining provides a general idea about the cell cycle stage of the cells, it cannot differentiate between G_1 and G_0 quiescent cells. Using a different DNA staining agent Hoescht dye and an RNA staining agent Pyronin Y it is possible to separate out active cells containing $2n$ amount of DNA and high RNA content (Q1) and quiescent cells that have $2n$ DNA but low RNA content (Q4). **Figure 5.14** below reveals that 48 hours after BRN2 inhibition the cells are arrested but have not entered a quiescent state as their RNA content is extremely high.

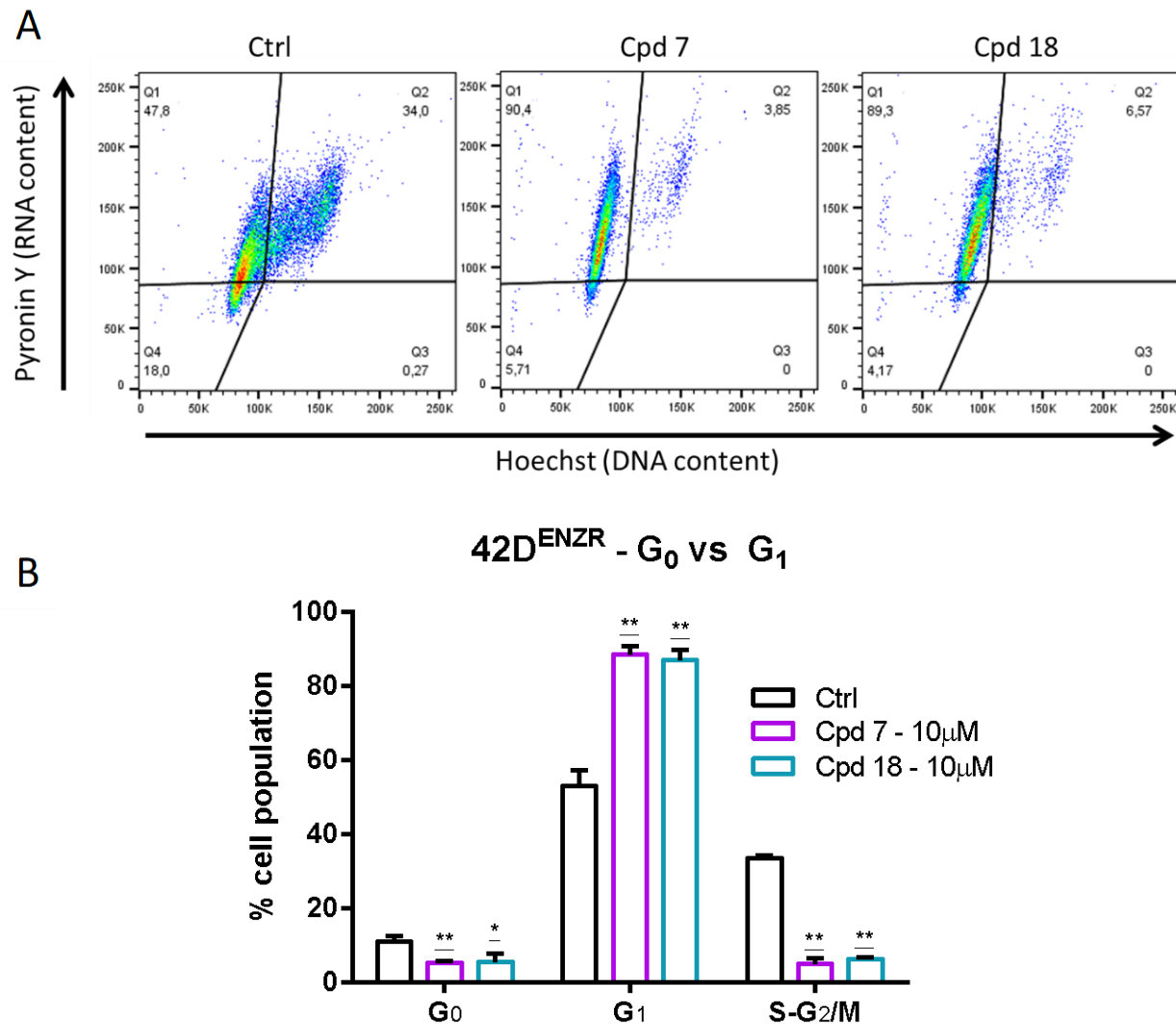


Figure 5.15 - G_0 / G_1 separation:

(A) Flow Cytometry analysis of Pyronin Y staining vs Hoescht staining in 42D^{ENZR} cells treated with BRN2i for 48 hours. Cells were Trypsinized, fixed and stained first with Pyronin Y and then with Hoescht. **(B)** Cell populations analyzed via FlowJo indicate cell cycle stages between the different treatments. Data presented is pooled from 3 independent experiments.

Delving further into the molecular mechanisms behind this cell cycle arrest, we mined our gene-profiling data for cell cycle inhibitory pathways that are activated in response to BRN2 inhibition. Strikingly, we discovered a modest yet significant recovery of p53 signaling, another major tumor suppressor lost in approximately 60-70% of NEPC patients (**Fig. 5.15 A**). The top genes in this pathway that were upregulated were cyclin dependent kinase inhibitors p21 (CDKN1A) and p27 (CDKN1B) (**Fig. 5.15 B**). These data were recapitulated at protein levels (**Fig. 5.15 C**). The cell cycle data from **Figure 5.8** also no changes in sub G0 levels suggesting a lack of apoptosis and consistent with this, we observed no PARP cleavage.

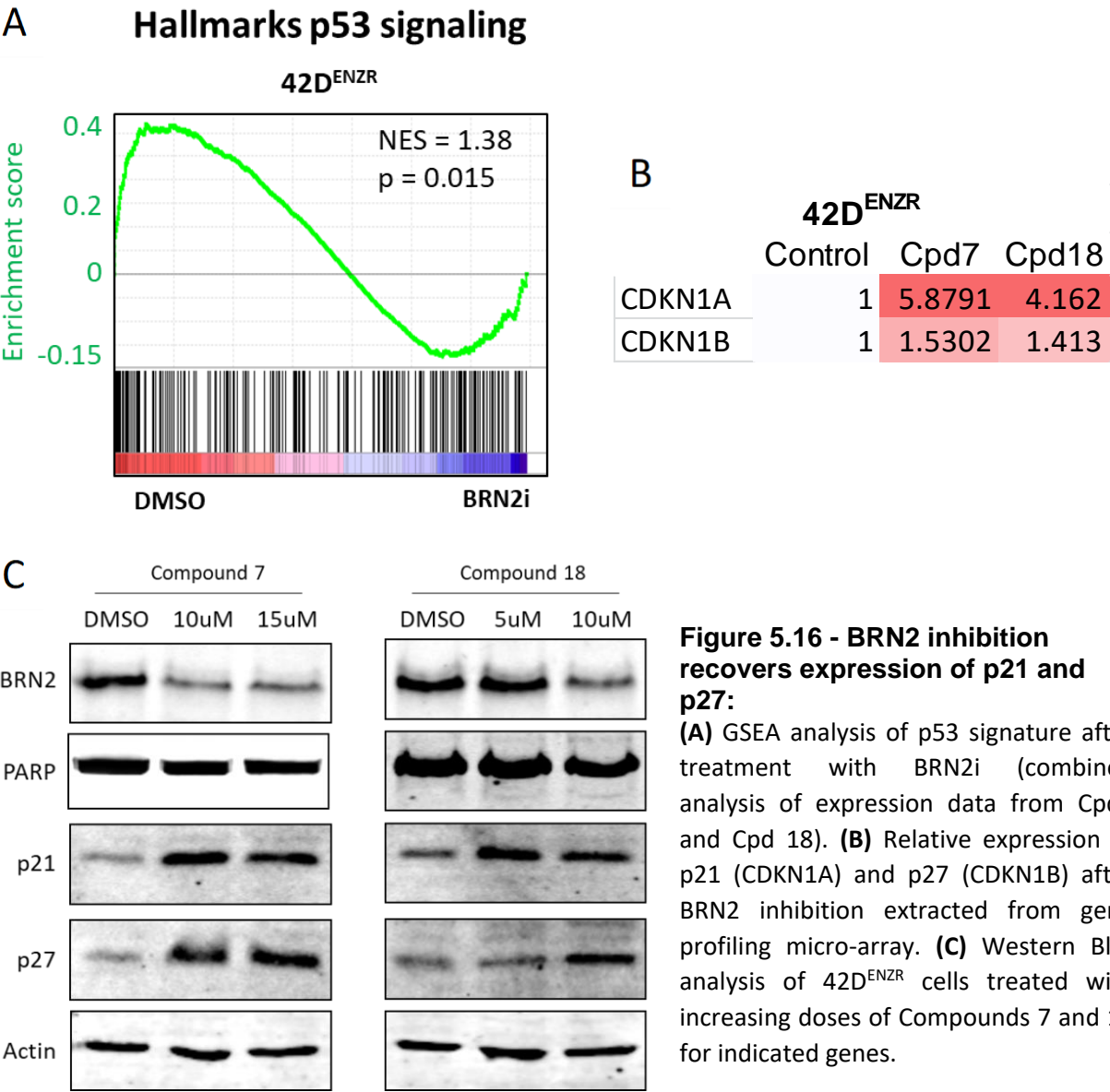


Figure 5.16 - BRN2 inhibition recovers expression of p21 and p27:
(A) GSEA analysis of p53 signature after treatment with BRN2i (combined analysis of expression data from Cpd7 and Cpd 18). **(B)** Relative expression of p21 (CDKN1A) and p27 (CDKN1B) after BRN2 inhibition extracted from gene profiling micro-array. **(C)** Western Blot analysis of 42D^{ENZR} cells treated with increasing doses of Compounds 7 and 18 for indicated genes.

As an important cross-validation, we first examined if this recovery of p21 was consistent between our inhibitors and siRNA treatment for BRN2 (**Figure 5.16A**). Moreover, transfection of BRN2 targeting guide RNA (gRNA) in a stable inducible eSpCas9 42D^{ENZ}R system for 48 hours caused in a dose dependent reduction in BRN2 and a concomitant increase in p21 (**Figure 5.16B**). Altogether, this data demonstrates the on target nature of the inhibitors as well as the consistency in the effects of inhibiting and downregulating BRN2.

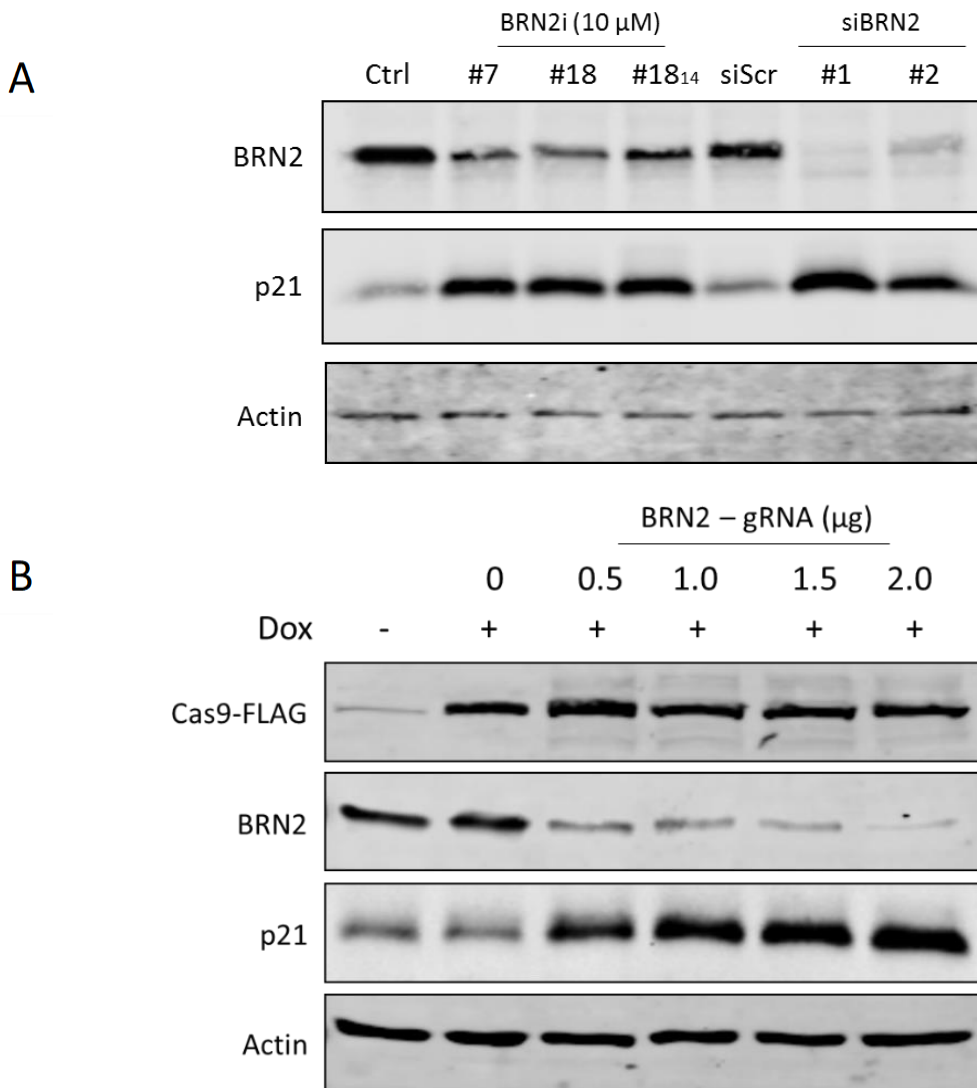


Figure 5.17 - Targeting BRN2 via different mechanisms:

(A) Western Blot analysis of indicated genes in 42D^{ENZ}R cells treated with 3 chemically different BRN2 inhibitors and 2 different siRNA for BRN2 for 48 hours. **(B)** 42D^{ENZ}R cells stably transfected with Dox. Inducible eSpCas9 cells were transfected with doses of guide RNA (gRNA) target Exon 1 of BRN2 and treated with 10ng/mL of Dox. Cells were lysed 48 hours later and Western Blot was performed for indicated genes.

5.2.5. Targeting BRN2 greatly sensitizes cells to AR pathway inhibition

Data from chapter 4 indicates that increased expression of BRN2 in can confer resistance to enzalutamide (Fig. 4.18D). Therefore, we posited that inhibition of BRN2 could bestow sensitivity to anti-androgen treatment. As shown previously, these compounds have no effect on 16D^{CRPC} cells under FBS (androgen positive) conditions (**Figure 5.18A**). However, once BRN2 expression is induced by maximal androgen blockade (CSS + enzalutamide), co-treatment with the BRN2 inhibitors severely reduces cell proliferation (**Figure 5.18A**). Interestingly, we found that androgen blockade drastically reduced the expression of p21, likely allowing CRPC cells to continue with cell proliferation. Yet again, co-treatment with BRN2i recovered levels of p21 likely causing the reduction in cell proliferation (**Figure 5.18B**).

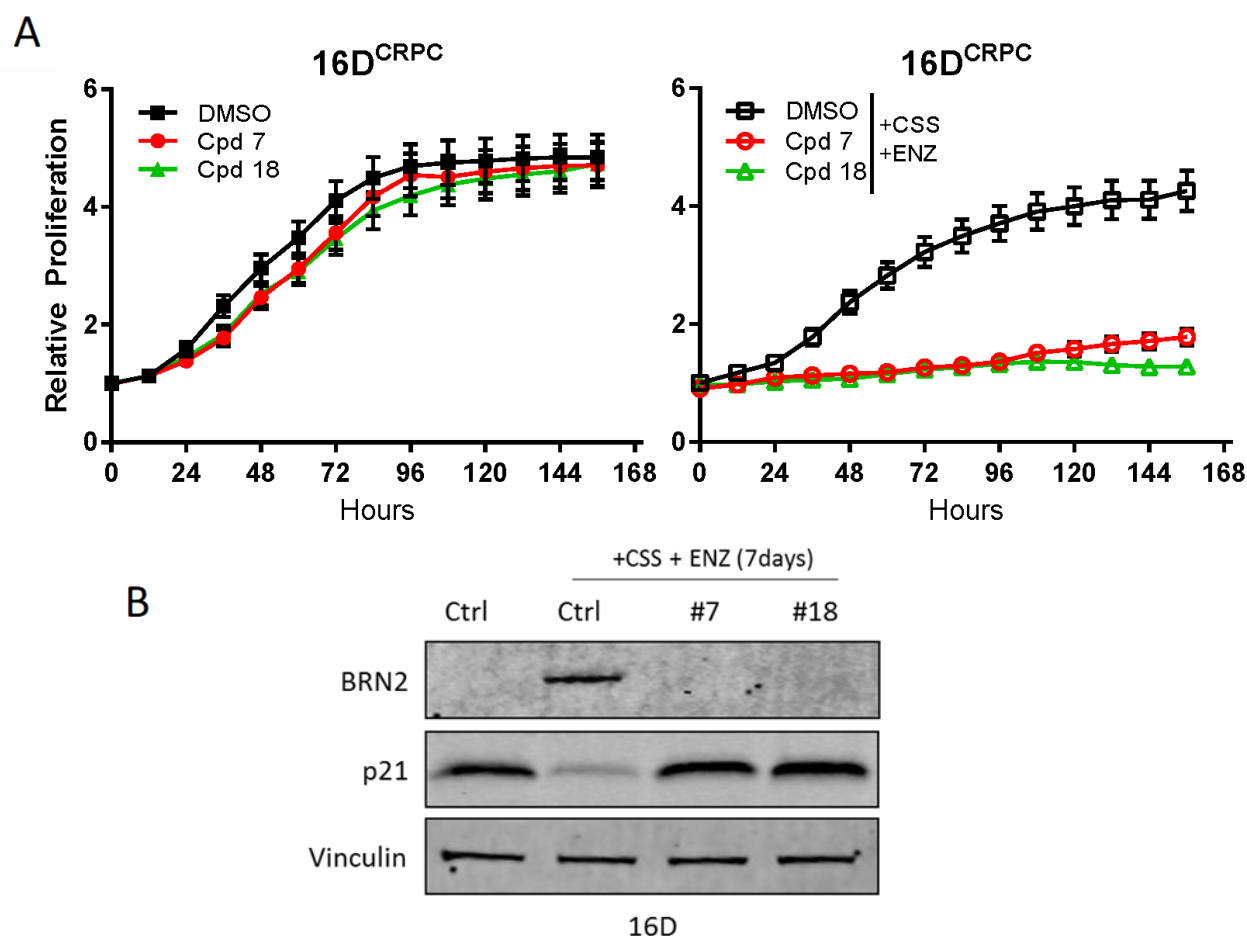


Figure 5.18 - Combination of AR and BRN2 inhibition on Proliferation:

(A) 16D^{CRPC} cells in CSS media treated +/- 10 μ M ENZ for 7 days in the presence or absence of Cpd 7 and Cpd 18. Cell proliferation was quantified using Incucyte Zoom. (B) Western Blot analysis comparing levels of BRN2 and p21 in 16D^{CRPC} cells cultured in CSS + 10 μ M ENZ with and without BRN2 inhibitors, Compounds 7 and 18.

One of the major effects of BRN2 inhibition demonstrated in the previous results chapter was its role in NE-differentiation after AR pathway inhibition, whereby knockdown of BRN2 hindered the ability of cells to undergo NE-differentiation (**Figure 4.16**). We see this recapitulated with BRN2i as the induction of the NE phenotype is reduced upon co-treatment with BRN2 inhibitors. This effect can be seen morphologically, as the spindle-like morphology created by AR inhibition is prevented when Cpd. 18 is co-administered (**Figure 5.19A**). This phenotypic change is reflected in qRT-PCR data as the upregulation of NEPC genes is diminished with the combination treatment (**Figure 5.19B**).

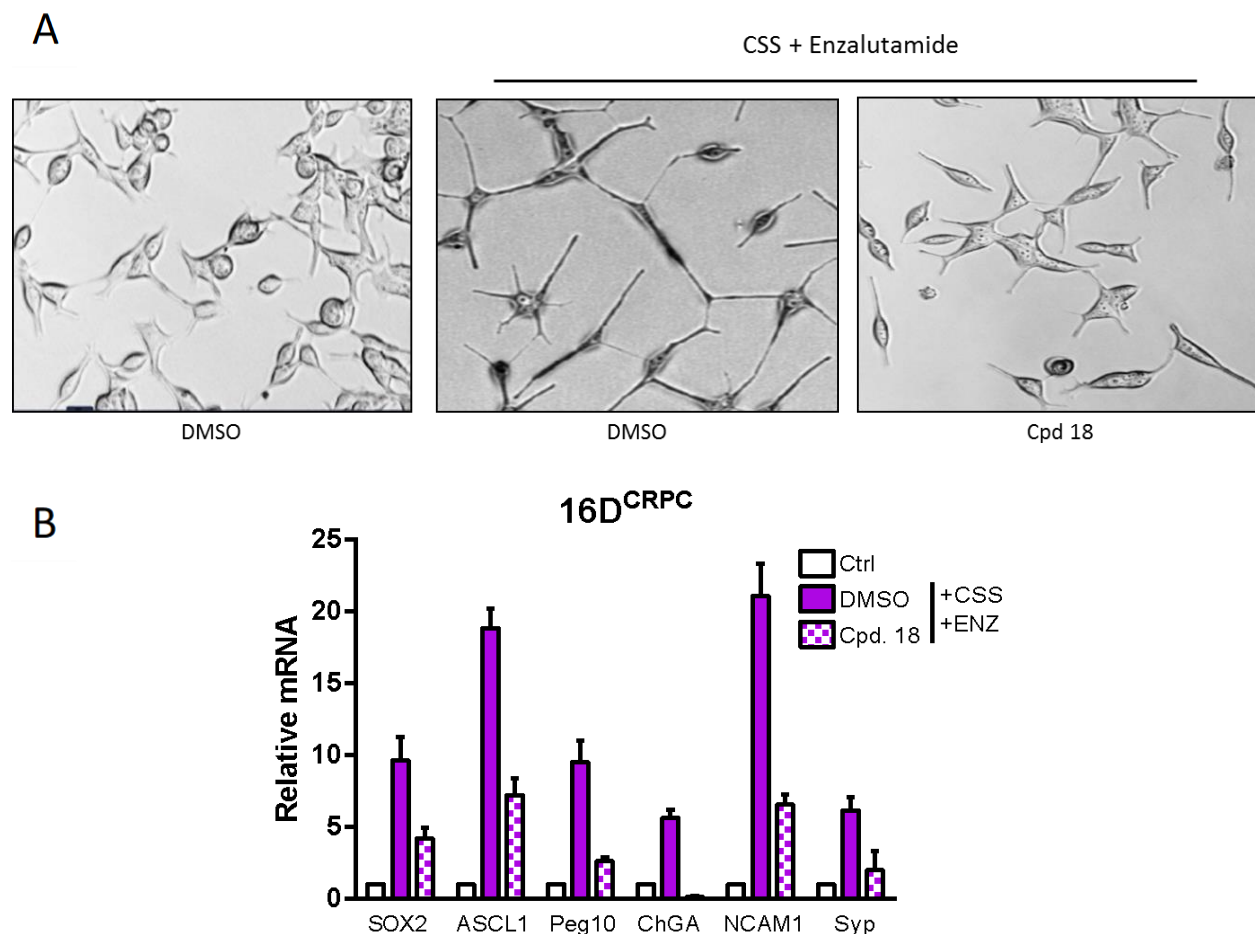


Figure 5.19 - BRN2 inhibition hinders NE-differentiation induced by AR pathway inhibition :

Cells treated with 10 μ M of Cpd 18 +/- 10 μ M ENZ for 7 days (**A**) Pictures were taken using bright field microscope. (**B**) mRNA expression of 16D^{CRPC} was analyzed for indicated genes.

5.3. Future Directions

Overall, our data shows that both chemically different scaffolds display high specificity to BRN2. Unfortunately, they both also suffer from low microsomal stability. With half-life of $T_{1/2} = 4$ minutes for Cpd.7 and $T_{1/2} = 3$ minutes for Cpd.18 (**Figure 5.20A**), these molecules serve as excellent tool compounds but require medicinal chemistry optimization before any in-vivo use is feasible. Our recent lead optimization efforts yielded compound 18-51 with a $T_{1/2} = \sim 47$ mins in microsomal stability, and an *in vivo* serum $T_{1/2} = \sim 50$ minutes (**Figure 5.20B**). 18-51 retains its specificity to 42D^{ENZR} cells, inhibits expression of BRN2 and downstream target genes (**Figure 5.20C-D**).

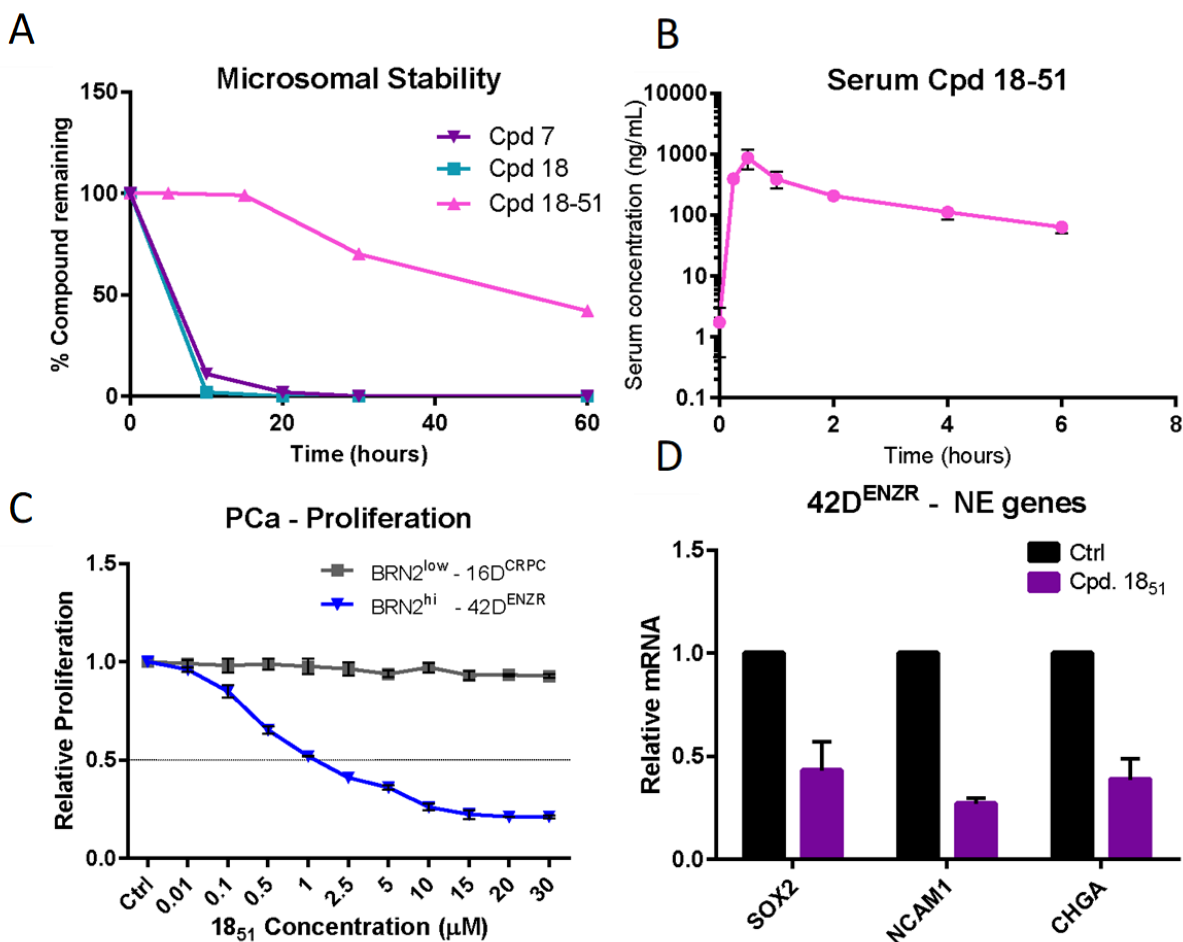


Figure 5.20 - Lead optimization:

(A) Metabolism in mice liver microsomes rate of Cpd 1851, compared to Cpd 18. (B) Serum levels of Cpd 18-51 collected over 6 hours from mice tail vein (n=3). (C) Proliferation of Cpd 18-51 in 42D^{ENZR} cells compared to 16D cells. (D) qRT-PCR of NEPC genes in 42D^{ENZR} cells treated with Cpd 18-51.

The improvements though significant, are not enough for a clinical candidate. While med-chem. optimization continues, future directions include testing 18-51 in multiple *in vivo* models. Xenograft studies will measure anti-cancer activity in 42D^{ENZ^R} cells as well as NCIH660 cells. Importantly, through collaborations we will examine the efficacy of these compounds in NEPC PDX models (**Figure 5.21**. (40) as well as in patient derived organoids both *in vitro* and *in vivo*. The last major priority moving forward will build upon the data presented in figure 5.17 highlighting the powerful synergy between AR and BRN2 inhibition. Employing a similar strategy, combination therapy experiments will be conducted using 16D^{CRPC} cells as well as a few of the “Adeno” PDX models presented in **Figure 5.21**.

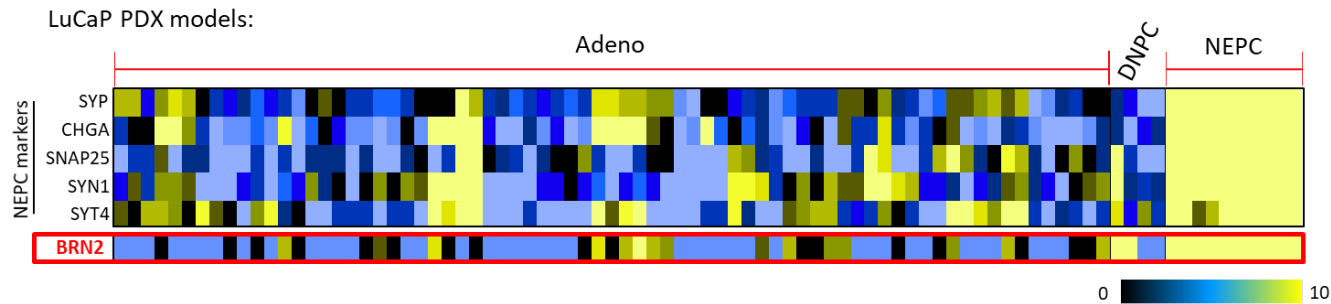


Figure 5.21 - BRN2 expression in NEPC patient derived xenograft models:
RNA-seq of PDX models from Adenocarcinoma, double negative prostate cancer (DNPC) and neuroendocrine prostate cancer (NEPC) characterized in Bleumn et. al in 2017.

6. Discussion – Treatment resistance and cell plasticity

A considerable body of research both old and new has delved into the notion of cellular plasticity. Historically, this field of research studied plasticity in response to growth factors like TGF β that induce EMT (357), or cocktails of chemicals and specific growth factors can induce neuronal differentiation as well as de-differentiation to a more pluripotent state (358-360). However, cancer therapy induced phenotypic plasticity is a relatively newer concept. Supporting evidence for treatment induced cell plasticity can be garnered from papers showing evidence of cell dormancy and the theory of cancer stem cells (CSC).

The relapse of cancer years after remission is a well-documented phenomenon. During remission cancer cells often survive through a process called tumor dormancy, whereby, cancer cells adopt a low proliferative quiescent phenotype in order to survive through treatments. This small collection of tumor cells likely exists in an equilibrium of cell renewal and death as there is little to no overall growth of the “tumor” (361). This growth equilibrium is also held in check by two major factors, immune evasion and localized angiogenesis for resources (361). Relapse occurs through some sort of trigger event years later and in the field of tumor dormancy, the biological understanding of this trigger event remains a major challenge as it could vary from macro-environment, to micro-environment but most likely through acquisition of specific mutations within the cells.

Tumor dormancy and the cancer stem cell hypotheses have considerable similarity as the low-proliferating, immune evasive dormant cells exhibit stem cell properties (362). The CSC theory specifically has two possible interpretations. One states that the stem-like cancer cells always exist as a small sub-population similar to normal developmental stem cell populations. CSCs are inherently drug-resistant and are expected to survive therapies and re-populate a tumor (363). On the other hand, recent research has promoted the hypothesis that some cancer cells gain enhanced self-renewal properties in response to external stressors (anti-cancer treatments) and this allows them to survive and re-populate a tumor (364). Furthermore, the sequence of events that lead a cell to become more CSC like, as well as the proteins involved in the process may also be different in response to different stressors like hypoxia, resource starvation, DNA-damage and cancer therapies (cytotoxic or targeted).

The arsenal of prostate cancer therapies has been relatively effective as seen from the decline of deaths (Figure 1.1). Outside of surgeries, patients receive a mix of radiotherapy, chemotherapies and hormone therapies over the course of their fight with the disease. The importance of the tumor dormancy and CSC hypotheses is emphasized by the long period of

dormancy observed in PCa after their initial hormone therapy and prior to gaining castration resistance (365, 366). Moreover, as patients progress through CRPC they receive more potent anti-androgen therapy, have months to years of response and once again relapse. Therefore, it is very important to understand the variety of malleable processes that occur within the cancer cells in response to hormone therapy. To this end, the research in this thesis explored cell plasticity at different stages of anti-androgen treatment. First, we studied how the upregulation of *LYN* kinase during ADT promotes the EMT processes and possibly feeds into the near 90% prevalence of metastatic disease at castration resistance. The last two-thirds of the thesis attempts to delineate the driver and target roles of transcription factor BRN2 behind neuroendocrine differentiation in response to 2nd generation anti-androgens.

AR pathway and Epithelial to Mesenchymal Transition/Plasticity (EMT/P)

The phrasing for epithelial to mesenchymal transition has recently been giving way to epithelial to mesenchymal plasticity due to the reversible nature of the process (367). While the identity of the EMT/P process is bonded to metastasis, the transition of cells to a more mesenchymal state in response to anti-cancer therapies has been reported in multiple cancer types (368-370). Moreover, many studies also demonstrate that mesenchymal cells are resistant to treatments like chemotherapy cementing the importance of this specific form of cell plasticity as a mechanism of treatment resistance (371, 372). This resemblance to properties described for CSCs is not accidental, as mesenchymal cells have long been hypothesized to share CSC characteristics. For example, transcription factor Snail regulates expression of Yamanaka factors Nanog and KLF4 (373, 374). Instead of chemotherapies, the major focus of this thesis is to study the molecular response of PCa cells to universally used anti-AR treatments in prostate cancer. Not surprisingly however, the relationship between AR signaling and the basic characteristics of EMT/P is not entirely straightforward.

This particular area of research examining epithelial to mesenchymal plasticity in response to positive and negative AR pathway stimulation is full of interesting and contradictory research. In simplistic terms, EMT/P can be broken down to loss of expression of cell adhesion molecule E-cadherin. Loss of AR signaling through androgen deprivation consistently results in downregulation of E-cadherin (119). The culprits suppressing E-cadherin are transcription factors Snail and Zeb1 whose expression is normally suppressed by AR activity. Furthermore, ADT has been shown to cause a shift from CDH1 (E-cadherin) to CDH2 (N-cadherin) (375) and CDH11 (376). Similarly, several studies have also shown that loss of AR expression promotes STAT3 activity creating a mixed mesenchymal and CSC phenotypes (377, 378). Conversely,

positive AR signaling has long been implicated in promoting metastasis. PCa metastatic tumor sites, specifically in the bone are generally AR positive (379). In ERG-fusion positive disease, ERG activity through AR activates SOX9 expression, which can enhance metastasis (380). Furthermore, AR signaling can also enhance expression of transcription factor Slug resulting in metastatic progression (124, 381). Slug expression and activity can enhance metastatic dissemination through upregulation of cytoskeletal proteins like Vimentin as well as a member of the matrix metalloprotease family (MMP) across multiple cancers (382-384). This family of proteins are crucial for metastatic dissemination as they are required for extra-cellular matrix (ECM) digestion, allowing cancer cells to maneuver through basement membrane (385).

These bivalent functions of AR create a difficult to reconcile a scenario where both over-active and inactive AR promotes progression of PCa to metastatic disease. Das et al. extensively reviewed this topic and the authors concluded that this differential activity is contextually dependent on AR co-activators that alter its cistrome (386). It is tempting to speculate that as cells gain resistance to ADT, this differential AR activity within the cancer cells of a single tumor (intra-tumor heterogeneity) may enable the tumor as a whole to gain advantage of both scenarios. Specifically, cells where resistance occurs independent of the AR, EMT/P could occur in some cells through E-cad suppression. While in cells that gain resistance by recovering their over-active AR signaling, metastasis may be supported through disintegration of the ECM at the leading edge of a tumor. Thus, identifying key signaling nodes that compromise canonical AR signaling as well as inhibit downstream metastasis promoters may help scientists prepare better treatment combinations.

Interestingly, the two reported functions of *LYN* kinase in PCa place it as a unique target for curbing EMT/metastasis. Previous research from our lab has shown that *LYN* tyrosine kinase expression is increased during CRPC (133). More importantly, the expression of *LYN* is upregulated soon after castration where it helps stabilize protein levels of the AR in order to help maintain its activity. Chapter 3 also demonstrates that *LYN* expression can also increase EMT/P transcription factors Slug and Snail as well as MMP activity (134). This dual-purpose activity may explain why *LYN* kinase is up-regulated during acquisition of castration resistance at a cellular level and why this increase is selected for and retained at metastatic sites in CRPC. It may be reasonable to conclude at this point that in AR signaling positive cells, inhibiting *LYN* would reduce AR expression, effectively reducing metastasis promoting AR signaling. While in cells with low AR signaling, targeting *LYN* would destabilize Slug and Snail impeding the metastatic capability of these cells as well.

One limitation in chapter 2 is the lack of experimental validation for targeting *LYN* in PCa, both as monotherapy and in combination with ADT. Over-expression of *LYN* in prostate cells was sufficient to trigger metastasis *in vivo*; however, targeting *LYN* at the CRPC disease state has not been tested. In recent years, the development of better CRPC models has expanded the toolset for these kinds of studies. For example, testing the effects of *LYN* inhibition on metastasis in the castration responsive Rapid-CAP model developed by Tortman and colleagues would be of interest (387). This experiment could also be conducted by crossing Rapid-CAP mice with a *LYN*^{-/-} model; however, using *LYN* inhibitor Bafetinib would be more clinically relevant.

AR pathway inhibition and NE-differentiation

The history of NE-differentiation research in prostate cancer is old but sparsely populated. In 1989, Drs. Abrahamsson and Grimelius reported the presence of focal neuroendocrine differentiation through staining of NEPC marker Chromogranin A in prostate adenocarcinoma (388) and hypothesized the following about its origin: (1) cancerous transformation of a prostate stem cell, (2) malignant transformation of a prostate neuroendocrine cell, and (3) de-differentiation followed by a new gene expression program in a PCa cell. The presentation of focal NE markers combined with the presence of neuroendocrine cells in the normal prostate lead most of the field to believe that NEPC likely stemmed from a transformation of a normal NE cells (389). Some contradictory evidence was presented in 1994, when Bang et al demonstrated for the first time “*direct evidence of plasticity in the lineage commitment of adenocarcinoma of the prostate*” through cyclic-AMP dependent mechanisms (390). In 1999, Cox et al. demonstrated the reversible nature of this transformation with cAMP exposure (391), followed by Deeble et al. demonstrating that IL-6 downstream of cyclic-AMP data promoted this plasticity (392). Interestingly, as androgen deprivation therapy evolved from Orchiectomy to LHRH agonists, researchers examined whether ADT may also induce a de-differentiation program. In 1997, Buttyan and colleagues showed that culturing LNCaP cells in media devoid of androgen suppressed AR signaling as expected, but also initiated NE-differentiation defined by morphological changes and upregulation of NEPC marker independent of cyclic-AMP (393). Soon after, clinical evidence of NE differentiation was observed in TURP samples from patients that received neo-adjuvant hormone therapy compared to control (394).

Due to the historical rarity of full NEPC, research into the disease was scarce up until 2011 when Dr. Beltran used next-gen sequencing to molecularly characterize 7 terminal NEPC tumors (135). The drastically increased incidence of NEPC with the advent of powerful anti-

androgens like enzalutamide and abiraterone has led many researchers to interrogate the plastic potential of adenocarcinoma cells subject to treatments. Revisiting the seminal papers described in the previous paragraph, researchers questioned whether this differentiation process was terminal as alluded to by Bang et al. or reversible, as we have come to observe with EMT/P and even CSCs (395). In support of the plasticity hypothesis, recent research demonstrated that ADT initiates NE-differentiation in AR-driven PCa cell lines and this process is reversed upon re-introduction of androgens (396). Importantly, the increase of NE markers like NSE and SYP was accompanied by an increase of established CSC markers like CD44, CD29 and CD133, also reversed with re-exposure to androgens. Strengthening this hypothesis further, Zou et al. conducted exquisite lineage tracing experiments *in vivo* and discovered that the NEPC can originate from luminal PCa adenocarcinoma cells (144). Furthermore, phylogenetic modeling of mutations in patients also show evidence of an adenocarcinoma cell of origin as the TMPRSS-ERG fusion is present in a similar ratio in NEPC patients (2).

Interestingly, a broader look at the research studying PCa cells undergoing anti-androgen treatment shows consistent cellular response across different stages of anti-androgen treatments. For example, the upregulation of NEPC markers like PEG10, CHGA and SYP has been observed after ADT (149) as well as after 2nd generation anti-androgens like enzalutamide and abiraterone (397). These findings are consistent with *in vitro* data showing concordance in gene expression patterns across multiple publications exposing AR-driven PCa cell lines to androgen deprivation conditions (CSS) or exposing them to AR inhibitor enzalutamide (145, 307, 398). Research conducted over the past few years has identified notable drivers of transcriptional programs leading to NEPC. Adapting the research done with SCLC on drivers such as N-Myc (151), SOX2 (153), EZH2 (154) and BRN2 (295), several researchers are studying their relevance to molecular mechanisms of NEPC in prostate cancer. In summary, the landscape of NEPC research can be segregated into the following groups: oncogenic over-expression models, tumor-suppressor knockout models and anti-androgen treatment models (Table 6-1).

Table 6-1: Models of NEPC

<i>Over-expression</i>	<i>Knockout</i>	<i>Anti-androgen</i>
nMYC + myrAKT	TRAMP	Castration PDX model
LNCaP nMYC	p53 ^{-/-} Rb1 ^{-/-} pTEN ^{-/-}	LNCaP serial transplant (Enz)
---	pTEN ^{-/-} p53 ^{-/-} combined with abiraterone treatment	
SRRM4 overexpression + knockout of p53 and Rb1		---

While the over-expression models demonstrate the capability of these proteins to drive NE-differentiation, the primary factor in the rise of NEPC diagnosis has been the powerful anti-androgen treatments. Therefore, the majority of this thesis utilized the model developed from serial transplantation of LNCaP cells under pressure of enzalutamide, attempting to mimic the “natural progression” to NEPC. The increased expression of master neuronal transcription factor BRN2 observed in this model was in concordance with the castration PDX model and terminal NEPC patients. BRN2 expression was shown to be required and sufficient to induce NE-differentiation as well as promote resistance to enzalutamide. The results in Chapter 2 also demonstrate that in this model, BRN2 maintained uni-directional control over SOX2 expression and could drive NE-differentiation in the absence of SOX2. It is likely that SOX2 is more involved in maintenance of the CSC phenotype observed during AR pathway inhibition. Most importantly, targeting BRN2 reduced proliferation of 42D^{ENZ^R} cells and NEPC NCI-H660 cells *in vitro* as well as 42F^{ENZ^R} cells *in vivo*. Prompting the use of *in silico* modeling for rational drug discovery of small molecule BRN2 inhibitors (Chapter 4).

Historically, use of GEM mouse models, which serve as a gold standard for illustrating specific biological processes and while reasonably comprehensive, Chapter 4, requires several key experiments to cement the role of BRN2 in NEPC. A few possible experimental avenues exist, for example similar to the experiments done by Lee et al. with N-Myc (142), BRN2 over-expressing prostatectomy tissue may be implanted into immune-compromised mice and NE markers evaluated by IHC. Moreover, generation of engineered mice with prostate specific K/O of BRN2 may be fruitful as they could be crossed with TRAMP mice to see if the rate of NEPC is reduced upon castration. Alternatively, the BRN2i developed in chapter 5 may also be utilized for the same experiment. These experiments are beyond the scope of this thesis, but they are intriguing research strategies for the future.

Targeting BRN2 in NEPC

In order to design the first-ever small molecule inhibitor for BRN2, we employed *in silico* homology modeling based on the DBD crystal structures of other POU domain proteins. Other than the POU^S and POU^H domains in the DNA binding region, BRN2 lacks defined protein domains (399) leading us to adopt the unorthodox approach of targeting the DBD. Positive hits from the modeling were subject to a series of exclusion criteria prior to designation as a “hit”. The selection pipeline and the *in silico* modeling were validated as the hits produced recapitulated many of the effects of BRN2 inhibition characterized in chapter 4. Specifically, BRN2i treatment reduced proliferation in BRN2^{hi} 42D^{ENZ^R} cells and NCIH660 cells and had no

effect on BRN2^{low} 16D^{CRPC} cells. The compounds downregulated NEPC markers, BRN2 target genes and most importantly, synergized with AR pathway inhibition to reduce NE-differentiation and cell proliferation. The consistency in the gene expression patterns between the two different chemical scaffolds display their specificity to BRN2. The on target nature of the molecules was further consolidated as other downstream effects like cell cycle arrest pattern and recovery of p21 was consistent across multiple siRNA as well as CRISPR/Cas9 knockouts.

If/When, a clinically usable molecule is designed; the stage of PCa where it is used will be an important topic to consider. While use at terminal NEPC is a reasonable first step, the option of early usage in combination with AR pathway inhibition will be an important consideration. As mentioned previously, NE-differentiation occurs after both ADT as well as after enzalutamide and abiraterone. The evaluation of these combination treatment regimens was mentioned in section 5.3 as an important part of the pre-clinical development of these molecules. Beyond PCa, BRN2 expression/activity has been implicated in several other disease like SCLC (294, 295), GBM (289) and Melanoma (291). These compounds will also serve as important tools to test relevance of BRN2 as a therapeutic option in these patients.

Typically, most targeted therapies used in the clinic are met by a predictable reaction, mutations in the target protein (400). Theoretically, targeting the DBD of transcription factors provides the advantage that the pool of possible mutations would decrease, as mutations in the DBD may compromise the activity of the protein itself. Importantly however, this strategy is not exempt from mutations that render the molecules inactive and continued research will be required to predict/identify these mutations and prepare appropriate responses. As a head start, the lead optimization mentioned in section 5.3 will be conducted on several different chemical scaffolds simultaneously in order to have 2nd and 3rd generation compounds ready for evaluation. The identification of these tool compounds also opens up several other strategies to target BRN2, for example, the compounds can be used as a hook for membrane anchoring as previously used for STAT3 (401). They may also be utilized to force interactions between BRN2 and E3 Ubiquitin ligases creating a “degrader” molecule with PROTAC technology (402).

The data presented in chapter 5 are promising but preliminary, and in addition to the future directions discussed in section 5.3 there are several key limitations that need to be addressed. Chief among them is the possibility of binding of BRN2i to other members of the POU3F family of proteins. BRN2 (POU3F2) shares 59%, 66% and 65% sequence homology to POU3F1, POU3F3 and POU3F4 respectively. Fortunately, the 42D^{ENZR} cells do not express any detectable levels of POU3F1, POU3F3 and POU3F4 at mRNA and protein levels, providing supporting evidence about the specificity of the effects observed in 42D^{ENZR} cells. However, this

does not eliminate possibility of binding to those family members and will require experimental confirmation. Furthermore, DARTS and BLI binding experiments are insightful but provide limited details about the binding of the inhibitors. As such, co-crystallization of BRN2i with the DBD of BRN2 will provide a more conclusive answer to the binding properties of these inhibitors.

In addition to the biophysical assays, another possible point of contention is the possibility of on-target toxicity. In an adult human, the expression of BRN2 is restricted to cells types present in the brain. Statistically, almost 99% of small molecules do not readily cross the blood brain barrier (403) and the brain should remain un-exposed to BRN2i. BRN2 however plays a crucial but redundant role in Schwann cell maturation (404). The duration and intensity of any possible side effects stemming from BRN2 inhibition in Schwann cells will need to be characterized flawlessly through *in vivo* toxicity experiments, both in acute and chronic timeframes.

Prostate Cancer Cell Plasticity: EMT + CSC + NE

As supporting evidence for cell plasticity post AR pathway inhibition mounts, a bird's eye view of the field reveals many intersecting lines of evidence between EMT, CSC and NE phenotypes across years of research. For example, IL-6 signalling inducing NEPC, initially investigated by Cox and colleagues has not only been reproduced, the major pathway effector STAT3 directly contributes towards enzalutamide resistance (405) and NE-differentiation (406). Evidence supporting importance of STAT3 in EMT and CSC processes across the entirety of cancer research is also considerable (407, 408). Another signaling node becoming increasingly apparent is the transcription factor Snail. Traditionally considered to be a driver of EMT due to its E-cadherin suppressing capabilities, its role in CSC phenotype was discovered by several different research groups. In 2010, Mckeithen et al. showed that over-expression of Snail in LNCaP cells triggered neurite formation and upregulation of NEPC markers CHGA and NSE (409). Snail is also AR suppressed gene (410) that is upregulated during NEPC transdifferentiation and co-operates with and another key NEPC protein PEG10 to promote the aggressiveness of NEPC (122).

In addition to NE phenotype, BRN2 itself has many studies examining its' role in metastasis (EMT/P) (291, 411) as well as maintenance of CSCs across several cancers (289, 412). The upregulation of CSC phenotype/genes within NEPC models is also common. In 2016, an excellent study uncovered that NEPC tumors are enriched for signatures resembling CD49F⁺/TROP2⁺ prostate cancer stem cells (413). N-Myc overexpression derived LASCPC-01

cells retain remarkable tumor initiating capacity and most importantly, have the ability to give rise to both Adenocarcinoma and NEPC tumors (142), providing near impeccable evidence for NEPC cells with CSC characteristics as they give rise to multiple lineages. Within the LNCaP enzalutamide resistance model used throughout this thesis, the 42D^{ENZR} and 42F^{ENZR} cells also display enhanced tumor initiating ability and are enriched for CSC phenotype (414, 415). Moreover, xenografts of DU145 cells sorted for CSC marker CD44 cells gave rise to tumors that are E-cadherin negative, Vimentin positive (EMT) and CHGA positive (NEPC), showcasing the intertwined relationship between these plasticity pathways (416, 417). Correlative clinical evidence of these overlapping cell states was measured by immunohistochemistry as prostatectomy samples show positive association between terminal NEPC marker CHGA with well established CSC proteins CD44 and OCT4 (418).

Once again, it would be tempting to speculate that upon inhibition of an identity defining protein like the Androgen Receptor, it may be possible that PCa cells exist in a gradient-like state with Adenocarcinoma at one end and a meta-stable cell type sharing EMT, CSC and NE properties at the other. Following this, trigger events in specific combinations and/or sequence may dictate whether resistant tumors become Adenocarcinoma, IAC, DNPC or NEPC tumors observed in patients (**Figure 6.1**).

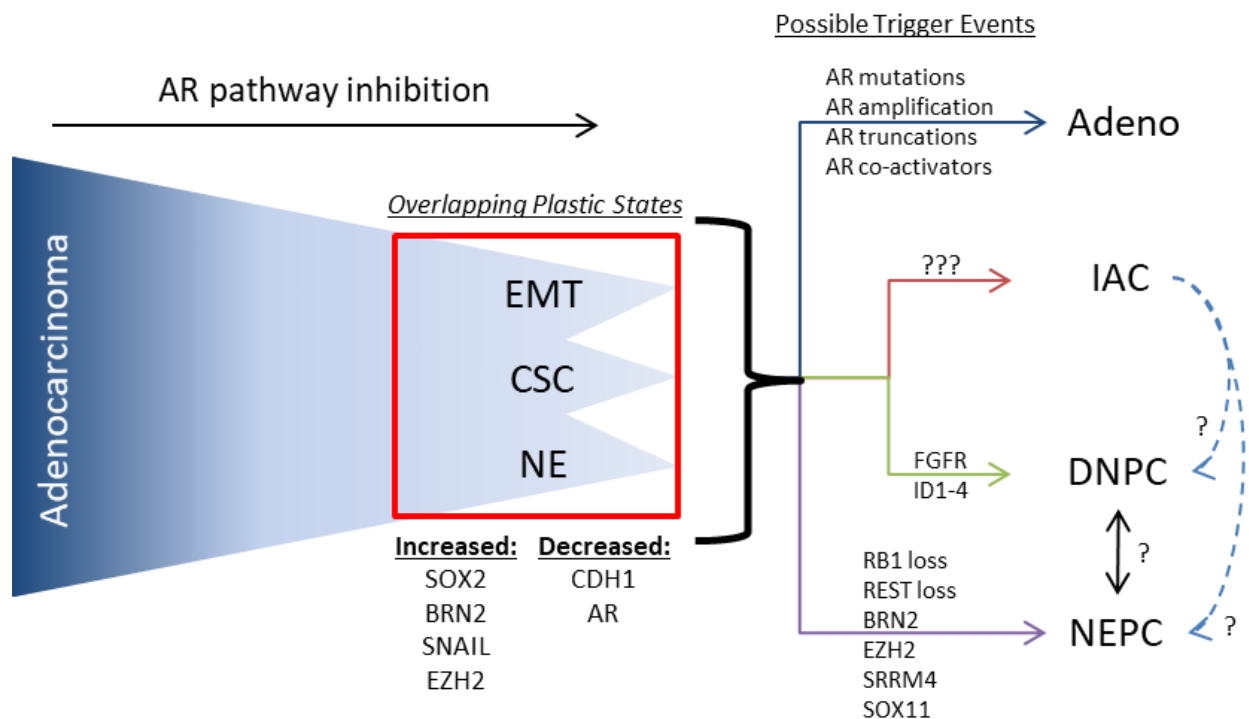


Figure 6.1 – Proposed model of PCa disease transformations:

The schematic above attempts to identify key components in a proposed roadmap of prostate cancer cell response to AR inhibition leading up disease stages presented in patients.

As 2nd generation anti-androgens are moved earlier in the treatment landscape (given with LHRH agonist/antagonist), PCa patients may present with these disease states at an earlier time. As treatments are developed for each of these sub-types of PCa, an important future research direction will be unraveling the relationship between the IAC, DNPC and NEPC disease states. Understanding these processes further will aid in designing rational combination treatment strategies that may ultimately abolish the paths leading IAC/DNPC/NEPC and greatly improve PCa patient survival.

Bibliography

1. Beltran H, Rickman DS, Park K, Chae SS, Sboner A, MacDonald TY, et al. Molecular characterization of neuroendocrine prostate cancer and identification of new drug targets. *Cancer discovery*. 2011 Nov;1(6):487-95. PubMed PMID: 22389870. Pubmed Central PMCID: 3290518. Epub 2012/03/06. eng.
2. Beltran H, Prandi D, Mosquera JM, Benelli M, Puca L, Cyrta J, et al. Divergent clonal evolution of castration-resistant neuroendocrine prostate cancer. *Nature medicine*. 2016 Mar;22(3):298-305. PubMed PMID: 26855148. Pubmed Central PMCID: 4777652.
3. Potosky AL, Miller BA, Albertsen PC, Kramer BS. The role of increasing detection in the rising incidence of prostate cancer. *Jama*. 1995 Feb 15;273(7):548-52. PubMed PMID: 7530782.
4. Andriole GL, Crawford ED, Grubb RL, 3rd, Buys SS, Chia D, Church TR, et al. Mortality results from a randomized prostate-cancer screening trial. *The New England journal of medicine*. 2009 Mar 26;360(13):1310-9. PubMed PMID: 19297565. Pubmed Central PMCID: 2944770.
5. Schroder FH, Hugosson J, Roobol MJ, Tammela TL, Ciatto S, Nelen V, et al. Screening and prostate-cancer mortality in a randomized European study. *The New England journal of medicine*. 2009 Mar 26;360(13):1320-8. PubMed PMID: 19297566.
6. Tsodikov A, Gulati R, Heijnsdijk EAM, Pinsky PF, Moss SM, Qiu S, et al. Reconciling the Effects of Screening on Prostate Cancer Mortality in the ERSPC and PLCO Trials. *Annals of internal medicine*. 2017 Oct 03;167(7):449-55. PubMed PMID: 28869989.
7. Wilt TJ, Jones KM, Barry MJ, Andriole GL, Culkin D, Wheeler T, et al. Follow-up of Prostatectomy versus Observation for Early Prostate Cancer. *The New England journal of medicine*. 2017 Jul 13;377(2):132-42. PubMed PMID: 28700844.
8. Epstein JI, Zelefsky MJ, Sjoberg DD, Nelson JB, Egevad L, Magi-Galluzzi C, et al. A Contemporary Prostate Cancer Grading System: A Validated Alternative to the Gleason Score. *European urology*. 2016 Mar;69(3):428-35. PubMed PMID: 26166626. Pubmed Central PMCID: 5002992.
9. Buyyounouski MK, Choyke PL, McKenney JK, Sartor O, Sandler HM, Amin MB, et al. Prostate cancer - major changes in the American Joint Committee on Cancer eighth edition cancer staging manual. *CA: a cancer journal for clinicians*. 2017 May 06;67(3):245-53. PubMed PMID: 28222223.
10. Edge SB, Compton CC. The American Joint Committee on Cancer: the 7th edition of the AJCC cancer staging manual and the future of TNM. *Annals of surgical oncology*. 2010 Jun;17(6):1471-4. PubMed PMID: 20180029.
11. Denmeade SR, Isaacs JT. A history of prostate cancer treatment. *Nature reviews Cancer*. 2002 May;2(5):389-96. PubMed PMID: 12044015. Pubmed Central PMCID: 4124639.
12. Dehm SM, Tindall DJ. Androgen receptor structural and functional elements: role and regulation in prostate cancer. *Molecular endocrinology*. 2007 Dec;21(12):2855-63. PubMed PMID: 17636035.
13. Vis AN, Schroder FH. Key targets of hormonal treatment of prostate cancer. Part 1: the androgen receptor and steroidogenic pathways. *BJU international*. 2009 Aug;104(4):438-48. PubMed PMID: 19558559.
14. Chen Y, Clegg NJ, Scher HI. Anti-androgens and androgen-depleting therapies in prostate cancer: new agents for an established target. *The Lancet Oncology*. 2009 Oct;10(10):981-91. PubMed PMID: 19796750. Pubmed Central PMCID: 2935850.
15. Parker C, Gillessen S, Heidenreich A, Horwich A, Committee EG. Cancer of the prostate: ESMO Clinical Practice Guidelines for diagnosis, treatment and follow-up. *Annals of oncology : official journal of the European Society for Medical Oncology*. 2015 Sep;26 Suppl 5:v69-77. PubMed PMID: 26205393.
16. Society AC. Treating Prostate Cancer. Available from: <https://www.cancer.org/cancer/prostate-cancer/treating.html>.

17. Rick FG, Block NL, Schally AV. An update on the use of degarelix in the treatment of advanced hormone-dependent prostate cancer. *OncoTargets and therapy*. 2013;6:391-402. PubMed PMID: 23620672. Pubmed Central PMCID: 3633549.
18. Furr BJ, Valcaccia B, Curry B, Woodburn JR, Chesterson G, Tucker H. ICI 176,334: a novel non-steroidal, peripherally selective antiandrogen. *The Journal of endocrinology*. 1987 Jun;113(3):R7-9. PubMed PMID: 3625091.
19. Peets EA, Henson MF, Neri R. On the mechanism of the anti-androgenic action of flutamide (alpha-alpha-alpha-trifluoro-2-methyl-4'-nitro-m-propionotoluidide) in the rat. *Endocrinology*. 1974 Feb;94(2):532-40. PubMed PMID: 4810387.
20. Raynaud JP, Bonne C, Bouton MM, Lagace L, Labrie F. Action of a non-steroid anti-androgen, RU 23908, in peripheral and central tissues. *Journal of steroid biochemistry*. 1979 Jul;11(1A):93-9. PubMed PMID: 385986.
21. Kolvenbag GJ, Blackledge GR, Gotting-Smith K. Bicalutamide (Casodex) in the treatment of prostate cancer: history of clinical development. *The Prostate*. 1998 Jan 1;34(1):61-72. PubMed PMID: 9428389.
22. Sarosdy MF. Which is the optimal antiandrogen for use in combined androgen blockade of advanced prostate cancer? The transition from a first- to second-generation antiandrogen. *Anti-cancer drugs*. 1999 Oct;10(9):791-6. PubMed PMID: 10587288.
23. Kent EC, Hussain MH. Neoadjuvant Therapy for Prostate Cancer: An Oncologist's Perspective. *Reviews in urology*. 2003;5 Suppl 3:S28-37. PubMed PMID: 16985947. Pubmed Central PMCID: 1502344.
24. Schulman CC, Debruyne FM, Forster G, Selvaggi FP, Zlotta AR, Witjes WP. 4-Year follow-up results of a European prospective randomized study on neoadjuvant hormonal therapy prior to radical prostatectomy in T2-3N0M0 prostate cancer. *European Study Group on Neoadjuvant Treatment of Prostate Cancer. European urology*. 2000 Dec;38(6):706-13. PubMed PMID: 11111188.
25. Kirby M, Hirst C, Crawford ED. Characterising the castration-resistant prostate cancer population: a systematic review. *International journal of clinical practice*. 2011 Nov;65(11):1180-92. PubMed PMID: 21995694.
26. de Bono JS, Logothetis CJ, Molina A, Fizazi K, North S, Chu L, et al. *Abiraterone* and increased survival in metastatic prostate cancer. *The New England journal of medicine*. 2011 May 26;364(21):1995-2005. PubMed PMID: 21612468. Pubmed Central PMCID: 3471149.
27. Scher HI, Fizazi K, Saad F, Taplin ME, Sternberg CN, Miller K, et al. Increased survival with enzalutamide in prostate cancer after chemotherapy. *The New England journal of medicine*. 2012 Sep 27;367(13):1187-97. PubMed PMID: 22894553.
28. Ryan CJ, Smith MR, Fizazi K, Saad F, Mulders PF, Sternberg CN, et al. Abiraterone acetate plus prednisone versus placebo plus prednisone in chemotherapy-naïve men with metastatic castration-resistant prostate cancer (COU-AA-302): final overall survival analysis of a randomised, double-blind, placebo-controlled phase 3 study. *The Lancet Oncology*. 2015 Feb;16(2):152-60. PubMed PMID: 25601341.
29. Mostaghel EA. Abiraterone in the treatment of metastatic castration-resistant prostate cancer. *Cancer management and research*. 2014;6:39-51. PubMed PMID: 24501545. Pubmed Central PMCID: 3912049.
30. Rehman Y, Rosenberg JE. Abiraterone acetate: oral androgen biosynthesis inhibitor for treatment of castration-resistant prostate cancer. *Drug design, development and therapy*. 2012;6:13-8. PubMed PMID: 22291466. Pubmed Central PMCID: 3267518.
31. Taplin ME, Montgomery B, Logothetis CJ, Bubley GJ, Richie JP, Dalkin BL, et al. Intense androgen-deprivation therapy with abiraterone acetate plus leuprolide acetate in patients with localized high-risk prostate cancer: results of a randomized phase II neoadjuvant study. *Journal of clinical oncology : official*

- journal of the American Society of Clinical Oncology. 2014 Nov 20;32(33):3705-15. PubMed PMID: 25311217. Pubmed Central PMCID: 4226804.
32. Fizazi K, Tran N, Fein L, Matsubara N, Rodriguez-Antolin A, Alekseev BY, et al. Abiraterone plus Prednisone in Metastatic, Castration-Sensitive Prostate Cancer. *The New England journal of medicine*. 2017 Jul 27;377(4):352-60. PubMed PMID: 28578607.
 33. Li R, Evaul K, Sharma KK, Chang KH, Yoshimoto J, Liu J, et al. Abiraterone inhibits 3beta-hydroxysteroid dehydrogenase: a rationale for increasing drug exposure in castration-resistant prostate cancer. *Clinical cancer research : an official journal of the American Association for Cancer Research*. 2012 Jul 1;18(13):3571-9. PubMed PMID: 22753664.
 34. Li Z, Bishop AC, Alyamani M, Garcia JA, Dreicer R, Bunch D, et al. Conversion of abiraterone to D4A drives anti-tumour activity in prostate cancer. *Nature*. 2015 Jul 16;523(7560):347-51. PubMed PMID: 26030522. Pubmed Central PMCID: 4506215.
 35. Li Z, Alyamani M, Li J, Rogacki K, Abazeed M, Upadhyay SK, et al. Redirecting abiraterone metabolism to fine-tune prostate cancer anti-androgen therapy. *Nature*. 2016 May 26;533(7604):547-51. PubMed PMID: 27225130. Pubmed Central PMCID: 5111629.
 36. McKay RR, Werner L, Mostaghel EA, Lis R, Voznesensky O, Zhang Z, et al. A Phase II Trial of Abiraterone Combined with Dutasteride for Men with Metastatic Castration-Resistant Prostate Cancer. *Clinical cancer research : an official journal of the American Association for Cancer Research*. 2017 Feb 15;23(4):935-45. PubMed PMID: 27683182. Pubmed Central PMCID: 5315609.
 37. Tran C, Ouk S, Clegg NJ, Chen Y, Watson PA, Arora V, et al. Development of a second-generation antiandrogen for treatment of advanced prostate cancer. *Science*. 2009 May 8;324(5928):787-90. PubMed PMID: 19359544. Pubmed Central PMCID: 2981508.
 38. Beer TM, Armstrong AJ, Rathkopf DE, Loriot Y, Sternberg CN, Higano CS, et al. Enzalutamide in metastatic prostate cancer before chemotherapy. *The New England journal of medicine*. 2014 Jul 31;371(5):424-33. PubMed PMID: 24881730. Pubmed Central PMCID: 4418931.
 39. Groenendijk FH, Bernards R. Drug resistance to targeted therapies: deja vu all over again. *Molecular oncology*. 2014 Sep 12;8(6):1067-83. PubMed PMID: 24910388. Pubmed Central PMCID: 5528618.
 40. Bluemn EG, Coleman IM, Lucas JM, Coleman RT, Hernandez-Lopez S, Tharakan R, et al. Androgen Receptor Pathway-Independent Prostate Cancer Is Sustained through FGF Signaling. *Cancer cell*. 2017 Oct 9;32(4):474-89 e6. PubMed PMID: 29017058.
 41. Robinson D, Van Allen EM, Wu YM, Schultz N, Lonigro RJ, Mosquera JM, et al. Integrative Clinical Genomics of Advanced Prostate Cancer. *Cell*. 2015 Jul 16;162(2):454. PubMed PMID: 28843286.
 42. Koivisto P, Kononen J, Palmberg C, Tammela T, Hyytinen E, Isola J, et al. Androgen receptor gene amplification: a possible molecular mechanism for androgen deprivation therapy failure in prostate cancer. *Cancer research*. 1997 Jan 15;57(2):314-9. PubMed PMID: 9000575.
 43. Barbieri CE, Baca SC, Lawrence MS, Demichelis F, Blattner M, Theurillat JP, et al. Exome sequencing identifies recurrent SPOP, FOXA1 and MED12 mutations in prostate cancer. *Nature genetics*. 2012 May 20;44(6):685-9. PubMed PMID: 22610119. Pubmed Central PMCID: 3673022.
 44. Zoubeidi A, Zardan A, Beraldi E, Fazli L, Sowery R, Rennie P, et al. Cooperative interactions between androgen receptor (AR) and heat-shock protein 27 facilitate AR transcriptional activity. *Cancer research*. 2007 Nov 1;67(21):10455-65. PubMed PMID: 17974989.
 45. Quigley DA, Dang HX, Zhao SG, Lloyd P, Aggarwal R, Alumkal JJ, et al. Genomic Hallmarks and Structural Variation in Metastatic Prostate Cancer. *Cell*. 2018 Jul 26;174(3):758-69 e9. PubMed PMID: 30033370.
 46. Dehm SM, Schmidt LJ, Heemers HV, Vessella RL, Tindall DJ. Splicing of a novel androgen receptor exon generates a constitutively active androgen receptor that mediates prostate cancer therapy

- resistance. *Cancer research*. 2008 Jul 1;68(13):5469-77. PubMed PMID: 18593950. Pubmed Central PMCID: 2663383.
47. Antonarakis ES, Lu C, Wang H, Lubber B, Nakazawa M, Roeser JC, et al. AR-V7 and resistance to enzalutamide and abiraterone in prostate cancer. *The New England journal of medicine*. 2014 Sep 11;371(11):1028-38. PubMed PMID: 25184630. Pubmed Central PMCID: 4201502.
 48. Guo Z, Yang X, Sun F, Jiang R, Linn DE, Chen H, et al. A novel androgen receptor splice variant is up-regulated during prostate cancer progression and promotes androgen depletion-resistant growth. *Cancer research*. 2009 Mar 15;69(6):2305-13. PubMed PMID: 19244107. Pubmed Central PMCID: 2672822.
 49. Li Y, Chan SC, Brand LJ, Hwang TH, Silverstein KA, Dehm SM. Androgen receptor splice variants mediate enzalutamide resistance in castration-resistant prostate cancer cell lines. *Cancer research*. 2013 Jan 15;73(2):483-9. PubMed PMID: 23117885. Pubmed Central PMCID: 3549016.
 50. Henzler C, Li Y, Yang R, McBride T, Ho Y, Sprenger C, et al. Truncation and constitutive activation of the androgen receptor by diverse genomic rearrangements in prostate cancer. *Nature communications*. 2016 Nov 29;7:13668. PubMed PMID: 27897170. Pubmed Central PMCID: 5141345 Medivation/Astellas. The remaining authors declare no competing financial interests.
 51. Feldman BJ, Feldman D. The development of androgen-independent prostate cancer. *Nature reviews Cancer*. 2001 Oct;1(1):34-45. PubMed PMID: 11900250.
 52. van de Wijngaart DJ, Molier M, Lusher SJ, Hersmus R, Jenster G, Trapman J, et al. Systematic structure-function analysis of androgen receptor Leu701 mutants explains the properties of the prostate cancer mutant L701H. *The Journal of biological chemistry*. 2010 Feb 12;285(7):5097-105. PubMed PMID: 20007693. Pubmed Central PMCID: 2836112.
 53. Steinkamp MP, O'Mahony OA, Brogley M, Rehman H, Lapensee EW, Dhanasekaran S, et al. Treatment-dependent androgen receptor mutations in prostate cancer exploit multiple mechanisms to evade therapy. *Cancer research*. 2009 May 15;69(10):4434-42. PubMed PMID: 19366804. Pubmed Central PMCID: 2765801.
 54. Lallous N, Volik SV, Awrey S, Leblanc E, Tse R, Murillo J, et al. Functional analysis of androgen receptor mutations that confer anti-androgen resistance identified in circulating cell-free DNA from prostate cancer patients. *Genome biology*. 2016 Jan 26;17:10. PubMed PMID: 26813233. Pubmed Central PMCID: 4729137.
 55. Hay CW, McEwan IJ. The impact of point mutations in the human androgen receptor: classification of mutations on the basis of transcriptional activity. *PloS one*. 2012;7(3):e32514. PubMed PMID: 22403669. Pubmed Central PMCID: 3293822.
 56. Chen S, Gulla S, Cai C, Balk SP. Androgen receptor serine 81 phosphorylation mediates chromatin binding and transcriptional activation. *The Journal of biological chemistry*. 2012 Mar 9;287(11):8571-83. PubMed PMID: 22275373. Pubmed Central PMCID: 3318700.
 57. Hsu FN, Chen MC, Chiang MC, Lin E, Lee YT, Huang PH, et al. Regulation of androgen receptor and prostate cancer growth by cyclin-dependent kinase 5. *The Journal of biological chemistry*. 2011 Sep 23;286(38):33141-9. PubMed PMID: 21799006. Pubmed Central PMCID: 3190877.
 58. Gordon V, Bhadel S, Wunderlich W, Zhang J, Ficarro SB, Mollah SA, et al. CDK9 regulates AR promoter selectivity and cell growth through serine 81 phosphorylation. *Molecular endocrinology*. 2010 Dec;24(12):2267-80. PubMed PMID: 20980437. Pubmed Central PMCID: 2999477.
 59. Xin L, Teitell MA, Lawson DA, Kwon A, Mellinghoff IK, Witte ON. Progression of prostate cancer by synergy of AKT with genotropic and nongenotropic actions of the androgen receptor. *Proceedings of the National Academy of Sciences of the United States of America*. 2006 May 16;103(20):7789-94. PubMed PMID: 16682621. Pubmed Central PMCID: 1458510.

60. Ha S, Iqbal NJ, Mita P, Ruoff R, Gerald WL, Lepor H, et al. Phosphorylation of the androgen receptor by PIM1 in hormone refractory prostate cancer. *Oncogene*. 2013 Aug 22;32(34):3992-4000. PubMed PMID: 22986532. Pubmed Central PMCID: 3527659.
61. Shu SK, Liu Q, Coppola D, Cheng JQ. Phosphorylation and activation of androgen receptor by Aurora-A. *The Journal of biological chemistry*. 2016 Oct 21;291(43):22854. PubMed PMID: 27825092. Pubmed Central PMCID: 5077229.
62. Gioeli D, Black BE, Gordon V, Spencer A, Kesler CT, Eblen ST, et al. Stress kinase signaling regulates androgen receptor phosphorylation, transcription, and localization. *Molecular endocrinology*. 2006 Mar;20(3):503-15. PubMed PMID: 16282370.
63. Mahajan K, Coppola D, Rawal B, Chen YA, Lawrence HR, Engelman RW, et al. Ack1-mediated androgen receptor phosphorylation modulates radiation resistance in castration-resistant prostate cancer. *The Journal of biological chemistry*. 2012 Jun 22;287(26):22112-22. PubMed PMID: 22566699. Pubmed Central PMCID: 3381169.
64. Mahajan K, Malla P, Lawrence HR, Chen Z, Kumar-Sinha C, Malik R, et al. ACK1/TNK2 Regulates Histone H4 Tyr88-phosphorylation and AR Gene Expression in Castration-Resistant Prostate Cancer. *Cancer cell*. 2017 Jun 12;31(6):790-803 e8. PubMed PMID: 28609657. Pubmed Central PMCID: 5512571.
65. Guo Z, Dai B, Jiang T, Xu K, Xie Y, Kim O, et al. Regulation of androgen receptor activity by tyrosine phosphorylation. *Cancer cell*. 2006 Oct;10(4):309-19. PubMed PMID: 17045208.
66. Chymkowitch P, Le May N, Charneau P, Compe E, Egly JM. The phosphorylation of the androgen receptor by TFIIH directs the ubiquitin/proteasome process. *The EMBO journal*. 2011 Feb 2;30(3):468-79. PubMed PMID: 21157430. Pubmed Central PMCID: 3034013.
67. Gregory CW, Fei X, Ponguta LA, He B, Bill HM, French FS, et al. Epidermal growth factor increases coactivation of the androgen receptor in recurrent prostate cancer. *The Journal of biological chemistry*. 2004 Feb 20;279(8):7119-30. PubMed PMID: 14662770.
68. Ponguta LA, Gregory CW, French FS, Wilson EM. Site-specific androgen receptor serine phosphorylation linked to epidermal growth factor-dependent growth of castration-recurrent prostate cancer. *The Journal of biological chemistry*. 2008 Jul 25;283(30):20989-1001. PubMed PMID: 18511414. Pubmed Central PMCID: 2475695.
69. Liu T, Li Y, Gu H, Zhu G, Li J, Cao L, et al. p21-Activated kinase 6 (PAK6) inhibits prostate cancer growth via phosphorylation of androgen receptor and tumorigenic E3 ligase murine double minute-2 (Mdm2). *The Journal of biological chemistry*. 2013 Feb 1;288(5):3359-69. PubMed PMID: 23132866. Pubmed Central PMCID: 3561555.
70. Zong H, Chi Y, Wang Y, Yang Y, Zhang L, Chen H, et al. Cyclin D3/CDK1p58 complex is involved in the repression of androgen receptor. *Molecular and cellular biology*. 2007 Oct;27(20):7125-42. PubMed PMID: 17698582. Pubmed Central PMCID: 2168904.
71. Yang CS, Xin HW, Kelley JB, Spencer A, Brautigan DL, Paschal BM. Ligand binding to the androgen receptor induces conformational changes that regulate phosphatase interactions. *Molecular and cellular biology*. 2007 May;27(9):3390-404. PubMed PMID: 17325038. Pubmed Central PMCID: 1899975.
72. Liu X, Han W, Gulla S, Simon NI, Gao Y, Cai C, et al. Protein phosphatase 1 suppresses androgen receptor ubiquitylation and degradation. *Oncotarget*. 2016 Jan 12;7(2):1754-64. PubMed PMID: 26636645. Pubmed Central PMCID: 4811495.
73. Ko S, Ahn J, Song CS, Kim S, Knapczyk-Stwora K, Chatterjee B. Lysine methylation and functional modulation of androgen receptor by Set9 methyltransferase. *Molecular endocrinology*. 2011 Mar;25(3):433-44. PubMed PMID: 21273441. Pubmed Central PMCID: 3045741.
74. Fu M, Rao M, Wang C, Sakamaki T, Wang J, Di Vizio D, et al. Acetylation of androgen receptor enhances coactivator binding and promotes prostate cancer cell growth. *Molecular and cellular biology*. 2003 Dec;23(23):8563-75. PubMed PMID: 14612401. Pubmed Central PMCID: 262657.

75. DePaolo JS, Wang Z, Guo J, Zhang G, Qian C, Zhang H, et al. Acetylation of androgen receptor by ARD1 promotes dissociation from HSP90 complex and prostate tumorigenesis. *Oncotarget*. 2016 Nov 1;7(44):71417-28. PubMed PMID: 27659526. Pubmed Central PMCID: 5342088.
76. Fu M, Liu M, Sauve AA, Jiao X, Zhang X, Wu X, et al. Hormonal control of androgen receptor function through SIRT1. *Molecular and cellular biology*. 2006 Nov;26(21):8122-35. PubMed PMID: 16923962. Pubmed Central PMCID: 1636736.
77. He B, Bai S, Hnat AT, Kalman RI, Minges JT, Patterson C, et al. An androgen receptor NH2-terminal conserved motif interacts with the COOH terminus of the Hsp70-interacting protein (CHIP). *The Journal of biological chemistry*. 2004 Jul 16;279(29):30643-53. PubMed PMID: 15107424.
78. Lin HK, Wang L, Hu YC, Altuwaijri S, Chang C. Phosphorylation-dependent ubiquitylation and degradation of androgen receptor by Akt require Mdm2 E3 ligase. *The EMBO journal*. 2002 Aug 1;21(15):4037-48. PubMed PMID: 12145204. Pubmed Central PMCID: 126152.
79. Locke JA, Guns ES, Lubik AA, Adomat HH, Hendy SC, Wood CA, et al. Androgen levels increase by intratumoral de novo steroidogenesis during progression of castration-resistant prostate cancer. *Cancer research*. 2008 Aug 1;68(15):6407-15. PubMed PMID: 18676866.
80. Yamaoka M, Hara T, Kusaka M. Overcoming persistent dependency on androgen signaling after progression to castration-resistant prostate cancer. *Clinical cancer research : an official journal of the American Association for Cancer Research*. 2010 Sep 1;16(17):4319-24. PubMed PMID: 20647476.
81. Grino PB, Griffin JE, Wilson JD. Testosterone at high concentrations interacts with the human androgen receptor similarly to dihydrotestosterone. *Endocrinology*. 1990 Feb;126(2):1165-72. PubMed PMID: 2298157.
82. Chang KH, Li R, Kuri B, Lotan Y, Roehrborn CG, Liu J, et al. A gain-of-function mutation in DHT synthesis in castration-resistant prostate cancer. *Cell*. 2013 Aug 29;154(5):1074-84. PubMed PMID: 23993097. Pubmed Central PMCID: 3931012.
83. Hearn JWD, Xie W, Nakabayashi M, Almassi N, Reichard CA, Pomerantz M, et al. Association of HSD3B1 Genotype With Response to Androgen-Deprivation Therapy for Biochemical Recurrence After Radiotherapy for Localized Prostate Cancer. *JAMA oncology*. 2017 Oct 12. PubMed PMID: 29049492.
84. Almassi N, Reichard C, Li J, Russell C, Perry J, Ryan CJ, et al. HSD3B1 and Response to a Nonsteroidal CYP17A1 Inhibitor in Castration-Resistant Prostate Cancer. *JAMA oncology*. 2017 Oct 12. PubMed PMID: 29049452.
85. Chang KH, Li R, Kuri B, Lotan Y, Roehrborn CG, Liu J, et al. A gain-of-function mutation in DHT synthesis in castration-resistant prostate cancer. *Cell*. 2013 Aug 29;154(5):1074-84. PubMed PMID: 23993097. Pubmed Central PMCID: 3931012.
86. York B, O'Malley BW. Steroid receptor coactivator (SRC) family: masters of systems biology. *The Journal of biological chemistry*. 2010 Dec 10;285(50):38743-50. PubMed PMID: 20956538. Pubmed Central PMCID: 2998129.
87. Culig Z. Androgen Receptor Coactivators in Regulation of Growth and Differentiation in Prostate Cancer. *Journal of cellular physiology*. 2016 Feb;231(2):270-4. PubMed PMID: 26201947.
88. He B, Lanz RB, Fiskus W, Geng C, Yi P, Hartig SM, et al. GATA2 facilitates steroid receptor coactivator recruitment to the androgen receptor complex. *Proceedings of the National Academy of Sciences of the United States of America*. 2014 Dec 23;111(51):18261-6. PubMed PMID: 25489091. Pubmed Central PMCID: 4280633.
89. Xu K, Wu ZJ, Groner AC, He HH, Cai C, Lis RT, et al. EZH2 oncogenic activity in castration-resistant prostate cancer cells is Polycomb-independent. *Science*. 2012 Dec 14;338(6113):1465-9. PubMed PMID: 23239736. Pubmed Central PMCID: 3625962.
90. Cai C, He HH, Chen S, Coleman I, Wang H, Fang Z, et al. Androgen receptor gene expression in prostate cancer is directly suppressed by the androgen receptor through recruitment of lysine-specific

demethylase 1. *Cancer cell*. 2011 Oct 18;20(4):457-71. PubMed PMID: 22014572. Pubmed Central PMCID: 3225024.

91. Zhong J, Ding L, Bohrer LR, Pan Y, Liu P, Zhang J, et al. p300 acetyltransferase regulates androgen receptor degradation and PTEN-deficient prostate tumorigenesis. *Cancer research*. 2014 Mar 15;74(6):1870-80. PubMed PMID: 24480624. Pubmed Central PMCID: 3971883.

92. Asangani IA, Dommeti VL, Wang X, Malik R, Cieslik M, Yang R, et al. Therapeutic targeting of BET bromodomain proteins in castration-resistant prostate cancer. *Nature*. 2014 Jun 12;510(7504):278-82. PubMed PMID: 24759320. Pubmed Central PMCID: 4075966.

93. Nadiminty N, Tummala R, Liu C, Yang J, Lou W, Evans CP, et al. NF-kappaB2/p52 induces resistance to enzalutamide in prostate cancer: role of androgen receptor and its variants. *Molecular cancer therapeutics*. 2013 Aug;12(8):1629-37. PubMed PMID: 23699654. Pubmed Central PMCID: 3941973.

94. Ueda T, Bruchovsky N, Sadar MD. Activation of the androgen receptor N-terminal domain by interleukin-6 via MAPK and STAT3 signal transduction pathways. *The Journal of biological chemistry*. 2002 Mar 1;277(9):7076-85. PubMed PMID: 11751884.

95. Mulholland DJ, Read JT, Rennie PS, Cox ME, Nelson CC. Functional localization and competition between the androgen receptor and T-cell factor for nuclear beta-catenin: a means for inhibition of the Tcf signaling axis. *Oncogene*. 2003 Aug 28;22(36):5602-13. PubMed PMID: 12944908.

96. Robinson JL, Hickey TE, Warren AY, Vowler SL, Carroll T, Lamb AD, et al. Elevated levels of FOXA1 facilitate androgen receptor chromatin binding resulting in a CRPC-like phenotype. *Oncogene*. 2014 Dec 11;33(50):5666-74. PubMed PMID: 24292680. Pubmed Central PMCID: 4051595.

97. Ewing CM, Ray AM, Lange EM, Zuhlke KA, Robbins CM, Tembe WD, et al. Germline mutations in HOXB13 and prostate-cancer risk. *The New England journal of medicine*. 2012 Jan 12;366(2):141-9. PubMed PMID: 22236224. Pubmed Central PMCID: 3779870.

98. Bennett NC, Gardiner RA, Hooper JD, Johnson DW, Gobe GC. Molecular cell biology of androgen receptor signalling. *The international journal of biochemistry & cell biology*. 2010 Jun;42(6):813-27. PubMed PMID: 19931639.

99. Small EJ, Huang J, Youngren J, Sokolov A, Aggarwal RR, Thomas G, et al. Characterization of neuroendocrine prostate cancer (NEPC) in patients with metastatic castration resistant prostate cancer (mCRPC) resistant to abiraterone (Abi) or enzalutamide (Enz): Preliminary results from the SU2C/PCF/AACR West Coast Prostate Cancer Dream Team (WCDT). 2015 ASCO Annual Meeting. *J Clin Oncol*: ASCO; 2015.

100. Purushottamachar P, Godbole AM, Gediya LK, Martin MS, Vasaitis TS, Kwegyir-Afful AK, et al. Systematic structure modifications of multitarget prostate cancer drug candidate galeterone to produce novel androgen receptor down-regulating agents as an approach to treatment of advanced prostate cancer. *Journal of medicinal chemistry*. 2013 Jun 27;56(12):4880-98. PubMed PMID: 23713567. Pubmed Central PMCID: 3959744.

101. Fizazi K, Jones R, Oudard S, Efsthathiou E, Saad F, de Wit R, et al. Phase III, randomized, double-blind, multicenter trial comparing orteronel (TAK-700) plus prednisone with placebo plus prednisone in patients with metastatic castration-resistant prostate cancer that has progressed during or after docetaxel-based therapy: ELM-PC 5. *Journal of clinical oncology : official journal of the American Society of Clinical Oncology*. 2015 Mar 1;33(7):723-31. PubMed PMID: 25624429. Pubmed Central PMCID: 4879718.

102. Toren PJ, Kim S, Pham S, Mangalji A, Adomat H, Guns ES, et al. Anticancer activity of a novel selective CYP17A1 inhibitor in preclinical models of castrate-resistant prostate cancer. *Molecular cancer therapeutics*. 2015 Jan;14(1):59-69. PubMed PMID: 25351916.

103. Moilanen AM, Riikonen R, Oksala R, Ravanti L, Aho E, Wohlfahrt G, et al. Discovery of ODM-201, a new-generation androgen receptor inhibitor targeting resistance mechanisms to androgen signaling-

- directed prostate cancer therapies. *Scientific reports*. 2015 Jul 3;5:12007. PubMed PMID: 26137992. Pubmed Central PMCID: 4490394.
104. Korpai M, Korn JM, Gao X, Rakiec DP, Ruddy DA, Doshi S, et al. An F876L mutation in androgen receptor confers genetic and phenotypic resistance to MDV3100 (enzalutamide). *Cancer discovery*. 2013 Sep;3(9):1030-43. PubMed PMID: 23842682.
 105. Azad AA, Volik SV, Wyatt AW, Haegert A, Le Bihan S, Bell RH, et al. Androgen Receptor Gene Aberrations in Circulating Cell-Free DNA: Biomarkers of Therapeutic Resistance in Castration-Resistant Prostate Cancer. *Clinical cancer research : an official journal of the American Association for Cancer Research*. 2015 May 15;21(10):2315-24. PubMed PMID: 25712683.
 106. Andersen RJ, Mawji NR, Wang J, Wang G, Haile S, Myung JK, et al. Regression of castrate-recurrent prostate cancer by a small-molecule inhibitor of the amino-terminus domain of the androgen receptor. *Cancer cell*. 2010 Jun 15;17(6):535-46. PubMed PMID: 20541699.
 107. Dalal K, Roshan-Moniri M, Sharma A, Li H, Ban F, Hassona MD, et al. Selectively targeting the DNA-binding domain of the androgen receptor as a prospective therapy for prostate cancer. *The Journal of biological chemistry*. 2014 Sep 19;289(38):26417-29. PubMed PMID: 25086042. Pubmed Central PMCID: 4176249.
 108. Watson PA, Chen YF, Balbas MD, Wongvipat J, Socci ND, Viale A, et al. Constitutively active androgen receptor splice variants expressed in castration-resistant prostate cancer require full-length androgen receptor. *Proceedings of the National Academy of Sciences of the United States of America*. 2010 Sep 28;107(39):16759-65. PubMed PMID: 20823238. Pubmed Central PMCID: 2947883.
 109. Hu R, Lu C, Mostaghel EA, Yegnasubramanian S, Gurel M, Tannahill C, et al. Distinct transcriptional programs mediated by the ligand-dependent full-length androgen receptor and its splice variants in castration-resistant prostate cancer. *Cancer research*. 2012 Jul 15;72(14):3457-62. PubMed PMID: 22710436. Pubmed Central PMCID: 3415705.
 110. Lu J, Lonergan PE, Nacusi LP, Wang L, Schmidt LJ, Sun Z, et al. The cistrome and gene signature of androgen receptor splice variants in castration resistant prostate cancer cells. *The Journal of urology*. 2015 Feb;193(2):690-8. PubMed PMID: 25132238. Pubmed Central PMCID: 4411637.
 111. Li H, Wang Z, Tang K, Zhou H, Liu H, Yan L, et al. Prognostic Value of Androgen Receptor Splice Variant 7 in the Treatment of Castration-resistant Prostate Cancer with Next generation Androgen Receptor Signal Inhibition: A Systematic Review and Meta-analysis. *European urology focus*. 2017 Jan 23. PubMed PMID: 28753843.
 112. Cucchiaro V, Cooperberg MR, Dall'Era M, Lin DW, Montorsi F, Schalken JA, et al. Genomic Markers in Prostate Cancer Decision Making. *European urology*. 2017 Nov 9. PubMed PMID: 29129398.
 113. Annala M, Vandekerckhove G, Khalaf D, Taavitsainen S, Beja K, Warner EW, et al. Circulating tumor DNA genomics correlate with resistance to abiraterone and enzalutamide in prostate cancer. *Cancer discovery*. 2018 Jan 24. PubMed PMID: 29367197.
 114. Varga J, Greten FR. Cell plasticity in epithelial homeostasis and tumorigenesis. *Nature cell biology*. 2017 Oct;19(10):1133-41. PubMed PMID: 28945230.
 115. Hay ED. An overview of epithelio-mesenchymal transformation. *Acta anatomica*. 1995;154(1):8-20. PubMed PMID: 8714286.
 116. Thiery JP, Acloque H, Huang RY, Nieto MA. Epithelial-mesenchymal transitions in development and disease. *Cell*. 2009 Nov 25;139(5):871-90. PubMed PMID: 19945376.
 117. Lamouille S, Xu J, Derynck R. Molecular mechanisms of epithelial-mesenchymal transition. *Nature reviews Molecular cell biology*. 2014 Mar;15(3):178-96. PubMed PMID: 24556840. Pubmed Central PMCID: 4240281.
 118. Haider M, Zhang X, Coleman I, Ericson N, True LD, Lam HM, et al. Epithelial mesenchymal-like transition occurs in a subset of cells in castration resistant prostate cancer bone metastases. *Clinical &*

- experimental metastasis. 2016 Mar;33(3):239-48. PubMed PMID: 26667932. Pubmed Central PMCID: 4777655.
119. Sun Y, Wang BE, Leong KG, Yue P, Li L, Jhunjhunwala S, et al. Androgen deprivation causes epithelial-mesenchymal transition in the prostate: implications for androgen-deprivation therapy. *Cancer research*. 2012 Jan 15;72(2):527-36. PubMed PMID: 22108827.
 120. Kwok WK, Ling MT, Lee TW, Lau TC, Zhou C, Zhang X, et al. Up-regulation of TWIST in prostate cancer and its implication as a therapeutic target. *Cancer research*. 2005 Jun 15;65(12):5153-62. PubMed PMID: 15958559.
 121. Tanaka H, Kono E, Tran CP, Miyazaki H, Yamashiro J, Shimomura T, et al. Monoclonal antibody targeting of N-cadherin inhibits prostate cancer growth, metastasis and castration resistance. *Nature medicine*. 2010 Dec;16(12):1414-20. PubMed PMID: 21057494. Pubmed Central PMCID: 3088104.
 122. Akamatsu S, Wyatt AW, Lin D, Lysakowski S, Zhang F, Kim S, et al. The Placental Gene PEG10 Promotes Progression of Neuroendocrine Prostate Cancer. *Cell reports*. 2015 Aug 11;12(6):922-36. PubMed PMID: 26235627.
 123. Jacob S, Nayak S, Fernandes G, Barai RS, Menon S, Chaudhari UK, et al. Androgen receptor as a regulator of ZEB2 expression and its implications in epithelial-to-mesenchymal transition in prostate cancer. *Endocrine-related cancer*. 2014 Jun;21(3):473-86. PubMed PMID: 24812058.
 124. Wu K, Gore C, Yang L, Fazli L, Gleave M, Pong RC, et al. Slug, a unique androgen-regulated transcription factor, coordinates androgen receptor to facilitate castration resistance in prostate cancer. *Molecular endocrinology*. 2012 Sep;26(9):1496-507. PubMed PMID: 22745193. Pubmed Central PMCID: 5416972.
 125. Cordonnier T, Bishop JL, Shiota M, Nip KM, Thaper D, Vahid S, et al. Hsp27 regulates EGF/beta-catenin mediated epithelial to mesenchymal transition in prostate cancer. *International journal of cancer Journal international du cancer*. 2015 Mar 15;136(6):E496-507. PubMed PMID: 25130271.
 126. Lu X, Kang Y. Epidermal growth factor signalling and bone metastasis. *British journal of cancer*. 2010 Feb 2;102(3):457-61. PubMed PMID: 20010942. Pubmed Central PMCID: 2822931.
 127. Graham TR, Zhau HE, Odero-Marrah VA, Osunkoya AO, Kimbro KS, Tighiouart M, et al. Insulin-like growth factor-I-dependent up-regulation of ZEB1 drives epithelial-to-mesenchymal transition in human prostate cancer cells. *Cancer research*. 2008 Apr 1;68(7):2479-88. PubMed PMID: 18381457.
 128. Liu ZC, Chen XH, Song HX, Wang HS, Zhang G, Wang H, et al. Snail regulated by PKC/GSK-3beta pathway is crucial for EGF-induced epithelial-mesenchymal transition (EMT) of cancer cells. *Cell and tissue research*. 2014 Nov;358(2):491-502. PubMed PMID: 25124796.
 129. Kao SH, Wang WL, Chen CY, Chang YL, Wu YY, Wang YT, et al. GSK3beta controls epithelial-mesenchymal transition and tumor metastasis by CHIP-mediated degradation of Slug. *Oncogene*. 2014 Jun 12;33(24):3172-82. PubMed PMID: 23851495. Pubmed Central PMCID: 4096338.
 130. Kim J, Bae S, An S, Park JK, Kim EM, Hwang SG, et al. Cooperative actions of p21WAF1 and p53 induce Slug protein degradation and suppress cell invasion. *EMBO reports*. 2014 Oct;15(10):1062-8. PubMed PMID: 25141863. Pubmed Central PMCID: 4253846.
 131. Sekimoto T, Miyamoto Y, Arai S, Yoneda Y. Importin alpha protein acts as a negative regulator for Snail protein nuclear import. *The Journal of biological chemistry*. 2011 Apr 29;286(17):15126-31. PubMed PMID: 21454664. Pubmed Central PMCID: 3083189.
 132. Yang Z, Rayala S, Nguyen D, Vadlamudi RK, Chen S, Kumar R. PAK1 phosphorylation of snail, a master regulator of epithelial-to-mesenchyme transition, modulates snail's subcellular localization and functions. *Cancer research*. 2005 Apr 15;65(8):3179-84. PubMed PMID: 15833848.
 133. Zardan A, Nip KM, Thaper D, Toren P, Vahid S, Beraldi E, et al. Lyn tyrosine kinase regulates androgen receptor expression and activity in castrate-resistant prostate cancer. *Oncogenesis*. 2014 Aug 18;3:e115. PubMed PMID: 25133482. Pubmed Central PMCID: 5189960.

134. Thaper D, Vahid S, Nip KM, Moskalev I, Shan X, Frees S, et al. Targeting Lyn regulates Snail family shuttling and inhibits metastasis. *Oncogene*. 2017 Jul 13;36(28):3964-75. PubMed PMID: 28288135.
135. Beltran H, Rickman DS, Park K, Chae SS, Sboner A, MacDonald TY, et al. Molecular characterization of neuroendocrine prostate cancer and identification of new drug targets. *Cancer discovery*. 2011 Nov;1(6):487-95. PubMed PMID: 22389870. Pubmed Central PMCID: 3290518.
136. Aggarwal R, Huang J, Alumkal JJ, Zhang L, Feng FY, Thomas GV, et al. Clinical and Genomic Characterization of Treatment-Emergent Small-Cell Neuroendocrine Prostate Cancer: A Multi-institutional Prospective Study. *Journal of clinical oncology : official journal of the American Society of Clinical Oncology*. 2018 Jul 9;JCO2017776880. PubMed PMID: 29985747.
137. Aggarwal R, Zhang T, Small EJ, Armstrong AJ. Neuroendocrine prostate cancer: subtypes, biology, and clinical outcomes. *Journal of the National Comprehensive Cancer Network : JNCCN*. 2014 May;12(5):719-26. PubMed PMID: 24812138.
138. Berruti A, Mosca A, Porpiglia F, Bollito E, Tucci M, Vana F, et al. Chromogranin A expression in patients with hormone naive prostate cancer predicts the development of hormone refractory disease. *The Journal of urology*. 2007 Sep;178(3 Pt 1):838-43; quiz 1129. PubMed PMID: 17631319.
139. Hirano D, Okada Y, Minei S, Takimoto Y, Nemoto N. Neuroendocrine differentiation in hormone refractory prostate cancer following androgen deprivation therapy. *European urology*. 2004 May;45(5):586-92; discussion 92. PubMed PMID: 15082200.
140. Sequist LV, Waltman BA, Dias-Santagata D, Digumarthy S, Turke AB, Fidias P, et al. Genotypic and histological evolution of lung cancers acquiring resistance to EGFR inhibitors. *Science translational medicine*. 2011 Mar 23;3(75):75ra26. PubMed PMID: 21430269. Pubmed Central PMCID: 3132801.
141. Mu P, Zhang Z, Benelli M, Karthaus WR, Hoover E, Chen CC, et al. SOX2 promotes lineage plasticity and antiandrogen resistance in TP53- and RB1-deficient prostate cancer. *Science*. 2017 Jan 6;355(6320):84-8. PubMed PMID: 28059768. Pubmed Central PMCID: 5247742.
142. Lee JK, Phillips JW, Smith BA, Park JW, Stoyanova T, McCaffrey EF, et al. N-Myc Drives Neuroendocrine Prostate Cancer Initiated from Human Prostate Epithelial Cells. *Cancer cell*. 2016 Apr 11;29(4):536-47. PubMed PMID: 27050099. Pubmed Central PMCID: 4829466.
143. Dardenne E, Beltran H, Benelli M, Gayvert K, Berger A, Puca L, et al. N-Myc Induces an EZH2-Mediated Transcriptional Program Driving Neuroendocrine Prostate Cancer. *Cancer cell*. 2016 Oct 10;30(4):563-77. PubMed PMID: 27728805. Pubmed Central PMCID: 5540451.
144. Zou M, Toivanen R, Mitrofanova A, Floch N, Hayati S, Sun Y, et al. Transdifferentiation as a Mechanism of Treatment Resistance in a Mouse Model of Castration-Resistant Prostate Cancer. *Cancer discovery*. 2017 Jul;7(7):736-49. PubMed PMID: 28411207. Pubmed Central PMCID: 5501744.
145. Bishop JL, Thaper D, Vahid S, Davies A, Ketola K, Kuruma H, et al. The Master Neural Transcription Factor BRN2 Is an Androgen Receptor-Suppressed Driver of Neuroendocrine Differentiation in Prostate Cancer. *Cancer discovery*. 2017 Jan;7(1):54-71. PubMed PMID: 27784708.
146. Rickman DS, Beltran H, Demichelis F, Rubin MA. Biology and evolution of poorly differentiated neuroendocrine tumors. *Nature medicine*. 2017 Jun 6;23(6):1-10. PubMed PMID: 28586335.
147. Heck MM, Thaler MA, Schmid SC, Seitz AK, Tauber R, Kubler H, et al. Chromogranin A and neurone-specific enolase serum levels as predictors of treatment outcome in patients with metastatic castration-resistant prostate cancer undergoing abiraterone therapy. *BJU international*. 2017 Jan;119(1):30-7. PubMed PMID: 27037533.
148. Burgio SL, Conteduca V, Menna C, Carretta E, Rossi L, Bianchi E, et al. Chromogranin A predicts outcome in prostate cancer patients treated with abiraterone. *Endocrine-related cancer*. 2014 Jun;21(3):487-93. PubMed PMID: 24741024.
149. Beltran H, Wyatt AW, Chedgy EC, Donoghue A, Annala M, Warner EW, et al. Impact of Therapy on Genomics and Transcriptomics in High-Risk Prostate Cancer Treated with Neoadjuvant Docetaxel and Androgen Deprivation Therapy. *Clinical cancer research : an official journal of the American Association*

- for Cancer Research. 2017 Nov 15;23(22):6802-11. PubMed PMID: 28842510. Pubmed Central PMCID: 5690882.
150. George J, Lim JS, Jang SJ, Cun Y, Ozretic L, Kong G, et al. Comprehensive genomic profiles of small cell lung cancer. *Nature*. 2015 Aug 6;524(7563):47-53. PubMed PMID: 26168399. Pubmed Central PMCID: 4861069.
 151. Nau MM, Brooks BJ, Jr., Carney DN, Gazdar AF, Battey JF, Sausville EA, et al. Human small-cell lung cancers show amplification and expression of the N-myc gene. *Proceedings of the National Academy of Sciences of the United States of America*. 1986 Feb;83(4):1092-6. PubMed PMID: 2869482. Pubmed Central PMCID: 323017.
 152. Funa K, Steinholtz L, Nou E, Bergh J. Increased expression of N-myc in human small cell lung cancer biopsies predicts lack of response to chemotherapy and poor prognosis. *American journal of clinical pathology*. 1987 Aug;88(2):216-20. PubMed PMID: 3039835.
 153. Rudin CM, Durinck S, Stawiski EW, Poirier JT, Modrusan Z, Shames DS, et al. Comprehensive genomic analysis identifies SOX2 as a frequently amplified gene in small-cell lung cancer. *Nature genetics*. 2012 Oct;44(10):1111-6. PubMed PMID: 22941189. Pubmed Central PMCID: 3557461.
 154. Gardner EE, Lok BH, Schneeberger VE, Desmeules P, Miles LA, Arnold PK, et al. Chemosensitive Relapse in Small Cell Lung Cancer Proceeds through an EZH2-SLFN11 Axis. *Cancer cell*. 2017 Feb 13;31(2):286-99. PubMed PMID: 28196596. Pubmed Central PMCID: 5313262.
 155. Murai F, Koinuma D, Shinozaki-Ushiku A, Fukayama M, Miyaozono K, Ehata S. EZH2 promotes progression of small cell lung cancer by suppressing the TGF-beta-Smad-ASCL1 pathway. *Cell discovery*. 2015;1:15026. PubMed PMID: 27462425. Pubmed Central PMCID: 4860843.
 156. Walter RF, Mairinger FD, Werner R, Ting S, Vollbrecht C, Theegarten D, et al. SOX4, SOX11 and PAX6 mRNA expression was identified as a (prognostic) marker for the aggressiveness of neuroendocrine tumors of the lung by using next-generation expression analysis (NanoString). *Future oncology*. 2015;11(7):1027-36. PubMed PMID: 25804118.
 157. Castillo SD, Matheu A, Mariani N, Carretero J, Lopez-Rios F, Lovell-Badge R, et al. Novel transcriptional targets of the SRY-HMG box transcription factor SOX4 link its expression to the development of small cell lung cancer. *Cancer research*. 2012 Jan 1;72(1):176-86. PubMed PMID: 22084397.
 158. Masumori N, Thomas TZ, Chaurand P, Case T, Paul M, Kasper S, et al. A probasin-large T antigen transgenic mouse line develops prostate adenocarcinoma and neuroendocrine carcinoma with metastatic potential. *Cancer research*. 2001 Mar 1;61(5):2239-49. PubMed PMID: 11280793.
 159. Kaplan-Lefko PJ, Chen TM, Ittmann MM, Barrios RJ, Ayala GE, Huss WJ, et al. Pathobiology of autochthonous prostate cancer in a pre-clinical transgenic mouse model. *The Prostate*. 2003 May 15;55(3):219-37. PubMed PMID: 12692788.
 160. Ku SY, Rosario S, Wang Y, Mu P, Seshadri M, Goodrich ZW, et al. Rb1 and Trp53 cooperate to suppress prostate cancer lineage plasticity, metastasis, and antiandrogen resistance. *Science*. 2017 Jan 6;355(6320):78-83. PubMed PMID: 28059767. Pubmed Central PMCID: 5367887.
 161. Otto T, Horn S, Brockmann M, Eilers U, Schuttrumpf L, Popov N, et al. Stabilization of N-Myc is a critical function of Aurora A in human neuroblastoma. *Cancer cell*. 2009 Jan 6;15(1):67-78. PubMed PMID: 19111882.
 162. Clermont PL, Lin D, Crea F, Wu R, Xue H, Wang Y, et al. Polycomb-mediated silencing in neuroendocrine prostate cancer. *Clinical epigenetics*. 2015;7:40. PubMed PMID: 25859291. Pubmed Central PMCID: 4391120.
 163. Tannock IF, de Wit R, Berry WR, Horti J, Pluzanska A, Chi KN, et al. Docetaxel plus prednisone or mitoxantrone plus prednisone for advanced prostate cancer. *The New England journal of medicine*. 2004 Oct 7;351(15):1502-12. PubMed PMID: 15470213.

164. Petrylak DP, Tangen CM, Hussain MH, Lara PN, Jr., Jones JA, Taplin ME, et al. Docetaxel and estramustine compared with mitoxantrone and prednisone for advanced refractory prostate cancer. *The New England journal of medicine*. 2004 Oct 7;351(15):1513-20. PubMed PMID: 15470214.
165. Herbst RS, Khuri FR. Mode of action of docetaxel - a basis for combination with novel anticancer agents. *Cancer treatment reviews*. 2003 Oct;29(5):407-15. PubMed PMID: 12972359.
166. Fabbri F, Amadori D, Carloni S, Brigliadori G, Tesei A, Ulivi P, et al. Mitotic catastrophe and apoptosis induced by docetaxel in hormone-refractory prostate cancer cells. *Journal of cellular physiology*. 2008 Nov;217(2):494-501. PubMed PMID: 18615564.
167. Zhu Y, Liu C, Nadiminty N, Lou W, Tummala R, Evans CP, et al. Inhibition of ABCB1 expression overcomes acquired docetaxel resistance in prostate cancer. *Molecular cancer therapeutics*. 2013 Sep;12(9):1829-36. PubMed PMID: 23861346. Pubmed Central PMCID: 3947549.
168. Ploussard G, Terry S, Maille P, Allory Y, Sirab N, Kheuang L, et al. Class III beta-tubulin expression predicts prostate tumor aggressiveness and patient response to docetaxel-based chemotherapy. *Cancer research*. 2010 Nov 15;70(22):9253-64. PubMed PMID: 21045157. Pubmed Central PMCID: 3290526.
169. de Bono JS, Oudard S, Ozguroglu M, Hansen S, Machiels JP, Kocak I, et al. Prednisone plus cabazitaxel or mitoxantrone for metastatic castration-resistant prostate cancer progressing after docetaxel treatment: a randomised open-label trial. *Lancet*. 2010 Oct 2;376(9747):1147-54. PubMed PMID: 20888992.
170. Oudard S, Fizazi K, Sengelov L, Daugaard G, Saad F, Hansen S, et al. Cabazitaxel Versus Docetaxel As First-Line Therapy for Patients With Metastatic Castration-Resistant Prostate Cancer: A Randomized Phase III Trial-FIRSTANA. *Journal of clinical oncology : official journal of the American Society of Clinical Oncology*. 2017 Oct 1;35(28):3189-97. PubMed PMID: 28753384.
171. Vrignaud P, Semiond D, Lejeune P, Bouchard H, Calvet L, Combeau C, et al. Preclinical antitumor activity of cabazitaxel, a semisynthetic taxane active in taxane-resistant tumors. *Clinical cancer research : an official journal of the American Association for Cancer Research*. 2013 Jun 1;19(11):2973-83. PubMed PMID: 23589177.
172. Sweeney CJ, Chen YH, Carducci M, Liu G, Jarrard DF, Eisenberger M, et al. Chemohormonal Therapy in Metastatic Hormone-Sensitive Prostate Cancer. *The New England journal of medicine*. 2015 Aug 20;373(8):737-46. PubMed PMID: 26244877. Pubmed Central PMCID: 4562797.
173. Kantoff PW, Higano CS, Shore ND, Berger ER, Small EJ, Penson DF, et al. Sipuleucel-T immunotherapy for castration-resistant prostate cancer. *The New England journal of medicine*. 2010 Jul 29;363(5):411-22. PubMed PMID: 20818862.
174. Anassi E, Ndefo UA. Sipuleucel-T (provenge) injection: the first immunotherapy agent (vaccine) for hormone-refractory prostate cancer. *P & T : a peer-reviewed journal for formulary management*. 2011 Apr;36(4):197-202. PubMed PMID: 21572775. Pubmed Central PMCID: 3086121.
175. Hodi FS, O'Day SJ, McDermott DF, Weber RW, Sosman JA, Haanen JB, et al. Improved survival with ipilimumab in patients with metastatic melanoma. *The New England journal of medicine*. 2010 Aug 19;363(8):711-23. PubMed PMID: 20525992. Pubmed Central PMCID: 3549297.
176. Wolchok JD, Kluger H, Callahan MK, Postow MA, Rizvi NA, Lesokhin AM, et al. Nivolumab plus ipilimumab in advanced melanoma. *The New England journal of medicine*. 2013 Jul 11;369(2):122-33. PubMed PMID: 23724867. Pubmed Central PMCID: 5698004.
177. Garon EB, Rizvi NA, Hui R, Leighl N, Balmanoukian AS, Eder JP, et al. Pembrolizumab for the treatment of non-small-cell lung cancer. *The New England journal of medicine*. 2015 May 21;372(21):2018-28. PubMed PMID: 25891174.
178. Mateo J, Carreira S, Sandhu S, Miranda S, Mossop H, Perez-Lopez R, et al. DNA-Repair Defects and Olaparib in Metastatic Prostate Cancer. *The New England journal of medicine*. 2015 Oct 29;373(18):1697-708. PubMed PMID: 26510020. Pubmed Central PMCID: 5228595.

179. Dziadkowiec KN, Gasiorowska E, Nowak-Markwitz E, Jankowska A. PARP inhibitors: review of mechanisms of action and BRCA1/2 mutation targeting. *Przegląd menopauzalny = Menopause review*. 2016 Dec;15(4):215-9. PubMed PMID: 28250726. Pubmed Central PMCID: 5327624.
180. Chedgy EC, Annala M, Beja K, Warner EW, Gleave ME, Chi KN, et al. Moving Toward Personalized Care: Liquid Biopsy Predicts Response to Cisplatin in an Unusual Case of BRCA2-Null Neuroendocrine Prostate Cancer. *Clinical genitourinary cancer*. 2016 Apr;14(2):e233-6. PubMed PMID: 26797585.
181. Kuruma H, Matsumoto H, Shiota M, Bishop J, Lamoureux F, Thomas C, et al. A novel antiandrogen, Compound 30, suppresses castration-resistant and MDV3100-resistant prostate cancer growth in vitro and in vivo. *Molecular cancer therapeutics*. 2013 May;12(5):567-76. PubMed PMID: 23493310. Epub 2013/03/16. eng.
182. Lin D, Wyatt AW, Xue H, Wang Y, Dong X, Haegert A, et al. High fidelity patient-derived xenografts for accelerating prostate cancer discovery and drug development. *Cancer research*. 2014 Feb 15;74(4):1272-83. PubMed PMID: 24356420. Epub 2013/12/21. eng.
183. Wyatt AW, Mo F, Wang K, McConeghy B, Brahmabhatt S, Jong L, et al. Heterogeneity in the inter-tumor transcriptome of high risk prostate cancer. *Genome biology*. 2014;15(8):426. PubMed PMID: 25155515. Pubmed Central PMCID: 4169643. Epub 2014/08/27. eng.
184. Goodall J, Wellbrock C, Dexter TJ, Roberts K, Marais R, Goding CR. The Brn-2 transcription factor links activated BRAF to melanoma proliferation. *Molecular and cellular biology*. 2004 Apr;24(7):2923-31. PubMed PMID: 15024080. Pubmed Central PMCID: 371133. Epub 2004/03/17. eng.
185. Jager W, Moskalev I, Janssen C, Hayashi T, Awrey S, Gust KM, et al. Ultrasound-guided intramural inoculation of orthotopic bladder cancer xenografts: a novel high-precision approach. *PloS one*. 2013;8(3):e59536. PubMed PMID: 23555699. Pubmed Central PMCID: 3608695.
186. Pai MY, Lomenick B, Hwang H, Schiestl R, McBride W, Loo JA, et al. Drug affinity responsive target stability (DARTS) for small-molecule target identification. *Methods in molecular biology*. 2015;1263:287-98. PubMed PMID: 25618353. Pubmed Central PMCID: 4442491.
187. Cabos-Siguier B, Steunou AL, Joseph G, Alazard R, Ducoux-Petit M, Nieto L, et al. Expression and purification of human full-length N Oct-3, a transcription factor involved in melanoma growth. *Protein expression and purification*. 2009 Mar;64(1):39-46. PubMed PMID: 18996486.
188. Singh K, Munuganti RS, Leblanc E, Lin YL, Leung E, Lallous N, et al. In silico discovery and validation of potent small-molecule inhibitors targeting the activation function 2 site of human oestrogen receptor alpha. *Breast cancer research : BCR*. 2015 Feb 25;17:27. PubMed PMID: 25848700. Pubmed Central PMCID: 4360945.
189. Gao J, Aksoy BA, Dogrusoz U, Dresdner G, Gross B, Sumer SO, et al. Integrative analysis of complex cancer genomics and clinical profiles using the cBioPortal. *Science signaling*. 2013 Apr 2;6(269):pl1. PubMed PMID: 23550210. Pubmed Central PMCID: 4160307.
190. Goldman M, Craft B, Swatloski T, Cline M, Morozova O, Diekhans M, et al. The UCSC Cancer Genomics Browser: update 2015. *Nucleic acids research*. 2015 Jan;43(Database issue):D812-7. PubMed PMID: 25392408. Pubmed Central PMCID: 4383911.
191. Oppermann H, Levinson AD, Varmus HE, Levintow L, Bishop JM. Uninfected vertebrate cells contain a protein that is closely related to the product of the avian sarcoma virus transforming gene (src). *Proceedings of the National Academy of Sciences of the United States of America*. 1979 Apr;76(4):1804-8. PubMed PMID: 221907. Pubmed Central PMCID: 383480.
192. Parsons SJ, Parsons JT. Src family kinases, key regulators of signal transduction. *Oncogene*. 2004 Oct 18;23(48):7906-9. PubMed PMID: 15489908.
193. Lowell CA. Src-family kinases: rheostats of immune cell signaling. *Molecular immunology*. 2004 Jul;41(6-7):631-43. PubMed PMID: 15220000.

194. Maness PF, Beggs HE, Klinz SG, Morse WR. Selective neural cell adhesion molecule signaling by Src family tyrosine kinases and tyrosine phosphatases. Perspectives on developmental neurobiology. 1996;4(2-3):169-81. PubMed PMID: 9168199.
195. Fidler IJ. The pathogenesis of cancer metastasis: the 'seed and soil' hypothesis revisited. Nature reviews Cancer. 2003 Jun;3(6):453-8. PubMed PMID: 12778135. Epub 2003/06/05. eng.
196. Zhang S, Yu D. Targeting Src family kinases in anti-cancer therapies: turning promise into triumph. Trends in pharmacological sciences. 2012 Mar;33(3):122-8. PubMed PMID: 22153719. Pubmed Central PMCID: 3675659.
197. Ingley E. Functions of the Lyn tyrosine kinase in health and disease. Cell communication and signaling : CCS. 2012 Jul 17;10(1):21. PubMed PMID: 22805580. Pubmed Central PMCID: 3464935.
198. Futami M, Zhu QS, Whichard ZL, Xia L, Ke Y, Neel BG, et al. G-CSF receptor activation of the Src kinase Lyn is mediated by Gab2 recruitment of the Shp2 phosphatase. Blood. 2011 Jul 28;118(4):1077-86. PubMed PMID: 21636860. Pubmed Central PMCID: 3148159.
199. Wang D, Esselman WJ, Cole PA. Substrate conformational restriction and CD45-catalyzed dephosphorylation of tail tyrosine-phosphorylated Src protein. The Journal of biological chemistry. 2002 Oct 25;277(43):40428-33. PubMed PMID: 12181320.
200. Somani AK, Yuen K, Xu F, Zhang J, Branch DR, Siminovitch KA. The SH2 domain containing tyrosine phosphatase-1 down-regulates activation of Lyn and Lyn-induced tyrosine phosphorylation of the CD19 receptor in B cells. The Journal of biological chemistry. 2001 Jan 19;276(3):1938-44. PubMed PMID: 11042209.
201. Scapini P, Pereira S, Zhang H, Lowell CA. Multiple roles of Lyn kinase in myeloid cell signaling and function. Immunological reviews. 2009 Mar;228(1):23-40. PubMed PMID: 19290919. Pubmed Central PMCID: 3248569.
202. Linnekin D, DeBerry CS, Mou S. Lyn associates with the juxtamembrane region of c-Kit and is activated by stem cell factor in hematopoietic cell lines and normal progenitor cells. The Journal of biological chemistry. 1997 Oct 24;272(43):27450-5. PubMed PMID: 9341198.
203. Sutton P, Borgia JA, Bonomi P, Plate JM. Lyn, a Src family kinase, regulates activation of epidermal growth factor receptors in lung adenocarcinoma cells. Molecular cancer. 2013 Jul 16;12:76. PubMed PMID: 23866081. Pubmed Central PMCID: 3725175.
204. Pereira S, Lowell C. The Lyn tyrosine kinase negatively regulates neutrophil integrin signaling. Journal of immunology. 2003 Aug 1;171(3):1319-27. PubMed PMID: 12874221.
205. Seong J, Ouyang M, Kim T, Sun J, Wen PC, Lu S, et al. Detection of focal adhesion kinase activation at membrane microdomains by fluorescence resonance energy transfer. Nature communications. 2011 Jul 26;2:406. PubMed PMID: 21792185. Pubmed Central PMCID: 3373894.
206. Takeda Y, Nakaseko C, Tanaka H, Takeuchi M, Yui M, Saraya A, et al. Direct activation of STAT5 by ETV6-LYN fusion protein promotes induction of myeloproliferative neoplasm with myelofibrosis. British journal of haematology. 2011 Jun;153(5):589-98. PubMed PMID: 21492125. Pubmed Central PMCID: 3091948.
207. Ingley E, Sarna MK, Beaumont JG, Tilbrook PA, Tsai S, Takemoto Y, et al. HS1 interacts with Lyn and is critical for erythropoietin-induced differentiation of erythroid cells. The Journal of biological chemistry. 2000 Mar 17;275(11):7887-93. PubMed PMID: 10713104.
208. Xu Y, Huntington ND, Harder KW, Nandurkar H, Hibbs ML, Tarlinton DM. Phosphatidylinositol-3 kinase activity in B cells is negatively regulated by Lyn tyrosine kinase. Immunology and cell biology. 2012 Oct;90(9):903-11. PubMed PMID: 22777522.
209. Huang TH, Huo L, Wang YN, Xia W, Wei Y, Chang SS, et al. Epidermal growth factor receptor potentiates MCM7-mediated DNA replication through tyrosine phosphorylation of Lyn kinase in human cancers. Cancer cell. 2013 Jun 10;23(6):796-810. PubMed PMID: 23764002. Pubmed Central PMCID: 3703149.

210. Golas JM, Arndt K, Etienne C, Lucas J, Nardin D, Gibbons J, et al. SKI-606, a 4-anilino-3-quinolinecarbonitrile dual inhibitor of Src and Abl kinases, is a potent antiproliferative agent against chronic myelogenous leukemia cells in culture and causes regression of K562 xenografts in nude mice. *Cancer research*. 2003 Jan 15;63(2):375-81. PubMed PMID: 12543790.
211. Warmuth M, Simon N, Mitina O, Mathes R, Fabbro D, Manley PW, et al. Dual-specific Src and Abl kinase inhibitors, PP1 and CGP76030, inhibit growth and survival of cells expressing imatinib mesylate-resistant Bcr-Abl kinases. *Blood*. 2003 Jan 15;101(2):664-72. PubMed PMID: 12393636.
212. Meyn MA, 3rd, Wilson MB, Abdi FA, Fahey N, Schiavone AP, Wu J, et al. Src family kinases phosphorylate the Bcr-Abl SH3-SH2 region and modulate Bcr-Abl transforming activity. *The Journal of biological chemistry*. 2006 Oct 13;281(41):30907-16. PubMed PMID: 16912036.
213. Wu J, Meng F, Lu H, Kong L, Bornmann W, Peng Z, et al. Lyn regulates BCR-ABL and Gab2 tyrosine phosphorylation and c-Cbl protein stability in imatinib-resistant chronic myelogenous leukemia cells. *Blood*. 2008 Apr 1;111(7):3821-9. PubMed PMID: 18235045. Pubmed Central PMCID: 2275035.
214. Ptasznik A, Nakata Y, Kalota A, Emerson SG, Gewirtz AM. Short interfering RNA (siRNA) targeting the Lyn kinase induces apoptosis in primary, and drug-resistant, BCR-ABL1(+) leukemia cells. *Nature medicine*. 2004 Nov;10(11):1187-9. PubMed PMID: 15502840.
215. Santos FP, Kantarjian H, Cortes J, Quintas-Cardama A. Bafetinib, a dual Bcr-Abl/Lyn tyrosine kinase inhibitor for the potential treatment of leukemia. *Current opinion in investigational drugs*. 2010 Dec;11(12):1450-65. PubMed PMID: 21154127.
216. O'Hare T, Shakespeare WC, Zhu X, Eide CA, Rivera VM, Wang F, et al. AP24534, a pan-BCR-ABL inhibitor for chronic myeloid leukemia, potently inhibits the T315I mutant and overcomes mutation-based resistance. *Cancer cell*. 2009 Nov 6;16(5):401-12. PubMed PMID: 19878872. Pubmed Central PMCID: 2804470.
217. Tauzin S, Ding H, Khatib K, Ahmad I, Burdevet D, van Echten-Deckert G, et al. Oncogenic association of the Cbp/PAG adaptor protein with the Lyn tyrosine kinase in human B-NHL rafts. *Blood*. 2008 Feb 15;111(4):2310-20. PubMed PMID: 18070987.
218. Hu Y, Liu Y, Pelletier S, Buchdunger E, Warmuth M, Fabbro D, et al. Requirement of Src kinases Lyn, Hck and Fgr for BCR-ABL1-induced B-lymphoblastic leukemia but not chronic myeloid leukemia. *Nature genetics*. 2004 May;36(5):453-61. PubMed PMID: 15098032.
219. Guarino M. Src signaling in cancer invasion. *Journal of cellular physiology*. 2010 Apr;223(1):14-26. PubMed PMID: 20049846.
220. Bougeret C, Jiang S, Keydar I, Avraham H. Functional analysis of Csk and CHK kinases in breast cancer cells. *The Journal of biological chemistry*. 2001 Sep 7;276(36):33711-20. PubMed PMID: 11445575. Epub 2001/07/11. eng.
221. Bates RC, Edwards NS, Burns GF, Fisher DE. A CD44 survival pathway triggers chemoresistance via lyn kinase and phosphoinositide 3-kinase/Akt in colon carcinoma cells. *Cancer research*. 2001 Jul 1;61(13):5275-83. PubMed PMID: 11431370.
222. Stettner MR, Wang W, Nabors LB, Bharara S, Flynn DC, Grammer JR, et al. Lyn kinase activity is the predominant cellular SRC kinase activity in glioblastoma tumor cells. *Cancer research*. 2005 Jul 1;65(13):5535-43. PubMed PMID: 15994925.
223. Guan H, Zhou Z, Gallick GE, Jia SF, Morales J, Sood AK, et al. Targeting Lyn inhibits tumor growth and metastasis in Ewing's sarcoma. *Molecular cancer therapeutics*. 2008 Jul;7(7):1807-16. PubMed PMID: 18644993. Pubmed Central PMCID: 2556989.
224. Choi YL, Bocanegra M, Kwon MJ, Shin YK, Nam SJ, Yang JH, et al. LYN is a mediator of epithelial-mesenchymal transition and a target of dasatinib in breast cancer. *Cancer research*. 2010 Mar 15;70(6):2296-306. PubMed PMID: 20215510. Pubmed Central PMCID: 2869247. Epub 2010/03/11. eng.
225. Kantarjian H, le Coutre P, Cortes J, Pinilla-Ibarz J, Nagler A, Hochhaus A, et al. Phase 1 study of INNO-406, a dual Abl/Lyn kinase inhibitor, in Philadelphia chromosome-positive leukemias after imatinib

resistance or intolerance. *Cancer*. 2010 Jun 1;116(11):2665-72. PubMed PMID: 20310049. Pubmed Central PMCID: 2876208.

226. Peinado H, Olmeda D, Cano A. Snail, Zeb and bHLH factors in tumour progression: an alliance against the epithelial phenotype? *Nature reviews Cancer*. 2007 Jun;7(6):415-28. PubMed PMID: 17508028.

227. Yu YP, Landsittel D, Jing L, Nelson J, Ren B, Liu L, et al. Gene expression alterations in prostate cancer predicting tumor aggression and preceding development of malignancy. *Journal of clinical oncology : official journal of the American Society of Clinical Oncology*. 2004 Jul 15;22(14):2790-9. PubMed PMID: 15254046.

228. Holzbeierlein J, Lal P, LaTulippe E, Smith A, Satagopan J, Zhang L, et al. Gene expression analysis of human prostate carcinoma during hormonal therapy identifies androgen-responsive genes and mechanisms of therapy resistance. *The American journal of pathology*. 2004 Jan;164(1):217-27. PubMed PMID: 14695335. Pubmed Central PMCID: 1602218.

229. Taylor BS, Schultz N, Hieronymus H, Gopalan A, Xiao Y, Carver BS, et al. Integrative genomic profiling of human prostate cancer. *Cancer cell*. 2010 Jul 13;18(1):11-22. PubMed PMID: 20579941. Pubmed Central PMCID: 3198787.

230. Tomlins SA, Mehra R, Rhodes DR, Cao X, Wang L, Dhanasekaran SM, et al. Integrative molecular concept modeling of prostate cancer progression. *Nature genetics*. 2007 Jan;39(1):41-51. PubMed PMID: 17173048.

231. Grasso CS, Wu YM, Robinson DR, Cao X, Dhanasekaran SM, Khan AP, et al. The mutational landscape of lethal castration-resistant prostate cancer. *Nature*. 2012 Jul 12;487(7406):239-43. PubMed PMID: 22722839. Pubmed Central PMCID: 3396711.

232. Hatzis C, Pusztai L, Valero V, Booser DJ, Esserman L, Lluch A, et al. A genomic predictor of response and survival following taxane-anthracycline chemotherapy for invasive breast cancer. *Jama*. 2011 May 11;305(18):1873-81. PubMed PMID: 21558518.

233. Kao KJ, Chang KM, Hsu HC, Huang AT. Correlation of microarray-based breast cancer molecular subtypes and clinical outcomes: implications for treatment optimization. *BMC cancer*. 2011;11:143. PubMed PMID: 21501481. Pubmed Central PMCID: 3094326.

234. Minn AJ, Siegel PM, Bos PD, Shu W, Giri DD, Viale A, Olshen AB, Gerald WL, Massagué J. Genes that mediate breast cancer metastasis to lung. *Nature*. 2011;436(July):518-24.

235. Bos PD, Nadal C, Shu W, Gomis RR, Nguyen DX, Minn AJ, van de Vijver MJ, Gerald WL, Foekens JA, Massague J. Genes that mediate breast cancer metastasis to the brain. *Nature*. 2009;459:1005-9.

236. Modlich O, Prisack HB, Pitschke G, Ramp U, Ackermann R, Bojar H, et al. Identifying superficial, muscle-invasive, and metastasizing transitional cell carcinoma of the bladder: use of cDNA array analysis of gene expression profiles. *Clinical cancer research : an official journal of the American Association for Cancer Research*. 2004 May 15;10(10):3410-21. PubMed PMID: 15161696.

237. Stransky N, Vallot C, Rey F, Bernard-Pierrot I, de Medina SG, Segraves R, et al. Regional copy number-independent deregulation of transcription in cancer. *Nature genetics*. 2006 Dec;38(12):1386-96. PubMed PMID: 17099711.

238. Dyrskjot L, Kruhoffer M, Thykjaer T, Marcussen N, Jensen JL, Moller K, et al. Gene expression in the urinary bladder: a common carcinoma in situ gene expression signature exists disregarding histopathological classification. *Cancer research*. 2004 Jun 1;64(11):4040-8. PubMed PMID: 15173019.

239. Sanchez-Carbajo M, Socci ND, Lozano J, Saint F, Cordon-Cardo C. Defining molecular profiles of poor outcome in patients with invasive bladder cancer using oligonucleotide microarrays. *Journal of clinical oncology : official journal of the American Society of Clinical Oncology*. 2006 Feb 10;24(5):778-89. PubMed PMID: 16432078.

240. Blaveri E, Simko JP, Korkola JE, Brewer JL, Baehner F, Mehta K, et al. Bladder cancer outcome and subtype classification by gene expression. *Clinical cancer research : an official journal of the American Association for Cancer Research*. 2005 Jun 1;11(11):4044-55. PubMed PMID: 15930339.
241. Pecina-Slaus N. Tumor suppressor gene E-cadherin and its role in normal and malignant cells. *Cancer cell international*. 2003 Oct 14;3(1):17. PubMed PMID: 14613514. Pubmed Central PMCID: 270068.
242. Kasahara K, Nakayama Y, Ikeda K, Fukushima Y, Matsuda D, Horimoto S, et al. Trafficking of Lyn through the Golgi caveolin involves the charged residues on alphaE and alphaI helices in the kinase domain. *The Journal of cell biology*. 2004 Jun 7;165(5):641-52. PubMed PMID: 15173188. Pubmed Central PMCID: 2172378.
243. Yokota A, Kimura S, Masuda S, Ashihara E, Kuroda J, Sato K, et al. INNO-406, a novel BCR-ABL/Lyn dual tyrosine kinase inhibitor, suppresses the growth of Ph+ leukemia cells in the central nervous system, and cyclosporine A augments its in vivo activity. *Blood*. 2007 Jan 1;109(1):306-14. PubMed PMID: 16954504.
244. Hibbs ML, Stanley E, Maglitto R, Dunn AR. Identification of a duplication of the mouse Lyn gene. *Gene*. 1995 Apr 24;156(2):175-81. PubMed PMID: 7758954.
245. Cancer Genome Atlas N. Comprehensive molecular portraits of human breast tumours. *Nature*. 2012 Oct 4;490(7418):61-70. PubMed PMID: 23000897. Pubmed Central PMCID: 3465532.
246. Shih JY, Yang PC. The EMT regulator slug and lung carcinogenesis. *Carcinogenesis*. 2011 Sep;32(9):1299-304. PubMed PMID: 21665887.
247. Zhou BP, Deng J, Xia W, Xu J, Li YM, Gunduz M, et al. Dual regulation of Snail by GSK-3beta-mediated phosphorylation in control of epithelial-mesenchymal transition. *Nature cell biology*. 2004 Oct;6(10):931-40. PubMed PMID: 15448698.
248. De Mesquita DD, Zhan Q, Crossley L, Badwey JA. p90-RSK and Akt may promote rapid phosphorylation/inactivation of glycogen synthase kinase 3 in chemoattractant-stimulated neutrophils. *FEBS letters*. 2001 Aug 3;502(3):84-8. PubMed PMID: 11583116.
249. Stambolic V, Woodgett JR. Mitogen inactivation of glycogen synthase kinase-3 beta in intact cells via serine 9 phosphorylation. *The Biochemical journal*. 1994 Nov 1;303 (Pt 3):701-4. PubMed PMID: 7980435. Pubmed Central PMCID: 1137602.
250. Brown JL, Stowers L, Baer M, Trejo J, Coughlin S, Chant J. Human Ste20 homologue hPAK1 links GTPases to the JNK MAP kinase pathway. *Current biology : CB*. 1996 May 1;6(5):598-605. PubMed PMID: 8805275.
251. Stebbins CC, Watzl C, Billadeau DD, Leibson PJ, Burshtyn DN, Long EO. VAV1 dephosphorylation by the tyrosine phosphatase SHP-1 as a mechanism for inhibition of cellular cytotoxicity. *Molecular and cellular biology*. 2003 Sep;23(17):6291-9. PubMed PMID: 12917349. Pubmed Central PMCID: 180957.
252. Teng Y, Xie X, Walker S, White DT, Mumm JS, Cowell JK. Evaluating human cancer cell metastasis in zebrafish. *BMC cancer*. 2013;13:453. PubMed PMID: 24089705. Pubmed Central PMCID: 3852235.
253. Weigelt B, Peterse JL, van 't Veer LJ. Breast cancer metastasis: markers and models. *Nature reviews Cancer*. 2005 Aug;5(8):591-602. PubMed PMID: 16056258. Epub 2005/08/02. eng.
254. Hochgrafe F, Zhang L, O'Toole SA, Browne BC, Pinese M, Porta Cubas A, et al. Tyrosine phosphorylation profiling reveals the signaling network characteristics of Basal breast cancer cells. *Cancer research*. 2010 Nov 15;70(22):9391-401. PubMed PMID: 20861192.
255. Gelman IH, Peresie J, Eng KH, Foster BA. Differential requirement for Src family tyrosine kinases in the initiation, progression, and metastasis of prostate cancer. *Molecular cancer research : MCR*. 2014 Oct;12(10):1470-9. PubMed PMID: 25053806. Pubmed Central PMCID: 4201973.
256. Tabaries S, Annis MG, Hsu BE, Tam CE, Savage P, Park M, et al. Lyn modulates Claudin-2 expression and is a therapeutic target for breast cancer liver metastasis. *Oncotarget*. 2015 Apr 20;6(11):9476-87. PubMed PMID: 25823815.

257. Ren X, Cao C, Zhu L, Yoshida K, Kharbanda S, Weichselbaum R, et al. Lyn tyrosine kinase inhibits nuclear export of the p53 tumor suppressor. *Cancer biology & therapy*. 2002 Nov-Dec;1(6):703-8. PubMed PMID: 12642697. Epub 2003/03/19. eng.
258. Wu ZQ, Li XY, Hu CY, Ford M, Kleer CG, Weiss SJ. Canonical Wnt signaling regulates Slug activity and links epithelial-mesenchymal transition with epigenetic Breast Cancer 1, Early Onset (BRCA1) repression. *Proceedings of the National Academy of Sciences of the United States of America*. 2012 Oct 9;109(41):16654-9. PubMed PMID: 23011797. Pubmed Central PMCID: 3478591.
259. Kim JY, Kim YM, Yang CH, Cho SK, Lee JW, Cho M. Functional regulation of Slug/Snail2 is dependent on GSK-3beta-mediated phosphorylation. *The FEBS journal*. 2012 Aug;279(16):2929-39. PubMed PMID: 22727060.
260. Vinas-Castells R, Beltran M, Valls G, Gomez I, Garcia JM, Montserrat-Sentis B, et al. The hypoxia-controlled FBXL14 ubiquitin ligase targets SNAIL1 for proteasome degradation. *The Journal of biological chemistry*. 2010 Feb 5;285(6):3794-805. PubMed PMID: 19955572. Pubmed Central PMCID: 2823521. Epub 2009/12/04. eng.
261. Wang SP, Wang WL, Chang YL, Wu CT, Chao YC, Kao SH, et al. p53 controls cancer cell invasion by inducing the MDM2-mediated degradation of Slug. *Nature cell biology*. 2009 Jun;11(6):694-704. PubMed PMID: 19448627.
262. Bid HK, Roberts RD, Manchanda PK, Houghton PJ. RAC1: an emerging therapeutic option for targeting cancer angiogenesis and metastasis. *Molecular cancer therapeutics*. 2013 Oct;12(10):1925-34. PubMed PMID: 24072884. Pubmed Central PMCID: 3823055.
263. Eswaran J, Li DQ, Shah A, Kumar R. Molecular pathways: targeting p21-activated kinase 1 signaling in cancer--opportunities, challenges, and limitations. *Clinical cancer research : an official journal of the American Association for Cancer Research*. 2012 Jul 15;18(14):3743-9. PubMed PMID: 22595609. Pubmed Central PMCID: 3399091.
264. Kumar R, Gururaj AE, Barnes CJ. p21-activated kinases in cancer. *Nature reviews Cancer*. 2006 Jun;6(6):459-71. PubMed PMID: 16723992.
265. Delaney MK, Liu J, Zheng Y, Berndt MC, Du X. The role of RAC1 in glycoprotein Ib-IX-mediated signal transduction and integrin activation. *Arteriosclerosis, thrombosis, and vascular biology*. 2012 Nov;32(11):2761-8. PubMed PMID: 22995516. Pubmed Central PMCID: 3523182.
266. Rahaman SO, Swat W, Febbraio M, Silverstein RL. VAV family Rho guanine nucleotide exchange factors regulate CD36-mediated macrophage foam cell formation. *The Journal of biological chemistry*. 2011 Mar 4;286(9):7010-7. PubMed PMID: 21209086. Pubmed Central PMCID: 3044957.
267. Yazawa N, Fujimoto M, Sato S, Miyake K, Asano N, Nagai Y, et al. CD19 regulates innate immunity by the toll-like receptor RP105 signaling in B lymphocytes. *Blood*. 2003 Aug 15;102(4):1374-80. PubMed PMID: 12714520.
268. Sturm RA, Herr W. The POU domain is a bipartite DNA-binding structure. *Nature*. 1988 Dec 8;336(6199):601-4. PubMed PMID: 2904656.
269. Herr W, Cleary MA. The POU domain: versatility in transcriptional regulation by a flexible two-in-one DNA-binding domain. *Genes & development*. 1995 Jul 15;9(14):1679-93. PubMed PMID: 7622033.
270. Cook AL, Sturm RA. POU domain transcription factors: BRN2 as a regulator of melanocytic growth and tumorigenesis. *Pigment cell & melanoma research*. 2008 Dec;21(6):611-26. PubMed PMID: 18983536.
271. Tomilin A, Remenyi A, Lins K, Bak H, Leidel S, Vriend G, et al. Synergism with the coactivator OBF-1 (OCA-B, BOB-1) is mediated by a specific POU dimer configuration. *Cell*. 2000 Dec 8;103(6):853-64. PubMed PMID: 11136971.
272. Alazard R, Bland M, Elbaz S, Vossen C, Icre G, Joseph G, et al. Identification of the 'NORE' (N-Oct-3 responsive element), a novel structural motif and composite element. *Nucleic acids research*. 2005;33(5):1513-23. PubMed PMID: 15767276. Pubmed Central PMCID: 1065252.

273. Lodato MA, Ng CW, Wamstad JA, Cheng AW, Thai KK, Fraenkel E, et al. SOX2 co-occupies distal enhancer elements with distinct POU factors in ESCs and NPCs to specify cell state. *PLoS genetics*. 2013;9(2):e1003288. PubMed PMID: 23437007. Pubmed Central PMCID: 3578749.
274. Urban S, Kobi D, Ennen M, Langer D, Le Gras S, Ye T, et al. A Brn2-Zic1 axis specifies the neuronal fate of retinoic-acid-treated embryonic stem cells. *Journal of cell science*. 2015 Jul 1;128(13):2303-18. PubMed PMID: 25991548.
275. Takahashi K, Yamanaka S. Induction of pluripotent stem cells from mouse embryonic and adult fibroblast cultures by defined factors. *Cell*. 2006 Aug 25;126(4):663-76. PubMed PMID: 16904174.
276. Pang ZP, Yang N, Vierbuchen T, Ostermeier A, Fuentes DR, Yang TQ, et al. Induction of human neuronal cells by defined transcription factors. *Nature*. 2011 May 26;476(7359):220-3. PubMed PMID: 21617644. Pubmed Central PMCID: 3159048.
277. Black JB, Adler AF, Wang HG, D'Ippolito AM, Hutchinson HA, Reddy TE, et al. Targeted Epigenetic Remodeling of Endogenous Loci by CRISPR/Cas9-Based Transcriptional Activators Directly Converts Fibroblasts to Neuronal Cells. *Cell stem cell*. 2016 Sep 1;19(3):406-14. PubMed PMID: 27524438. Pubmed Central PMCID: 5010447.
278. Chanda S, Ang CE, Davila J, Pak C, Mall M, Lee QY, et al. Generation of induced neuronal cells by the single reprogramming factor ASCL1. *Stem cell reports*. 2014 Aug 12;3(2):282-96. PubMed PMID: 25254342. Pubmed Central PMCID: 4176533.
279. Wapinski OL, Vierbuchen T, Qu K, Lee QY, Chanda S, Fuentes DR, et al. Hierarchical mechanisms for direct reprogramming of fibroblasts to neurons. *Cell*. 2013 Oct 24;155(3):621-35. PubMed PMID: 24243019. Pubmed Central PMCID: 3871197.
280. Wapinski OL, Lee QY, Chen AC, Li R, Corces MR, Ang CE, et al. Rapid Chromatin Switch in the Direct Reprogramming of Fibroblasts to Neurons. *Cell reports*. 2017 Sep 26;20(13):3236-47. PubMed PMID: 28954238. Pubmed Central PMCID: 5646379.
281. Treutlein B, Lee QY, Camp JG, Mall M, Koh W, Shariati SA, et al. Dissecting direct reprogramming from fibroblast to neuron using single-cell RNA-seq. *Nature*. 2016 Jun 16;534(7607):391-5. PubMed PMID: 27281220. Pubmed Central PMCID: 4928860.
282. Castro DS, Skowronska-Krawczyk D, Armant O, Donaldson IJ, Parras C, Hunt C, et al. Proneural bHLH and Brn proteins coregulate a neurogenic program through cooperative binding to a conserved DNA motif. *Developmental cell*. 2006 Dec;11(6):831-44. PubMed PMID: 17141158.
283. Rakic P. Evolution of the neocortex: a perspective from developmental biology. *Nature reviews Neuroscience*. 2009 Oct;10(10):724-35. PubMed PMID: 19763105. Pubmed Central PMCID: 2913577.
284. Xue Y, Qian H, Hu J, Zhou B, Zhou Y, Hu X, et al. Sequential regulatory loops as key gatekeepers for neuronal reprogramming in human cells. *Nature neuroscience*. 2016 Jun;19(6):807-15. PubMed PMID: 27110916. Pubmed Central PMCID: 4882254.
285. Ambasadhan R, Talantova M, Coleman R, Yuan X, Zhu S, Lipton SA, et al. Direct reprogramming of adult human fibroblasts to functional neurons under defined conditions. *Cell stem cell*. 2011 Aug 5;9(2):113-8. PubMed PMID: 21802386. Pubmed Central PMCID: 4567246.
286. Goodall J, Carreira S, Denat L, Kobi D, Davidson I, Nuciforo P, et al. Brn-2 represses microphthalmia-associated transcription factor expression and marks a distinct subpopulation of microphthalmia-associated transcription factor-negative melanoma cells. *Cancer research*. 2008 Oct 1;68(19):7788-94. PubMed PMID: 18829533.
287. Eccles MR, He S, Ahn A, Slobbe LJ, Jeffs AR, Yoon HS, et al. MITF and PAX3 Play Distinct Roles in Melanoma Cell Migration; Outline of a "Genetic Switch" Theory Involving MITF and PAX3 in Proliferative and Invasive Phenotypes of Melanoma. *Frontiers in oncology*. 2013 Sep 11;3:229. PubMed PMID: 24062982. Pubmed Central PMCID: 3769631.

288. Zhao J, He H, Zhou K, Ren Y, Shi Z, Wu Z, et al. Neuronal transcription factors induce conversion of human glioma cells to neurons and inhibit tumorigenesis. *PloS one*. 2012;7(7):e41506. PubMed PMID: 22859994. Pubmed Central PMCID: 3409237.
289. Suva ML, Rheinbay E, Gillespie SM, Patel AP, Wakimoto H, Rabkin SD, et al. Reconstructing and reprogramming the tumor-propagating potential of glioblastoma stem-like cells. *Cell*. 2014 Apr 24;157(3):580-94. PubMed PMID: 24726434. Pubmed Central PMCID: 4004670.
290. Thurber AE, Douglas G, Sturm EC, Zabierowski SE, Smit DJ, Ramakrishnan SN, et al. Inverse expression states of the BRN2 and MITF transcription factors in melanoma spheres and tumour xenografts regulate the NOTCH pathway. *Oncogene*. 2011 Jul 7;30(27):3036-48. PubMed PMID: 21358674. Pubmed Central PMCID: 3591523.
291. Fane ME, Chhabra Y, Hollingsworth DEJ, Simmons JL, Spoerri L, Oh TG, et al. NFIB Mediates BRN2 Driven Melanoma Cell Migration and Invasion Through Regulation of EZH2 and MITF. *EBioMedicine*. 2017 Feb;16:63-75. PubMed PMID: 28119061. Pubmed Central PMCID: 5474438.
292. Simmons JL, Pierce CJ, Al-Ejeh F, Boyle GM. MITF and BRN2 contribute to metastatic growth after dissemination of melanoma. *Scientific reports*. 2017 Sep 7;7(1):10909. PubMed PMID: 28883623. Pubmed Central PMCID: 5589904.
293. Roesch A, Fukunaga-Kalabis M, Schmidt EC, Zabierowski SE, Brafford PA, Vultur A, et al. A temporarily distinct subpopulation of slow-cycling melanoma cells is required for continuous tumor growth. *Cell*. 2010 May 14;141(4):583-94. PubMed PMID: 20478252. Pubmed Central PMCID: 2882693.
294. Sakaeda M, Sato H, Ishii J, Miyata C, Kamma H, Shishido-Hara Y, et al. Neural lineage-specific homeoprotein BRN2 is directly involved in TTF1 expression in small-cell lung cancer. *Laboratory investigation; a journal of technical methods and pathology*. 2013 Apr;93(4):408-21. PubMed PMID: 23358112.
295. Ishii J, Sato H, Sakaeda M, Shishido-Hara Y, Hiramatsu C, Kamma H, et al. POU domain transcription factor BRN2 is crucial for expression of ASCL1, ND1 and neuroendocrine marker molecules and cell growth in small cell lung cancer. *Pathology international*. 2013 Mar;63(3):158-68. PubMed PMID: 23530560.
296. Brohl AS, Solomon DA, Chang W, Wang J, Song Y, Sindiri S, et al. The genomic landscape of the Ewing Sarcoma family of tumors reveals recurrent STAG2 mutation. *PLoS genetics*. 2014 Jul;10(7):e1004475. PubMed PMID: 25010205. Pubmed Central PMCID: 4091782.
297. Ferraldeschi R, Welte J, Luo J, Attard G, de Bono JS. Targeting the androgen receptor pathway in castration-resistant prostate cancer: progresses and prospects. *Oncogene*. 2015 Apr 2;34(14):1745-57. PubMed PMID: 24837363. Pubmed Central PMCID: 4333106. Epub 2014/05/20. eng.
298. Beltran H, Tomlins S, Aparicio A, Arora V, Rickman D, Ayala G, et al. Aggressive variants of castration-resistant prostate cancer. *Clinical cancer research : an official journal of the American Association for Cancer Research*. 2014 Jun 1;20(11):2846-50. PubMed PMID: 24727321. Pubmed Central PMCID: 4040316. Epub 2014/04/15. eng.
299. Epstein JI, Amin MB, Beltran H, Lotan TL, Mosquera JM, Reuter VE, et al. Proposed morphologic classification of prostate cancer with neuroendocrine differentiation. *The American journal of surgical pathology*. 2014 Jun;38(6):756-67. PubMed PMID: 24705311. Pubmed Central PMCID: 4112087. Epub 2014/04/08. eng.
300. Aparicio A, Logothetis CJ, Maity SN. Understanding the lethal variant of prostate cancer: power of examining extremes. *Cancer discovery*. 2011 Nov;1(6):466-8. PubMed PMID: 22586648. Pubmed Central PMCID: 4133693. Epub 2012/05/16. eng.
301. Alanee S, Moore A, Nutt M, Holland B, Dynda D, El-Zawahry A, et al. Contemporary Incidence and Mortality Rates of Neuroendocrine Prostate Cancer. *Anticancer research*. 2015 Jul;35(7):4145-50. PubMed PMID: 26124369. Epub 2015/07/01. eng.

302. Tan HL, Sood A, Rahimi HA, Wang W, Gupta N, Hicks J, et al. Rb loss is characteristic of prostatic small cell neuroendocrine carcinoma. *Clinical cancer research : an official journal of the American Association for Cancer Research*. 2014 Feb 15;20(4):890-903. PubMed PMID: 24323898. Pubmed Central PMCID: 3931005. Epub 2013/12/11. eng.
303. Tzelepi V, Zhang J, Lu JF, Kleb B, Wu G, Wan X, et al. Modeling a lethal prostate cancer variant with small-cell carcinoma features. *Clinical cancer research : an official journal of the American Association for Cancer Research*. 2012 Feb 1;18(3):666-77. PubMed PMID: 22156612. Pubmed Central PMCID: 3923417. Epub 2011/12/14. eng.
304. Chen H, Sun Y, Wu C, Magyar CE, Li X, Cheng L, et al. Pathogenesis of prostatic small cell carcinoma involves the inactivation of the P53 pathway. *Endocrine-related cancer*. 2012 Jun;19(3):321-31. PubMed PMID: 22389383. Pubmed Central PMCID: 3433057. Epub 2012/03/06. eng.
305. Lapuk AV, Wu C, Wyatt AW, McPherson A, McConeghy BJ, Brahmbhatt S, et al. From sequence to molecular pathology, and a mechanism driving the neuroendocrine phenotype in prostate cancer. *The Journal of pathology*. 2012 Jul;227(3):286-97. PubMed PMID: 22553170. Pubmed Central PMCID: 3659819. Epub 2012/05/04. eng.
306. Zhang X, Coleman IM, Brown LG, True LD, Kollath L, Lucas JM, et al. SRRM4 expression and the loss of REST activity may promote the emergence of the neuroendocrine phenotype in Castration-Resistant Prostate Cancer. *Clinical cancer research : an official journal of the American Association for Cancer Research*. 2015 Oct 15;21(20):4698-708. Epub 2015 Jun 12.
307. Svensson C, Ceder J, Iglesias-Gato D, Chuan YC, Pang ST, Bjartell A, et al. REST mediates androgen receptor actions on gene repression and predicts early recurrence of prostate cancer. *Nucleic acids research*. 2014 Jan;42(2):999-1015. PubMed PMID: 24163104. Pubmed Central PMCID: 3902919.
308. Wee ZN, Li Z, Lee PL, Lee ST, Lim YP, Yu Q. EZH2-mediated inactivation of IFN-gamma-JAK-STAT1 signaling is an effective therapeutic target in MYC-driven prostate cancer. *Cell reports*. 2014 Jul 10;8(1):204-16. PubMed PMID: 24953652. Epub 2014/06/24. eng.
309. Li Y, Donmez N, Sahinalp C, Xie N, Wang Y, Xue H, et al. SRRM4 Drives Neuroendocrine Transdifferentiation of Prostate Adenocarcinoma Under Androgen Receptor Pathway Inhibition. *European urology*. 2016 May 11. PubMed PMID: 27180064. Epub 2016/05/18. Eng.
310. Abrahamsson PA. Neuroendocrine differentiation and hormone-refractory prostate cancer. *The Prostate Supplement*. 1996;6:3-8. PubMed PMID: 8630226. Epub 1996/01/01. eng.
311. Burchardt T, Burchardt M, Chen MW, Cao Y, de la Taille A, Shabsigh A, et al. Transdifferentiation of prostate cancer cells to a neuroendocrine cell phenotype in vitro and in vivo. *The Journal of urology*. 1999 Nov;162(5):1800-5. PubMed PMID: 10524938. Epub 1999/10/19. eng.
312. Kani K, Malihi PD, Jiang Y, Wang H, Wang Y, Ruderman DL, et al. Anterior gradient 2 (AGR2): blood-based biomarker elevated in metastatic prostate cancer associated with the neuroendocrine phenotype. *The Prostate*. 2013 Feb 15;73(3):306-15. PubMed PMID: 22911164. Epub 2012/08/23. eng.
313. Rapa I, Volante M, Migliore C, Farsetti A, Berruti A, Vittorio Scagliotti G, et al. Human ASH-1 promotes neuroendocrine differentiation in androgen deprivation conditions and interferes with androgen responsiveness in prostate cancer cells. *The Prostate*. 2013 Aug;73(11):1241-9. PubMed PMID: 23657976.
314. Zhang X, Coleman I, Brown LG, True LD, Kollath L, Lucas JM, et al. SRRM4 Expression and the Loss of REST Activity May Promote the Emergence of the Neuroendocrine Phenotype in Castration-Resistant Prostate Cancer. *Clinical cancer research : an official journal of the American Association for Cancer Research*. 2015 Jun 12. PubMed PMID: 26071481. Epub 2015/06/14. Eng.
315. Arora VK, Schenkein E, Murali R, Subudhi SK, Wongvipat J, Balbas MD, et al. Glucocorticoid receptor confers resistance to antiandrogens by bypassing androgen receptor blockade. *Cell*. 2013 Dec 5;155(6):1309-22. PubMed PMID: 24315100. Pubmed Central PMCID: 3932525. Epub 2013/12/10. eng.

316. Balbas MD, Evans MJ, Hosfield DJ, Wongvipat J, Arora VK, Watson PA, et al. Overcoming mutation-based resistance to antiandrogens with rational drug design. *eLife*. 2013;2:e00499. PubMed PMID: 23580326. Pubmed Central PMCID: 3622181. Epub 2013/04/13. eng.
317. Joseph JD, Lu N, Qian J, Sensintaffar J, Shao G, Brigham D, et al. A clinically relevant androgen receptor mutation confers resistance to second-generation antiandrogens enzalutamide and ARN-509. *Cancer discovery*. 2013 Sep;3(9):1020-9. PubMed PMID: 23779130. Epub 2013/06/20. eng.
318. Hubbard GK, Mutton LN, Khalili M, McMullin RP, Hicks JL, Bianchi-Frias D, et al. Combined MYC Activation and Pten Loss Are Sufficient to Create Genomic Instability and Lethal Metastatic Prostate Cancer. *Cancer research*. 2016 Jan 15;76(2):283-92. PubMed PMID: 26554830. Epub 2015/11/12. eng.
319. Shappell SB, Thomas GV, Roberts RL, Herbert R, Ittmann MM, Rubin MA, et al. Prostate pathology of genetically engineered mice: definitions and classification. The consensus report from the Bar Harbor meeting of the Mouse Models of Human Cancer Consortium Prostate Pathology Committee. *Cancer research*. 2004 Mar 15;64(6):2270-305. PubMed PMID: 15026373. Epub 2004/03/18. eng.
320. Dominguez MH, Ayoub AE, Rakic P. POU-III transcription factors (Brn1, Brn2, and Oct6) influence neurogenesis, molecular identity, and migratory destination of upper-layer cells of the cerebral cortex. *Cereb Cortex*. 2013 Nov;23(11):2632-43. PubMed PMID: 22892427. Pubmed Central PMCID: 3792741. Epub 2012/08/16. eng.
321. Small EJ, J. Huang, J. Youngren, A. Sokolov, R. Raj Aggarwal, G. Thomas, L. D. True, L. Zhang, A. Foye, J. J. Alumkal, C. J. Ryan, M. Rettig, C. P. Evans, M.E. Gleave, R. Baertsch, J. Stuart, R.E. Reiter, P. Lara, K.N. Chi, T.M. Beer. Characterization of neuroendocrine prostate cancer (NEPC) in patients with metastatic castration resistant prostate cancer (mCRPC) resistant to abiraterone (Abi) or enzalutamide (Enz): Preliminary results from the SU2C/PCF/AACR West Coast Prostate Cancer Dream Team (WCDT). ASCO Annual Meeting; Chicago, IL: J Clin Oncol; 2015.
322. Tarhini AA, Edington H, Butterfield LH, Lin Y, Shuai Y, Tawbi H, et al. Immune monitoring of the circulation and the tumor microenvironment in patients with regionally advanced melanoma receiving neoadjuvant ipilimumab. *PloS one*. 2014;9(2):e87705. PubMed PMID: 24498358. Pubmed Central PMCID: 3912016. Epub 2014/02/06. eng.
323. Barton BE, Murphy TF, Shu P, Huang HF, Meyenhofer M, Barton A. Novel single-stranded oligonucleotides that inhibit signal transducer and activator of transcription 3 induce apoptosis in vitro and in vivo in prostate cancer cell lines. *Molecular cancer therapeutics*. 2004 Oct;3(10):1183-91. PubMed PMID: 15486184. Epub 2004/10/16. eng.
324. Yu X, Cates JM, Morrissey C, You C, Grabowska MM, Zhang J, et al. SOX2 expression in the developing, adult, as well as, diseased prostate. *Prostate cancer and prostatic diseases*. 2014 Dec;17(4):301-9. PubMed PMID: 25091041. Pubmed Central PMCID: 4227931. Epub 2014/08/06. eng.
325. Dailey L, Basilico C. Coevolution of HMG domains and homeodomains and the generation of transcriptional regulation by Sox/POU complexes. *Journal of cellular physiology*. 2001 Mar;186(3):315-28. PubMed PMID: 11169970. Epub 2001/02/15. eng.
326. Kregel S, Kiriluk KJ, Rosen AM, Cai Y, Reyes EE, Otto KB, et al. Sox2 is an androgen receptor-repressed gene that promotes castration-resistant prostate cancer. *PloS one*. 2013;8(1):e53701. PubMed PMID: 23326489. Pubmed Central PMCID: 3543364. Epub 2013/01/18. eng.
327. Iwafuchi-Doi M, Yoshida Y, Onichtchouk D, Leichsenring M, Driever W, Takemoto T, et al. The Pou5f1/Pou3f-dependent but SoxB-independent regulation of conserved enhancer N2 initiates Sox2 expression during epiblast to neural plate stages in vertebrates. *Developmental biology*. 2011 Apr 15;352(2):354-66. PubMed PMID: 21185279. Epub 2010/12/28. eng.
328. Endo T, Yazawa T, Shishido-Hara Y, Fujiwara M, Shimoyamada H, Ishii J, et al. Expression of developing neural transcription factors in lung carcinoid tumors. *Pathology international*. 2014 Aug;64(8):365-74. PubMed PMID: 25143124. Epub 2014/08/22. eng.

329. Berlin I, Denat L, Steunou AL, Puig I, Champeval D, Colombo S, et al. Phosphorylation of BRN2 modulates its interaction with the Pax3 promoter to control melanocyte migration and proliferation. *Molecular and cellular biology*. 2012 Apr;32(7):1237-47. PubMed PMID: 22290434. Pubmed Central PMCID: 3302439. Epub 2012/02/01. eng.
330. Boyle GM, Woods SL, Bonazzi VF, Stark MS, Hacker E, Aoude LG, et al. Melanoma cell invasiveness is regulated by miR-211 suppression of the BRN2 transcription factor. *Pigment cell & melanoma research*. 2011 Jun;24(3):525-37. PubMed PMID: 21435193. Epub 2011/03/26. eng.
331. Pinner S, Jordan P, Sharrock K, Bazley L, Collinson L, Marais R, et al. Intravital imaging reveals transient changes in pigment production and Brn2 expression during metastatic melanoma dissemination. *Cancer research*. 2009 Oct 15;69(20):7969-77. PubMed PMID: 19826052. Pubmed Central PMCID: 2763120. Epub 2009/10/15. eng.
332. Bae KM, Su Z, Frye C, McClellan S, Allan RW, Andrejewski JT, et al. Expression of pluripotent stem cell reprogramming factors by prostate tumor initiating cells. *The Journal of urology*. 2010 May;183(5):2045-53. PubMed PMID: 20303530. Epub 2010/03/23. eng.
333. Jia X, Li X, Xu Y, Zhang S, Mou W, Liu Y, et al. SOX2 promotes tumorigenesis and increases the anti-apoptotic property of human prostate cancer cell. *Journal of molecular cell biology*. 2011 Aug;3(4):230-8. PubMed PMID: 21415100. Epub 2011/03/19. eng.
334. Lin F, Lin P, Zhao D, Chen Y, Xiao L, Qin W, et al. Sox2 targets cyclinE, p27 and survivin to regulate androgen-independent human prostate cancer cell proliferation and apoptosis. *Cell proliferation*. 2012 Jun;45(3):207-16. PubMed PMID: 22469032. Epub 2012/04/04. eng.
335. Graham V, Khudyakov J, Ellis P, Pevny L. SOX2 functions to maintain neural progenitor identity. *Neuron*. 2003 Aug 28;39(5):749-65. PubMed PMID: 12948443. Epub 2003/09/02. eng.
336. Catena R, Tiveron C, Ronchi A, Porta S, Ferri A, Tatangelo L, et al. Conserved POU binding DNA sites in the Sox2 upstream enhancer regulate gene expression in embryonic and neural stem cells. *The Journal of biological chemistry*. 2004 Oct 1;279(40):41846-57. PubMed PMID: 15262984. Epub 2004/07/21. eng.
337. Ugolkov AV, Eisengart LJ, Luan C, Yang XJ. Expression analysis of putative stem cell markers in human benign and malignant prostate. *The Prostate*. 2011 Jan 1;71(1):18-25. PubMed PMID: 20583131. Epub 2010/06/29. eng.
338. Sholl LM, Long KB, Hornick JL. Sox2 expression in pulmonary non-small cell and neuroendocrine carcinomas. *Applied immunohistochemistry & molecular morphology : AIMM / official publication of the Society for Applied Immunohistochemistry*. 2010 Jan;18(1):55-61. PubMed PMID: 19661786. Epub 2009/08/08. eng.
339. Morise M, Hishida T, Takahashi A, Yoshida J, Ohe Y, Nagai K, et al. Clinicopathological significance of cancer stem-like cell markers in high-grade neuroendocrine carcinoma of the lung. *Journal of cancer research and clinical oncology*. 2015 May 12. PubMed PMID: 25963795. Epub 2015/05/13. Eng.
340. Laga AC, Lai CY, Zhan Q, Huang SJ, Velazquez EF, Yang Q, et al. Expression of the embryonic stem cell transcription factor SOX2 in human skin: relevance to melanocyte and merkel cell biology. *The American journal of pathology*. 2010 Feb;176(2):903-13. PubMed PMID: 20042675. Pubmed Central PMCID: 2808095. Epub 2010/01/01. eng.
341. Larischa de Wet AW, Marc Gillard, Steve Kregel, Tzintzuni Garcia, Erin McAuley, Ryan Brown, Donald Vander Griend. . The role of SOX2 in promoting resistance to AR-targeted therapies in prostate cancer. *Cancer research*. 2018;78(13).
342. Shimozaki K. Sox2 transcription network acts as a molecular switch to regulate properties of neural stem cells. *World journal of stem cells*. 2014 Sep 26;6(4):485-90. PubMed PMID: 25258670. Pubmed Central PMCID: 4172677.

343. Cox JL, Mallanna SK, Luo X, Rizzino A. Sox2 uses multiple domains to associate with proteins present in Sox2-protein complexes. *PloS one*. 2010 Nov 12;5(11):e15486. PubMed PMID: 21103394. Pubmed Central PMCID: 2980493.
344. Eric Jay Small JH, Jack Youngren, Artem Sokolov, Rahul Raj Aggarwal, George Thomas, Lawrence D. True, Li Zhang, Adam Foye, Joshi J. Alumkal, Charles J. Ryan, Matthew Rettig, Christopher P. Evans, Martin Edwin Gleave, Robert Baertsch, Josh Stuart, Robert Evan Reiter, Primo Lara, Kim N. Chi, Tomasz M. Beer. Characterization of neuroendocrine prostate cancer (NEPC) in patients with metastatic castration resistant prostate cancer (mCRPC) resistant to abiraterone (Abi) or enzalutamide (Enz): Preliminary results from the SU2C/PCF/AACR West Coast Prostate Cancer Dream Team (WCDT). *J Clin Oncol*. 2015;33.
345. Robinson D, Van Allen EM, Wu YM, Schultz N, Lonigro RJ, Mosquera JM, et al. Integrative clinical genomics of advanced prostate cancer. *Cell*. 2015 May 21;161(5):1215-28. PubMed PMID: 26000489. Pubmed Central PMCID: 4484602.
346. Darnell JE, Jr. Transcription factors as targets for cancer therapy. *Nature reviews Cancer*. 2002 Oct;2(10):740-9. PubMed PMID: 12360277.
347. Yeh JE, Toniolo PA, Frank DA. Targeting transcription factors: promising new strategies for cancer therapy. *Current opinion in oncology*. 2013 Nov;25(6):652-8. PubMed PMID: 24048019.
348. Bordoli L, Kiefer F, Arnold K, Benkert P, Battey J, Schwede T. Protein structure homology modeling using SWISS-MODEL workspace. *Nature protocols*. 2009;4(1):1-13. PubMed PMID: 19131951.
349. Wang J, Wolf RM, Caldwell JW, Kollman PA, Case DA. Development and testing of a general amber force field. *Journal of computational chemistry*. 2004 Jul 15;25(9):1157-74. PubMed PMID: 15116359.
350. do Vale Coelho IE, Arruda DC, Taranto AG. In silico studies of the interaction between BRN2 protein and MORE DNA. *Journal of molecular modeling*. 2016 Sep;22(9):228. PubMed PMID: 27568376.
351. Sterling T, Irwin JJ. ZINC 15--Ligand Discovery for Everyone. *Journal of chemical information and modeling*. 2015 Nov 23;55(11):2324-37. PubMed PMID: 26479676. Pubmed Central PMCID: 4658288.
352. Friesner RA, Banks JL, Murphy RB, Halgren TA, Klicic JJ, Mainz DT, et al. Glide: a new approach for rapid, accurate docking and scoring. 1. Method and assessment of docking accuracy. *Journal of medicinal chemistry*. 2004 Mar 25;47(7):1739-49. PubMed PMID: 15027865.
353. Miteva MA, Lee WH, Montes MO, Villoutreix BO. Fast structure-based virtual ligand screening combining FRED, DOCK, and Surflex. *Journal of medicinal chemistry*. 2005 Sep 22;48(19):6012-22. PubMed PMID: 16162004.
354. Klock HE, Lesley SA. The Polymerase Incomplete Primer Extension (PIPE) method applied to high-throughput cloning and site-directed mutagenesis. *Methods in molecular biology*. 2009;498:91-103. PubMed PMID: 18988020.
355. Rubin SM. Deciphering the retinoblastoma protein phosphorylation code. *Trends in biochemical sciences*. 2013 Jan;38(1):12-9. PubMed PMID: 23218751. Pubmed Central PMCID: 3529988.
356. Bertoli C, Skotheim JM, de Bruin RA. Control of cell cycle transcription during G1 and S phases. *Nature reviews Molecular cell biology*. 2013 Aug;14(8):518-28. PubMed PMID: 23877564. Pubmed Central PMCID: 4569015.
357. Xu J, Lamouille S, Derynck R. TGF-beta-induced epithelial to mesenchymal transition. *Cell research*. 2009 Feb;19(2):156-72. PubMed PMID: 19153598. Pubmed Central PMCID: 4720263.
358. Hou P, Li Y, Zhang X, Liu C, Guan J, Li H, et al. Pluripotent stem cells induced from mouse somatic cells by small-molecule compounds. *Science*. 2013 Aug 9;341(6146):651-4. PubMed PMID: 23868920.
359. Cheng L, Hu W, Qiu B, Zhao J, Yu Y, Guan W, et al. Generation of neural progenitor cells by chemical cocktails and hypoxia. *Cell research*. 2014 Jun;24(6):665-79. PubMed PMID: 24638034. Pubmed Central PMCID: 4042166.

360. Zhang M, Lin YH, Sun YJ, Zhu S, Zheng J, Liu K, et al. Pharmacological Reprogramming of Fibroblasts into Neural Stem Cells by Signaling-Directed Transcriptional Activation. *Cell stem cell*. 2016 May 5;18(5):653-67. PubMed PMID: 27133794. Pubmed Central PMCID: 4864020.
361. Yeh AC, Ramaswamy S. Mechanisms of Cancer Cell Dormancy--Another Hallmark of Cancer? *Cancer research*. 2015 Dec 1;75(23):5014-22. PubMed PMID: 26354021. Pubmed Central PMCID: 4668214.
362. Kleffell S, Schatton T. Tumor dormancy and cancer stem cells: two sides of the same coin? *Advances in experimental medicine and biology*. 2013;734:145-79. PubMed PMID: 23143979.
363. Fabian A, Vereb G, Szollosi J. The hitchhikers guide to cancer stem cell theory: markers, pathways and therapy. *Cytometry Part A : the journal of the International Society for Analytical Cytology*. 2013 Jan;83(1):62-71. PubMed PMID: 22997049.
364. Batlle E, Clevers H. Cancer stem cells revisited. *Nature medicine*. 2017 Oct 6;23(10):1124-34. PubMed PMID: 28985214.
365. Crea F, Nur Saidy NR, Collins CC, Wang Y. The epigenetic/noncoding origin of tumor dormancy. *Trends in molecular medicine*. 2015 Apr;21(4):206-11. PubMed PMID: 25771096.
366. Ruppender NS, Morrissey C, Lange PH, Vessella RL. Dormancy in solid tumors: implications for prostate cancer. *Cancer metastasis reviews*. 2013 Dec;32(3-4):501-9. PubMed PMID: 23612741. Pubmed Central PMCID: 3796576.
367. Ye X, Weinberg RA. Epithelial-Mesenchymal Plasticity: A Central Regulator of Cancer Progression. *Trends in cell biology*. 2015 Nov;25(11):675-86. PubMed PMID: 26437589. Pubmed Central PMCID: 4628843.
368. Kurrey NK, Jalgaonkar SP, Joglekar AV, Ghanate AD, Chaskar PD, Doiphode RY, et al. Snail and slug mediate radioresistance and chemoresistance by antagonizing p53-mediated apoptosis and acquiring a stem-like phenotype in ovarian cancer cells. *Stem cells*. 2009 Sep;27(9):2059-68. PubMed PMID: 19544473.
369. Cheng GZ, Chan J, Wang Q, Zhang W, Sun CD, Wang LH. Twist transcriptionally up-regulates AKT2 in breast cancer cells leading to increased migration, invasion, and resistance to paclitaxel. *Cancer research*. 2007 Mar 1;67(5):1979-87. PubMed PMID: 17332325.
370. Vesuna F, Lisok A, Kimble B, Domek J, Kato Y, van der Groep P, et al. Twist contributes to hormone resistance in breast cancer by downregulating estrogen receptor- α . *Oncogene*. 2012 Jul 5;31(27):3223-34. PubMed PMID: 22056872. Pubmed Central PMCID: 3276743.
371. Fischer KR, Durrans A, Lee S, Sheng J, Li F, Wong ST, et al. Epithelial-to-mesenchymal transition is not required for lung metastasis but contributes to chemoresistance. *Nature*. 2015 Nov 26;527(7579):472-6. PubMed PMID: 26560033. Pubmed Central PMCID: 4662610.
372. Zheng X, Carstens JL, Kim J, Scheible M, Kaye J, Sugimoto H, et al. Epithelial-to-mesenchymal transition is dispensable for metastasis but induces chemoresistance in pancreatic cancer. *Nature*. 2015 Nov 26;527(7579):525-30. PubMed PMID: 26560028. Pubmed Central PMCID: 4849281.
373. Liu CW, Li CH, Peng YJ, Cheng YW, Chen HW, Liao PL, et al. Snail regulates Nanog status during the epithelial-mesenchymal transition via the Smad1/Akt/GSK3 β signaling pathway in non-small-cell lung cancer. *Oncotarget*. 2014 Jun 15;5(11):3880-94. PubMed PMID: 25003810. Pubmed Central PMCID: 4116528.
374. De Craene B, Gilbert B, Stove C, Bruyneel E, van Roy F, Berx G. The transcription factor snail induces tumor cell invasion through modulation of the epithelial cell differentiation program. *Cancer research*. 2005 Jul 15;65(14):6237-44. PubMed PMID: 16024625.
375. Jennbacken K, Tesan T, Wang W, Gustavsson H, Damber JE, Welen K. N-cadherin increases after androgen deprivation and is associated with metastasis in prostate cancer. *Endocrine-related cancer*. 2010 Jun;17(2):469-79. PubMed PMID: 20233707.

376. Lee YC, Cheng CJ, Huang M, Bilen MA, Ye X, Navone NM, et al. Androgen depletion up-regulates cadherin-11 expression in prostate cancer. *The Journal of pathology*. 2010 May;221(1):68-76. PubMed PMID: 20191612. Pubmed Central PMCID: 2936767.
377. Schroeder A, Herrmann A, Cherryholmes G, Kowolik C, Buettner R, Pal S, et al. Loss of androgen receptor expression promotes a stem-like cell phenotype in prostate cancer through STAT3 signaling. *Cancer research*. 2014 Feb 15;74(4):1227-37. PubMed PMID: 24177177. Pubmed Central PMCID: 4539262.
378. Izumi K, Fang LY, Mizokami A, Namiki M, Li L, Lin WJ, et al. Targeting the androgen receptor with siRNA promotes prostate cancer metastasis through enhanced macrophage recruitment via CCL2/CCR2-induced STAT3 activation. *EMBO molecular medicine*. 2013 Sep;5(9):1383-401. PubMed PMID: 23982944. Pubmed Central PMCID: 3799493.
379. Hornberg E, Ylitalo EB, Crnalic S, Antti H, Stattin P, Widmark A, et al. Expression of androgen receptor splice variants in prostate cancer bone metastases is associated with castration-resistance and short survival. *PloS one*. 2011 Apr 28;6(4):e19059. PubMed PMID: 21552559. Pubmed Central PMCID: 3084247.
380. Cai C, Wang H, He HH, Chen S, He L, Ma F, et al. ERG induces androgen receptor-mediated regulation of SOX9 in prostate cancer. *The Journal of clinical investigation*. 2013 Mar;123(3):1109-22. PubMed PMID: 23426182. Pubmed Central PMCID: 3582143.
381. Jing Y, Cui D, Guo W, Jiang J, Jiang B, Lu Y, et al. Activated androgen receptor promotes bladder cancer metastasis via Slug mediated epithelial-mesenchymal transition. *Cancer letters*. 2014 Jun 28;348(1-2):135-45. PubMed PMID: 24662746.
382. Yue B, Ren QX, Su T, Wang LN, Zhang L. ERK5 silencing inhibits invasion of human osteosarcoma cell via modulating the Slug/MMP-9 pathway. *European review for medical and pharmacological sciences*. 2014;18(18):2640-7. PubMed PMID: 25317798.
383. Zhang K, Chen D, Jiao X, Zhang S, Liu X, Cao J, et al. Slug enhances invasion ability of pancreatic cancer cells through upregulation of matrix metalloproteinase-9 and actin cytoskeleton remodeling. *Laboratory investigation; a journal of technical methods and pathology*. 2011 Mar;91(3):426-38. PubMed PMID: 21283078. Pubmed Central PMCID: 3125102.
384. Huang CH, Yang WH, Chang SY, Tai SK, Tzeng CH, Kao JY, et al. Regulation of membrane-type 4 matrix metalloproteinase by SLUG contributes to hypoxia-mediated metastasis. *Neoplasia*. 2009 Dec;11(12):1371-82. PubMed PMID: 20019845. Pubmed Central PMCID: 2794518.
385. Nagase H, Visse R, Murphy G. Structure and function of matrix metalloproteinases and TIMPs. *Cardiovascular research*. 2006 Feb 15;69(3):562-73. PubMed PMID: 16405877.
386. Das R, Gregory PA, Hollier BG, Tilley WD, Selth LA. Epithelial plasticity in prostate cancer: principles and clinical perspectives. *Trends in molecular medicine*. 2014 Nov;20(11):643-51. PubMed PMID: 25262538.
387. Cho H, Herzka T, Zheng W, Qi J, Wilkinson JE, Bradner JE, et al. RapidCaP, a novel GEM model for metastatic prostate cancer analysis and therapy, reveals myc as a driver of Pten-mutant metastasis. *Cancer discovery*. 2014 Mar;4(3):318-33. PubMed PMID: 24444712. Pubmed Central PMCID: 4084646.
388. Abrahamsson PA, Falkmer S, Falt K, Grimelius L. The course of neuroendocrine differentiation in prostatic carcinomas. An immunohistochemical study testing chromogranin A as an "endocrine marker". *Pathology, research and practice*. 1989 Sep;185(3):373-80. PubMed PMID: 2813190.
389. Isaacs JT. The biology of hormone refractory prostate cancer. Why does it develop? *The Urologic clinics of North America*. 1999 May;26(2):263-73. PubMed PMID: 10361549.
390. Bang YJ, Pirnia F, Fang WG, Kang WK, Sartor O, Whitesell L, et al. Terminal neuroendocrine differentiation of human prostate carcinoma cells in response to increased intracellular cyclic AMP. *Proceedings of the National Academy of Sciences of the United States of America*. 1994 Jun 7;91(12):5330-4. PubMed PMID: 8202489. Pubmed Central PMCID: 43988.

391. Cox ME, Deeble PD, Lakhani S, Parsons SJ. Acquisition of neuroendocrine characteristics by prostate tumor cells is reversible: implications for prostate cancer progression. *Cancer research*. 1999 Aug 1;59(15):3821-30. PubMed PMID: 10447001.
392. Deeble PD, Murphy DJ, Parsons SJ, Cox ME. Interleukin-6- and cyclic AMP-mediated signaling potentiates neuroendocrine differentiation of LNCaP prostate tumor cells. *Molecular and cellular biology*. 2001 Dec;21(24):8471-82. PubMed PMID: 11713282. Pubmed Central PMCID: 100010.
393. Shen R, Dorai T, Szaboles M, Katz AE, Olsson CA, Buttyan R. Transdifferentiation of cultured human prostate cancer cells to a neuroendocrine cell phenotype in a hormone-depleted medium. *Urologic oncology*. 1997 Mar-Apr;3(2):67-75. PubMed PMID: 21227062.
394. Jiborn T, Bjartell A, Abrahamsson PA. Neuroendocrine differentiation in prostatic carcinoma during hormonal treatment. *Urology*. 1998 Apr;51(4):585-9. PubMed PMID: 9586611.
395. Dragu DL, Necula LG, Bleotu C, Diaconu CC, Chivu-Economescu M. Therapies targeting cancer stem cells: Current trends and future challenges. *World journal of stem cells*. 2015 Oct 26;7(9):1185-201. PubMed PMID: 26516409. Pubmed Central PMCID: 4620424.
396. Nouri M, Caradec J, Lubik AA, Li N, Hollier BG, Takhar M, et al. Therapy-induced developmental reprogramming of prostate cancer cells and acquired therapy resistance. *Oncotarget*. 2017 Mar 21;8(12):18949-67. PubMed PMID: 28145883. Pubmed Central PMCID: 5386661.
397. Pal SK, He M, Chen L, Yang L, Pillai R, Twardowski P, et al. Synaptophysin expression on circulating tumor cells in patients with castration resistant prostate cancer undergoing treatment with abiraterone acetate or enzalutamide. *Urologic oncology*. 2017 Dec 27. PubMed PMID: 29289429.
398. Wang C, Peng G, Huang H, Liu F, Kong DP, Dong KQ, et al. Blocking the Feedback Loop between Neuroendocrine Differentiation and Macrophages Improves the Therapeutic Effects of Enzalutamide (MDV3100) on Prostate Cancer. *Clinical cancer research : an official journal of the American Association for Cancer Research*. 2017 Nov 30. PubMed PMID: 29191973.
399. Kang J, Shakya A, Tantin D. Stem cells, stress, metabolism and cancer: a drama in two Acts. *Trends in biochemical sciences*. 2009 Oct;34(10):491-9. PubMed PMID: 19733480.
400. Housman G, Byler S, Heerboth S, Lapinska K, Longacre M, Snyder N, et al. Drug resistance in cancer: an overview. *Cancers*. 2014 Sep 5;6(3):1769-92. PubMed PMID: 25198391. Pubmed Central PMCID: 4190567.
401. Avadisian M, Fletcher S, Liu B, Zhao W, Yue P, Badali D, et al. Artificially induced protein-membrane anchorage with cholesterol-based recognition agents as a new therapeutic concept. *Angewandte Chemie*. 2011 Jul 4;50(28):6248-53. PubMed PMID: 21721078.
402. Zengerle M, Chan KH, Ciulli A. Selective Small Molecule Induced Degradation of the BET Bromodomain Protein BRD4. *ACS chemical biology*. 2015 Aug 21;10(8):1770-7. PubMed PMID: 26035625. Pubmed Central PMCID: 4548256.
403. Pardridge WM. The blood-brain barrier: bottleneck in brain drug development. *NeuroRx : the journal of the American Society for Experimental NeuroTherapeutics*. 2005 Jan;2(1):3-14. PubMed PMID: 15717053. Pubmed Central PMCID: 539316.
404. Ghislain J, Charnay P. Control of myelination in Schwann cells: a Krox20 cis-regulatory element integrates Oct6, Brn2 and Sox10 activities. *EMBO reports*. 2006 Jan;7(1):52-8. PubMed PMID: 16311519. Pubmed Central PMCID: 1369227.
405. Liu C, Zhu Y, Lou W, Cui Y, Evans CP, Gao AC. Inhibition of constitutively active Stat3 reverses enzalutamide resistance in LNCaP derivative prostate cancer cells. *The Prostate*. 2014 Feb;74(2):201-9. PubMed PMID: 24307657. Pubmed Central PMCID: 4437226.
406. Spiotto MT, Chung TD. STAT3 mediates IL-6-induced growth inhibition in the human prostate cancer cell line LNCaP. *The Prostate*. 2000 Feb 1;42(2):88-98. PubMed PMID: 10617865.

407. Yuan J, Zhang F, Niu R. Multiple regulation pathways and pivotal biological functions of STAT3 in cancer. *Scientific reports*. 2015 Dec 3;5:17663. PubMed PMID: 26631279. Pubmed Central PMCID: 4668392.
408. Bishop JL, Thaper D, Zoubeidi A. The Multifaceted Roles of STAT3 Signaling in the Progression of Prostate Cancer. *Cancers*. 2014 Apr 9;6(2):829-59. PubMed PMID: 24722453. Pubmed Central PMCID: 4074806.
409. McKeithen D, Graham T, Chung LW, Odero-Marrah V. Snail transcription factor regulates neuroendocrine differentiation in LNCaP prostate cancer cells. *The Prostate*. 2010 Jun 15;70(9):982-92. PubMed PMID: 20166136. Pubmed Central PMCID: 2877267.
410. Ware KE, Somarelli JA, Schaeffer D, Li J, Zhang T, Park S, et al. Snail promotes resistance to enzalutamide through regulation of androgen receptor activity in prostate cancer. *Oncotarget*. 2016 Aug 2;7(31):50507-21. PubMed PMID: 27409172. Pubmed Central PMCID: 5226599.
411. Zeng H, Jorapur A, Shain AH, Lang UE, Torres R, Zhang Y, et al. Bi-allelic Loss of CDKN2A Initiates Melanoma Invasion via BRN2 Activation. *Cancer cell*. 2018 Jul 9;34(1):56-68 e9. PubMed PMID: 29990501.
412. Naoko Kobayashi DH, Chun Wang, Joyce Yamashiro, Johnny Guan, and Robert E. Reiter. The role of POU3F2 in the aggressive behavior of neuroendocrine prostate cancer. *Cancer research*. 2018;78(13):5901.
413. Smith BA, Sokolov A, Uzunangelov V, Baertsch R, Newton Y, Graim K, et al. A basal stem cell signature identifies aggressive prostate cancer phenotypes. *Proceedings of the National Academy of Sciences of the United States of America*. 2015 Nov 24;112(47):E6544-52. PubMed PMID: 26460041. Pubmed Central PMCID: 4664352.
414. Davies A, Ahmed M, Bostock C, Gleave A, Ketola K, Johnson F, et al. Abstract 5025: EZH2 reprogramming confers intrinsic stem cell properties and developmental plasticity driving neuroendocrine prostate cancer. *Cancer research*. 2017;77(13 Supplement):5025-.
415. Ketola K, Munuganti RSN, Davies A, Nip KM, Bishop JL, Zoubeidi A. Targeting Prostate Cancer Subtype 1 by Forkhead Box M1 Pathway Inhibition. *Clinical Cancer Research*. 2017;23(22):6923-33.
416. Palapattu GS, Wu C, Silvers CR, Martin HB, Williams K, Salamone L, et al. Selective expression of CD44, a putative prostate cancer stem cell marker, in neuroendocrine tumor cells of human prostate cancer. *The Prostate*. 2009 May 15;69(7):787-98. PubMed PMID: 19189306.
417. Salvatori L, Caporuscio F, Verdina A, Starace G, Crispi S, Nicotra MR, et al. Cell-to-cell signaling influences the fate of prostate cancer stem cells and their potential to generate more aggressive tumors. *PloS one*. 2012;7(2):e31467. PubMed PMID: 22328933. Pubmed Central PMCID: 3273473.
418. Sotomayor P, Godoy A, Smith GJ, Huss WJ. Oct4A is expressed by a subpopulation of prostate neuroendocrine cells. *The Prostate*. 2009 Mar 1;69(4):401-10. PubMed PMID: 19058139. Pubmed Central PMCID: 2865184.